

Methods to assess the impact of geographic interdependencies induced by extreme rainfall on the resilience of public transport networks

Georgia Boura

Department of Civil & Environmental Engineering
Faculty of Engineering, University of Strathclyde

A thesis submitted for the requirements for the degree of
Doctor of Philosophy

April 2025

Contents

Declaration of Authenticity and Author's Rights	x
Abstract.....	xi
Acknowledgements.....	xiii
List of Author's Contributions.....	xiv
List of Notations.....	xv
List of Abbreviations	xviii
Glossary of Key Definitions	xix
1. Introduction.....	1
1.1. Identification of the problem and context of research	1
1.2. Background.....	8
1.2.1. Spatial extent of rainfall events and estimated impacts of climate change	8
1.2.2. Vulnerability assessment of public transport networks to disruptions	14
1.2.3. Vulnerability assessment of transport networks to area-wide events	20
1.3. Research aim and objectives.....	24
1.4. Structure of Thesis	29
2. Incorporating geographic interdependencies into the resilience assessment of multimodal public transport networks.....	31
2.1. Introduction.....	31
2.2. Background.....	35
2.3. Methods	37
2.3.1. Network representation	37
2.3.2. Redundancy indicator	38
2.3.3. Substitutability indicator.....	42
2.4. Application to rail and long-distance bus networks in mainland Scotland.....	43
2.5. Results	48
2.5.1. Redundancy of options and geographic interdependencies between modes.....	50
2.5.2. Substitutability of options accounting for geographic interdependencies between modes	55
2.6. Conclusions and Discussion.....	58
3. Empirical assessment of the impact of rainfall-related geographic interdependencies on multimodal public transport networks.....	63
3.1. Introduction.....	63

3.2.	Key literature on importance, weakness and criticality of network elements.....	65
3.2.1.	Importance.....	65
3.2.2.	Weakness and criticality	66
3.2.3.	Research gaps	67
3.3.	Methods	68
3.3.1.	Network representation	68
3.3.2.	Assessing the geographic interdependency between discrete public transport networks due to heavy rainfall.....	69
3.3.3.	Assessment of importance in the public transport networks	73
3.3.4.	Assessment of criticality in the public transport networks	75
3.4.	Application of importance and criticality models	79
3.4.1.	Network representation	79
3.4.2.	Historical incident dataset for the bus network.....	82
3.4.3.	Historical incident dataset for the railway network	89
3.5.	Results	93
3.5.1.	Geographic interdependencies between the public transport modes due to rainfall	94
3.5.2.	Impact of rainfall-related geographic interdependencies on the importance of public transport links	98
3.5.3.	Impact of rainfall-related geographic interdependencies on the criticality of public transport links	105
3.6.	Conclusions and Discussion.....	117
4.	Assessment of the impact of extreme rainfall on interdependent public transport networks	123
4.1.	Introduction.....	123
4.2.	Key literature.....	126
4.3.	Methods	129
4.3.1.	Characteristics of critical rainfall events resulting in the closure of public transport links.....	129
4.3.2.	Assessing the geographic interdependencies between public transport modes due to extreme rainfall.....	130
4.3.3.	Assessing the impact of extreme rainfall on the redundancy of interdependent public transport networks	132
4.4.	Application of the impact assessment of flooding to the long-distance public transport network in mainland Scotland	138

4.5.	Results	139
4.5.1.	Characteristics of critical rainfall events causing the closure of public transport links	139
4.5.2.	Spatial dependence of critical rainfall events.....	143
4.5.3.	Impact of pluvial flooding on the redundancy of travel options between locations	146
4.6.	Conclusions and Discussion.....	153
5.	Discussion	158
5.1.	Completion of the research aim and objectives	158
5.2.	Conclusions and Discussion.....	162
5.3.	Limitations and recommendations for future research directions.....	166
5.4.	Contributions of research to theory and practice	171
6.	Conclusions.....	177
	References	178
	Appendices.....	193
	Appendix A: Supplementary Material for Chapter 2	193
	Appendix B: Supplementary Material for Chapter 3	200
	Appendix C: Supplementary Material for Chapter 4.....	210

List of Figures

Figure 1-1 The relationship between vulnerability and components of resilience (adapted from Mattsson and Jenelius, 2015).....	6
Figure 2-1 Comparison of redundancy and substitutability, with and without geographical interdependency. All figures show a choice set containing a total of four options (A-D) which is equal to the unweighted redundancy of options. The size of options indicates the attractiveness of each option; thus, Option A is the preferred option. The intersection of options $A \cap B$ plus $C \cap D$ is the degree of geographical interdependency in each choice set. In Figures 1(a) and 1(c), the sum of weighted options ($A \cup B \cup C \cup D$) is the weighted redundancy which is equivalent to the accessibility presented by the options. In Figures 1(b) and 1(d), Option A is unavailable, thus the remaining accessibility is equal to $((A' \cap B) \cup (C \cup D))$ which is the substitutability of each choice set.....	33
Figure 2-2 Example of a route of the substitute transport mode (purple line) located in the neighbourhood (grey area) of the primary route (red line).....	39
Figure 2-3 Travel paths of the long-distance public transport network in mainland Scotland, along with selected Scottish cities and towns and their respective population.	46
Figure 2-4 Histograms of accessibility for the (A) railway and (B) bus routes for OD pairs served by both modes on Monday between 07:30am and 09:30am. Accessibility values for a particular mode range from approximately 0 to 1. Low values of accessibility indicate long travel times close to 12 hours, while high accessibility values indicate short travel times.	49
Figure 2-5 Maps showing accessibility-based redundancy values of zones connected by both modes for (a) travel from origins (b) travel to destinations, when ignoring geographic interdependencies between the two networks. Non-shaded zones are those not served by both modes. Zones in lighter colours are characterised by lower accessibility than those in darker colours.	50
Figure 2-6 Relative losses in redundancy of O-D Pairs when considering geographic interdependencies related to various neighbourhood sizes. Larger values indicate higher susceptibility of travel options between an O-D pair to accessibility loss due to geographic interdependencies, while lower values indicate lower susceptibility.....	51
Figure 2-7 O-D Pairs associated with particularly high redundancy losses where primary mode is (a) rail and (b) bus in the case of 100 m-wide buffers, along with sections of (c) rail and (d) bus (road) networks (in red) used by routes connecting these O-D pairs.	52
Figure 2-8 Losses in redundancy for origins (a) in absolute terms due to hazards of 100 m footprint (b) in absolute terms due to hazards of 1.5 km footprint (c) in absolute terms due to hazards	

of 10 km footprint (d) in relative terms due to hazards of 100m footprint in relative terms due to hazards of 1.5 km footprint, and (f) in relative terms due to hazards of 10 km footprint, when rail is considered as primary travel mode and bus as alternative. Non-shaded zones are those origins not served by both modes. Zones in lighter colours are less susceptible to losses due to geographic interdependencies.53

Figure 2-9 Losses in normalised substitutability values of alternative routes of each mode for buffers of varying widths. The box plots for bus (orange colour) show substitutability losses when bus is the primary mode and railway is substitute and express the reduction in the extent to which railway routes replace the corresponding bus routes when the latter become unavailable. Likewise, box plots for railway (green colour) reflect the drop in extent to which bus routes replace the accessibility provided by railway routes.55

Figure 2-10 O-D Pairs associated with high outliers of substitutability losses for travel by (a) rail and (b) bus, in the case of 100 m-wide buffers, along with sections of (c) rail and (d) bus (road) networks that the routes connecting these O-D Pairs use.....56

Figure 2-11 Losses in normalised substitutability for origins (a) in absolute terms due to hazards of 100m footprint (b) in absolute terms due to hazards of 1.5 km footprint (c) in absolute terms due to hazards of 10 km footprint (d) in relative terms due to hazards of 100m footprint (e) in relative terms due to hazards of 1.5 km footprint, and (f) in relative terms due to hazards of 10 km footprint, when rail is considered as primary travel mode and bus as substitute. Non-shaded zones are those origins not served by both modes. Zones in lighter colours are less susceptible to losses due to geographic interdependencies.57

Figure 3-1 The identification of public transport trips traversing the road links connecting road nodes with ID's "706670", "706607", "706596" and "706525" based on the mapping of bus segments 1 and 2 on which the sets of trips {t1, t2} and {t3, t4, t5} run, respectively.69

Figure 3-2 Schematic figure on the method used to compute the conditional probability of a link of mode m_2 experiencing disruption given that a link of mode m_1 is already disrupted. The blue link is that of m_1 that is already disrupted, the grey links are links of m_2 and the red links are those of m_2 concurrently disrupted.....72

Figure 3-3 The geographical representation of the Scottish public transport network consisting of long-distance bus and rail services, along with selected main localities that these services connect and their corresponding population.81

Figure 3-4 Steps of process (blue rectangles) and data sources (yellow rectangles) for the formation of the historical incident dataset for the long-distance bus network in Scotland...86

Figure 3-5 Plots of probability of (A) bus links being disrupted given that a railway link at a certain distance is disrupted (B) railway links being disrupted given that a bus link at a certain distance is disrupted. The red lines are the exponential regression lines fitted to the data. Note the different scales of the y-axis of the plots.95

Figure 3-6 Relative increases in importance of (a) rail and (b) bus links as a result of their geographic interdependencies due to rainfall. Note the different classification scales in the two maps. The classification of values was done using the Jenks natural breaks classification method.....100

Figure 3-7 Importance of (a) railway links and (b) 4 km railway buffers. Note the different classification scales in the two maps. High values suggest that a significant number of public transport trips traverse the link or buffer. It should be also noted that in the map referring to 4 km buffers of links, the widths of the buffers are not included in order for the results to be clearly shown.102

Figure 3-8 Importance of (a) bus links and (b) 4 km bus buffers. Note the different classification scales in the two maps. High values suggest that a significant number of public transport trips traverse the link or buffer. It should be also noted that in the map referring to 4 km buffers of links, the widths of the buffers are not included in order for the results to be clearly shown.104

Figure 3-9 Empirical and fitted probability distribution functions for the weekly frequency of flooding incidents on the (a) railway network and (b) bus network.....106

Figure 3-10 Scatterplots of criticality of (A) railway and (B) bus links against the respective values of their corresponding 4 km buffers. Note the difference in the x-axis and y-axis values between plots A and B.....109

Figure 3-11 Criticality of (a) railway links and (b) 4 km railway buffers. Note the different classification scales in the two maps. High values suggest that a significant number of public transport trips traverse the link or buffer.....111

Figure 3-12 Criticality of (a) bus links and (b) 4 km bus buffers. Note the different classification scales in the two maps. High values suggest that a significant number of public transport trips traverse the link or buffer.114

Figure 4-1 Histogram of computed minimum inter-event time (MIT) of rain stations in mainland Scotland.140

Figure 4-2 Total depth and duration of rainfall events that caused full closure of (a) rail and (b) bus links, along with the fitted median regression lines.141

Figure 4-4 Depth and duration of rainfall events that led to full closures of bus and railway links, along with the fitted median regression line.142

Figure 4-4 Box plots of proportion of rain stations that recorded a critical rainfall event on the same day of occurrence of a critical event at the origin station, along with the mean value of proportions for each distance bin (denoted by diamond symbols).144

Figure 4-5 Fitted exponential regression model to the estimated conditional probabilities of rainfall.145

Figure 4-6 Scatterplots of (a) importance of rail links, when considering the spatial dependence of flood events that may occur on the bus network concurrently with those on rail (Case III), against the importance of rail links when assuming that floods on the bus network are independent (Case I), and (b) importance of rail links, when considering the spatial dependence of flood events that may occur on the bus network concurrently with those on rail (Case III), against the importance of rail links when assuming complete dependence of floods on the bus network to them (Case II). In both plots, data points below (above) the 45-degree reference line (in red colour) indicate increase (decrease) in importance of the link compared to Case III, while those falling onto the reference line indicate no change.147

Figure 4-7 Losses in redundancy of origins due to the failure of link spanning from Croy to Greenhill Upper Junction (a) when assuming complete independence of flooding-induced closures on bus routes, in absolute terms (b) when assuming complete dependence of flooding-induced closures, in absolute terms (c) when assuming spatial dependence of flooding-induced closures on bus routes, in absolute terms (d) when assuming complete independence of flooding-induced closures on bus routes, in relative terms (e) when assuming complete dependence of flooding-induced closures on bus routes, in relative terms (f) when assuming spatial dependence of flooding-induced closures on bus routes, in relative terms. Non-shaded zones correspond to origins either not served by both modes or not directly affected by closure of the link.150

Figure 4-8 Losses in redundancy of origins due to the failure of link spanning from Pitlochry to Dunkeld & Birnam, (a) when assuming complete independence of flooding-induced closures on bus routes, in absolute terms (b) when assuming complete dependence of flooding-induced closures, in absolute terms (c) when assuming spatial dependence of flooding-induced closures on bus routes, in absolute terms (d) when assuming complete independence of flooding-induced closures on bus routes, in relative terms (e) when assuming complete dependence of flooding-induced closures on bus routes, in relative terms (f) when assuming spatial dependence of flooding-induced closures on bus routes, in relative

terms. Non-shaded zones correspond to origins either not served by both modes or not directly affected by closure of the link.152

List of Tables

Table 1-1 Examples of interdependencies in the transport network in relation to pluvial flooding .	3
Table 1-2 Studies assessing the spatial scale of rainfall events and potential changes due to climate change.....	11
Table 3-1 Types of flood impacts on Stagecoach services and re-classified impacts on the road infrastructure availability.....	84
Table 3-2 Variables of the historical dataset of flood events for the long-distance bus network	86
Table 3-3 Variables in the historical incident dataset of flood events on the railway network.	91
Table 3-4 Average annual number of flooding incidents on bus links from May 2017 to May 2020.	93
Table 3-5 Average annual number of flooding incidents on railway links from May 2017 to May 2020.	93
Table 3-6 Parameters and diagnostics of the fitted exponential model predicting the conditional probability of a bus link being disrupted given that a railway link is disrupted due to pluvial flooding.	97
Table 3-7 Parameters and diagnostics of the fitted exponential model predicting the conditional probability of a railway link being disrupted given that a bus link is disrupted due to pluvial flooding.	97
Table 3-8 Parameters of the fitted Negative Binomial distribution function to the weekly frequency of flooding incidents on the railway network due to rainfall.	105
Table 3-9 Parameters of the fitted Negative Binomial distribution function to the weekly frequency of flooding incidents on the bus network due to rainfall.	105
Table 3-10 Goodness-of-fit criteria for the fitted probability functions to the weekly frequency of flooding incidents on the railway network.	106
Table 3-11 Goodness-of-fit criteria for the fitted probability functions to the weekly frequency of flooding incidents on the bus network.	106
Table 3-12 Expected annual number of flood events on bus links due to rainfall.	107
Table 3-13 Expected annual number of pluvial flood events on rail links due to rainfall.	107
Table 3-14 Weakness of bus and rail links to rainfall.	108
Table 3-15 Five most critical rail links	112

Table 3-16 Five most critical rail links, when considering their rainfall-related geographic interdependency to bus links.....	112
Table 3-17 Five most critical bus links.	115
Table 3-18 Five most critical bus links, when considering their rainfall-related geographic interdependency to rail links.	116
Table 4-1 Fitted parameters of the median regression model that represents the critical rainfall thresholds for rail and bus.	143
Table 4-2 Parameters of the fitted exponential decay model to the estimated conditional probabilities of co-occurrences of critical rainfall events.....	145
Table 4-3 Top 20 rail links identified using the importance measure for Case III, along with their ranking according to their importance under Cases I and II.	149
Table 5-1 Research objectives achieved in this thesis.	159

Declaration of Authenticity and Author's Rights

This thesis is the result of the author's original research. It has been composed by the author and has not been previously submitted for examination which has led to the award of a degree.

The copyright of this thesis belongs to the author under the terms of the United Kingdom Copyright Acts as qualified by University of Strathclyde Regulation 3.50. Due acknowledgement must always be made of the use of any material contained in, or derived from, this thesis.

Signed: Georgia Boura

Date: 06/04/2025

Abstract

Severe rainfall events can concurrently affect components of public transport modes operating on discrete infrastructure networks which are co-located within the spatial extent of these events, thereby revealing geographic interdependencies between them. These interdependencies may in turn disrupt the functionality of public transport services, consequently reducing the available travel options or, in more extreme cases, causing complete loss of connectivity between locations. Despite the growing risk of these events, existing research has largely overlooked the potential of concurrent disruptions across interdependent networks. This thesis presents a novel framework for the assessment of resilience and vulnerability of geographically interdependent public transport networks using the Scottish long-distance public transport networks as a case study.

The framework initially evaluates the potential impacts of area-wide events of varying spatial scales on the accessibility provided by two discrete public transport networks. Indicators are developed which quantify the contributions of alternative travel options to the accessibility of locations while also considering the geographic interdependencies between them arising from their close spatial proximity. Building on this, an empirical method is proposed to estimate the geographic interdependencies between public transport networks for a given hazard (in this case, rainfall) and integrate them into the vulnerability assessment of public transport links. The estimation of geographic interdependencies is based on historical disruption records which are analysed to determine the proximity of past concurrent flooding incidents due to rainfall. The research is then further extended by modelling the rainfall-related geographic interdependencies in probabilistic terms and incorporating them into the resilience assessment of interdependent networks, therefore providing a more realistic estimation of concurrent failures compared to deterministic approaches.

Results reveal that the potential losses in accessibility can be substantial even for localised hazards and that these are positively correlated with the spatial scale of event. This suggests that the contribution of alternative travel options to accessibility of locations may be significantly reduced due to the occurrence of area-wide events and that ignoring the potential for concurrent disruptions, significantly underestimates the true consequences. When analysing rainfall as the hazard of interest, the empirical analysis confirms the existence of geographic interdependencies between rail and bus networks and reveals that the

vulnerability of public transport links is significantly affected when geographic interdependencies are considered, especially within and around urban centres where many public transport services operate in close spatial proximity. This observation is further validated through probabilistic modelling, reinforcing the need to incorporate interdependencies into impact assessments. Although the findings focus on Scotland's long-distance public transport networks, they are applicable to other regions and countries exposed to heavy rainfall.

This research provides infrastructure managers and public transport operators with practical and easily implementable methods for the evaluation of resilience of geographically interdependent networks that can be implemented using readily available data and tools to identify locations and parts of their networks that require further scrutiny.

Keywords: Resilience, Vulnerability, Public transport, Geographic interdependency, Accessibility, Connectivity, Redundancy, Substitutability, Flooding, Rainfall.

Acknowledgements

I would like to thank my supervisor, Dr Neil S. Ferguson, for his continuous support and guidance throughout my PhD studies. I am also grateful to my second supervisor, Dr. Stella Pytharouli, for her advice and support throughout this journey.

I am grateful to all those who contributed to this research – directly or indirectly. This PhD was funded by the University of Strathclyde and, without this support, this thesis would not have been possible. I would also like to thank Network Rail for providing spatial data and flooding incident data for the rail network in Scotland. Equally, thanks to Transport Scotland and the Scottish local authorities for making available flooding incident data for the road network, and to SEPA for providing rainfall data. Further, I would like to thank Christos and Haifa, two close friends of mine whom I met during the early years of my PhD studies, for all the fun moments and experiences in and out of the University as well as our virtual group study sessions during the pandemic.

Special thanks to my family, especially my mother, Eva, and sister, Theoni, for their emotional support, love and encouragement, and for trusting my abilities to complete this research. I'd like to specifically thank Theoni for our chats on statistics and for encouraging me early on in my PhD journey to familiarise myself with the principles of statistical programming – acquiring this skill proved to be vital for the implementation of this research.

I would like to thank my partner, Jonathan, for taking care of me and keeping me sane, but also for reminding me to rest and to not always be glued at my desk studying. I am also grateful to my four-legged feline buddy, Mitsy, for all the fun moments at home and for being a pleasant everyday distraction from work.

Despite all the difficulties throughout this journey, I deeply appreciate all the lessons learnt, as these contributed significantly to my professional and personal growth. Unbeknownst to me, by testing the resilience of transport networks, I tested and improved my personal resilience as well.

List of Author's Contributions

The research presented in Chapter 2 has been published in the *Journal of Transport Geography*, as shown below.

Boura, G. and Ferguson, N. S. (2024) "Incorporating geographic interdependencies into the resilience assessment of multimodal public transport networks". *Journal of Transport Geography*, 118, 12 p., 103934.

In addition, the following manuscripts are being prepared for publication.

Manuscript 1: "Empirical assessment of the impact of flooding-related geographic interdependencies on multimodal public transport networks".

Manuscript 2: "Assessment of the impact of pluvial flooding on interdependent public transport networks".

List of Notations

Notation	Description
\mathbf{G}	Graph that represents a public transport network
$N = \{n_1, n_2, \dots, n_K\}$	Set of nodes of a graph.
$E = \{e_1, e_2, \dots, e_M\}$	Set of segments of a graph.
$T = \{t_1, t_2, \dots, t_S\}$	Set of public transport trips.
$L = \{l_1, l_2, \dots\}$	Set of links of the transport infrastructure network on which a public transport mode operates.
m_1	Primary transport mode.
m_2	Alternative transport mode.
OD	Origin-Destination pair.
p_m	Route of mode m .
$C(p_m)$	Cost of travel along route of mode m .
β_m	Maximum travel cost by mode m acceptable to travellers.
acc_{OD}^m	Accessibility of OD pair for travel by mode m .
$acc_{OD}^{m_1 \leftarrow m_2}$	Redundancy of travel between OD pair offered by primary mode m_1 and alternative mode m_2 .
$R_C(p_{m_2}, p_{m_1})$	Neighbourhood coefficient for primary route p_{m_1} and alternative route p_{m_2} .
$l(p_{m_2}, p_{m_1})$	Length of alternative route located in the neighbourhood of the primary route.
$l(p_m)$	Length of a route.
i	Origin of travel.
j	Destination of travel.
$Acc_i^{(m_1 \leftarrow m_2)}$	Redundancy of origin zone i for travel by m_1 and substituted by m_2 .
$\Delta Acc_{i,m_1}^{(ab)}$	Absolute change in redundancy of origin zone i for travel by m_1 .
$\Delta Acc_{i,m_1}^{(rel)}$	Relative change in redundancy of origin zone i for travel by m_1 .
S_{OD}	Substitutability of travel options between OD .
\widehat{S}_{OD}	Normalised substitutability of travel options between OD .
LS_{OD}	The total accessibility (i.e. the maximum expected utility) of all options between OD under normal conditions.
$LS_{OD}^{Y=i}$	The accessibility of remaining options when the preferred choice i is unavailable.

$LS_{OD}^{m_1 \leftarrow m_2, y=1}$	The total accessibility when the preferred option of m_1 is unavailable and may be substituted by m_2 .
d	The width of a buffer or buffer ring.
$P(m_2 m_1)$	Conditional probability of a link of m_2 experiencing disruption given that a link of m_1 at a certain distance is disrupted.
$I^{m_1}(a)$	Importance of link a of mode m_1 .
$t^{m_1}(a)$	Number of trips that traverse link a of mode m_1 .
$D_a = \{x d_{min}(x, a) \leq d\}$	The neighbourhood (buffer) of link a of mode m_1 , which represents each point in space x with a minimum Euclidean distance from a , denoted as $d_{min}(x, a)$, that is less than or equal to the selected buffer width d .
$I^{m_1, m_2}(a)$	Importance of link a of mode m_1 when considering its geographic interdependency to links of mode m_2 .
n	The number of weeks over a year.
$E(f_m)$	Expected annual network-wide frequency of flooding on mode m .
$E(f_{m,w})$	Expected network-wide frequency of flood events on week w .
$E(f_a^m)$	Expected frequency of flood events on link a of mode m .
l_a	Length of link a .
L_m	Total length of all links of mode m .
f_a^m	Average annual frequency of flood events on link a .
$W^m(a)$	Weakness of link a of mode m .
$C^m(a)$	Criticality of link a of mode m .
$C^{m_1, m_2}(a)$	Criticality link a of mode m_1 when considering its geographic interdependency to links of mode m_2 .
$E(f_{D_a}^{m_2})$	Expected number of incidents on links of mode m_2 within the buffer of link a .
$E_{cr}(m)$	Critical rainfall event for mode m .
V_{cr}	Total depth of a critical rainfall event.
D_{cr}	Duration of a critical rainfall event.
$P(E_{cr}(m_1) E_{cr}(m_2))$	Conditional probability of a critical rainfall event for m_1 occurring given the occurrence of a critical rainfall event for m_2 .
$E_A = \{E_{A1}, E_{A2}, E_{A3}, \dots\}$	Set of rainfall events recorded by rain station A.
Dr	Standardised conditional probability.
d_0	Decorrelation distance of rainfall.
$P(E_{cr}(m_1))$	Unconditional probability of critical rainfall event for m_1 .

d_{ij}	The demand for travel between the OD pair.
$v_{ij(a)}$	The consequences for the OD pair between i and j due to the closure of link a .
$acc_{ij(0)}$	The accessibility from i to j under normal conditions.
$acc_{ij(a)}$	The accessibility from i to j when link a has failed.
D_j	The attractiveness of destination zone j , which captures the number of opportunities available at j .
$P(p_{m_2}^{flood} p_{m_1}^{flood})$	Conditional probability of substitute route experiencing flooding-induced closure given the flooding-induced closure of primary route.
A	A flood event that is considered to have occurred at the preferred route p_{m_1} .
B $= \{B_1, B_2, \dots, B_m\}$	The set of flood events that may occur in the alternative route p_{m_2} according to the flood map.
B' $= \{B_1, B_2, \dots, B_n\}$	The set of flood events in the alternative route p_{m_2} that is considered to have occurred concurrently with A . Note that B' is a subset of B , i.e. $B' \subseteq B$ and $n \leq m$.
$P(\cup B_i A)$	Conditional probability of at least one B_i event occurring given the occurrence of event A .
RP	Return period of flooding.

List of Abbreviations

Abbreviation	Description
CVA	Coefficient of Variation Analysis
GIS	Geographic Information System
GTFS	General Transit Feed Specification
IDW	Inverse Distance Weighted
IETD	Inter-Event Time Interval
IRIS	Integrated Road Information System
MIT	Minimum Inter-event Time
OD	Origin-Destination (pair)
OTP	OpenTripPlanner
SEPA	Scottish Environment Protection Agency

Glossary of Key Definitions

Term	Definition
Accessibility	The extent to which land use and transport systems enable (groups of) individuals to reach activities or destinations.
Exposure	The network elements located within the area that a given hazard may occur.
Critical rainfall event	A rainfall event with characteristics (e.g., depth, duration, intensity) that can result in the full closure of a transport link due to flooding.
Criticality	The criticality of a network element represents its likelihood (or frequency) of closures due to a certain type of disruption as well as the consequences to the network because of its closure.
Geographic interdependency	The concurrent change of state of two or more spatially proximate infrastructure networks due to an event affecting them at the same time.
Minimum inter-event time	The minimum dry period that needs to elapse between two rain events for them to be considered as independent.
Importance	The importance of a network element reflects the severity of impact on the functionality of the network if that element is failed.
Interdependency	The bidirectional interaction between two or more infrastructure networks, where the state of one affects the state and/or operation of the others.
Rapidity	The capacity of the system to timely restore its operation back to normal.
Redundancy	The availability of multiple elements within a system that can be used in the event of disruptions to maintain performance.
Resilience	The ability of a system to absorb the effects of hazards and quickly recover from hazard impacts.

Resourcefulness	The ability of a system to identify and utilise resources to tackle disruptions.
Risk	Potential for adverse consequences.
Robustness	The ability of the system to withstand disruptions.
Substitutability	The extent to which the preferred travel alternative can be substituted by other initially less preferred alternatives.
Vulnerability	The susceptibility of the transport network to loss of performance.
Weakness	The weakness of a network element represents its likelihood (or frequency) of closure due to a certain type of disruptive event occurring.

1. Introduction

1.1. Identification of the problem and context of research

Public transport networks are essential for the functioning of societies as they ensure the seamless mobility of people between locations. However, they are exposed to various types of disruptive incidents that can damage their assets and degrade their operation thus resulting in socioeconomic losses, such as longer travel times and business interruption (Pregolato *et al.*, 2020). Hazardous events stemming from hydrometeorological phenomena, such as heavy rainfall, are one of the costliest hazards globally (Westra, 2014) and pose significant threats for transportation infrastructure networks (Steen *et al.*, 2022). These events may span wide areas and, as such, have the potential to concurrently inflict damages to assets of all transport networks located within their spatial footprint, consequently disrupting all public transport modes and leaving travellers with no option to complete their trips.

Indicatively, in July 2021, a heavy precipitation event led to widespread flooding, which affected multiple countries in western Europe, including Belgium, Germany and the Netherlands, and inflicted major damages of both roads and railways (Koks *et al.*, 2021). More recently, a storm event that was characterised by heavy, persistent and widespread rainfall, affected most of England, Wales and eastern Scotland, and resulted in extensive damages to bridges, flooding-induced closures of roads and cancellation of rail services (Met Office, 2023). Projected changes of future climate patterns indicate that precipitation and, by extension, the potential for flood events will exacerbate in both frequency and intensity in many parts of the world (Seneviratne *et al.*, 2021), including the UK (Slingo, 2021). Considering this increasing trend, growing efforts have been devoted to understanding current and future impacts of extreme rainfall on transportation to ultimately identify measures to reduce them (Chen *et al.*, 2015; Pregolato *et al.*, 2017; Pyatkova *et al.*, 2019; Evans *et al.*, 2020; Zhu *et al.*, 2022).

The aforementioned examples demonstrate that multiple flood events may occur within the spatial footprint of heavy rainfall. These events, often referred to as pluvial (or surface water) flooding, occur when the amount of water reaching the surface exceeds the capacity of the natural or engineered drainage of the area, consequently leading to water flowing and

concentrating onto the surface, rather than infiltrating into it (Rosenzweig *et al.*, 2018). When pluvial flooding occurs due to convective rainfall, i.e., events of high intensity and short duration, it is characterised by a sudden and rapid onset and high intensity and, in this case, is commonly referred to as flash flooding (Mishra *et al.*, 2022).

The impacts of pluvial flooding on infrastructure networks can be classified as direct or indirect (Rogelis *et al.*, 2015). *Direct* impacts are those that occur on infrastructure assets and vehicles due to their physical contact with floodwater, such as flooding-induced closure of roads or rail sections, embankments failures and vehicles being swept away by floodwaters. A well-developed body of research exists on the susceptibility of infrastructure and vehicle assets directly affected by flooding, which seeks to model the extent of infrastructure damage as a function of the flooding intensity (e.g., Vanneuville *et al.*, 2003; Huizinga *et al.*, 2017; van Ginkel *et al.*, 2021). *Indirect* impacts are knock-on effects to the users of infrastructure systems located outside of the area directly affected by flooding, such as cancellation of public transport services and increased travel times due to detours (Rogelis *et al.*, 2015). Although the indirect impacts can potentially be much larger than direct costs (Hackl *et al.*, 2018), this body of research is much more limited compared to that assessing direct impacts of flooding (Rebally *et al.*, 2021).

The scope of this thesis is on heavy rainfall and its impact on transport networks and, therefore, only pluvial flood events are considered, with a focus on their indirect impacts on public transport networks. Although riverine flooding may also occur when heavy rainfall exceeds the capacity of rivers and watercourses, causing the excess water to overflow onto adjacent areas (Forbes *et al.*, 2015), it falls outside the scope of this research, as it may occur beyond the immediate footprint of rainfall and requires separate analysis. Similarly, coastal flooding is not considered, as it is primarily driven by high winds, tides, and storm surges rather than predominantly by rainfall (Hunt, 2005) and may impact transport networks differently than pluvial flooding.

The transport system consists of various modes that may operate either on the same infrastructure networks (e.g., bus and taxis) or different ones (e.g., bus and rail), which makes it particularly difficult to assess the indirect impacts of rainfall events on the entire transport system comprehensively. This is because these modes that make up the transport network do not operate independently and, even when they are not physically connected, they may

interact with and influence the state of each other in a complex way. As such, disruptions induced by flooding may affect all transport modes concurrently.

The concept of this bidirectional interconnectedness between infrastructure networks that can emerge in normal or disruption conditions, known as *interdependency*, was described by Rinaldi *et al.* (2001). The authors classified interdependencies between infrastructure networks into four types, namely physical, cyber, geographic and logical. *Physical interdependency* occurs when the state or operation of one network depends on its physical connections with the other network. In other words, the operation of one network is dependent on the material output of the other network. *Cyber interdependency* occurs when the operation of an infrastructure network is dependent on the functioning of information systems. *Geographic interdependency* occurs when an environmental event concurrently affects the state of all networks co-located within its spatial footprint, and therefore is driven by the proximity of assets of these networks, rather than the interaction between them. Lastly, *logical interdependency* refers to interconnectedness between networks that cannot be classified into one of the three abovementioned types of interdependencies, and it often relates to human decisions.

The occurrence of rainfall may reveal any of these interdependencies that exist within the transport system, which may or may not be apparent under normal conditions. Table 1-1 provides examples for each type of interdependency that may arise in transport networks in the event of flooding.

Table 1-1 Examples of interdependencies in the transport network in relation to pluvial flooding

Interdependency	Example
Physical	Cancellation of rail and bus services due to train and bus drivers' inability to arrive at termini of routes, because of flooding on the road network.
Cyber	Cancellation of rail services due to flooding-induced failures on the electricity, signalling and/or telecommunication systems.
Geographic	Concurrent surface water flooding on road and rail infrastructure that is co-located in the spatial footprint of an intense rainfall event.

Logical	Limited allocation of resources leading to sub-optimal measures for the adaptation of transport infrastructure to climate change, which in turns results in more frequent and/or extensive flooding-induced damages of transport assets.
---------	--

From Table 1-1 and as previously mentioned, it becomes clear that since rainfall events directly affect areas rather than a single point in space, their direct impacts may include concurrent flood events on separate transport infrastructure networks (e.g., road and rail) and may, therefore, reveal geographic interdependencies that exist between them. In terms of indirect impacts, these concurrent flood events may cause simultaneous disruptions on all public transport modes that operate on these interdependent infrastructure networks. This in turn may result in some of the available public transport options within the affected area becoming unavailable and, in more extreme cases, no options may remain functional, thereby leaving travellers without any alternative to undertake their trips. Although research has been done to understand how various disruptions directly affecting one transport mode may cause knock-on effects to other modes (negative physical interdependency) (e.g., Ma *et al.*, 2019; Ferrari and Santagata, 2023) or how undisrupted modes can be used to help manage incidents of the disrupted mode (positive physical interdependency) (e.g., Ouyang *et al.*, 2015; Hong *et al.*, 2017; Fang *et al.*, 2022), limited work has been undertaken so far to understand the impact of geographic interdependencies on discrete transport networks.

Therefore, this thesis will focus on the geographic interdependency between discrete transport infrastructure networks and concurrent disruptions of the public transport modes operating on these networks, due to the same rainfall event. Since the nature and extent of geographic interdependencies between networks depend on the spatial scale and intensity of the hazardous event, this study defines 'rainfall-related geographic interdependency' as the simultaneous disruption of transport networks due to their co-location within the spatial footprint of a heavy rainfall event, which can trigger multiple flooding incidents within its spatial scale.

The expected impacts of pluvial flooding are commonly analysed through risk assessment methods. *Risk* is defined as the “potential for adverse consequences” (IPCC, 2022) and

encompasses the probability of the hazardous event occurring and resulting consequences to the system of concern (Liu *et al.*, 2018). The consequences of a pluvial flood event to the transport network reflect its *vulnerability*, which, in indirect terms, is defined as the susceptibility of the network to loss of performance (Berdica, 2002). The framework of flood risk assessment includes estimating the expected consequences of flooding to the transport system for a range of possible event magnitudes, ultimately resulting in a risk curve that captures the expected annual economic costs of flooding-induced disruptions as a function of the hazard intensity (Nicholson and Dalziell, 2003).

The vulnerability of transport networks can also be explored through the resilience assessment framework. *Resilience* is broadly defined as the ability to “absorb and recover from hazard impacts” (White *et al.*, 2005). Bruneau *et al.* (2013) further defined four components of resilience, namely *robustness* (the ability of the system to withstand disruptions); *redundancy* (the availability of multiple elements or options within the system that fulfil the same function); *resourcefulness* (the ability of the system to identify and utilise existing resources to tackle disruptions); and *rapidity* (the capacity of the system to timely restore its operation back to normal). The elements of robustness and redundancy relate to the preparedness of the system to reduce the impacts of anticipated disruptions (ex-ante mitigation), while resourcefulness and rapidity refer to the ability of the system to adapt in order to ultimately manage and timely resolve disruptions when these occur (ex-post adaptation). Figure 1-1 shows the relationship between resilience, its individual components and vulnerability. In this case, vulnerability is considered as the opposite of resilience and it corresponds to the area between the horizontal dotted line and the curve that represents the performance of the system during the disruption conditions (Mattsson and Jenelius, 2015).

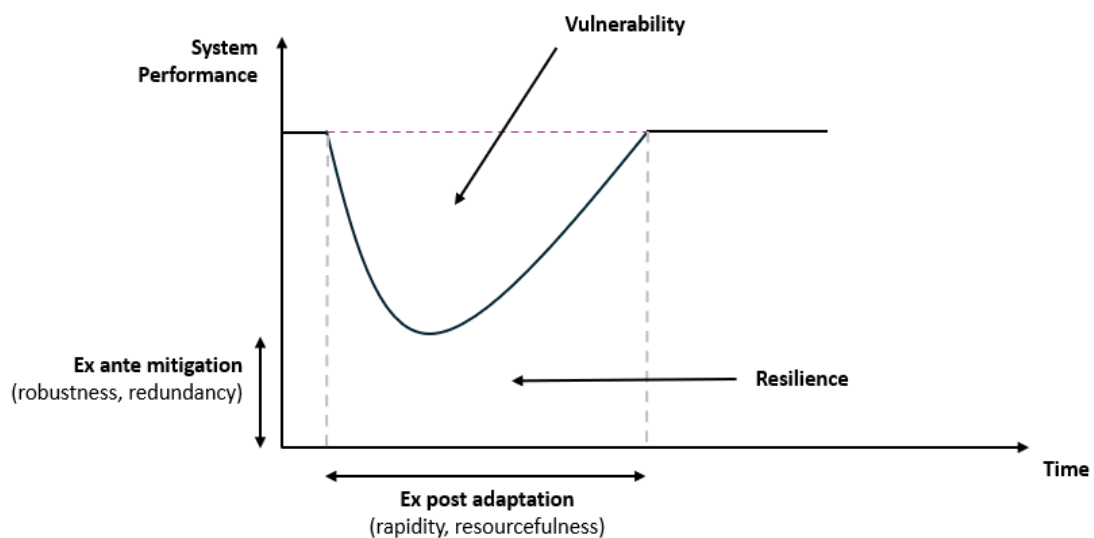


Figure 1-1 The relationship between vulnerability and components of resilience (adapted from Mattsson and Jenelius, 2015)

From the above, it is clear that there is not a universally accepted definition of vulnerability. Specifically, in the resilience assessment framework, vulnerability explicitly considers both the loss of network performance and duration of disruption given the occurrence of a hazardous event. On the other hand, the risk assessment framework places more emphasis on the reduction in network performance and does not explicitly consider the duration of disruptions as part of the vulnerability, although examples also exist which incorporate the duration of disruptions in the risk assessment process (Dalziell and Nicholson, 2001).

The focus of this thesis is on the components of resilience related to the ex-ante mitigation capacity of the system. The time required for the system to restore its functionality is not considered and, thus, vulnerability is here used to describe the susceptibility of public transport networks to loss of performance given the occurrence of flood events. Furthermore, the research on this thesis is specifically concerned with the redundancy of public transport networks rather than their robustness. This is because robustness is a more general concept which reflects the capacity of the system to “maintain its basic functionality under the failure of some of its components” (Klau and Weiskircher, 2004) and, in some cases, it may encompass redundancy as well (e.g., Laporte *et al.* 2011; Liao and van Wee, 2017).

Since the extent of impacts of disruptions on transport networks varies depending on where these occur, considerable work has been undertaken seeking to identify network elements, of which the failure results in the highest losses of network performance (Jenelius *et al.*, 2005). These network elements are defined as *important*. Elements that have a higher probability of failure due to the occurrence of event of concern are considered *weak*, while those that are both weak and important are considered as *critical* (Cats *et al.*, 2016).

The concept of importance has been further defined for areas, which represent the spatial scale of the hazard. Therefore, areas where the occurrence of the hazard inflicts the most significant impacts on the performance of network, are considered as *important* (Johansson and Hassel, 2010). Based on the abovementioned definitions, it can be argued that identifying important and critical elements is appropriate when exploring impacts of events that may directly affect only one element of the network at a time (e.g., one link or station), while it is more pertinent to identify important areas when assessing area-wide events, which typically relate to severe weather.

Although much work has been done to identify important elements of transport networks (Jenelius *et al.*, 2006; Taylor *et al.*, 2006; Rodriguez-Nunez and Garcia-Palomares, 2014; Cats and Jenelius, 2014), studies on the assessment of their weakness or criticality are much scarcer, mostly because of the limited availability of historical data that may allow estimating them (Cats *et al.*, 2016). Furthermore, for area-wide events, only a few studies have been proposed for transport networks (Jenelius and Mattsson, 2012; Schintler *et al.*, 2007; Thacker *et al.*, 2017). Therefore, the importance of areas that contain multiple transport infrastructure networks and where geographic interdependencies between them may occur, has not been appropriately assessed. Finally, as the spatial scale of an event depends on the nature and severity of the hazard of concern, the assessment of importance should make sensible selection of the size of areas that represent the event footprint. However, most works to date have developed general frameworks for the vulnerability assessment of networks to area-wide events and, as such, arbitrarily select their potential scale (e.g., Mattsson and Jenelius, 2012; Ouyang *et al.*, 2019; Du *et al.*, 2023; Kays *et al.*, 2023).

The exposure of heavy rainfall on infrastructure networks is estimated using flood maps that show the spatial extent, location and depth of floodwater across the area of interest. However, these maps cannot be used to estimate the impacts of flooding-related geographic

interdependencies between infrastructure networks, as they do not capture the temporal propagation of rainfall and, thus, they do not indicate which locations may experience flooding at the same time. A commonly used approach to estimate the impact of concurrent rainfall-induced flood events to transport networks on the urban or sub-urban scale involves modelling the occurrence and propagation of a design rainfall event at a hydrological catchment, which is produced using a stochastic rainfall generator, and subsequently using a hydrological model to estimate the resulting flood flows over the area of interest at various time steps (e.g., Pregolato *et al.*, 2015; Pyatkova *et al.*, 2019). According to Brunner *et al.* (2020), an alternative approach to model concurrent pluvial flood events over an area requires the use of spatial extreme value models predicting the intensity and duration of rainfall events of certain frequencies, which also account for the conditional probability of extreme values being observed in spatially separated locations (e.g., Hefferman and Tawn, 2004; Renard and Lang, 2007; Le *et al.*, 2018). However, it is not always possible to use these sophisticated approaches either because of the unavailability of appropriate rainfall and/or hydrological models for the area of interest, or because of the significant computational requirements to perform these processes for larger areas.

The aim of this thesis is to assess the vulnerability of geographically interdependent public transport modes that operate on discrete transport infrastructure networks to area-wide events, with a particular focus on heavy rainfall.

For the purposes of this thesis, a literature review was conducted on research works seeking to estimate the current and future spatial scales of rainfall (Section 1.2.1). In addition, a literature review on the vulnerability of transport networks to disruptions (Sections 1.2.2), including to area-wide events (Section 1.2.3) has been carried out in order to identify important gaps that will be addressed as part of this research.

1.2. Background

1.2.1. Spatial extent of rainfall events and estimated impacts of climate change

In the past years, the adverse impacts of precipitation and flooding on societies have resulted in growing efforts to estimate the spatial scale of rainfall events in various areas globally, and how this may change as temperatures increase due to human-caused climate change. Notable

works have been undertaken on this area of research, which are further summarised in Table 1-2.

Lochbihler *et al.* (2017) investigated the spatial properties of convective precipitation, which typically relates to high-intensity and short-duration rainfall events, and showed that most events span up to 4 km and only a few of them may extend up to 12 km. Touma *et al.* (2018) investigated the spatial extent of daily extreme rainfall over the United States and how it varies seasonally and regionally. The results of this work revealed significant variations across the regions and seasons, with the longest length scales of rainfall and greatest regional variations being observed in winter. Gvozdikova *et al.* (2019) explored rainfall patterns for a wider geographical area, as their work focused on 1-day to 10-day rainfall totals in central Europe. The authors found that heavy rainfall can simultaneously affect river sub-catchments located in distant regions with similar topography and showed that the maximum size of areas affected can potentially be up to 100,000 km². Lengfeld *et al.* (2019) analysed the spatial extent of daily and hourly rainfall events in Germany and revealed that the footprint of the former is significantly larger compared to the latter.

These works assess the spatial scale of historical rainfall events and do not consider the effects of climate change to the spatial properties of precipitation. Several studies have been undertaken to fill this gap, which, however, have provided conflicting results. Guinard *et al.* (2015) explored various characteristics of rainfall events in North America, including spatial area, and their potential changes due to climate change. They found that spatial areas did not exhibit any statistically significant changes in the future. Chang *et al.* (2016) assessed the change in spatial extent of rainfall in the United States and found that the extent of precipitation events becomes smaller in both winter and summer. Similarly, Wasko *et al.* (2016) found that in a warming climate, the rainfall events in Australia are anticipated to increase in magnitude and shrink spatially, and thus, are expected to be more intense and concentrated. Lochbihler *et al.* (2019) performed climate simulations to understand the effect of increased temperatures to the spatial scale of summer convective rainfall in the Netherlands and, as opposed to the previous studies, revealed that future conditions associated with higher temperatures and moisture will lead to both higher intensities and spatial extents of events.

Matte *et al.* (2021) analysed the change in spatial extent of the most extreme precipitation events in Europe for different levels of global warming, namely 1°C, 2°C and 3°C. The authors concluded that temperatures and spatial extents of events are positively correlated and that 20-year rainfall events will become more frequent and widespread at the expense of smaller events. In a similar direction, Bevacqua *et al.* (2021) found that the rainfall events in the Northern Hemisphere extratropics, including parts of North America, Europe and east-central Asia, will exhibit significant increases in their spatial extents and highlighted that increased global temperatures at 2°C may lead to disproportionately higher increases in the spatial scales of rainfall events compared to those at 1.5°C. Considering these contradictory results, with a view to obtain more comprehensive insights of the anticipated changes of scale of rainfall events, Ghanghas *et al.* (2023) performed a global assessment which revealed that the impact of climate change on the spatial extent of rainfall significantly varies across the globe, with reduced extents being anticipated only in tropical regions and significant increases in arid regions and in central Europe.

The above literature reviewed shows that, although there is no consensus on the expected changes of spatial footprint of rainfall due to climate change, the range of spatial extents in current conditions is well-documented, as shown in Table 1-2. However, to the author's knowledge, this evidence has not been used in the context of resilience assessments of infrastructure networks.

Table 1-2 Studies assessing the spatial scale of rainfall events and potential changes due to climate change

Reference	Scale of analysis	Location	Study period	Rainfall event	Spatial scale of rainfall*	
					Current conditions	Future changes
Lochgbihler <i>et al.</i> (2017)	National	Netherlands	2008 to 2016	Convective, summer rainfall.	Up to 12 km.	
Touma <i>et al.</i> (2018)	National	United States	1965 to 2014	Extreme daily rainfall (above 90 th percentile) (winter and summer).	eastern US: up to 400 km in winter and 200 km in summer. northern US: up to 150 km throughout the year.	
Gvodzikova <i>et al.</i> (2019)	International	Central Europe	1961 to 2013	Extreme 1-day to 10-day rainfall (winter and summer).	Up to 100,000 km ² .	
Lengfeld <i>et al.</i> (2019)	National	Germany	2001 to 2017	Daily and hourly rainfall.	On average 68 km for daily events, and 17 km for hourly.	
Guinard <i>et al.</i> (2015)	Continental	North America	1961 to 1990, 1992 to 2011 & 2071 to 2100	Rainfall events with intensity greater than 0.2 mm/hr.	2·10 ⁴ to 7·10 ⁴ km ² .	No change.
Wasko <i>et al.</i> (2016)	National	Australia		Extreme 1hr and 3hr rainfall at higher temperatures	Up to 50 km below 18°C and 30 km above 35°C.	Reduced extent of (degree of reduction)

				(above 90 th percentile).		depends on location).
Chang <i>et al.</i> (2016)	National	United States	1995 to 2004 & 2085 to 2094	Rainfall intensity than (summer and winter).	with greater than 1mm/3h and	2·10 ⁴ to 8·10 ⁴ km ² in summer, and 5·10 ⁴ to 50·10 ⁴ km ² in winter. Reduced extent (up to 80% in summer and 40% in winter).
Lochbihler <i>et al.</i> (2019)	National	Netherlands		Convective rainfall with intensity greater than 0.6 mm/hr (summer).		Up to 12 km. Increased extent (estimated value up to 20 km).
Matte <i>et al.</i> (2021)	Continental	Europe		Daily rainfall (above 90 th and 99 th percentiles).	extreme events	Up to 512 km. Increased extent of large events.
Bevacqua <i>et al.</i> (2021)	Intercontinental	Northern Hemisphere extratropics		Wintertime rainfall (return greater than 10 years).	extreme events period greater than 10 years).	Varies based on location (e.g., a 100-year event in UK, may span between 900 and 1300 km, while 100 to 300 km in France). Increased extent in most areas. E.g., up to 190% in Northern Europe and 250% in central-east Asia.
Ghanghas <i>et al.</i> (2023)	Global		2014 to 2021	Short duration, extreme rainfall.		Reduced extent in tropics.

Increased extent
in arid regions
and parts of
central Europe.

*Spatial extent of rainfall is reported in terms of area (km²) or length scale of event (km). The latter is equal to the squared root of the former.

1.2.2. Vulnerability assessment of public transport networks to disruptions

The vulnerability assessment of transportation networks aims to identify parts of the network, of which the failure leads to the most significant consequences to the network performance and, thus, are considered the most important to the functionality of the network. The approaches to test the vulnerability of transport networks, including public transport, can be classified into two distinct categories, namely topological and system-based (Mattsson and Jenelius, 2015). In both these approaches, the public transport system is represented by a graph consisting of nodes and links, where the former typically correspond to public transport stops (or stations), and the latter refer to linear infrastructure (e.g., roads, rail tracks) connecting nodes served by a public transport route.

The topological vulnerability assessment seeks to identify important elements of the network (links or nodes), which, if failed, result in the greatest degradation of its topology. For instance, an indicator used to measure network topology is global efficiency, which is the average value of reciprocals of the path distances between all node pairs of the network (Latora and Marchiori, 2001). On the other hand, the system-based approach incorporates functional properties of the system in the network representation and adopted methods can be further classified into accessibility-based and serviceability-based.

Accessibility-based methods analyse the vulnerability in terms of the changes in the level of accessibility of locations, which reflects the “the extent to which land use and transport systems enable (groups of) individuals to reach activities or destinations” (Geurs and van Wee, 2004). In this case, the vulnerability assessment seeks to identify the network elements, of which the failure inflicts the highest losses of accessibility, such as in terms of travel time or distance (D’Este and Taylor, 2003). While the serviceability-based approach may partly assess vulnerability in terms of change in travel time, it places more emphasis on the demand-side of transport system. For example, this is done by considering the passenger flows across the various routes of the network and using sophisticated tools to capture congestion effects of disruption on parts of the network (Taylor, 2017). In this case, vulnerability

may also be perceived in terms of number of passengers that experience delays or those that cannot complete their trips due to disruptions (unsatisfied demand).

Topological vulnerability assessment

Topological vulnerability is assessed in terms of network connectedness and is typically measured by successively removing a node or link of the network, at random or based on a certain attack strategy, until the network becomes completely disintegrated. Topological importance metrics of elements are used to identify these attack strategies, examples being the degree of node, which is equal to the number of links directly connected to the node; betweenness centrality of node, which is the number of shortest paths between each two pair of nodes traversing the node of concern; and betweenness centrality of link, i.e. the number of shortest paths traversing the link of concern.

Extensive research has been devoted to analysing the vulnerability of public transport networks to disruptions from a topological standpoint. Han and Liu (2009) assessed the vulnerability of ten Chinese subway systems to random or intentional attacks. Separate scenarios were developed where nodes representing subway stations were successively removed based on their degree or betweenness centrality. For some of these scenarios, at each removal step, the degree or betweenness centrality value of the nodes remained the same (static approach), while, for others, it was recalculated (dynamic approach). Across all these scenarios, nodes were removed until the relative size of the largest component of the network that remained connected fell below a predefined threshold. Using the same approach, Wang *et al.* (2015) studied the vulnerability of 33 metro networks by removing nodes at random or based on their degree values. Cats and Krishnakumari (2020) assessed and compared the vulnerability of three metropolitan networks by removing both nodes and links at random or based on their dynamic degree and betweenness centrality values. The effects to all lines traversing the disrupted nodes or links were assessed by removing them to account for cascading impacts to the operation of

services, and then the impact of disruptions was assessed in terms of the relative size of the largest component of network remaining connected (proxy for passengers' ability to travel), but also in terms of the normalised average shortest path between each pair of nodes (proxy for detours incurred). A similar study was conducted by Cao and Cao (2020), albeit for the urban bus network.

The aforementioned studies explore the topological vulnerability of networks consisting of only one mode and thus provide partial insights on the topology of the multimodal public transport network. Several notable studies have focused on the analysis of multiple public transport modes. Berche *et al.* (2009) studied the vulnerability of fourteen multimodal public transport networks subject to random disruptions and intentional attacks to nodes and assessed the impacts in terms of global efficiency and the relative size of largest component of network remaining connected. The modes considered included bus, tramway, trolleybus, subway and urban train. This work was further extended to assess the vulnerability based on the removal of both links and nodes (Berche *et al.*, 2012). Aparicio *et al.* (2022) adopted a similar approach for the vulnerability of the network consisting of tram, metro, bus, rail and riverway, and further considered consequences to the public transport lines traversing the removed elements in a similar way to that of Cats and Krishnakumari (2020). The impacts of disruptions were assessed in terms of several metrics, namely average path length between nodes, number of isolated network components and size of largest connected component.

Although these works considered the vulnerability of multiple public transport modes, they overlooked interdependencies between them. Very limited research has been carried out to incorporate the interdependencies between modes into the topological assessment of vulnerability. Ferrari and Santagata (2023) incorporated the geographical and functional interdependency between the regional rail and road networks within the vulnerability assessment. The former interdependency was captured by nodes that represent overpasses between networks, e.g. motorway bridges overpassing the rail network, while the latter as inter-links between motorway exits and rail stations where modal shifts can take place. The vulnerability

of the multimodal network was then assessed by measuring the number of nodes required to be removed until the network collapses. By repeating the process for each single network and comparing it to that of the interdependent networks, the impact of interdependencies on the vulnerability was estimated, and important nodes and links of the interdependent networks were identified according to the severity of impacts of their removal.

Xu *et al.* (2024) assessed the vulnerability of the urban multimodal network consisting of bus and rail, while also considering both positive and negative functional interdependencies, where the former pertain to neighbouring stops that can be accessed by walking or bicycle, while the latter correspond to failures that progressively cascade to neighbouring stops. These studies showed that it is imperative to consider interdependencies between disrupted networks as this allows identifying nodes and links of the network, of which the failure results in greater consequences than it was previously thought because of concurrent and propagating disruptions.

System-based vulnerability assessment

Similarly with the topological assessment, the system-based approach of vulnerability assessment involves removing nodes or links of the network and estimating the consequences of their failure to the performance of the network. Two system-based approaches exist for the identification of important nodes or links. In the first method, known as full-scan approach, each network element is separately failed, and the resulting vulnerability is estimated in terms of reductions in network performance. Because this process is resource-intensive, the second approach is particularly favourable for large-scale networks.

The second approach a priori characterises the importance of network elements based on performance-based metrics and then filters only the most important ones for the next step of the process where the vulnerability of the network to their failure is computed. The most common metrics of system-based importance are the

passengers betweenness centrality of links, which reflects the percentage of the total passengers that use a public transport link, and operators betweenness centrality, which denotes the percentage of total public transport trips that traverse the link (Cats and Jenelius, 2014).

In the past decade, the literature on the system-based vulnerability assessment of public transport networks has increased considerably. Using real-world data on public transport trips and adopting a full-scan approach, Rodríguez-Núñez and García-Palomares (2014) measured the vulnerability of the metro network of Madrid by removing one metro link at a time and measuring the disruption consequences in terms of number of cancelled trips and increase in travel times, thus revealing the most important links of the network. Shelat and Cats (2017) assessed the vulnerability of the urban rail network to link failures in terms of the potential for propagation of disruption resulting from passengers choosing alternative routes. These knock-on effects were captured in terms of congestion on trains and denied boarding of travellers at stations. By adopting a full-scan approach, the rail links were ranked based on the extent of knock-on effects that their failure may induce to the network.

Adjetey-Bajun *et al.* (2016) assessed the system-based vulnerability of the urban rail network by further considering its physical interdependencies with other systems, namely power, telecommunication and organisation. To achieve this, a detailed representation of each network was constructed as well as the interrelationships between them. Disruptions on power network were then considered that cascaded to rail by causing either speed reductions of trains or complete closure of links. Pant *et al.* (2016) performed a national vulnerability assessment of the rail network while considering both its physical and geographic interdependencies with the electricity and telecommunication networks. The former interdependencies reflect dependencies of rail assets with assets of other infrastructure networks, such as signalling, lighting, and monitoring systems, and were captured using inter-links between them. The latter interdependencies were identified for a specific flood scenario by identifying the flooded assets of the three networks and then assessing

the vulnerability of rail to these failures. By considering the physical and geographic interdependencies of rail with other networks, more realistic insights into the susceptible parts of former were provided.

Although some of the above works go beyond exploring the effects of a single disruption to the public transport network, e.g. by assessing cascading or concurrent failures of network elements, they focus on one individual public transport mode. Notable studies have been carried out to test the system-based vulnerability of multimodal public transport networks as well. Cats and Jenelius (2014) proposed a novel dynamic and stochastic representation of the multimodal public transport network that captures the interaction between system supply and passenger demand and assessed its vulnerability to disruptions of links. Rather than performing a full-scan analysis, potentially important links were initially identified based on the passenger and operators' betweenness centrality value of links, and the impacts of their disruptions were estimated in terms of a composite index that encompasses passengers' travel time and transfers between services. Using the same dynamic and stochastic approach, Cats and Jenelius (2015) explored strategies to reduce vulnerability of the multimodal network by increasing the capacity on lines that can serve as alternatives when important links are disrupted.

In both of these studies, the approach adopted allowed modelling in more realistic terms the progression and impacts of disruptions, thus revealing useful insights into their cascading effects to modes. However, the interdependencies between the individual modes that make up the network were not explicitly explored. Hong *et al.* (2019) proposed a method to study the vulnerability of the integrated bus and subway network from the perspective of accessibility to critical services, such as commercial and education services. The positive interdependencies between the modes were represented by inter-links between geographically proximate stations to account for passengers' potential modal shift in the event of disruptions. Various types of disruption were considered to the bus network, namely random, degree-based and betweenness-based failures, as well as flood events according to the flood map of a historical event. Similar works that considered these interdependencies

were those of Ouyang *et al.* (2015) and Wang *et al.* (2023). Apart from positive interdependencies, Zhang *et al.* (2023) further assessed the geographic interdependency between individual modes of the national transport network by estimating the impacts on travel time of concurrent disruptions to all elements within the province that a historical storm event occurred.

Gaps in the literature of vulnerability assessment of public transport networks

The above literature on the vulnerability assessment of public transport networks reveals several important gaps. Firstly, in both topological and system-based approaches, most works to date have focused on the vulnerability of a single public transport mode, typically railway, while bus remains largely under-explored. Secondly, studies on the multimodal public transport networks have mostly assessed the physical interdependencies between various modes, either from a positive perspective (modal shift of passenger demand) or negative (cascading disruptions); however, the disruptions considered directly affect only one mode, while the other either remains completely unaffected or suffers disruptions due to cascading effects. Therefore, the geographic interdependency between public transport modes that operate on discrete networks has not been analysed so far. Lastly, most works on vulnerability assessment to date have analysed urban public transport networks, while research on inter-city and national networks that are used for long-distance travel is much scarcer. Consequently, the implications of disruptions, and particularly those relating to the geographic interdependency between modes, to the operation of transport systems at the national scale is still lacking.

1.2.3. Vulnerability assessment of transport networks to area-wide events

Since the geographic interdependencies between networks occur as a result of man-made or natural hazards that may affect geographical areas, it is important to understand the degree to which the vulnerability of transportation networks to area-wide disruptions has been explored and how these disruptions are captured.

Similarly with the network vulnerability of single-link and single-node failures, the aim of the vulnerability assessment to area-wide events is to identify areas, where, if the event occurs (and consequently all network links and nodes located within are failed), the degradation of the network performance is the most severe (Johansson and Hassel, 2010).

Several works on the vulnerability analysis to spatial events have been identified in the literature. Jenelius and Mattsson (2012) assessed the vulnerability of the Swedish regional road network to area-covering disruptions using an impact-based approach, commonly referred to as the cell space method (Johansson and Hassel, 2010; Ouyang, 2015). The spatial events were captured by cells of a square grid, which was superimposed on the network. By failing one grid cell at a time and assuming that all road links located in or traversing the cell are closed, the consequences of the cell-wide failures to the network performance were estimated. Similarly with the full-scan approach, by repeating the process for all cells, the most important areas (cells) were identified. The analysis was performed for various grid sizes, namely 12.5x12.5 km², 25x25 km² and 50x50 km² and revealed that the cell size has a significant effect on the results. Du *et al.* (2023) adopted the same approach to test the vulnerability of urban road networks in China, but for significantly smaller sizes of square cells, namely 1x1 km², 2x2 km² and 4x4 km², therefore focusing on considerably more localised events.

Another approach was developed by Ouyang *et al.* (2019), who proposed three types of spatially localised disruptions, namely node-centred, district-based and circle-based, and applied them to the Chinese rail network. In the node-centred event, a certain node is assumed to be disrupted and a specified fraction of nodes that have the nearest distance from this disrupted node are further considered to have concurrently failed. The district-based event is defined by administrative boundaries (e.g., province, county), while the circle-based event pertains to a disruption occurring in a circular area of a certain radius, anywhere on the network. According to the authors, the node-centred and circle-based events are applicable to intentional attacks, whilst the district-based event pertains to localised natural

hazards. Similarly with the cell-space method, the process involved assuming the occurrence of an event of a certain extent at a given part of the network and thus all nodes and links within the footprint of event are closed, and subsequently computing the consequences of these failures to the network performance.

Li *et al.* (2019) adopted the circle-based model proposed by Ouyang *et al.* (2019) to assess the vulnerability of the coupled high-speed rail and air transport system of China in order to ultimately determine the most important circle-based areas. Areas of various circular sizes were applied, with the considered radius ranging from 10 km to 500 km. Fang *et al.* (2020) analysed the vulnerability of the high-speed rail to province-based disruptions due to geological and hydrological events. The authors extended the work of Ouyang *et al.* (2019) by exploring the possibility of discrete area-wide events occurring simultaneously, which was achieved by initially establishing the natural disaster probability of each province based on historic data and subsequently developing multiple scenarios of concurrent province-based disruptions using Monte-Carlo simulations.

The aforementioned works explored the vulnerability of transport networks to spatial events using impact-based approaches, which require carrying out multiple disruption scenarios in order to identify important areas. This may prove to be a very resource-intensive task for large-scale networks. In the absence of non-impact-based approaches focusing on transport only, several works were identified that explored the impact of spatial events on the geographic interdependency between transport and other critical infrastructure networks. Schintler *et al.* (2007) identified important areas in the multimodal transportation network consisting of roads and railway by estimating the importance of links based on the number of shortest paths traversing them and performing spatial density analysis to create a continuous raster surface, which captures the importance of co-located railway and road links. Thacker *et al.* (2017) assessed the vulnerability of multiple national infrastructure networks, including road and rail, while considering the proximity between their assets. The importance of nodes of each network was estimated based on a disruption metric that reflects the number of direct and indirect users of the node, and areas containing

clusters of highly important nodes (hotspots) were identified. This was achieved using kernel density estimation, which provided a map showing the density of assets weighted by their importance value over the study area. Kays *et al.* (2023) assessed the vulnerability stemming from the geographic interdependency between the road and stormwater networks by computing the importance of each link and subsequently identifying areas with co-located important road and stormwater links using autocorrelation metrics. With a primary focus on the road network, Hughes *et al.* (2020) analysed the geographic interdependency between road links and links of the power, water and wastewater networks, by delineating buffer-based neighbourhoods around each road. By comparing the importance of the road to that of its corresponding buffer, which includes the road itself and neighbouring assets, the effect of geographic interdependencies to vulnerability was explored. The same buffer-based approach was also used by Islam and Moselhi (2012) to estimate the extent to which assets of the road and water network are geographically interdependent.

Gaps in the literature of vulnerability assessment of transport networks to area-wide events

This review of studies developing general models and frameworks to assess the vulnerability of transport networks to area-wide events revealed several gaps. Firstly, while the impact of area-wide disruptions on transportation networks has been explored, in most cases, only one transport mode has been considered at a time, namely road or rail. No study was identified that explores the concurrent impact of spatial events on multiple public transport modes, such as rail and bus. Secondly, while a range of approaches has been proposed to test the area-wide vulnerability of transport networks, consideration was given only to the shape of area affected, such as square and circular areas, while the spatial footprint of events was arbitrarily set without considering the nature of hazards that it corresponds to. While these approaches are accompanied by sensitivity analysis of the vulnerability for various sizes of areas, no effort has been made so far to relate area size to a specific hazard,

and, therefore, it is not clear how these approaches can be made hazard-specific. This could be achieved by performing empirical research to link general vulnerability assessments with historical evidence on spatial scale of events.

Furthermore, with the exception of the work of Fang *et al.* (2020), none of these studies considered the probability of concurrent events occurring and thus only important areas can be derived from the approaches proposed to date. Specifically, in the case of pluvial flooding, this limitation could be systematically overcome with the aid of pluvial flood maps that show the water depth and extent and extent for a certain return period on the network (or networks). However, as previously mentioned in Section 1.1, these maps may capture concurrent flood events only when they have been produced using a stochastic rainfall generator and flood model or using intensity-duration-frequency curves for rainfall events whilst accounting for the conditional probabilities of rainfall co-occurrences across the area.

1.3. Research aim and objectives

As previously stated in Section 1.1, this thesis aims to assess the resilience of geographically interdependent public transport modes that operate on discrete transport infrastructure networks to area-wide events, with a particular focus on flooding.

The literature review carried out in the previous sections identified several significant gaps. These include:

1. The potential impact of geographic interdependencies that may arise from area-wide events (including rainfall) on the resilience of public transport modes operating on discrete infrastructure networks and how this may vary depending on the spatial extent of events.
2. The empirical assessment of geographic interdependencies that may occur between discrete infrastructure networks due to a weather-related hazardous event and exploring their impact on the importance and criticality assessment of public transport modes operating on these networks.

3. Modelling the extent of weather-related geographic interdependencies between transport networks and incorporating it to the importance assessment of interdependent public transport modes, for a certain hazard of interest – in this case, rainfall.

Therefore, the research aim is further divided into a number of research objectives, which will enable to answer key research questions and ultimately address the three aforementioned gaps, as shown in Table 1-3.

Table 1-3 Identification of research questions and objectives

Research question	Research objective	Chapter
RQ1. How can redundancy be quantified for geographically interdependent public transport networks?	OBJ1.1. Review metrics proposed in the existing literature that quantify the redundancy of travel options between locations.	2
RQ2. How can the geographic interdependency between transport networks be quantified for various hazards?	OBJ2.1. Review how geographic interdependencies have been previously quantified. OBJ2.2. Propose a metric that captures the geographic interdependency between networks.	2
RQ3. What are the implications of geographic interdependencies between public transport modes on the redundancy, and how do they vary based on the spatial extent of area-wide events?	OBJ3.1. Incorporate metric of geographic interdependencies between networks into selected metrics of redundancy. OBJ3.2. Develop a general framework to analyse the impact of geographic interdependencies on the redundancy due to area-wide hazardous events. OBJ3.3. Perform sensitivity analysis to assess how the loss of redundancy changes for varying spatial scales of hazardous events.	2

<p>RQ4. How can the importance and criticality of public transport links be quantified?</p>	<p>OBJ4.1. Review metrics that capture the importance and criticality of transport links.</p>	<p>3</p>
<p>RQ5. How can the rainfall-related geographic interdependencies between transport infrastructure networks be empirically characterised?</p>	<p>OBJ5.1. Review and select method to quantify the likelihood of simultaneous events occurring based on the separation distance of locations.</p> <p>OBJ5.2. Identify the data requirements for the empirical estimation of flooding-related geographic interdependencies and construct datasets for the public transport networks of concern.</p>	<p>3</p>
<p>RQ6. What is the impact of the geographic interdependency between networks on the importance and criticality of public transport links?</p>	<p>OBJ6.1. Incorporate the empirical extent of geographic interdependencies into the selected metrics of importance and criticality of public transport links.</p> <p>OBJ6.2. Compute link importance and criticality with and without considering geographic interdependencies and compare ranking of links in these two cases.</p>	<p>3</p>

<p>RQ7. What is the current state-of-the-art on assessing the risk of transport networks to concurrent rainfall-related flood events?</p>	<p>OBJ7.1. Review the literature that seeks to quantify and assess the risk of transport networks to flood events.</p>	<p>4</p>
<p>RQ8. How can the rainfall-related geographic interdependencies between transport modes be modelled?</p>	<p>OBJ8.1. Select a method to model the likelihood of concurrent rainfall-induced flood events occurring at spatially proximate locations.</p>	<p>4</p>
<p>RQ9. How can the model of rainfall-related geographic interdependency be incorporated into the pluvial flood impact assessment of discrete public transport networks?</p>	<p>OBJ9.1. Propose a framework for the development of scenarios of concurrent pluvial flood events and incorporate them into the impact assessment.</p> <p>OBJ9.2. Compute losses in redundancy for pluvial flood scenarios with and without considering concurrency of events in geographically interdependent public transport networks.</p>	<p>4</p>

1.4. Structure of Thesis

With a view to produce and submit three separate papers for publication in academic journals, three discrete studies were carried out, which are reported in Chapters 2, 3 and 4 of this PhD thesis.

Therefore, this thesis is divided into five chapters. Chapter 1 includes the introduction and review of key literature that informed the identification of gaps in research.

Chapter 2 presents a general framework for the assessment of the impact of geographic interdependencies between public transport modes operating on separate infrastructure networks on components of resilience, namely redundancy and substitutability of travel options. The method adopts an accessibility-based concept of resilience and is applied to the Scottish long-distance bus and railway networks.

In Chapter 3, an empirical method to assess the impact of geographic interdependencies between public transport modes on the importance and criticality of links is reported. Historical data of flood incidents are used in order to derive information on the characteristics of the hazard of concern – in this case, rainfall – that are typically ignored in the vulnerability assessment of transport networks to area-wide disruptions. The method uses a topological approach and is again applied to the Scottish long-distance bus and railway networks.

Chapter 4 presents a method to systematically assess the concurrent impacts of extreme rainfall events on the accessibility of locations offered by interdependent public transport networks by considering the spatial dependence structure of flooding-producing rainfall co-occurrences. The method identified important links from an impact-based perspective and takes a similar accessibility-based approach as that of Chapter 2. The analysis is applied to the Scottish rail network which may be substituted by long-distance bus services.

Finally, Chapter 5 includes the general conclusions drawn from this thesis, contributions of research to the academic theory as well as practice, along with directions of future research.

2. Incorporating geographic interdependencies into the resilience assessment of multimodal public transport networks

This chapter addresses the first objective of the thesis, which is to explore the potential consequences of geographic interdependencies due to weather-related events on the resilience of public transport modes operating on discrete infrastructure networks and how these consequences may vary depending on the spatial extent of events. As such, this chapter introduces a general framework for the evaluation of potential concurrent impacts of area-wide events on travel options offered by two discrete public transport modes and the implications of these impacts to the connectivity of locations. This chapter lays the foundation for the subsequent analyses in Chapters 3 and 4 by providing an approach to quantify geographic interdependencies between public transport modes and to incorporate these into metrics of network vulnerability.

Note that this chapter has been published in the *Journal of Transport Geography* as follows: Boura, G. and Ferguson, N. S. (2024) "Incorporating geographic interdependencies into the resilience assessment of multimodal public transport networks". *Journal of Transport Geography*, 118, 12 p., 103934.

2.1. Introduction

The effective functioning of the public transport system is placed at risk by naturally-occurring, spatially-defined events such as earthquakes, rainfall, flooding and landslides. These events have the capacity to disrupt transport infrastructure and, in areas affected by such events, discrete transport networks carrying separate public transport modes (e.g. railway and bus) are at risk of concurrent disruption. For example, heavy snowfall in March 2018 caused widespread railway and road closures in Scotland affecting train and bus services (Network Rail, 2020). More recently, in July 2021, heavy and prolonged rainfall caused extensive flooding in central Germany and Belgium, leading to damage of railway lines, roads and bridges (Fathom Global,

2021). Human-caused climate change is expected to intensify and alter patterns of extreme weather around the world in the coming decades, including increases in heavy precipitation, flooding and heat, thereby increasing the risk of transport disruption (Lee *et al.*, 2023).

As mentioned in Section 1.1, infrastructure networks which are located in close proximity to each other are said to be geographically (or spatially) interdependent if a hazardous event can disrupt both networks at the same time (Rinaldi *et al.*, 2001; Zimmerman, 2004; Dudenhoeffer *et al.*, 2006). As such, discrete public transport networks located in corridors defined by the natural landscape or built environment are particularly susceptible to concurrent disruption. From the public transport users' perspective, geographical interdependency reduces the added benefit of flexibility which exists when more than one transport mode is available.

Redundancy is a key component of transport system resilience (Bruneau *et al.*, 2003) and in its simplest form is equal to the total number of (feasible) options, such as paths and transport modes, which exist between locations (Berdica, 2002). By weighting each option by a function of travel deterrence, a generalised measure of redundancy is obtained which is equivalent to established measures of accessibility (Ben-Akiva and Lerman, 1985; Anas, 1983; Xi *et al.*, 2018). High levels of redundancy help maintain connectivity between locations in the event of disruption. However, it is also evident that spatially-defined events may reduce redundancy in geographically interdependent systems. Although a number of studies have considered the redundancy of single and multimodal networks with shared infrastructure (e.g. Frappier *et al.*, 2018; Liao and van Wee, 2017), and whilst there is a growing body of research addressing geographical interdependencies between civil infrastructure systems (Patterson and Apostolakis, 2007; Johansson and Hassel, 2010; Pant *et al.*, 2016; Thacker *et al.*, 2017; Kays *et al.*, 2023), to the authors' knowledge there has been no attention paid to the effect of geographical interdependencies on the redundancy of discrete transport networks carrying separate public transport modes.

Recently the concept of substitutability was introduced into the literature (van Wee *et al.*, 2019). Substitutability is defined as the level of accessibility which is preserved in the event of the unavailability of a preferred option and reflects the capacity of the transport system to absorb the impact of disruptive events. As with redundancy, the level of substitutability will be reduced as a result of geographical interdependencies between public transport modes. A comparison of the concepts of redundancy and substitutability, with and without consideration of geographical interdependency, is given in Figure 2-1. Whilst the attractiveness of preferred option (A) relative to the attractiveness of other options (B, C and D) does not affect the level of redundancy (or accessibility) offered by the set of options, it does affect the level of substitutability. Consequently, it is argued that both redundancy and substitutability can give important and complementary insights into public transport system resilience when considered within an accessibility framework.

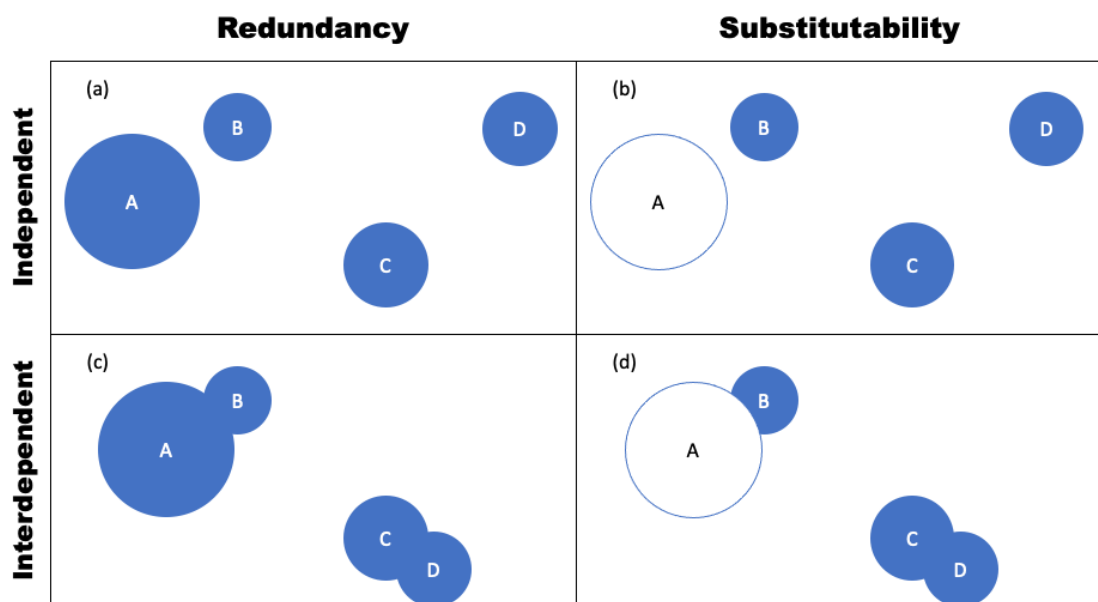


Figure 2-1 Comparison of redundancy and substitutability, with and without geographical interdependency. All figures show a choice set containing a total of four options (A-D) which is equal to the unweighted redundancy of options. The size of options indicates the attractiveness of each option; thus, Option A is the preferred option. The intersection of options $A \cap B$ plus $C \cap D$ is the degree of geographical interdependency in each choice set. In Figures 1(a) and 1(c), the sum of weighted options ($A \cup B \cup C \cup D$) is the weighted redundancy which is equivalent to the accessibility presented by the options. In Figures

1(b) and 1(d), Option A is unavailable, thus the remaining accessibility is equal to $((A' \cap B) \cup (CUD))$ which is the substitutability of each choice set.

Redundancy and substitutability are closely related to but distinct from the robustness of a transport system which reflects its capacity to withstand an adverse event without disproportionate consequences (Bruneau *et al.*, 2003). Thus, they contribute to robustness (Agarwal, 2015; van Wee *et al.*, 2019) and are, by extension, negatively correlated to vulnerability. As presented in Section 1.2.2, previous studies have assessed the vulnerability of single and multimodal transport systems in terms of loss in network performance (from a topological or system-based perspective) resulting from infrastructure failures, typically by removing one network component at a time to identify the most important components (Rodriguez-Nunez and Garcia-Palomarez, 2014; Cats and Jenelius, 2014; Mattsson and Jenelius, 2015). Building on this concept, the cell-space method assesses the vulnerability of geographically interdependent networks to spatially-defined events by overlaying them with a grid and computing the impact of infrastructure failures within each cell (Johansson and Hassel, 2010; Ouyang, 2014).

Whilst transport vulnerability has been comprehensively researched in recent years, these studies often reveal issues stemming from a lack of system redundancy. Therefore, gaining insight into the redundancy (and substitutability) of a system has the potential to shed light on the root cause of these issues and to identify key areas for improvement. Methodologically, vulnerability studies require the development of disruption scenarios with which to test the network whereas redundancy analyses do not require any prior assumption of disruption. Moreover, these scenarios are predominately based on the failure of single links (or adjacent links within defined cells) whereas redundancy focusses on the quality of route options between Origin-Destination (O-D) pairs. This route-based approach is particularly pertinent when considering geographical interdependency since higher levels of interdependency reduces the level of redundancy between O-D pairs which is not something that would be evident from vulnerability analysis.

This study aims to assess the impact of geographic interdependencies on the redundancy and substitutability of discrete public transport infrastructure networks. This aim is achieved by developing two resilience measures which consider the contributions of each network to accessibility whilst accounting for the spatial proximity between network components. The measures are then applied to the Scottish public transport network consisting of long-distance bus and railway services.

The rest of the chapter is organised as follows. Section 2.2 provides a review of relevant literature and Section 2.3 includes the research methods. In Section 2.4 the case study is presented, followed by the results in Section 2.5. Finally, Section 2.6 includes conclusions and discussion.

2.2. Background

In the past decade, the redundancy of transport networks has received growing attention. Xu *et al.* (2018) proposed two measures capturing the number of connections with realistic travel times between locations and applied these to an urban road network. Similar approaches were developed by Jing *et al.* (2019) who measured redundancy between each pair of stations in a metro network, and by Yang *et al.* (2016) who proposed a network-level redundancy index reflecting the average number of routes between all stations of an urban rail network. The metrics discussed above assess redundancy from a topological perspective. Taking a different approach, Liao and van Wee (2017) developed an indicator for the diversity of travel options considering each option's travel time and the extent of overlap between options, and subsequently applied it to a regional multimodal network. Mamun *et al.* (2013) measured the redundancy of bus travel options between census zones by developing and applying an index that considered the number of available routes and their associated travel times. Li *et al.* (2024) proposed route diversity measures reflecting the number of routes between origin-destination pairs, their corresponding travel costs and the level of overlap between them, and subsequently

used these to evaluate the redundancy offered by urban multimodal bus and metro networks.

In contrast, limited work has been undertaken on substitutability within the context of resilience. Van Wee *et al.* (2019) defined substitutability as the reduction in accessibility occurring when the preferred option becomes unavailable. Building on this idea, Bondemark *et al.* (2021) measured substitutability between transport modes as the reduction in accessibility of locations, when a mode becomes unavailable. Chan *et al.* (2023) developed a metric that captures available options based on their travel time and monetary cost, and further examined how unappealing alternatives could be adjusted to improve spatial equity of options, thus providing insights into how substitutability of options can be enhanced. Another body of research has explored substitutability between travel modes from an impact-based perspective. For example, Ouyang *et al.* (2015) measured the extent to which rail can substitute the airline network of China when the latter experiences disruptions, by comparing the accessibilities of locations offered by the airline network with and without considering the substitute rail services. Taking a similar approach, Hong *et al.* (2017) examined how well the urban bus and subway networks can substitute for each other, when one of them is disrupted. Although still in its infancy, current research shows that, by focusing on the attractiveness of options, substitutability provides further insights into the characteristics of resilience of networks, and how well alternative options can replace a preferred one.

These substitutability measures pertain to events affecting only one option at a time and cannot be applied directly to the situation when area-wide events concurrently disrupt more than one modal option. As argued in Section 1.3, while geographic interdependencies have been explored between transport and other networks (e.g., Dong *et al.*, 2020; Li *et al.* (2019); Pant *et al.*, 2016; Patterson and Apostolakis, 2007; Zorn *et al.*, 2020), no study has assessed this interdependency between transport modes which use discrete infrastructure networks.

2.3. Methods

2.3.1. Network representation

Each public transport network is represented by a graph G consisting of a set of nodes $N = \{n_1, n_2, \dots, n_K\}$ and a set of segments $E = \{e_1, e_2, \dots, e_M\}$, where K is the number of nodes and M is the number of segments. Each node corresponds to a public transport stop and each segment represents the transport infrastructure connecting two nodes (e.g., railway tracks, roads) consecutively serviced by a public transport trip. The segment is characterised by a shape, which is dictated by the travel paths that public transport vehicles take along the infrastructure. A set of trips, denoted by $T = \{t_1, t_2, \dots, t_S\}$ operates on each segment, where S is the total number of trips. Each trip is associated with a schedule defined by a sequence of nodes. Thus, a trip t is expressed as $t = \{n_{lO}, n_{l1}, n_{l2}, \dots, n_{lT}\}$, where n_{lO} is the origin station and n_{lT} is the terminal station of the trip.

In the following sections indicators of redundancy and substitutability are proposed which reflect the potential for concurrent disruption to alternative routes from spatially-defined events. These indicators are extensions of previous work which adjusted redundancy or substitutability on the basis of the shared use of infrastructure as discussed above. Here, the adjustment reflects the extent to which alternative routes fall within a specified distance of each other and thus would be exposed to the impact of the same event.

Redundancy can be viewed as the total accessibility offered by alternative routes minus the contribution to accessibility from spatially proximate infrastructure. Similarly, substitutability can be viewed as the total accessibility minus the accessibility offered by the preferred route and the contribution to the remaining accessibility from spatially proximate infrastructure.

2.3.2. Redundancy indicator

The following redundancy indicator is based on an indicator of “robustness”¹ proposed by Liao and van Wee (2017) which is adapted in this paper to consider the degree of geographic interdependency between two networks by introducing a term based on spatial proximity.

When considering a single mode m_1 , let p_{m_1} denote the least-cost route connecting an origin-destination pair, OD . The accessibility offered by m_1 is expressed in Equation 2-1 (Liao and van Wee, 2017). The negative exponential form is derived from the widely used gravity-based measure, based on which higher costs of options result in lower accessibility values (Geurs and van Wee, 2004).

$$acc_{OD}^{m_1} = exp\left(-\frac{C(p_{m_1})}{\beta_{m_1}}\right) \quad 2-1$$

Where $C(p_{m_1})$ represents the cost of travel along p_{m_1} and β_{m_1} indicates the maximum travel cost acceptable to travellers. If the indicator refers to the same region and the same types of destinations, then β_{m_1} can be set arbitrarily as all indicator values are corrected equally (Liao and van Wee, 2017).

Now consider that mode m_2 is an alternative to m_1 . Following Liao and van Wee (2017), the measure in Equation 2-1 can be extended by adding the accessibility offered by m_2 , $acc_{OD}^{m_2}$. When routes p_{m_1} and p_{m_2} are not spatially proximate to each other, and, thus, not subject to geographic independencies, the contribution of m_2 to the overall level of accessibility is $acc_{OD}^{m_2}$ and hence the redundancy between OD is the sum of $acc_{OD}^{m_1}$ and $acc_{OD}^{m_2}$, as shown in Equation 2-2 below. This extended measure reflects the degree of redundancy offered by the two modes.

$$acc_{OD}^{m_1 \leftarrow m_2} = acc_{OD}^{m_1} + acc_{OD}^{m_2} \quad 2-2$$

¹ Because in their work, robustness was perceived as the number of travel options available between an origin-destination pair, we argue that redundancy is a more pertinent term; hence, the adapted indicator will be referred to as redundancy indicator.

However, in case that p_{m_2} is in the vicinity of p_{m_1} , a correction factor is introduced to account for the geographic interdependency between m_1 and m_2 . This factor is referred to as the neighbourhood coefficient and denotes the share of length of p_{m_2} which lies within a specified distance of p_{m_1} . This formulation is presented in Equation 2-3. The reduced contribution of m_2 to the accessibility of OD via m_1 , due to the proximity between the routes is included in Equation 2-4.

$$R_C(p_{m_2}, p_{m_1}) = l(p_{m_2}, p_{m_1})/l(p_{m_2}) \quad 2-3$$

$$acc_{OD}^{m_1 \leftarrow m_2} = \exp\left(-\frac{C(p_{m_1})}{\beta_{m_1}}\right) + \exp\left(-\frac{C(p_{m_2})}{\beta_{m_2}}\right) [1 - R_C(p_{m_2}, p_{m_1})] \quad 2-4$$

Where $R_C(p_{m_2}, p_{m_1})$ is the neighbourhood coefficient, $l(p_{m_2})$ is the length of p_{m_2} , and $l(p_{m_2}, p_{m_1})$ is the length of p_{m_2} in the neighbourhood of p_{m_1} .

The neighbourhood of routes was represented by buffer zones constructed around them. Figure 2-2 illustrates an example of p_{m_2} lying partially in the neighbourhood of p_{m_1} .

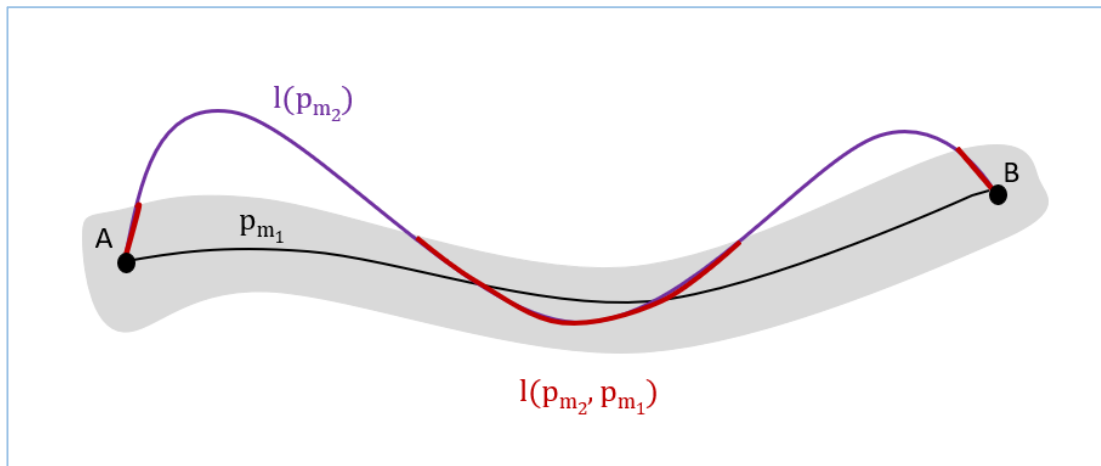


Figure 2-2 Example of a route of the substitute transport mode (purple line) located in the neighbourhood (grey area) of the primary route (red line)

Equation 2-4 includes the positive effects of the alternative mode m_2 to the primary mode m_1 in connecting a pair of locations, whilst considering geographic interdependencies.

Similarly, $acc_{OD}^{m_2 \leftarrow m_1}$ reflects the redundancy offered by m_2 and m_1 , when taking into account the spatial proximity of the two routes. These two indicators are not necessarily equal, because the share of length of p_{m_2} in the neighbourhood of p_{m_1} is not equal to the share of length of p_{m_1} in the neighbourhood of p_{m_2} , and therefore both indicators were computed. For example, for a pair of locations where accessibilities acc^{m_1} and acc^{m_2} are approximately equal, if the share of p_{m_2} in the neighbourhood of p_{m_1} is lower than the share of p_{m_1} in the neighbourhood of p_{m_2} , i.e., $R_c(p_{m_2}, p_{m_1})$ is lower than $R_c(p_{m_1}, p_{m_2})$, then the redundancy $acc^{m_1 \leftarrow m_2}$ will be higher than $acc^{m_2 \leftarrow m_1}$. This in turn indicates that using m_1 as the primary mode of travel and m_2 as alternative provides more resilient connectivity between the pair of locations than when m_2 is the primary mode.

If p_{m_2} is entirely within the neighbourhood of p_{m_1} , then $R_c(p_{m_2}, p_{m_1})$ takes the value of 1, and therefore $acc_{OD}^{m_1 \leftarrow m_2, y=1}$ takes its minimum value given by Equation 2-1, while if p_{m_2} is entirely outside of the neighbourhood of p_{m_1} , then $R_c(p_{m_2}, p_{m_1})$ is zero and, as such, $acc_{OD}^{m_1 \leftarrow m_2, y=1}$ takes its maximum value (Equation 2-2).

The redundancy indicator can be aggregated by origin i or destination j , as shown in Equations 2-5 and 2-6 respectively, to assess the redundancy of travel options from each origin to all zones (Equation 2-5) or from all zones to each destination (Equation 2-6).

$$Acc_i^{(m_1 \leftarrow m_2)} = \sum_{j=1}^N (acc_{ij}^{m_1 \leftarrow m_2}) \quad 2-5$$

$$Acc_j^{(m_1 \leftarrow m_2)} = \sum_{i=1}^M (acc_{ij}^{m_1 \leftarrow m_2}) \quad 2-6$$

Where $j = \{1, 2, \dots, N\}$ is the set of destinations and $i = \{1, 2, \dots, M\}$ is the set of origins.

For this study, the redundancy indicator was used to determine the loss in redundancy because of area-wide events concurrently affecting two modes m_1 and m_2 .

The opportunities available at the destination zones were not considered, as the scope of this work focuses on the impacts of geographic interdependency on the connectivity offered by two discrete networks, rather than the wider implications on the activity system.

In the absence of empirical data, it was assumed that both β_{m_1} and β_{m_2} were equal to 12 hours which was considered as the maximum travel time that users of both m_1 and m_2 are willing to travel. In reality these coefficients may not be equal because users may place different limits on the maximum time they would be willing to spend on different modes, for example due to variations in the levels of comfort provided.

The redundancy indicator was computed as follows:

Case I: The positive effects of m_2 were added to the level of accessibility, without accounting for geographic interdependencies between m_1 and m_2 .

For each O-D pair, the neighbourhood coefficient was zero, and therefore $acc_{ij}^{(m_1 \leftarrow m_2)I}$ was estimated from Equation 2-2. The redundancy indicator was computed for each origin zone, $Acc_i^{(m_1 \leftarrow m_2)I}$ using Equation 2-5.

Case II: The positive effects of m_2 were added to the level of accessibility, accounting for geographic interdependencies between m_1 and m_2 .

For each OD pair, the redundancy $acc_{ij}^{(m_1 \leftarrow m_2)II}$ was quantified using Equation 2-4. The value of neighbourhood coefficient was computed using Equation 2-3. The redundancy indicator was again computed for each origin zone, $Acc_i^{(m_1 \leftarrow m_2)II}$ from Equation 2-5.

The losses in redundancy for each origin because of geographic interdependencies were computed using Equations 2-7 and 2-8 below.

$$\Delta Acc_{i,m_1}^{(ab)} = Acc_i^{(m_1 \leftarrow m_2)II} - Acc_i^{(m_1)I} \quad 2-7$$

$$\Delta Acc_{i,m_1}^{(rel)} = (Acc_i^{(m_1 \leftarrow m_2)II} - Acc_i^{(m_1)I}) / Acc_i^{(m_1)I} \quad 2-8$$

2.3.3. Substitutability indicator

The model of substitutability developed by van Wee *et al.*, (2019) was adapted to incorporate geographic interdependencies between two modes. Van Wee *et al.* (2019) defined substitutability as the change in accessibility when the least-cost option is unavailable (Equation 2-9). The normalised substitutability, which ranges between 0 and 1, is shown in Equation 2-10. When the normalised measure is close to 0, the substitutability between the O-D pair is very poor, whilst when the value is 1, the preferred option can be fully substituted by alternatives without any accessibility loss.

$$S_{OD} = \frac{1}{LS_{OD} - LS_{OD}^{Y=i}} \quad 2-9$$

$$\hat{S}_{OD} = 1 - \frac{1}{1 + S_{OD}} \quad 2-10$$

Where S_{OD} is the degree of substitutability for an O-D pair and \hat{S}_{OD} is the normalised substitutability measure. LS_{OD} is the total accessibility (i.e. the maximum expected utility) of all options between OD under normal conditions and $LS_{OD}^{Y=i}$ is the accessibility of remaining options when the preferred choice i is unavailable.

Although Equations 2-9 and 2-10 remain unchanged, the remaining utility was adapted to incorporate the geographic interdependency between m_1 and m_2 . When both p_{m_1} and p_{m_2} are available, where the former is the preferred option and the latter is the alternative, their maximum utility, $LS_{OD}^{m_1 \leftarrow m_2}$, is as shown in Equation 2-11. When p_{m_1} becomes unavailable and the two routes are distant from each

other, and thus there are no geographic interdependencies, the remaining utility $LS_{OD}^{m_1 \leftarrow m_2, y=1}$ is given in Equation 2-12.

$$LS_{OD}^{m_1 \leftarrow m_2} = \ln(acc_{OD}^{m_1} + acc_{OD}^{m_2}) \quad 2-11$$

$$LS_{OD}^{m_1 \leftarrow m_2, y=1} = \ln(acc_{OD}^{m_2}) \quad 2-12$$

Where $acc_{OD}^{m_1}$ and $acc_{OD}^{m_2}$ can be computed using Equation 2-1.

However, when p_{m_2} is in the vicinity of p_{m_1} , the neighbourhood coefficient of Equation 2-3 is introduced to reflect the potential for that part of p_{m_2} which lies in the neighbourhood of p_{m_1} , to be concurrently disrupted. The remaining utility in this case is shown in Equation 2-13.

$$LS_{OD}^{m_1 \leftarrow m_2, y=1} = \ln(acc_{OD}^{m_2} [1 - R_c(p_{m_2}, p_{m_1})]) \quad 2-13$$

In case that p_{m_2} is entirely within the neighbourhood of p_{m_1} , and thus $R_c(p_{m_2}, p_{m_1})$ is one, the remaining utility of Equation 2-13 approaches negative infinity and, therefore, substitutability is zero.

Similarly with redundancy, the normalised substitutability indicator was obtained for origins, without accounting for geographic interdependencies between the two modes (**Case I**) and when accounting for them (**Case II**). In the former case, the neighbourhood coefficient of substitute routes was set to zero, while in the latter case it was computed using Equation 2-3. Consequently, the absolute and relative losses in substitutability for the origins were computed in a similar way to the indicator of redundancy.

2.4. Application to rail and long-distance bus networks in mainland Scotland

The services provided by the public transport system range from local, operating mainly in urban areas (e.g., local bus, subway), to regional and long-distance services, which provide connectivity between cities and regions (e.g., certain railway, long-

distance bus/coach services). Because the focus of this work is on services that can act as alternatives to each other, modes operating on the same functional scale were selected. Thus, discrete public transport networks for long-distance travel consisting of railway and coach/bus services in mainland Scotland were used to illustrate the application of measures described in Section 3.

The main data sources for the networks were the publicly-available General Transit Feed Specification (GTFS) data for railway (Association of Train Operating Companies, 2020) and bus (Traveline, 2019). For each mode, the data contains information on the stops, routes, trips and timetable of services of the relevant operating companies. The GTFS datasets were initially filtered based on the rail stations and bus stops located within the mainland of Scotland. Contrary to the rail dataset that relates to regional and long-distance routes exclusively, the available dataset for bus made no distinction between urban and long-distance services (i.e. all bus routes were recorded as belonging to the same route type) and, therefore, it was not possible to directly extract data associated exclusively with long-distance bus travel. While most long-distance services in Scotland are operated by certain companies, such as National Express, Stagecoach and Megabus, there are multiple operators for urban travel that also provide longer-distance services. Therefore, with a view to retaining only long-distance bus routes, the length of bus routes was used to characterise long-distance travel. Because there is no consensus on how long-distance travel is defined (Aultman-Hall, 2018), with thresholds ranging between 24 km in the UK (van de Velde, 2013) and over 80 km in the United States (Outwater *et al.*, 2015), a 30 km threshold was selected in this study which removed bus routes within urban areas and also between adjacent urban areas from the final dataset. OpenTripPlanner (OTP) (OpenTripPlanner, 2022) was used to obtain travel distances between the termini, and only those routes longer than 30 km long were retained.

The GTFS data was then related to spatially accurate models of the railway and bus infrastructure networks. For bus, the OS MasterMap Highways Network (Ordnance Survey, 2021) was used and, for railway, a model was created using spatial data on railway lines and junctions provided by Network Rail (Network Rail, personal

communication, 7 June 2021). In each case, routes were constructed by finding the shortest path between consecutive stops/stations for each unique service contained in the GTFS data. The final representation of these two discrete public transport networks is shown in Figure 2-3.

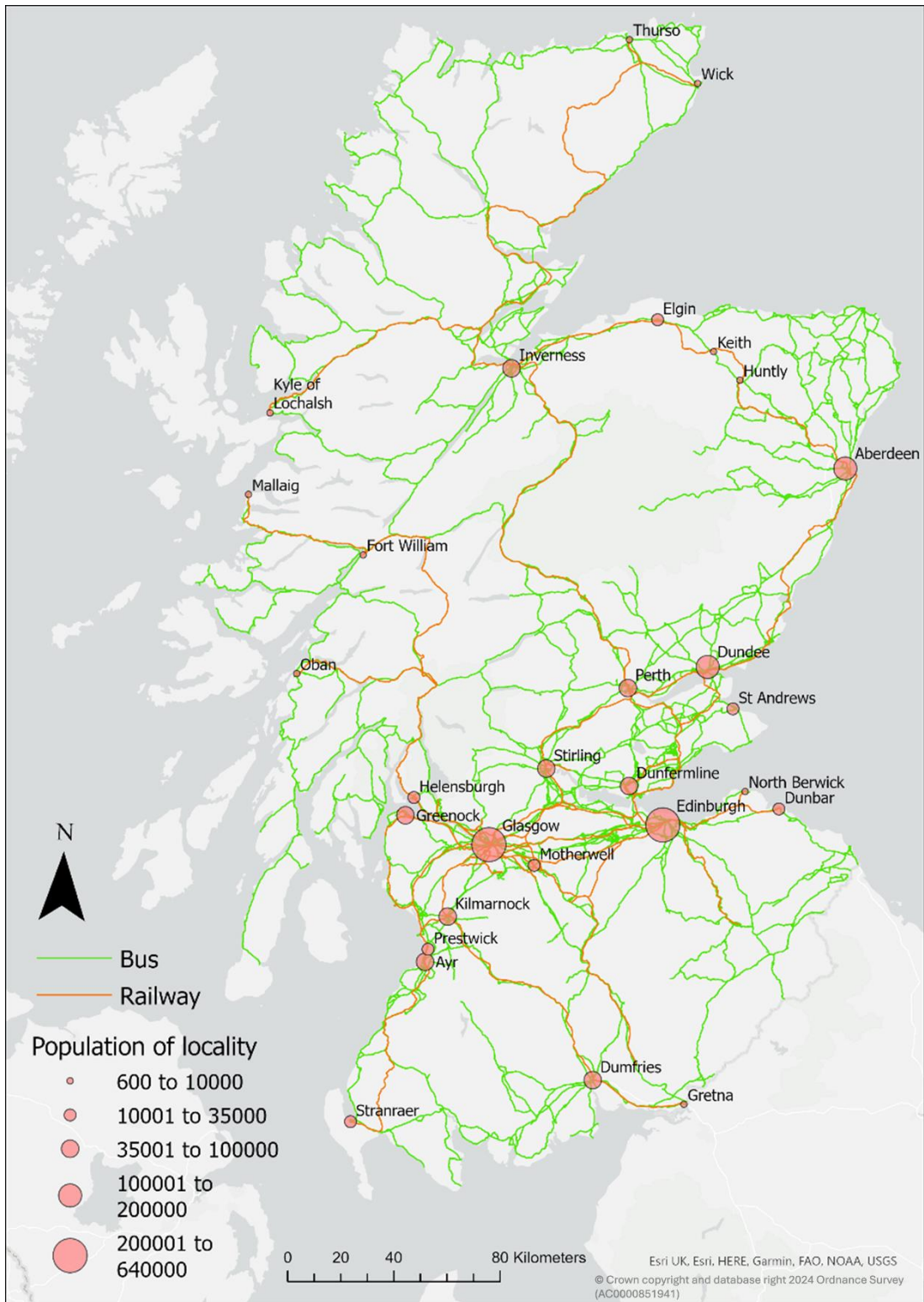


Figure 2-3 Travel paths of the long-distance public transport network in mainland Scotland, along with selected Scottish cities and towns and their respective population (Scottish Government, 2023).

To measure accessibility between locations, a grid was formed dividing the study area into cells representing travel zones. A hexagonal grid was selected because it is preferred when exploring connectivity (Birch *et al.*, 2007). Using the same reasoning as that for the identification of long-distance bus routes, the cell size was selected to have a 30km long diagonal to exclude short trips. Proximity analysis between localities (cities and towns in Scotland with population of more than 500) revealed that only 8% of locality pairs were related to separation distances of less than 30km. These are adjacent localities (e.g., Prestwick to Ayr) forming parts of the same continuous urban area and thus travel between them was not considered long-distance. Therefore, it was concluded that the selected cell size was appropriate for this work. For zones partly located outside of Scotland, only the part lying within the country was considered in the analysis. Furthermore, zones separated by un-spanned stretches of coastal water were subdivided to avoid problems in connectivity with the rest of the zoning system. As the focus is on locations serviced by both modes, only zones containing at least one stop of each mode were considered.

OTP was used to estimate the least-cost routes between zones. Two joint public transport-walk networks were constructed, one for each mode, using the street network provided by OpenStreetMap (OpenStreetMap, 2022) and relevant GTFS dataset. Owing to the nature of the GTFS data, the models were schedule-based, rather than frequency-based, as they use the actual timetable of services. Subsequently, route analysis was performed between all OD pairs. The day of journeys was set to Monday and potential times of departure were set for a time window between 7:30am and 9:30am, the former time being the earliest possible time of departure and the latter being the latest. This time window was selected to be relatively long to avoid excluding from the analysis infrequent rail and bus services that connect rural and remote areas.

Since access to long-distance services can be achieved via various modes, e.g. walking, bus and taxi, the start and end point of travel were taken to be the stops closest to the centroid of origin and destination zones. The maximum walking distance when transferring between services was restricted to 5km to prohibit

excessive walking, and the maximum number of transfers was set to 2 on the assumption that travellers making longer-distance journeys have a higher willingness to transfer between routes than those on shorter journeys.

Then, route analysis was performed between all combinations of candidate stops in the origin and destination zones, and the least-cost route identified across all possible departure times within the two-hour time window was selected on the basis of travel time.

The output itineraries derived from OTP included the start and end journey times, number of transfers, duration of journey, service (or services) used, boarding and alighting stops, and boarding and alighting times for each service. Owing to the travellers' flexibility to start their journey within the defined time window, there was no waiting time at the start of each journey, however the waiting time arising from transfers between services was included. A spatial representation of these itineraries was then constructed by identifying the routes of services used by the traveller and linking them to the spatially accurate travel paths of networks (Figure 2-3), to enable geographical proximity between alternative bus and railway routes to be estimated.

2.5. Results

Based on the travel times of least-cost routes between O-D pairs, the accessibility offered by bus and rail routes were calculated using Equation 2-1. For simplicity, routes connecting O-D pairs served by both modes will be henceforth referred to as alternative routes. Figure 2-4 shows the distribution of accessibility values characterising the alternative routes.

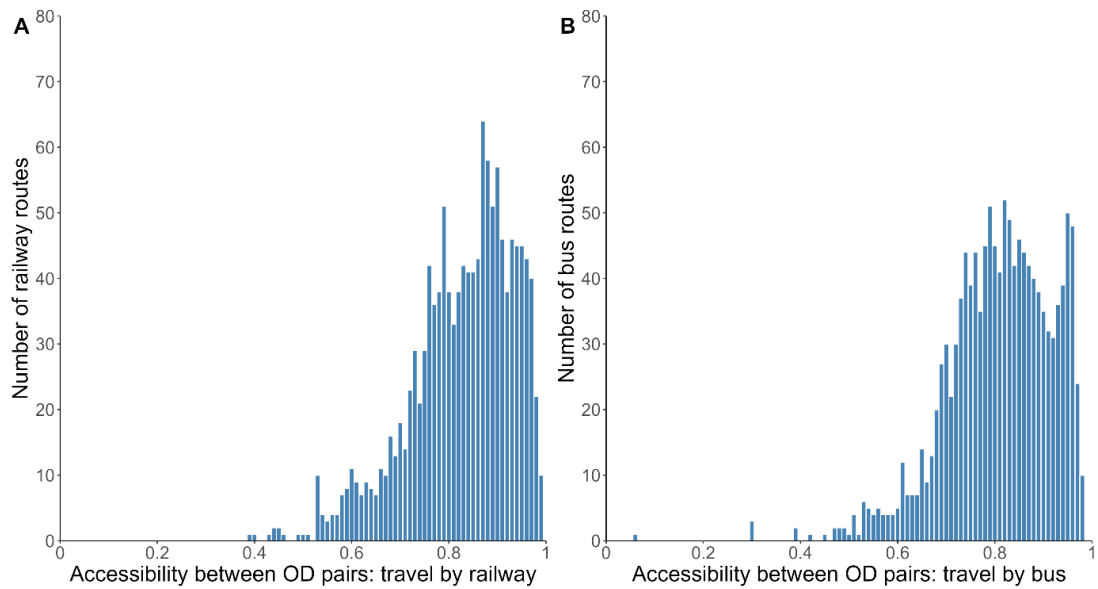


Figure 2-4 Histograms of accessibility for the (A) railway and (B) bus routes for OD pairs served by both modes on Monday between 07:30am and 09:30am. Accessibility values for a particular mode range from approximately 0 to 1. Low values of accessibility indicate long travel times close to 12 hours, while high accessibility values indicate short travel times.

Figure 2-4 shows that high accessibility values, especially those higher than 0.8, are more prevalent to each mode than low values. Furthermore, the distributions show that travel by rail is associated with slightly higher accessibility than bus which was expected as travel times by train are generally lower than travel times by bus.

To assess the geographic distribution of accessibility offered by rail and bus jointly, accessibility values of routes were aggregated for origins and destinations (Equations 2-5 and 2-6), as shown in Figure 2-5.

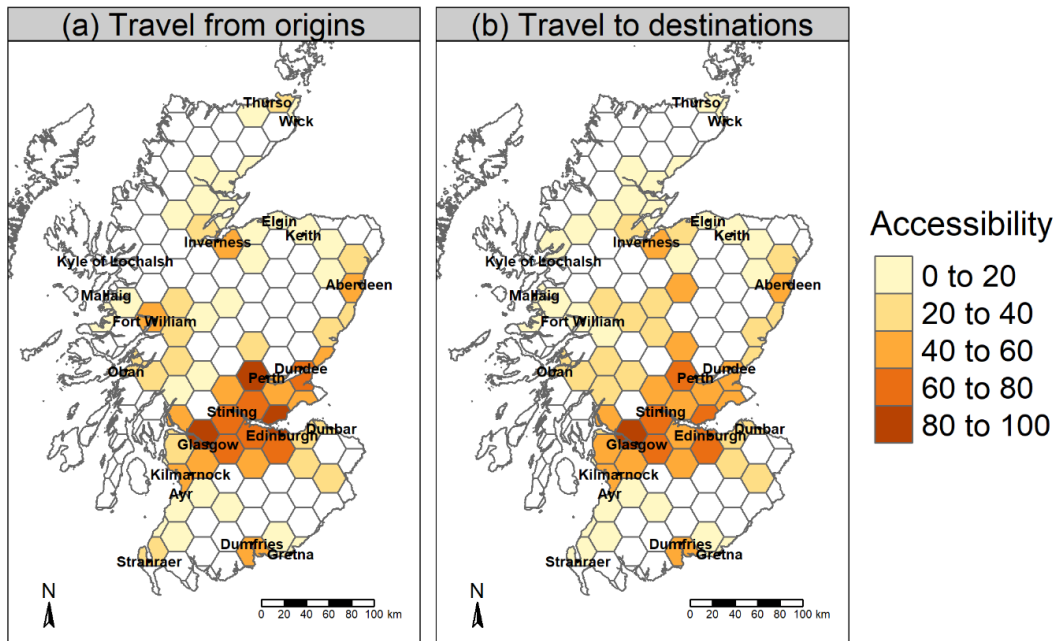


Figure 2-5 Maps showing accessibility-based redundancy values of zones connected by both modes for (a) travel from origins (b) travel to destinations, when ignoring geographic interdependencies between the two networks. Non-shaded zones are those not served by both modes. Zones in lighter colours are characterised by lower accessibility than those in darker colours.

Figure 2-5 reveals significant similarities in the accessibility for travel from origins and to destinations. In both cases, a cluster of high accessibility is observed in the central part of Scotland (“Central Belt”), where the largest and most populated cities are located, such as Glasgow and Edinburgh. Zones containing less populated localities in North Scotland (e.g., Oban, Mallaig, Inverness) and South Scotland (e.g., Ayr, Stranraer, Dumfries), but also in the area above the Central Belt are associated with lower accessibility values. Finally, other zones where smaller settlements are located (e.g., Elgin, Thurso, Wick) are related to the lowest accessibility values.

2.5.1. Redundancy of options and geographic interdependencies between modes

To assess how the positive effects of redundancy diminish due to potential geographic interdependencies, the redundancy indicator (Equation 2-4) was computed for various buffer widths and the losses in redundancy due to geographic interdependencies were obtained (Figure 2-6).

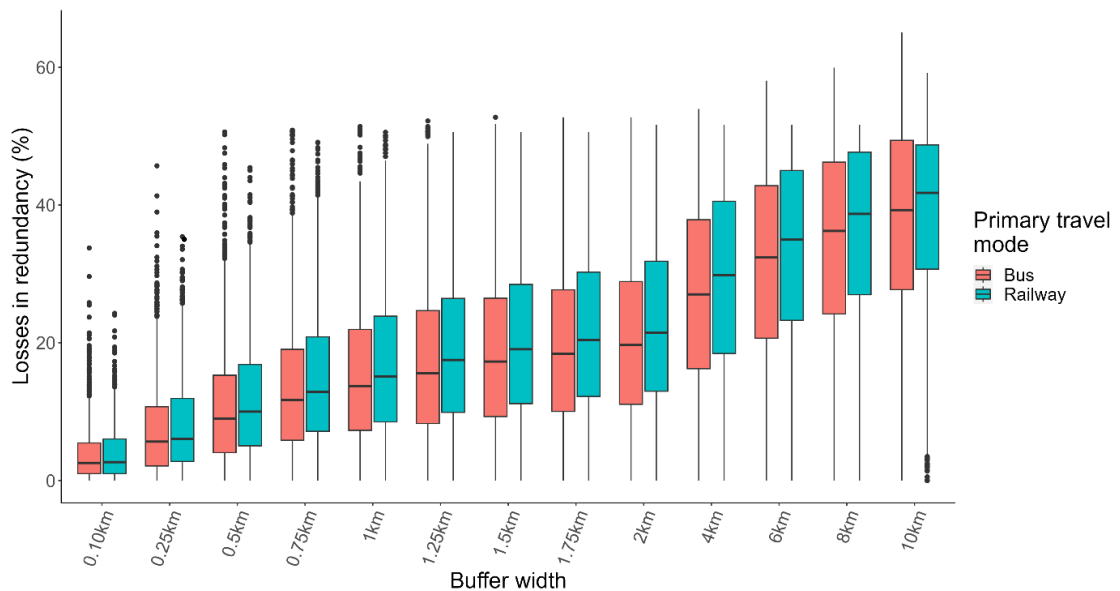


Figure 2-6 Relative losses in redundancy of O-D Pairs when considering geographic interdependencies related to various neighbourhood sizes. Larger values indicate higher susceptibility of travel options between an O-D pair to accessibility loss due to geographic interdependencies, while lower values indicate lower susceptibility.

Figure 2-6 reveals that, as expected, for hazards related to a 100 m buffer width, the redundancy of O-D pairs exhibits slight losses, and as the buffer widths increase, the losses continue to increase gradually. For the most localised hazard, the relative losses for most O-D pairs are less than 15%, which indicates that only a small part of the alternative route is within the 100 m-wide buffer of the primary route and, thus, the contribution of former to the redundancy is reduced only by a small percentage. On the other hand, for the most large-scale hazard, losses can be as much as 60%, revealing that a significant part of the substitute route is in the 10 km-wide buffer of the primary, consequently reducing markedly the contribution of substitute mode to the redundancy. Post-hoc comparisons of redundancy values were performed between the case where proximity is ignored and all other cases using Dunn’s test (Table S1) which revealed that the losses are statistically significant in all cases, indicating that, regardless of their spatial extent, hazards markedly influence redundancy of travel options.

For small buffer widths, the outliers of Figure 2-6 represent location pairs related to particularly high redundancy losses and thus particularly susceptible to geographic interdependencies. The O-D pairs related to outliers for 100 m-wide buffers, along with the sections of routes that contribute to this susceptibility, are shown in Figure 2-7.

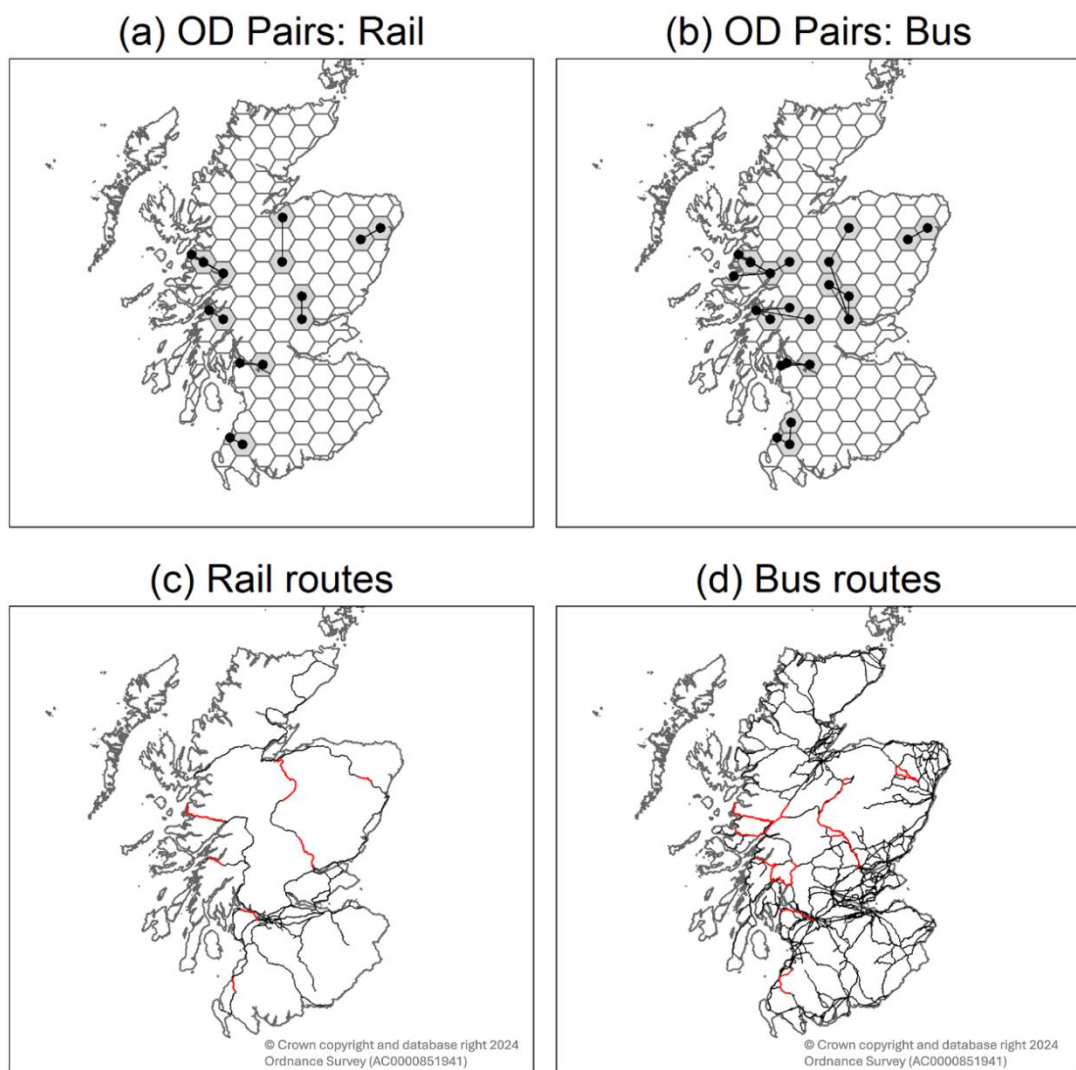


Figure 2-7 O-D Pairs associated with particularly high redundancy losses where primary mode is (a) rail and (b) bus in the case of 100 m-wide buffers, along with sections of (c) rail and (d) bus (road) networks (in red) used by routes connecting these O-D pairs.

The results reveal that the most susceptible O-D pairs are similar for rail and bus (Figure 2-7(a) and Figure 2-7(b)). It is observed that these pairs of locations share the

same region, particularly the northern part of the country, while a few O-D pairs are also scattered in the rest of the country. Sections of routes that contribute to these high losses are identified in Figure 2-7(c) and Figure 2-7(d). Most of these sections are located in North Scotland and are located in very close proximity to each other, thus revealing that even the most localised events may concurrently disrupt these alternative rail and bus routes and result in high accessibility losses.

Finally, the redundancy indicator was aggregated by origin to ascertain the geographic distribution of potential redundancy loss due to geographic interdependencies, shown in Figure 2-8. Based on the mean relative losses in redundancy between O-D pairs due to geographic interdependencies (Table S1), the buffer widths of 100 m, 1.5 km and 10 km were selected for the zone-level aggregation.

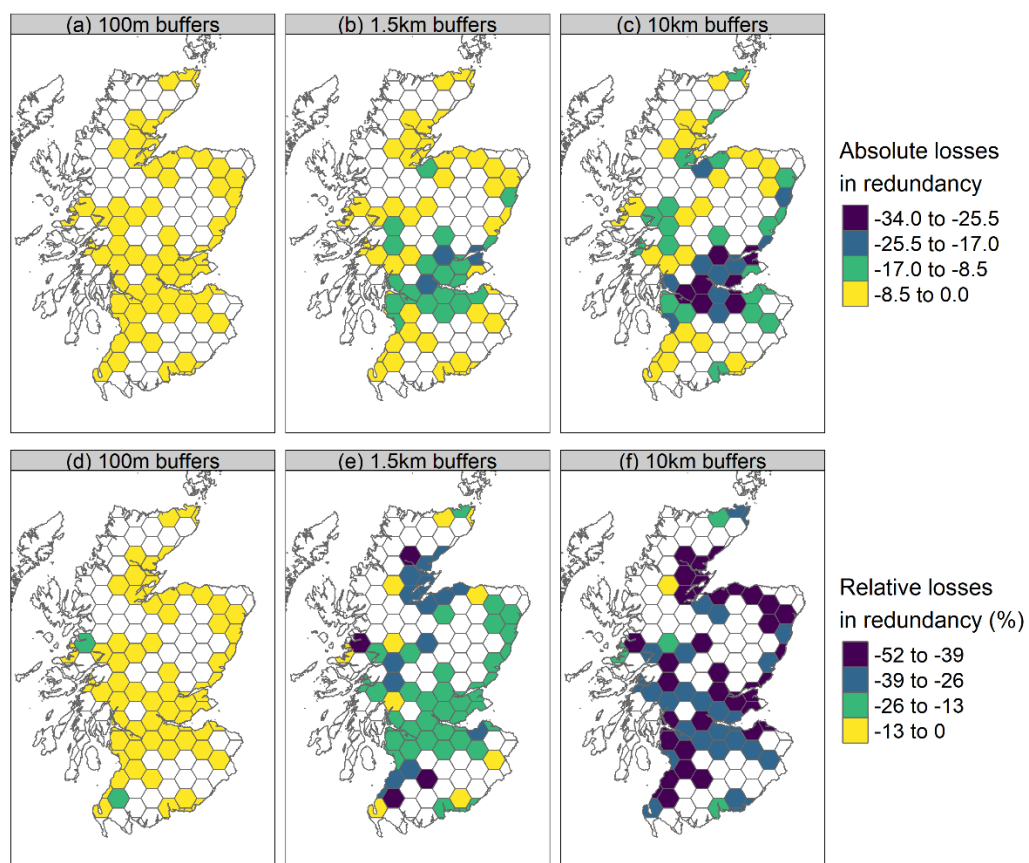


Figure 2-8 Losses in redundancy for origins (a) in absolute terms due to hazards of 100 m footprint (b) in absolute terms due to hazards of 1.5 km footprint (c) in absolute terms

due to hazards of 10 km footprint (d) in relative terms due to hazards of 100m footprint in relative terms due to hazards of 1.5 km footprint, and (f) in relative terms due to hazards of 10 km footprint, when rail is considered as primary travel mode and bus as alternative. Non-shaded zones are those origins not served by both modes. Zones in lighter colours are less susceptible to losses due to geographic interdependencies.

Figure 2-8 reveals that, for the 100 m hazard footprint, all zones experience low absolute losses in redundancy (Figure 2-8(a)), and only two origins suffer slightly higher relative losses (Figure 2-8(d)). For the 1.5 km footprint, absolute losses in redundancy increase for densely populated zones in Central Belt (Figure 2-8(b)). For the rest of Scotland, while absolute losses remain low, they are high in relative terms (Figure 2-8(e)), ranging for most zones between 13% and 26%, but also 26% to 39% in some cases. This indicates that as the hazard footprint increases, zones may lose a relatively large percentage of their initial redundancy due to alternative routes connecting them being concurrently disrupted. Finally, for the 10 km footprint, absolute losses are very high in Central Belt, and considerably lower in the rest of the country (Figure 2-8(c)). However, when considering these in relative terms (Figure 2-8(f)), less populated zones outside of Central Belt are the most susceptible to losses arising from geographic interdependencies. Generally, it is observed that relative losses due to large-scale hazards result in significantly high losses across the entire country and especially in less populated zones, revealing that in many cases those zones may lose larger percentage of their initial accessibility than urban zones, when the correlated risk of alternative routes being concurrently disrupted is considered.

Figure S1 shows the loss in redundancy for origins due to geographic interdependencies when bus is the primary mode and rail is substitute, and the results are very similar to those of Figure 2-8.

2.5.2. Substitutability of options accounting for geographic interdependencies between modes

Figure 2-9 shows the distributions of normalised substitutability losses for alternative routes for various buffer widths.

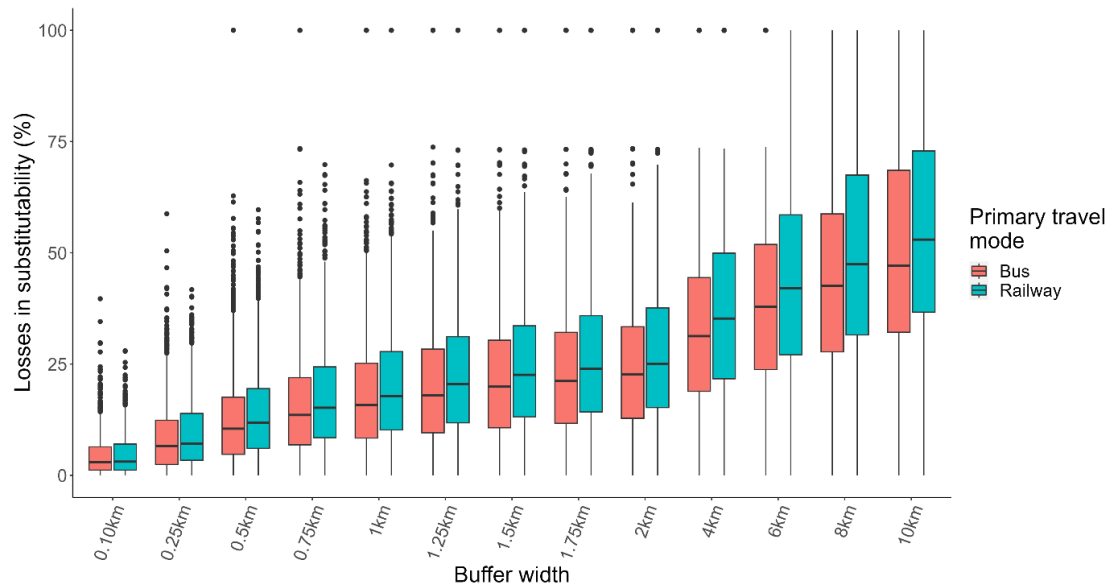


Figure 2-9 Losses in normalised substitutability values of alternative routes of each mode for buffers of varying widths. The box plots for bus (orange colour) show substitutability losses when bus is the primary mode and railway is substitute and express the reduction in the extent to which railway routes replace the corresponding bus routes when the latter become unavailable. Likewise, box plots for railway (green colour) reflect the drop in extent to which bus routes replace the accessibility provided by railway routes.

As with redundancy, the box plots of Figure 2-9 reveal that losses in substitutability of O-D pairs exhibit an upward trend as the buffer widths around primary routes increase. Post-hoc comparisons using Dunn’s test (Table S2) showed that geographic interdependencies result in significantly different substitutability values, even for the smallest-scale hazards considered.

As with the redundancy indicator, the routes associated with the high outliers of substitutability losses in the case of 100 m-wide buffers were identified, as shown in Figure 2-11, along with the section of public transport routes that contribute to these

losses. The results reveal that the O-D pairs related to these outliers are in similar locations to those of redundancy (Figure 2-7), however they appear to be significantly more, when considering either mode as primary. This shows that while significant discrepancies in the redundancy and substitutability losses do not exist, it further reinforces the observation that it is possible for an O-D pair to experience very high losses in substitutability but not in redundancy. Thus, for an O-D pair where the primary route is characterised as high accessibility and the alternative route is entirely within the neighbourhood of the former, the redundancy indicator will still be high, while substitutability will be zero.

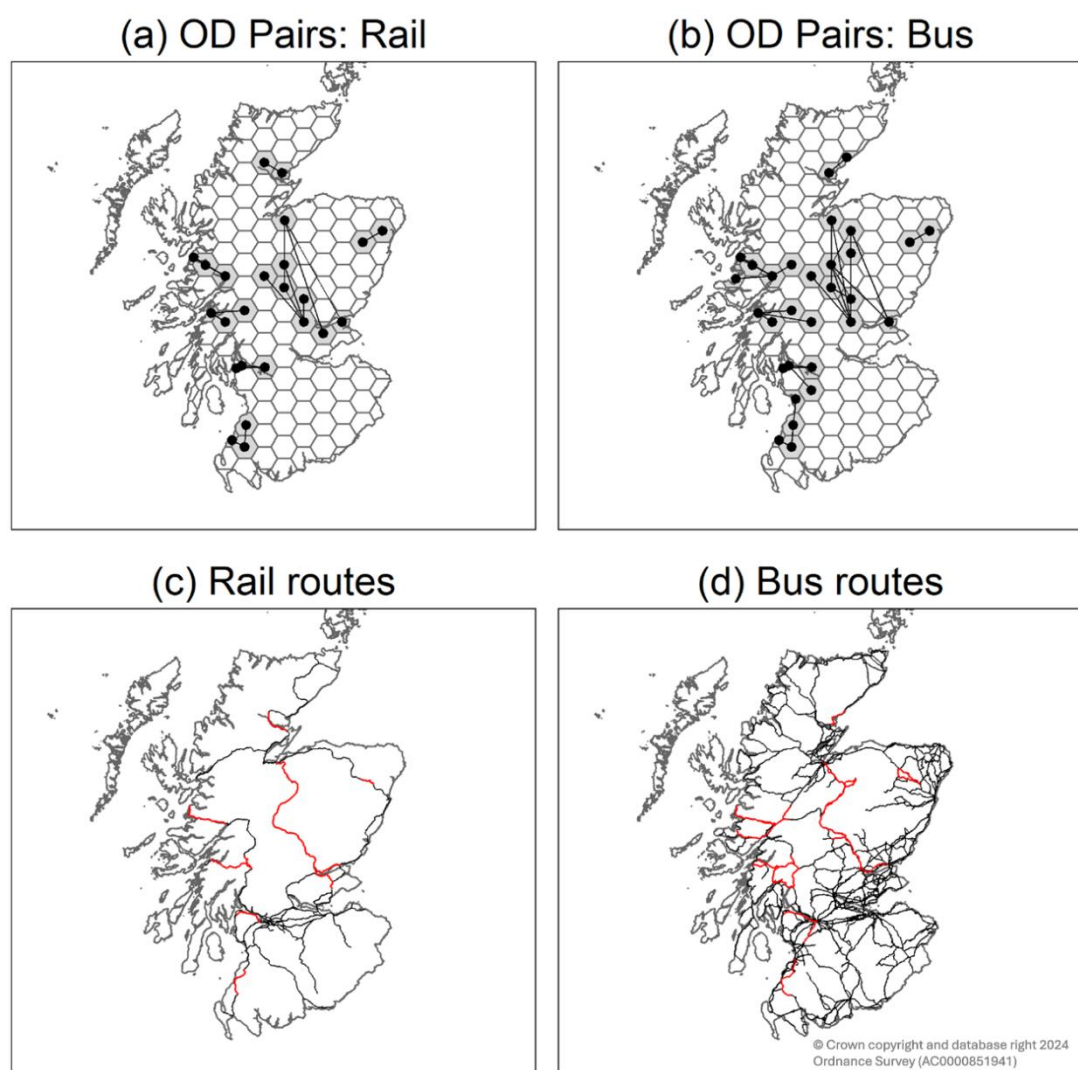


Figure 2-10 O-D Pairs associated with high outliers of substitutability losses for travel by (a) rail and (b) bus, in the case of 100 m-wide buffers, along with sections of (c) rail and (d) bus (road) networks that the routes connecting these O-D Pairs use.

Regarding the sections of the rail and bus networks that contribute to these high losses in substitutability, Figure 2-10(c) and Figure 2-10(d) show that these are the same as those for redundancy (Figure 2-7), thus revealing that regardless an O-D pair is characterised by extremely high losses in redundancy, substitutability (or both), its corresponding routes use specific parts of the network that contribute to its susceptibility to geographic interdependencies.

The normalised substitutability of routes was aggregated for origins for the 100 m, 1.5km and 10km footprints, as shown in Figure 2-11.

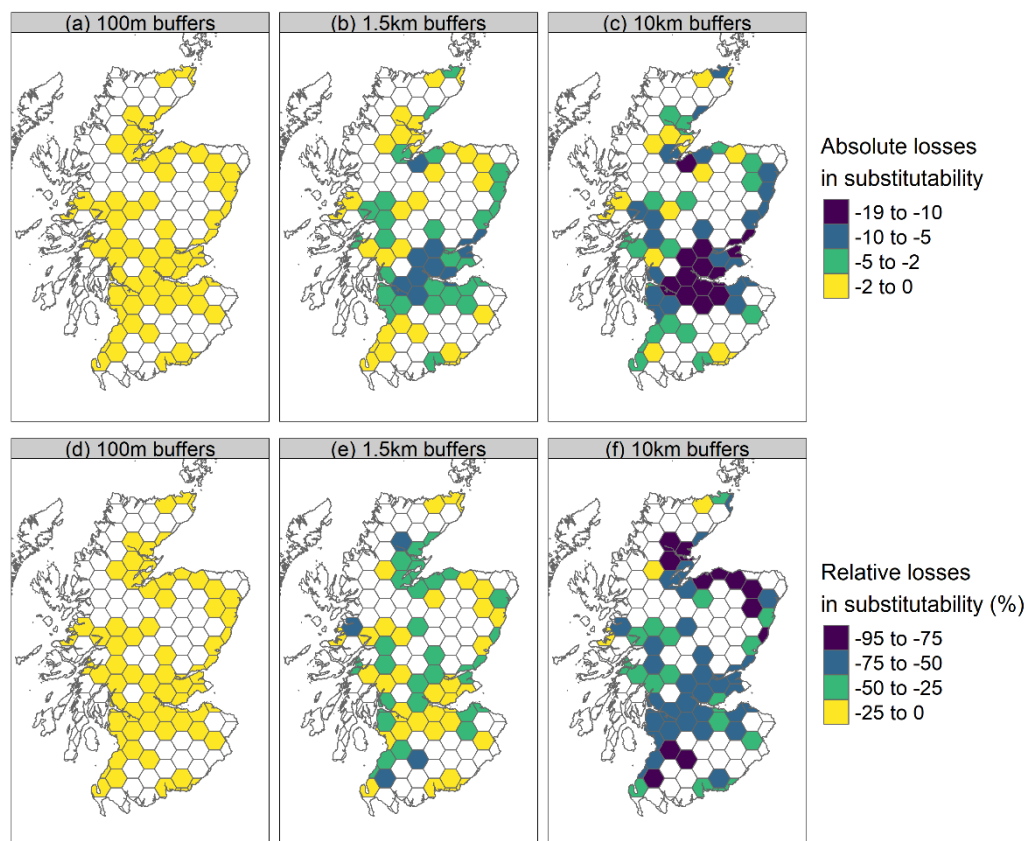


Figure 2-11 Losses in normalised substitutability for origins (a) in absolute terms due to hazards of 100m footprint (b) in absolute terms due to hazards of 1.5 km footprint (c) in absolute terms due to hazards of 10 km footprint (d) in relative terms due to hazards of 100m footprint (e) in relative terms due to hazards of 1.5 km footprint, and (f) in relative terms due to hazards of 10 km footprint, when rail is considered as primary travel mode and bus as substitute. Non-shaded zones are those origins not served by both modes. Zones in lighter colours are less susceptible to losses due to geographic interdependencies.

The results for localised hazards (Figure 2-11(a) and Figure 2-11(d)) suggest that all zones exhibit very low losses in substitutability, which is consistent with those of redundancy (Figure 2-8(a) and Figure 2-8(d)). However, as the scale of hazard increases, differences between the two indicator values are revealed. While the geographic distribution of absolute losses in redundancy for the 1.5 km-wide buffers (Figure 2-8(b)) shares significant similarities with that of normalised substitutability (Figure 2-11(b)), the distributions of relative losses exhibit differences as Figure 2-11(e) indicates that fewer zones are related to high substitutability losses due to geographic interdependencies than Figure 2-8(e). These differences are even more significant for the 10km-wide buffers (Figure 2-11(f)) and Figure 2-8(f)). This indicates that while a zone may experience very high losses in terms of redundancy, its losses in terms of substitutability may be lower. It is further worth noting that zones that rank high in substitutability losses but low in redundancy are not observed, indicating that using the redundancy indicator to assess losses in accessibility of locations provides more conservative results than the substitutability indicator.

The origin-level losses in substitutability were also computed (Figure S2) when considering bus as primary mode and reveal very similar results to those of Figure 2-11.

2.6. Conclusions and Discussion

In this chapter, an approach is presented to assess the role of geographic interdependencies between two discrete public transport networks for two components of resilience, namely redundancy and substitutability of travel options. Measures were developed to represent each of these components using an accessibility-based approach. The degree of geographic interdependencies was introduced by reducing the contributions of total accessibility of alternative routes based on the proximity between them. The results reveal that while an alternative mode provides significant resilience benefits, its contributions are potentially

reduced when geographic interdependency is considered. The extent of this reduction depends on the spatial footprint of hazards and the degree of proximity of alternative routes, highlighting the importance of careful selection of buffer size. A very small value will result in narrow buffers that underestimate the risk of routes being concurrently disrupted by large-scale events, while wide buffers could overestimate the risk of concurrent disruptions caused by localised events. In the example presented, the redundancy and substitutability of most routes between OD pairs were not significantly affected by small-scale events, however losses became significantly more noticeable for larger-scale hazards.

Furthermore, the results of the example show that, although urban, densely populated areas are associated with the highest redundancy and substitutability losses in absolute terms, rural areas that are less densely populated lose a higher percentage of their initial values as a result of area-wide events. This is because, although absolute losses in zones located in less populated areas due to geographic interdependency were low, their initial values in redundancy and substitutability (i.e., when ignoring geographic interdependency) were also low. In contrast, absolute losses due to geographic interdependency in urban zones were high, but their initial values in redundancy and substitutability were also high; therefore, these high absolute losses were only a small proportion of their initial indicator values. An important observation of the results highlighted differences in the ranking of OD pairs and locations in terms of redundancy and substitutability, which is attributed to the fact that the former metric places more emphasis on the contribution of the primary option to the accessibility, while the latter focuses more on the remaining accessibility when the primary option is unavailable. These indicators therefore complement each other when assessing the accessibility of locations, with or without accounting for geographic interdependency.

The work presented comes with several limitations. Firstly, the redundancy and substitutability measures were assessed in terms of travel time, however other elements of travel deterrence could be considered, such as distance and economic cost of travel. Secondly, for the proposed indicators, rail and bus operating on the

same functional level were identified based on the travel distance of their services. However, although the modes selected were largely interchangeable, each has different capacities and flexibilities. For example, typically a bus service may more easily detour in the event of a road closure, while rail can put on replacement buses when trains are disrupted. Thirdly, due to the fact that the available GTFS data for bus services in Scotland made no distinction between local and long-distance routes, the latter were selected based solely on the length of each bus route. This selection could be further refined by retaining bus services with termini in different localities which exceed a given route distance threshold. Another limitation is that the impact of geographic interdependencies on components of resilience was assessed for a certain time-window on a weekday. Choosing a different day or time-of-day may have resulted in different itineraries and, as such, different redundancy and substitutability values. Repeating the analysis for various time-windows (e.g., peak and off-peak times) would allow ascertaining hours-of-day and days-of-week, where resilience of networks is mostly affected by geographic interdependencies.

Furthermore, the geographic interdependencies were estimated using a buffer-based approach where only those parts of alternative routes which lie within the buffer of preferred route were considered, while those parts lying outside of that buffer were ignored. The method could be extended to avoid this “cliff-edge” effect by allowing the degree of geographic interdependency to decay with separation distance between routes. However, capturing the distance-decay effect would be challenging and computationally intensive, as proximity between alternative routes varies along their length. Another limitation of this work is that the potential of two travel options being concurrently disrupted arises purely from their proximity. Whilst horizontal distance is an important determinant for concurrent failures, other factors may influence this, depending on the hazard of concern, such as vertical separation of routes and slope. To better account for these factors, risk maps showing the spatial footprint and intensity of hazards of interest could be used instead of buffers.

Finally, because the focus of this work was to assess the effects of the geographic interdependency between two discrete public transport modes, only the shortest

path route of each mode was considered. The method could also include other feasible routes of these modes following the approach of Liao and van Wee (2017), in which the accessibility offered by each additional route is reduced by the extent to which it falls within the buffers of routes which have already been included in the calculation. Likewise, this approach could be extended to include more than two transport modes, as well as the attractiveness of destinations. A general model of redundancy that considers both the value of destination opportunities and the connectivity provided by multiple options is presented in the Supplementary Material (Equation S1 of Appendix A).

Despite these limitations, the findings provide novel indications on the impacts of geographic interdependencies related to area-wide events on components of resilience of transport networks. The approach presented enables policy makers and network managers to explore the potential severity of consequences of area-wide events on multimodal transportation networks and identify areas of the network which, if impacted, would lead to the highest losses in accessibility.

This chapter developed a general framework for assessing the impact of geographic interdependencies on the resilience of public transport modes which operate on spatially proximate infrastructure networks. However, this framework was applied for events of varying spatial extent and, therefore, did not assess specifically the geographic interdependencies that arise due to extreme rainfall. The next chapter builds upon this foundation by empirically assessing the impact of rainfall-related geographic interdependencies using historical flood incident data for the two networks of concern.

3. Empirical assessment of the impact of rainfall-related geographic interdependencies on multimodal public transport networks

The general framework developed in Chapter 2 can be used to examine the impact of weather-related area-wide events on the accessibility of geographically interdependent public transport networks and the connectivity of locations, however it does not explicitly pertain to extreme rainfall. This chapter addresses this gap by empirically characterising the geographic interdependencies between modes specifically due to rainfall, and by further considering the potential for the same rainfall event to inundate neighbouring links of the two public transport networks of concern. Chapter 3 address the second objective of this thesis which is concerned with the empirical assessment of geographic interdependencies due to a weather-related hazardous event – in this case, rainfall – and their impact on the importance and criticality of public transport links using historical rainfall-related flood disruption records for the rail and bus networks.

3.1. Introduction

Hydrometeorological hazards, such as precipitation and flooding, can cause severe damage to transport infrastructure, thus inflicting disruption to road and railway networks, and resulting in adverse socio-economic impacts (Bowyer *et al.*, 2020; Palko *et al.*, 2017; Pyatkova *et al.*, 2019; van Ginkel *et al.*, 2022). For example, in the west of England in 2007, the flood event caused by extreme rainfall inflicted extensive closures in both the railway and road networks, consequently leaving people stranded and affecting others, even outside flooded areas (Pitt, 2007). More recently, in September 2023 a heavy rainfall event, known as storm Daniel, resulted in extensive flooding of Thessaly region in Greece, consequently closing both the main motorway and train route between the two biggest cities of the country (Chatzigeorgiadis *et al.*, 2023). Future climate projections consistently show that

rainfall and flooding are expected to increase in both magnitude and frequency in many countries (IPCC, 2022), including the UK (Betts and Brown, 2021). In light of this increasing trend, it is imperative that vulnerabilities of the transportation system to extreme weather events are assessed in order to improve resilience (Bowyer *et al.*, 2020; National Infrastructure Commission, 2020).

Since the location of a disruptive incident in a network influences the extent of network-wide consequences, particular emphasis has been placed on characterising which network elements would result in the greatest adverse consequences, when failed (Cats *et al.*, 2016). As previously mentioned in Section 1.1, the importance of a network element reflects the severity of impacts on the network if that element were to fail, while weakness expresses the probability of an element failing when exposed to the hazardous event (Cats *et al.*, 2016). The concept of criticality encompasses both the weakness and importance of elements (Jenelius *et al.*, 2006).

Although the concept of importance has been extended to apply to spatial areas when assessing the vulnerability of networks to area-wide events (Johansson and Hassel, 2010), no similar extensions to the definition of weakness and, by extension, criticality have been proposed to date. In the context of geographic interdependencies, it is here argued that weakness of the area indicates the probability of it being directly affected by the event of concern, while criticality of the area would reflect the resulting risk associated with the event that occurs and directly affects the area of concern. Therefore, criticality encompasses both the importance and weakness of the area to the hazardous event of concern.

The study in this chapter aims to assess the extent to which geographic interdependencies exist between discrete transport infrastructure networks in the event of heavy rainfall, and to use the estimated characteristics of this interdependency to assess its impact on the importance and criticality of public transport links.

The Scottish public transport network that consists of long-distance bus and railway services is used for the application of the proposed method. To explore the spatial

patterns of rainfall-related geographic interdependencies and estimate the weakness of network elements from an empirical standpoint, datasets were used containing the date, location and impact of historical flooding incidents that disrupted each mode due to heavy rainfall. Since a readily available single dataset for bus and rail networks was not available, data from various sources were processed and combined.

The rest of the chapter is organised as follows. Section 3.2 presents key literature on the importance and criticality of elements and areas. Section 3.3 includes the methods of analysis, followed by Section 3.4, where the representation of the Scottish public transport network and the steps to construct datasets of historical flood events that disrupted it are presented. In Section 3.5, the results of the analysis are shown, and Section 3.6 includes the conclusions arising from this work.

3.2. Key literature on importance, weakness and criticality of network elements

3.2.1. Importance

The assessment of importance has received considerable attention within the existing literature. As previously mentioned in Section 1.2.2, methods developed so far to assess the vulnerability of networks can be classified into two distinct approaches. These methods can be equally used to measure the importance of elements. As previously discussed, the first one, known as full-scan approach, involves sequentially failing each network element and estimating the resulting consequences for the network performance and, therefore, estimates the importance of elements through an impact-based approach. Indicatively, Taylor *et al.* (2006) developed a measure of importance that expresses the increase in population-weighted travel times between locations, when a link of the road network is closed, and based on this, performed a full-scan of the Australian strategic road network. Similarly, Jenelius *et al.* (2006) performed a full-scan of the Swedish road network by computing several measures of importance of links, namely increase in travel time between locations, demand-weighted increase in travel time, and

number of missed trips, referred to as unsatisfied demand. Similarly, for the public transport network, While the impact-based full-scan approach thoroughly studies the consequences of element failures to the network, it is computationally intensive, and therefore challenging to implement for large-scale transport networks (Cats *et al.*, 2016).

In the second approach, the importance of network elements reflects the extent to which each element is central to the topology or function of the network under normal conditions. The most common measure is a topological measure, known as betweenness centrality, which expresses the number of shortest paths between locations traversing the elements of concern (Freeman *et al.*, 1991; Crucitti *et al.*, 2006). In several works, this measure has been augmented to include functional network characteristics. Lowry (2014) extended the betweenness centrality of road links to include the trip production and attraction rates in the origins and destinations of paths traversing the links. Similarly, Sarlas *et al.* (2020) proposed a set of accessibility-based indicators, which augmented the betweenness centrality of links by incorporating the population and employment opportunities in the origins and destinations of paths using the links, but also the cost of interaction between them in the form of travel times. Because centrality-based metrics of importance do not require the implementation of multiple disruption scenarios, their estimation is less computationally intensive compared to the full-scan approaches.

3.2.2. Weakness and criticality

Works assessing the criticality of network elements are much scarcer compared to importance. Cats *et al.* (2016) computed the criticality of public transport links by combining their importance and weakness, which was represented by the expected duration of disruptions on each link per year. The computation of weakness was facilitated by a dataset containing historical incidents that had disrupted the network. Using the same dataset, Yap *et al.* (2018) estimated the criticality of public transport links, in which weakness included both the expected annual duration of a

link being disrupted due to events directly occurring on it (first-order effects) as well as the knock-on effects from disruptions occurring on other links of the network (second-order effects). Yap and Cats (2021) proposed a supervised learning approach to predict the weakness of stations, represented by the expected frequency of station disruptions, thus reducing the requirements for large datasets of disruptive incidents. This approach involved establishing a model to predict the probability of stations experiencing a certain type of disruption based on location and station-specific variables. This probability was then translated to frequency over a time period of interest and, based on this, the most critical stations were identified.

3.2.3. Research gaps

Previous works that assessed the importance and criticality of elements of the transport network were concerned with events affecting only one element at a time and therefore did not consider the correlated exposure of multiple elements to the same event. However, area-wide events, such as those stemming from adverse weather, may result in concurrent disruptions on all infrastructure networks located within the hazard footprint.

In the case of area-wide disruptive events, where geographic interdependencies between infrastructure networks occur, a similar impact-based approach is applied to assess the importance of areas (Johansson and Hassel, 2010). Centrality measures for such events are much scarcer and have been only applied to capture the geographic interdependency between transport and other civil infrastructure systems (Schintler *et al.*, 2007; Islam and Moselhi, 2012; Thacker *et al.*, 2017; Hughes *et al.*; 2020). Previous works assessing the importance of areas did not pertain to specific hazards, hence ignoring the probability of infrastructure elements experiencing disruption as a result of a particular hazardous event occurring. Therefore, the weakness and, by extension, criticality were not assessed. Furthermore, they did not consider the size of cells and corridor neighbourhoods capturing the spatial footprint of the hazard as these were arbitrarily selected. In

contrast, the approach proposed in this study explicitly considers the characteristics of the hazard into the assessment of importance and criticality, by initially evaluating the geographic interdependencies between infrastructure networks and subsequently incorporating its spatial footprint and probability of occurrence in the metrics of importance and criticality.

3.3. Methods

3.3.1. Network representation

As previously described in Section 2.3.1 of Chapter 2, the bus network is represented as a graph $G_B = (N_B, E_B, T_B)$ consisting of nodes, segments and bus trips operating according to a certain timetable. Nodes correspond to bus stops, and segments to paths between stops consecutively serviced by a trip. The bus operates on the road infrastructure network, which is also represented by a graph $G_R = (N_R, L_R)$ consisting of a set of nodes $N_R = \{n_{R1}, n_{R2}, \dots\}$ and a set of links $L_R = \{l_{R1}, l_{R2}, \dots\}$. Road nodes correspond to road ends or intersections between roads. Links represent the physical infrastructure connecting two nodes that are geographically consecutive, and thus do not overlap with each other. Each road link can be traversed by one or more bus segments. For example, for road link l_{R1} , this can be expressed as $l_{R1} = \{e_{Bi}, e_{Bj}, e_{Bk} \dots\}$. Because each segment can be used by one or more bus trips, then it can be stated that each road link is traversed by all bus trips that use its corresponding segments. Thus, for road link l_{R1} , this can be expressed as, $l_{R1} = \{t_{B1}, t_{B2}, t_{Bk} \dots\}$.

Figure 3-1 below shows a schematic example of the bus trips traversing distinct bus segments, which in turn use certain road links. Figure 3-1(b) shows three consecutive non-overlapping road links which connect four road nodes, namely nodes with ID's "706670", "706607", "706596" and "706525". These road links are traversed by two overlapping bus segments of which the first is used by two bus trips denoted as t_1 and t_2 (Figure 3-1(a)) and the second is used by three trips denoted as t_3 , t_4 and t_5

(Figure 3-1(c)). Therefore, by mapping the bus network onto the road network, it is shown that trips of both bus segments traverse the four road links of concern.

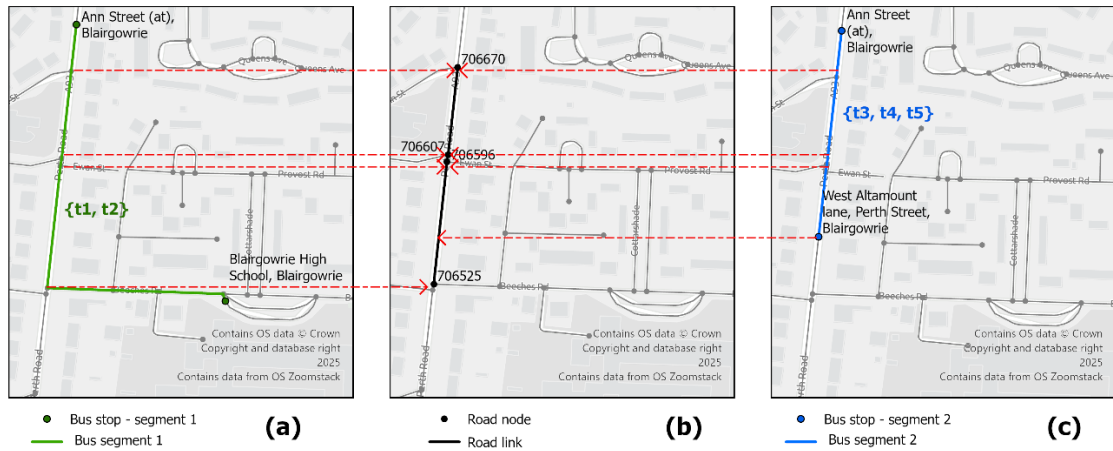


Figure 3-1 The identification of public transport trips traversing the road links connecting road nodes with ID's "706670", "706607", "706596" and "706525" based on the mapping of bus segments 1 and 2 on which the sets of trips {t1, t2} and {t3, t4, t5} run, respectively.

Similar to the bus network, the railway network, represented by the graph $G_R = (N_R, E_R, T_R)$, operates on the physical rail infrastructure network, which is also a graph $G_{RI} = (N_{RI}, L_{RI})$ consisting of a set of nodes $N_{RI} = \{n_{RI1}, n_{RI2}, \dots\}$, and a set of non-overlapping links $L_{RI} = \{e_{RI1}, e_{RI2}, \dots\}$ that span between geographically consecutive nodes. Therefore, a rail link may be used by one or more rail segments, i.e. $l_{RI1} = \{e_{RI}, e_{RIj}, e_{RIk} \dots\}$, and thus by one or more rail trips, i.e. $l_{RI1} = \{t_{R1}, t_{R2}, t_{Rk} \dots\}$.

3.3.2. Assessing the geographic interdependency between discrete public transport networks due to heavy rainfall

In order to explore the extent to which distinct modes of public transport are subject to geographic interdependencies due to rainfall, the spatial patterns between concurrent rainfall-induced flood events on the railway and bus networks were assessed.

The approach adopted builds on established methods for the detection of spatial patterns in plant ecology (Galiano, 1982) and estimation of spatial dependence in hydro-meteorological phenomena (Israelsson *et al.*, 2020; Ricciardulli and Sardeshmukh, 2002). Specifically, to detect spatial patterns in plant populations, Galiano (1982) developed a method, known as “plant-to-all-plant” analysis, which involved computing the conditional probability of finding a plant at a certain distance from another plant. By computing the conditional probabilities for all plants and for a wide range of distances, the “conditioned probability spectrum” showing the conditional probabilities against separation distance is derived. The shape of this spectrum indicates patterns in the plant population deviating from spatial randomness. This method was applied to cross-sectional data, thus capturing patterns at a given time. Similarly, Ricciardulli and Sardeshmukh (2002) and Israelsson *et al.* (2020) used this method of conditional probabilities to detect the spatial dependence structure of rainfall based on time series data, thus capturing the average spatial patterns over long time periods.

The empirical method of conditional probabilities (Israelsson *et al.* 2020; Ricciardulli and Sardeshmukh, 2002) was adapted to detect spatial patterns in concurrent disruptions of discrete public transport modes. This enabled the estimation of the extent to which geographic interdependencies occur between the two modes operating on separate infrastructure networks due to rainfall events. Because the method required the date and location of historic rainfall-induced flood events that disrupted bus and railway networks, the historic datasets described in Section 3.4 were used. Each dataset contained the date of each flood event, location of flooded link as well as the disruption caused, i.e. whether the link fully closed or remained partially open due to lane closures or speed restrictions imposed.

For a given public transport mode, the conditional probability of a disruptive flood event occurring on a link given the occurrence of flooding on a link of the other mode at a certain distance interval was computed for each day in the resulting time series. Since the flood events for both railway and bus were recorded at link-level, rather than spatial points, the distance intervals used for the computation of conditional

probabilities from the link of concern were defined on the basis of non-overlapping buffer rings of equal width around the link. The smallest buffer ring of width d covers the link plus its buffer-shaped neighbourhood. A second buffer ring (of the same width d) was formed around the smallest buffer, while the third buffer was formed around the second, etc (see Figure 3-2 below).

For a public transport network consisting of two modes m_1 and m_2 , the former being the primary mode of interest and the latter being the alternative, let a_i be a link of m_1 that has been disrupted at least once throughout the study period. The conditional probabilities were estimated using the following algorithm.

1. Form buffer rings of equal width d around link a_i . In this case, 2km-wide bins were formed spanning up to 100 km from the link of concern.
2. Identify all links b_j of m_2 located within each buffer ring from a_i .
3. For each day that a_i was disrupted, identify the number of links b_j within each buffer ring that were concurrently disrupted and compute the corresponding proportion with respect to the total number of links b_j located in the respective buffer ring.
4. Repeat step 3, for each day of disruption of railway link a_i .
5. Repeat steps 2-4, for each link a_i of m_1 .
6. Compute the average value of proportions of step 5 for each buffer ring. This represents the conditional probability of a link of m_2 experiencing disruption given that a link of m_1 at a certain distance is disrupted; denoted as $P(m_2|m_1)$.

Figure 3-2 illustrates the process to calculate the conditional probability of links of m_2 experiencing disruption given that a link of m_1 which is located at a certain distance from these links is already disrupted. Note that in case that a link b_j spatially extended across two or more buffer rings of a_i , then it was considered that b_j fell into the buffer ring closer to a_i . In other words, the minimum distance between a_i and b_j was taken.

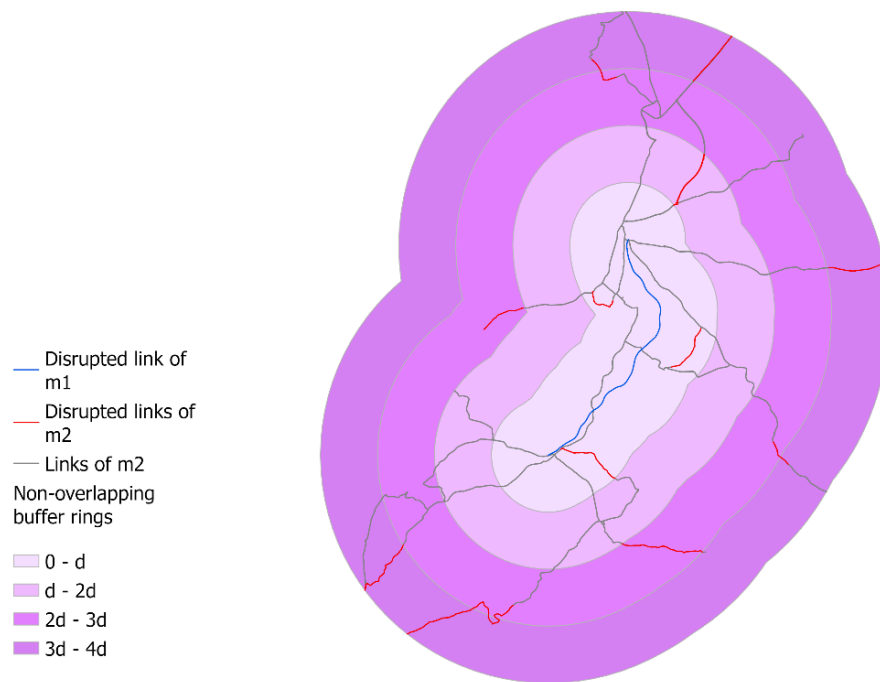


Figure 3-2 Schematic figure on the method used to compute the conditional probability of a link of mode m_2 experiencing disruption given that a link of mode m_1 is already disrupted. The blue link is that of m_1 that is already disrupted, the grey links are links of m_2 and the red links are those of m_2 concurrently disrupted.

Where geographic interdependencies exist, it was expected that links of the two modes closer to one another, were more likely to be concurrently disrupted compared to those farther apart. By plotting the conditional probability $P(m_2|m_1)$ against the separation distance, d , between links of m_1 and m_2 , the spatial pattern of concurrent flooding-induced disruptions on the two networks was derived.

To determine whether spatial association exists between concurrent disruptions on modes m_1 and m_2 , the shape of the plot was assessed. Generally, in case that the plot does not exhibit any shape, the concurrent disruptions between links of m_1 and m_2 were considered as spatially random. Otherwise, the existence of a shape indicates the existence of relationship between the conditional probability and separation distance. Specifically in the case of geographic interdependencies, it was expected that the shape would follow a distance-decay form, where low values of

d exhibit higher probabilities compared to large values of d . The degree of fit to the data of various functions was explored, and the relationship between $P(m_2|m_1)$ and d was obtained, and thus the statistical significance of the role of d on the conditional probabilities was tested. The existence of a statistically significant relationship in which $P(m_2|m_1)$ is higher for lower values of distance separation between elements of m_1 and m_2 provided evidence that the two modes were subject to geographic interdependencies as a result of the hazard.

This process was undertaken by taking in turn each public transport mode as primary mode of concern and, thus, plots for both $P(Bus|Rail)$ and $P(Rail|Bus)$ were constructed.

3.3.3. Assessment of importance in the public transport networks

Similar to the operators-based centrality measure proposed by Cats and Jenelius (2014), important links were here considered as those traversed by the largest number of public transport trips. To incorporate the geographic interdependency between two networks, the approach proposed by Islam and Mosehli (2012) and Hughes *et al.* (2020) was used. This involved delineating buffers around the links of the mode of concern to identify the links of the other mode that are at risk of concurrent disruption and adding their importance values to the importance of that link.

Recalling that for a mode m_1 , each link a is associated with a number of public transport trips (Section 3.3.1), the importance of the link was here defined as the number of trips of m_1 that traverse it on a typical weekday, as shown in Equation 3-1.

$$I^{m_1}(a) = t^{m_1}(a) \tag{3-1}$$

Where $t^{m_1}(a)$ is the number of public transport trips of m_1 traversing link a on a typical weekday.

Consider now two modes m_1 and m_2 operating on two separate infrastructure networks, where the former is the primary and the latter is the alternative. When link a of m_1 is affected by an area-wide hazardous event, links of mode m_2 located close to a and within the spatial footprint of the event can be also concurrently disrupted. In this case, the importance of link a is extended to account for the geographic interdependency between m_1 and m_2 . Because the assessment of importance here pertains to transport corridors, buffers around the links are preferred over grid cells to identify co-located infrastructure elements subject to geographic interdependencies (Hughes *et al.*, 2020). Therefore, the importance of a buffer of link a , includes the importance of the link itself, as well as the importance of neighbouring links of m_2 lying within the buffer zone of a . The importance of buffer of a is expressed in Equation 3-2.

$$I^{m_1, m_2}(a) = t^{m_1}(a) + t^{m_2}(D_a) \quad 3-2$$

Where D_a is the neighbourhood (buffer) of link a , which is mathematically defined as $D_a = \{x | d_{min}(x, a) \leq d\}$, i.e. each point in space x with a minimum Euclidean distance from a , denoted as $d_{min}(x, a)$, that is less than or equal to the selected buffer width d . Finally, $t_l^{m_2}(D_a)$ is the number of unique public transport trips of m_2 traversing the buffer zone D_a . The identification of public transport trips of m_2 traversing the buffer zone D_a allows considering only each neighbouring public transport trip in the importance of the buffer zone only once.

To assess the impact of rainfall-related geographic interdependencies between link a of m_1 and neighbouring links of m_2 on the importance of a , the importance value of Equation 3-2 was compared to that of Equation 3-1. In case that a significant number of trips of m_2 traverse the neighbouring links lying within the buffer zone of a , then the additional importance of m_2 significantly increases the importance of $I^{m_1}(a)$ (Equation 3-1) and thus a large number of trips of m_2 can be potentially disrupted concurrently with the trips of m_1 traversing link a . Conversely, if only a few trips of m_2 traverse the buffer of a , the increase in $I^{m_1}(a)$ is not considerable.

An important consideration is the selection of buffer width for the primary links of concern. Contrary to previous works on the assessment of importance, where the size of buffers or cells was arbitrarily selected, the spatial footprint of the hazard of concern was here explicitly considered. Specifically, because the importance was computed for flooding, the evidence from the spatial association between concurrent flood events, as presented in Section 3.3.2, was used to inform the size of buffers. This was done by identifying in the plots of conditional probabilities, the separation distances between railway and bus links that were associated with the highest probability values.

3.3.4. Assessment of criticality in the public transport networks

The criticality of a link encompasses both the probability of failure (weakness) and the consequences of failure (importance). The computation of weakness was here performed specifically for flooding, based on the historical datasets which are presented in Section 3.4. Similarly with the measure of importance in Section 3.3.3, acknowledging that concurrent flood events may occur within an area, the criticality of links was extended to account for the geographic interdependency between the two networks based on the results of the analysis in Section 3.3.2.

There are two methods in the literature for the empirical estimation of weakness of public transport links; the first method involves computing the frequency of incidents at the network level and then using it to estimate the incident frequency on links (Cats *et al.*, 2016; Hong *et al.*, 2015; Yap *et al.*, 2018), while the second method develops link-level fragility models (Yap and Cats, 2021). The former approach initially fits a probability distribution function to historical frequencies of incidents, which determines the expected incident frequency on the whole network. The expected number of incidents on a link is then derived from the network-wide frequency using explanatory variables (predictors). This is done by multiplying the network-wide frequency of events by the ratio of the value of variable for the link to the total value of the variable for all network links (Yap *et al.*, 2018). The advantage

of the method is that the estimation of incident frequency at the link-level is straightforward and does not require long datasets of historic events containing sufficient observations for each network link. However, because the predictor variables used typically refer to general network characteristics, such as link length, characteristics relevant to the hazard of concern may not be considered, potentially leading to less accurate predictions of link weakness (Yap and Cats, 2021).

The second method directly develops a model that predicts the probability of incidents occurring on a link based on explanatory variables relevant to both the hazard and link. The probability estimated is then translated to incident frequency for a time period of interest (e.g., one year). While this method may lead to more accurate estimates of link weakness, it requires identifying hazard-specific information that can be used to predict the probability of incidents, which can be a data-intensive task.

Specifically for flooding incidents caused by rainfall, the development of models that predict the probability of flood events occurring on links requires detailed data on the hazard (e.g., flood depth, rainfall intensity) and surrounding environment (e.g., slope, elevation, type and condition of drainage of the link) (Hong *et al.*, 2015; Lyu *et al.*, 2018; Liu *et al.*, 2018). However, detailed information on these variables was not available. Therefore, the estimation of weakness was based on the first method that was previously presented.

The expected network-wide frequency of rainfall-induced flooding incidents per week for each public transport mode m was computed. From a theoretical perspective, the Poisson and negative binomial distributions were regarded as suitable candidates to model frequency of events. For each mode m , both distributions were fitted to the observed frequency of flood events for each week of the study period and the best-fit function was selected on the basis of visual inspection and goodness-of-fit criteria. Then, from the weekly frequencies, the expected annual flooding frequency for each mode on the network level were obtained, as shown in Equation 3-3.

$$E(f_m) = n \cdot E(f_{m,w}) \quad 3-3$$

Where $E(f_m)$ is the expected annual network-wide frequency of flooding on mode m , n is the number of weeks over a year, and $E(f_{m,w})$ is the expected network-wide frequency of flood events on a week w .

Link length has been used in the literature to estimate the link-level frequency of various types of non-weather-related disturbances from the network-wide frequency (Cats *et al.*, 2016; Yap *et al.*, 2018), but also flooding (Hong *et al.*, 2015). Therefore, the expected frequency of flooding incidents on link a of mode m per year is as shown in Equation 3-4.

$$E(f_a^m) = E(f_m) \cdot \frac{l_a}{L_m} \quad 3-4$$

Where $E(f_a^m)$ is the expected frequency of flood events on link a , l_a is the length of link a and L_m is the total length of all links of mode m .

Using link lengths to estimate the flooding frequency is based on the assumption that longer links are more likely to experience flooding than shorter links, all things being equal. To take into account the potential effect of unobserved factors, the historical frequency of flooding on each link was introduced such that link weakness was defined as the difference between the average annual frequency and the expected annual frequency of flood events on a link, as shown in Equation 3-5.

$$W^{m_1}(a) = f_a^{m_1} - E(f_a^{m_1}) \quad 3-5$$

Where $f_a^{m_1}$ is the average annual frequency of flood events on link a , and $W^{m_1}(a)$ is the weakness of the link.

The metric $W^m(a)$ reflects the extent to which link a experienced a greater (or fewer) number of days of disruption than expected based on its length. When $f_a^{m_1}$ is higher than $E(f_a^{m_1})$, then it means that link a was disrupted more times than

expected, and therefore it is susceptible to flooding and requires further assessment. On the other hand, if $f_a^{m_1}$ is lower than or equal to $E(f_a^{m_1})$, then the link is much more robust to flooding than expected.

As previously stated, the criticality of a network element is the product of its weakness and importance and is expressed as in Equation 3-6.

$$C^{m_1}(a) = W^{m_1}(a) \cdot I^{m_1}(a) \quad 3-6$$

Following the same process with the measure of importance, when considering two modes m_1 and m_2 , and bearing in mind the joint exposure of them to flooding, criticality encompasses both the criticality of link a of m_1 as well as the criticality of neighbouring links of m_2 . The latter term is introduced to reflect the fact that links of m_2 located in close spatial proximity to link a may experience concurrent flooding-induced disruptions. Thus, the criticality is expressed as in Equation 3-7.

$$C^{m_1, m_2}(a) = C^{m_1}(a) + C^{m_2}(D_a) \quad 3-7$$

Where,

$$C^{m_2}(D_a) = (f_{D_a}^{m_2} - E(f_{D_a}^{m_2})) \cdot I^{m_2}(D_a) \quad 3-8$$

Where $f_{D_a}^{m_2}$ is the historic average of number of incidents on m_2 within buffer D_a and $E(f_{D_a}^{m_2})$ is the expected number of incidents on m_2 in D_a , which is given from Equation 3-4 based on the total length of links of m_2 located within the buffer.

Similarly with the importance of the buffer, the historic average and expected number of incidents was considered as a whole for the part of the network of m_2 within the buffer D_a , rather than for each link of m_2 separately.

3.4. Application of importance and criticality models

3.4.1. Network representation

Similarly with Chapter 2, discrete public transport networks consisting of rail and bus services in mainland Scotland were used to apply the models of importance and criticality; however, based on the availability of historical incident data, a subset of the bus network was used. As will be further explained in Section 3.4.2, while an incident dataset for the entire rail network was available, this was not the case for bus. Owing to the difficulty in acquiring and fusing these records, only several operating companies were selected to represent the bus network, namely Stagecoach, Scottish Citylink, National Express and Megabus. Although Stagecoach runs also shorter-distance services on the regional level, it was selected to keep these in the bus network, because incident data were retrieved for the entire network of Stagecoach (see Section 3.4.2) and, thus, valuable information would be discarded if these routes were removed from the analysis. Therefore, the subset of GTFS data for these four operators was extracted from the GTFS dataset of UK bus services.

For each public transport mode, the computation of importance and criticality requires the location of rail and bus links to be known, along with the public transport trips traversing each link. The location of links was derived from the rail and bus segments that were previously estimated, as described in Section 2.4. For bus, the route analysis that was performed to estimate the shape of bus segments in GIS provided also the road links of the OS MasterMap Highways Network (Ordnance Survey, 2021) that each segment uses, consequently providing the location and shape of each bus link and a lookup table between the links used by each segment. Furthermore, the trips that traverse each bus link were identified by determining from the GTFS dataset the trips that traverse each bus segment, and, by extension, the corresponding bus links based on the lookup table acquired from the previous step.

The process to derive rail links was similar to that of bus; however, it was selected to define infrastructure links in the corresponding infrastructure model for rail as those spanning between geographically consecutive rail stations or junctions, as defined in

the Scotland Route Specification (Network Rail, 2017). This was done because the incident records that were obtained by Network Rail, were used as the main source of data for rail incidents (Section 3.4.3) and were reported to occur on links between stations or junctions. The representation of the public transport network is shown in Figure 3-3.

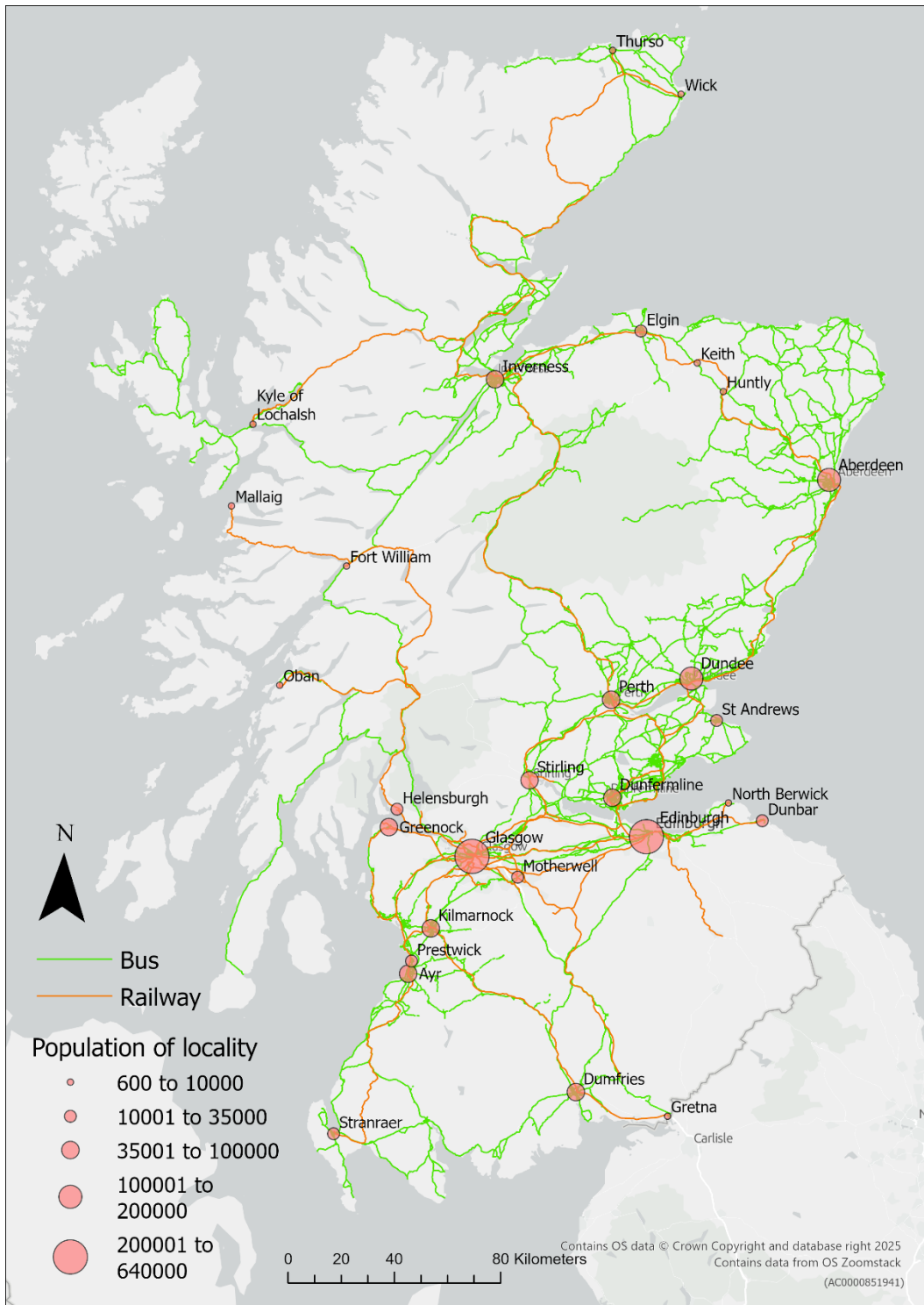


Figure 3-3 The geographical representation of the Scottish public transport network consisting of long-distance bus and rail services, along with selected main localities that these services connect and their corresponding population (Scottish Government, 2023).

3.4.2. Historical incident dataset for the bus network

For each mode, datasets were constructed containing historical flood events that disrupted each network between May 2017 and May 2020. Each dataset contained the date and location of the flood event, along with its impact on the flooded link, i.e. whether the link fully closed or remained partially open due to speed restrictions imposed or lane closures.

As can be seen in Figure 3-3, bus services included in this analysis use both trunk and local roads. Communication with the bus operating companies of interest revealed the absence of readily available records of flooding incidents which disrupted their services. Therefore, data from various sources were fused. These included official records of flood events for trunk roads used by the bus services, data retrieved from the operators' social media accounts and data from requests submitted to local authorities.

The main source of information was the dataset of flood events for the Scottish trunk road network acquired from Transport Scotland. These records are included in the agency's Integrated Road Information System (IRIS). This dataset spanned the period between 2013 and 2020 and included the start and end dates, duration, location, description of event and impact of the flooding on the availability of road (e.g., full closure, lane closure). Further information is included in Table S3 of Appendix B. Incidents that occurred from May 2017 to May 2020 were extracted and, based on the description of events, those that did not occur due to adverse weather, such as those caused by burst water mains, were excluded. Moreover, incidents that did not cause any disruption to the trunk road section, according to the relevant variable ("disruption caused"), were filtered out from the dataset, as it was assumed that the severity of flooding was not acute enough to cause disruption to the vehicular traffic traversing the road. For the events of interest, the types of flooding impacts on road infrastructure availability were re-classified to *full capacity reduction*, *partial capacity reduction* and *unknown*. Further information on this process is available in Table S4 of Appendix B.

In GIS, the flood events reported in the IRIS dataset were mapped onto the spatial layer of the road links used by bus services. For each incident, the coordinates of the location of flooding were available, along with the identification number of the respective trunk road section that was flooded. However, mapping of the coordinates onto the spatial layer of trunk road network revealed that these referred to the start node of each section, rather than the actual location of flooding. Therefore, it was selected to assume that the flooded location is the point at the mid-span of each trunk section. These points were subsequently snapped to the nearest trunk road link used by bus, which was considered as the link directly impacted by flooding. Points of IRIS incidents that were not snapped to any road link used by bus services were incidents that occurred outside of the bus network and were therefore excluded.

Although the IRIS dataset provided the flood events that occurred on the trunk road links used by bus, there were parts of the bus network that these do not cover. As such, relevant information was extracted from the Twitter accounts of all bus operators of concern. The data retrieval was carried out in two distinct stages. In the first stage, the latest posts (tweets) were pulled from each account to determine whether the operator makes regular announcements of service disruptions, to extract information on historical floods that affected the operator's services, and to identify relevant keywords used in the posts announcing flooding incidents. The tweets extracted in this first stage covered only a short time period, and therefore in the second stage, queries were submitted to Twitter to obtain data for a longer time period. For these queries, the keywords identified in the first stage were used, namely *flood, flooding, flooded, floods, surface water, floodwater, rain, rainfall*. The period covered by these queries spans between May 2017 to May 2020.

From the first stage, it was observed that only Stagecoach provided consistent updates via Twitter, and it was therefore selected to retrieve further data from the account of this operator only. The information extracted from the tweets included the date and time of the post announcing the incident, which was assumed to be the start date and time of the incident; location of flooding; the impact to services (e.g.,

cancellation, diversion, delay); and date and time of the post announcing the end of incident, which was assumed to be the end date and time of the incident. From the reported types of impacts on services, the impact of flooding on infrastructure availability of the flooded road was derived using the assumptions shown in Table 3-1.

Table 3-1 Types of flood impacts on Stagecoach services and re-classified impacts on the road infrastructure availability.

Information announced by Stagecoach	Type of impact for the bus dataset
Diversion of bus services to avoid specific location due to flooding	Full capacity reduction
Cancellation of bus services due to flooding at a specific location	
Termination of bus services at a location before the final stop of the trip to avoid specific location due to flooding	
Road passable with care	Partial capacity reduction
No information provided on the impact of flooding on a certain road or bus service	Unknown
Delay of bus service	

In GIS, the flood events reported by Stagecoach were mapped onto the road infrastructure layer containing the road links used by the bus services. The road infrastructure links that were directly impacted by each flood event were thus identified by mapping the reported incidents and then performing intersection between the spatial layer of incidents and road links. The mapping process presented challenges because the nature of reported location of flooding varied, and thus it was performed in a semi-automatic way. Further information on the mapping of events is included in Table S5 of Appendix B.

The mapping of incidents onto the road layer revealed that in several cases, the flooded locations reported were vague (e.g., long road stretch between two localities), therefore resulting in a significant number of road links being assumed to be flooded. To overcome this issue, it was assumed that flooding occurred at the point in the mid-span of this stretch, and the road link containing that point was the link directly impacted by flooding.

Because some of the local roads used by the services of Scottish Citylink, Megabus and National Express did not lie on the Stagecoach network, requests for flood incident data were submitted to local authorities responsible for these roads between May 2017 and May 2020. However, the responses from all local authorities, with the exception of Perth and Kinross council, did not provide any additional data, because the requested information was either refused or not available (Aberdeen City Council; Aberdeenshire Council; Angus Council; Argyll and Bute Council; Clackmannanshire Council; Dundee City Council; East Dunbartonshire Council; Falkirk Council; Fife Council; Perth and Kinross Council, personal communication, 16 November 2021). The information for the incidents provided for the local roads in Perth and Kinross included the start date and time of the event, name of the flooded road, type of flood impact on the road (e.g., road closed or passable with care), and, in some cases, the end date and time of event. These incidents were mapped and the impact types on the road infrastructure availability were re-classified using the processes previously described for the mapping of Stagecoach incidents.

Finally, to construct the dataset of historical flood events for the bus network, the various datasets were cross-referenced to identify duplicate events, which resulted in the removal of 9 duplicated incidents. Figure 3-4 summarises the process and steps that were carried out for the construction of the incident dataset of the bus network. The variables included within the final dataset are shown in Table 3-2.

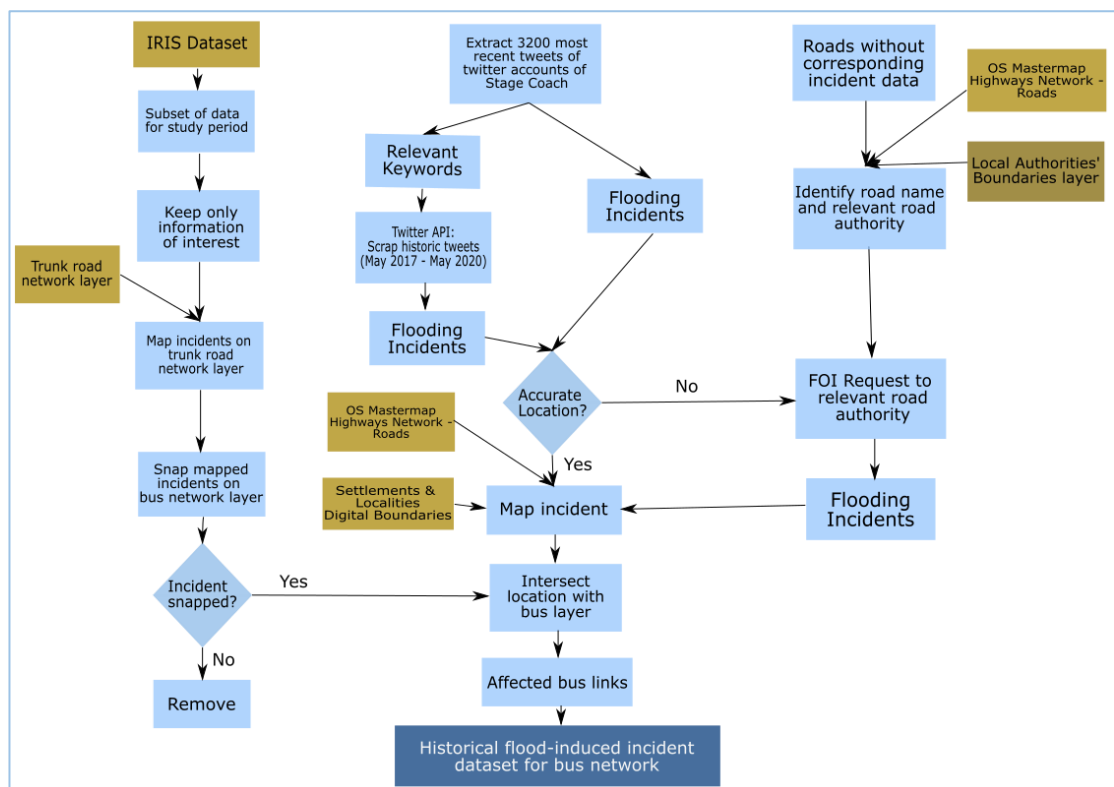


Figure 3-4 Steps of process (blue rectangles) and data sources (yellow rectangles) for the formation of the historical incident dataset for the long-distance bus network in Scotland

Table 3-2 Variables of the historical dataset of flood events for the long-distance bus network

Variable	Description
Incident ID	Unique identification number for the incident.
Start date	Date that the incident reportedly occurred.
Location	Textual description of the location of flood event as it appears in the original data source, such as Auchmill Road, Aberdeen.
Impact	The impact of the flood event on the infrastructure availability of the road that was directly impacted by the event. The possible values of this variable are: <ul style="list-style-type: none"> · Full capacity reduction: <p>This denotes the full closure of the road, i.e. no traffic was allowed to traverse it.</p> · Partial capacity reduction:

This refers to cases where the road can be used by traffic but less than normal, and corresponds to the cases of speed reduction, individual lane closures or where it was announced by the relevant authority or operator that the road is passable with care.

- Unknown.

Reasoning for impact value In case that the event impact on the infrastructure availability of the road has been formed based on assumptions (see Table S4 of Appendix B), the relevant information used to make these assumptions is included.

For example, in case that a full road closure was assumed for an incident due to a bus service having to divert to avoid a certain location, the value of this variable would be noted as “Diversion”.

gml_id Unique identification code of the flooded road link, as it appears in the road links used by the long-distance bus services, which is a subset of the OS Mastermap Highways Network spatial layer (Ordnance Survey, 2021).

Duration The duration of flooding incident, expressed in hours.

Source The dataset in which the incident was originally recorded. For example, IRIS Dataset, Stagecoach Twitter, Perth and Kinross Council.

Several limitations were observed in the dataset pertaining to the uncertainty associated with the duration and location of events, but also the spatial coverage of the network due to the unavailability of incident data for several local roads. Firstly, regarding the duration of events, in the case of the 194 incidents provided by the IRIS dataset, although the start and end dates of events were provided, the exact times of day that the incidents occurred and ended were not known; hence, this did not allow to validate the duration of events. Because it was observed in the wider IRIS

dataset spanning from 2013 that negative or unrealistically high duration values were present, it was concluded that the recorded durations cannot be considered as accurate. Furthermore, for 60 out of the 98 incidents in the final dataset reported by Stagecoach, the end date and time of events was not known, and therefore the duration could not be computed. For 5 incidents provided by the local authorities, the duration of the incident was also unknown. Thus, for 65 out of the 345 incidents, the duration was unavailable and, for 194 events, confirming the accuracy of their duration was not possible. Due to this missing information, the incident duration was not considered in the calculation of weakness of links.

Another important limitation of the final bus dataset relates to the accuracy of incident locations. Specifically in the IRIS dataset, flood events were reported to occur on trunk road sections, which, however, span in length from a few metres to several kilometres and thus resulted in more than one bus link being assumed to be flooded. This was also the case for the incidents reported by Stagecoach and local authorities, where, in several instances, long roads containing multiple bus links were reported to be directly affected by flooding. For only 39 out of 345 incidents in the final dataset, the location of flooding was originally reported as one link. In the Stagecoach dataset, the location of flooding was not given in all cases. For incidents where the location of flooding was not stated, internet searches were carried out using related keywords and requests were made to the relevant local authorities² to obtain further information. In cases that no road incidents were identified in the internet search or by the local transport authorities, then the incident was omitted from the dataset due to insufficient information, and, as such, 8 incidents were excluded.

A final limitation was that, because 9 local authorities did not provide data on past flood events that occurred within their network, the incident dataset did not cover

² The local authorities to which requests were made were the West Lothian Council, Moray Council, Fife Council, Dumfries and Galloway Council, Ayrshire Roads Alliance, Highway Council, Perth and Kinross Council, and City of Edinburgh Council. However, the Dumfries and Galloway Council, City of Edinburgh Council and Ayrshire Roads Alliance did not provide the requested data.

5,714 local road links used by Scottish Citylink, Megabus and National Express, which amounts to less than 10% of all bus links. These links were located mainly in central Scotland and connect Glasgow, Edinburgh and Stirling, but also a few links in South-East and North-East Scotland. Because most of the road links without associated incident data were located in central Scotland, where the density of the railway network is high and proximity between bus and rail links is also high, it is possible that a number of concurrent flooding events were not included in the data set (due to the unavailability of bus incident data) and that the extent of geographic interdependencies between the networks was underestimated in the subsequent analysis.

3.4.3. Historical incident dataset for the railway network

Two main sources of information contributed to the incident dataset for the railway network, namely official records of flooding incidents acquired from Network Rail, the railway infrastructure manager of the UK, and data retrieved from the Twitter accounts of Network Rail as well as ScotRail which is the main operator of railway services in Scotland. The official incident dataset of Network Rail was the main source of information, whilst the latter was used to augment the former.

To maintain consistency with the bus network incident dataset, data was obtained from Network Rail for the period from May 2017 to May 2020. For each flooding incident, the dataset included the start and end dates and times, brief description and location of incident. Further information on the variables included is presented in Table S6 of Appendix B. Incidents that occurred outside of Scotland were excluded from the dataset. Moreover, a variable was created that captured the impact of flooding on the railway infrastructure. This was based on the description of incidents, which in several cases included whether the directly impacted railway line was closed or subjected to speed restrictions. However, the impact was documented for only 22 out of the 279 incidents.

The incidents were mapped on the layer of rail infrastructure network in GIS based on their reported locations. Specifically, these were reported to occur either on nodes (stations, junctions) or rail sections between two stations. In the former case, the flooded links were considered as those starting from or ending at the flooded node and in the latter case, flooded links were those spanning between the two stations. Further information on the mapping of events is included in Table S7 of Appendix B. The mapping process revealed that, in most cases, the railway sections that were originally assumed to be flooded, contained multiple railway links, unlikely to be simultaneously inundated.

Due to the limitations of the acquired dataset on the accuracy of incident location and impact, further data were retrieved from Twitter. The same process for data extraction was followed as with the bus incident dataset (Section 3.4.2). The latest tweets from the official Twitter accounts of Network Rail and ScotRail were extracted to identify flooding incidents that disrupted the network, and to identify relevant keywords used to announce flooding-induced disruptions to the public. Based on the identified keywords, which were the same as those for bus, relevant posts from May 2017 to May 2020 were retrieved from the two accounts of interest. These provided the date and time of the post announcing the incident, which was assumed to be the start date and time of the incident, the flooded location, type of flood impact on the infrastructure availability (e.g., line closed, speed restriction of rail vehicles), and date and time of the post announcing the end of event, which was considered as the end date and time of the incident. Finally, the incidents were mapped using the same process as for the dataset acquired from Network Rail.

After constructing the dataset from posts of the Twitter accounts, it was cross-referenced to the Network Rail's dataset to identify duplicate events. In the case that an event was reported in both datasets, then, the additional information included in the Twitter dataset was used to augment the official record from Network Rail. This process resulted in the final incident dataset for rail. Table 3-3 includes the variables of the dataset and a summary for each one of them. Note that although the time of

day was available for both the start and end days of incidents, it was decided not to include it for the sake of consistency with the incident dataset of the bus network.

Table 3-3 Variables in the historical incident dataset of flood events on the railway network.

Variable	Description
Incident ID	Unique identification number for the incident.
Start date	Date that the incident reportedly occurred.
Location	Textual description of the location of flood event as it appears in the original data source, such as Glasgow Central to Pollokshields East.
Impact	<p>The impact of the flood event on the infrastructure availability of the road that was directly impacted by the event. The possible values of this variable are:</p> <ul style="list-style-type: none"> · Full capacity reduction: This denotes the full closure of the railway link, i.e. no railway trips were allowed to traverse it. · Partial capacity reduction: This refers to cases where the link was passable but could be used less than normal and corresponds to the cases of speed restrictions, reduced frequency of railway trips, and prohibition of electric vehicles traversing the link. · Unknown.
Link ID	The unique identification code of the flooded railway link.
Duration	The duration of flooding incident, expressed in hours.
Information from tweets	The variable includes a brief description of the Twitter information (if any) used to augment the records, such as impact category on infrastructure availability, location of event.

Similarly with the incident dataset for bus, there are several limitations associated with the dataset of the railway network. The main limitation was that for 61 out of 279 incidents, the reporting of flooded location was not specific enough which resulted in multiple infrastructure links of the network being assumed as flooded. Further communication with Network Rail revealed that more accurate information on the location of inundation was not available (Network Rail, personal communication, 30 September 2021). Therefore, for incidents that more than one infrastructure link was reported to be flooded, the same strategy as with the bus network was adopted, which involved assuming the point at the mid-span of the series of presumably flooded links was the location of inundation, and the rail infrastructure link coinciding to that point was assumed to be the flooded link. Exceptions to this process were incidents that occurred on nodes, as in this case all links starting from or ending to the node were considered as flooded.

Another limitation of the dataset is the lack of reporting of the type of flooding impact on the link infrastructure availability. Although the data retrieved from social media provided this information for some incidents, for most events (approximately 62%), the type of impact was still unknown. This created challenges in estimating the weakness of railway links in terms of the distinct impact categories of flooding on infrastructure availability, and therefore, the weakness of links and buffers was estimated without making distinction between the various types of impact that flooding can have on the links.

3.5. Results

In the study period, 343 rainfall-related flooding incidents disrupted the bus network based on the dataset for bus (Section 3.4.2), consequently leading to either speed restrictions on bus links or their full closure. As a result, 265 bus links were directly affected by flooding at least once, which corresponds to approximately 0.45% of the total bus links (after excluding the links for which no incident data could be obtained). Table 3-4 shows the distribution of the average annual frequency of flood incidents across the bus network which reveals that most links were not disrupted in the study period, and that for those links which were disrupted, the average annual frequency of flooding did not exceed one.

Table 3-4 Average annual number of flooding incidents on bus links from May 2017 to May 2020.

Average annual frequency of flood event	Number of road links	Percentage of road links
No events	57,029	99.54 %
0 < events ≤ 1	259	0.45 %
1 < events ≤ 2	4	0.007 %
More than 2 events	2	0.003 %

On the railway network there were 279 flooding incidents, and 162 railway links were directly affected by flood events at least once, which amounts to 42.41% of the railway links in total. Table 3-5 shows the distribution of the average annual frequency of flood incidents across the railway network.

Table 3-5 Average annual number of flooding incidents on railway links from May 2017 to May 2020.

Average annual frequency of flood event	Number of rail links	Percentage of rail links
No events	220	57.59 %
0 < events ≤ 1	130	34.03 %
1 < events ≤ 2	26	6.81 %
More than 2 events	6	1.57 %

On 68 out of the 1,096 days within the study period, concurrent flooding incidents on the bus and railway networks occurred. To confirm if concurrent disruptions on the two networks are correlated, Cramer's V association test was performed for two categorical variables indicating the existence of at least one flood event on each network, for each day of study period. Cramer's V test hypothesises that the variables are independent of each other and thus no correlation exists between them. The computed statistic of the test takes values between 0 and 1, with the former indicating very weak association, while the latter strong association. In this case, the Cramer's V results ($ES = 0.43, p = 0$) indicated a statistically significant, moderate association between events on the two networks. This means that flooding incidents tend to co-occur on both networks to a moderate degree. Although Cramer's V association test revealed association between flood events on the system-level, it does not provide indications on geographic interdependencies between the two networks.

3.5.1. Geographic interdependencies between the public transport modes due to rainfall

The method of conditional probabilities (Section 3.3.2) was applied to detect spatial patterns between concurrent flooding incidents caused by a rainfall event and assess the existence of geographic interdependency between modes. It should be noted that bus links for which no incident data could be obtained were excluded from the analysis.

Figure 3-5 shows the conditional probability plots for each public transport mode and corresponding fitted exponential regression lines.

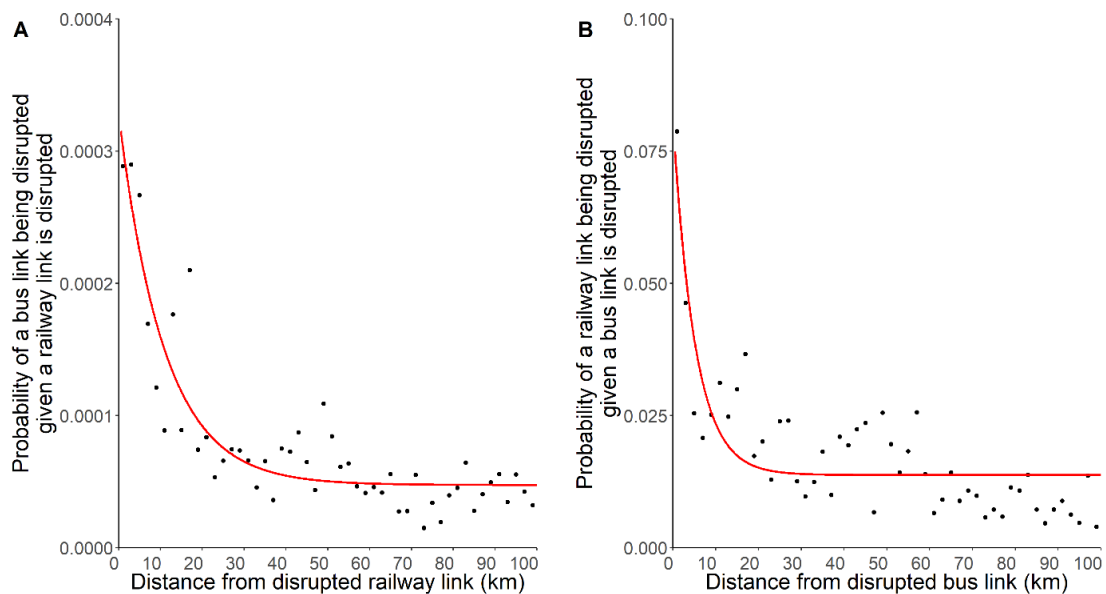


Figure 3-5 Plots of probability of (A) bus links being disrupted given that a railway link at a certain distance is disrupted (B) railway links being disrupted given that a bus link at a certain distance is disrupted. The red lines are the exponential regression lines fitted to the data. Note the different scales of the y-axis of the plots.

Both probability plots are characterised by a distance decay function, which shows that links of the two modes lying in close proximity are more likely to be concurrently flooded than links separated by larger distances. This confirms that geographic interdependencies between railway and road infrastructure links used for long-distance travel in Scotland indeed exist as a result of rainfall. For $P(Bus|Rail)$ in Plot A of Figure 3-5, the highest probability values are observed for the first 4 km of separation distances. Furthermore, it is generally observed that the first 20 km are associated with higher values of conditional probabilities compared to larger values of separation distance between railway and bus links probabilities. Similarly with Plot A, for $P(Rail|Bus)$ (Plot B of Figure 3-5) the highest probability values are also observed for the first 4 km of separation distances.

Furthermore, it is worth noting that the conditional probability values of $P(Bus|Rail)$ are significantly lower than those of $P(Rail|Bus)$. This may be attributed to the structure of the two networks. Specifically, the bus network consists of a significantly high number of road links which are of short length, while the rail network comprises fewer and longer links. Thus, there are typically more bus links

within the buffer ring of a given rail link compared to the number of rail links in a given bus buffer ring. Therefore, when a flood event is recorded on one bus link within the rail buffer ring of concern, the resulting proportion of bus links being flooded, which reflects the conditional probability of flood co-occurrences, is typically low due to the high number of bus links located in the buffer ring. Conversely, when there is a flood event recorded on a rail link within a specific bus buffer ring, the resulting proportion of rail links being concurrently flooded with the bus link of concern is typically high because only a few longer rail links are within the bus buffer ring. This, in conjunction with the fact that the average frequency of flooding on bus being just slightly higher than that of rail (see Section 3.5.3), resulted in lower conditional probabilities for the former compared to the latter mode.

The parameters of the fitted exponential model for $P(Bus|Rail)$ and diagnostics are included in Table 3-6. The results suggest that the distance of bus links to disrupted railway links plays a statistically significant role in concurrent disruptions for the network of the case study. Similarly, Table 3-7 includes the parameters and diagnostics of the exponential model for $P(Rail|Bus)$, which also confirms that the separation distance from flooded bus links is a statistically significant predictor of the likelihood of railway links being flooded. The residual standard error of the fitted model ($8.5 \cdot 10^{-3}$) indicates high goodness of fit.

Based on the plots of Figure 3-5 and the statistically significant role of separation distances to the conditional probabilities, it can be concluded that geographic interdependencies exist between the modes of the Scottish public transport network, specifically for rainfall. This means that railway and bus links in close proximity may be concurrently flooded in the event of heavy rainfall. Since in both plots of Figure 3-5 separation distances of up to 4 km are associated with the highest conditional probability values, a 4 km buffer width was selected to assess the impact of geographic interdependencies on the importance and criticality of links within the public transport network. This 4km-wide buffer represents the typical spatial scale of rainfall events that may result in the concurrent flooding of rail and bus links.

Table 3-6 Parameters and diagnostics of the fitted exponential model predicting the conditional probability of a bus link being disrupted given that a railway link is disrupted due to pluvial flooding.

	Value	Standard error	t value	p-value	2.5% confidence interval value	97.5% confidence interval value
alpha (α)	$2.80 \cdot 10^{-4}$	$2.43 \cdot 10^{-5}$	11.54	< 0.001	$2.31 \cdot 10^{-4}$	$3.29 \cdot 10^{-4}$
beta (β)	$-9.19 \cdot 10^{-2}$	$1.32 \cdot 10^{-2}$	-6.95	< 0.001	$-1.19 \cdot 10^{-1}$	$-6.53 \cdot 10^{-2}$
theta (θ)	$4.74 \cdot 10^{-5}$	$5.28 \cdot 10^{-6}$	8.99	< 0.001	$3.68 \cdot 10^{-5}$	$5.81 \cdot 10^{-5}$

Table 3-7 Parameters and diagnostics of the fitted exponential model predicting the conditional probability of a railway link being disrupted given that a bus link is disrupted due to pluvial flooding.

	Value	Standard error	t value	p-value	2.5% confidence interval value	97.5% confidence interval value
alpha (α)	0.067	0.010	6.73	<0.001	0.04	0.08
beta (β)	-0.19	0.042	-4.53	< 0.001	-0.28	-0.11
theta (θ)	0.013	0.001	11.29	< 0.001	0.011	0.016

3.5.2. Impact of rainfall-related geographic interdependencies on the importance of public transport links

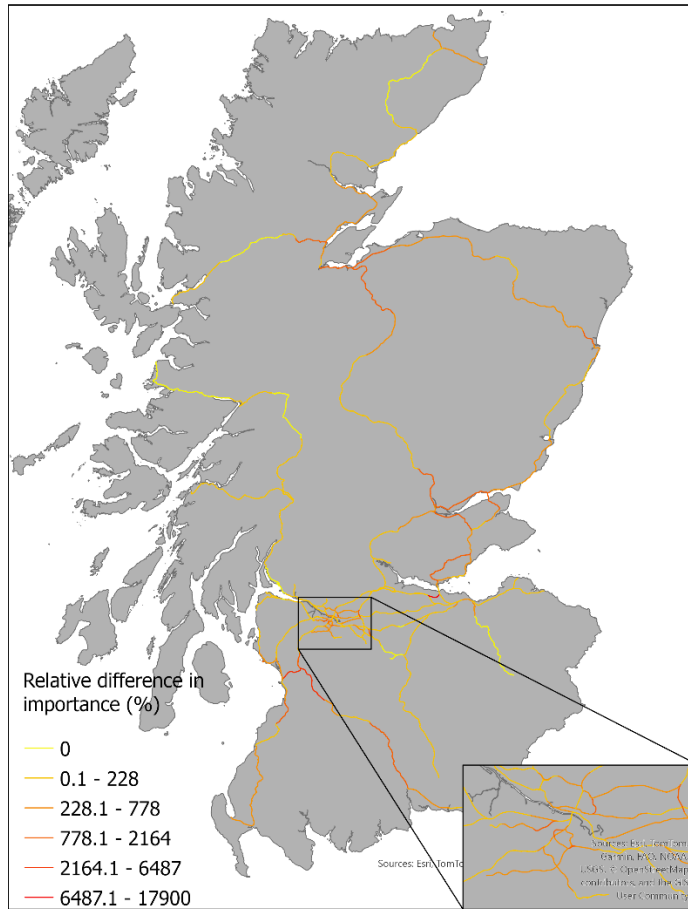
The analysis on spatial patterns of concurrent disruptions between railway and bus links revealed the existence of geographic interdependencies between the two modes due to rainfall. To incorporate this interdependency into the analysis of importance, buffers were formed around each public transport link and the trips traversing the links of the other mode located within these buffers were considered in the measure of importance. Based on the evidence revealed from the spatial association between concurrent events, the width of buffers was set to 4 km.

To assess whether the ranking of importance of links is significantly different from that of their corresponding 4 km buffers, Spearman's correlation test was performed, which measures the strength and direction of relationship between two variables. The test hypothesises that there is no significant relationship between the two variables and its statistic ρ takes values between -1 and 1. Values of ρ close to -1 indicate strong negative relationship between the ranks of the variable, and those close to 1 reflect strong positive relationship. In this case, the test revealed a statistically significant, moderate (positive) relationship between importance of links and buffers, for both rail ($\rho = 0.57, p < 0.001$) and bus ($\rho = 0.49, p < 0.001$). This suggests that public transport links and their respective buffers are characterised by similar importance values, however exceptions to this also exist which is further confirmed by the scatterplot of Figure S3 of Appendix B.

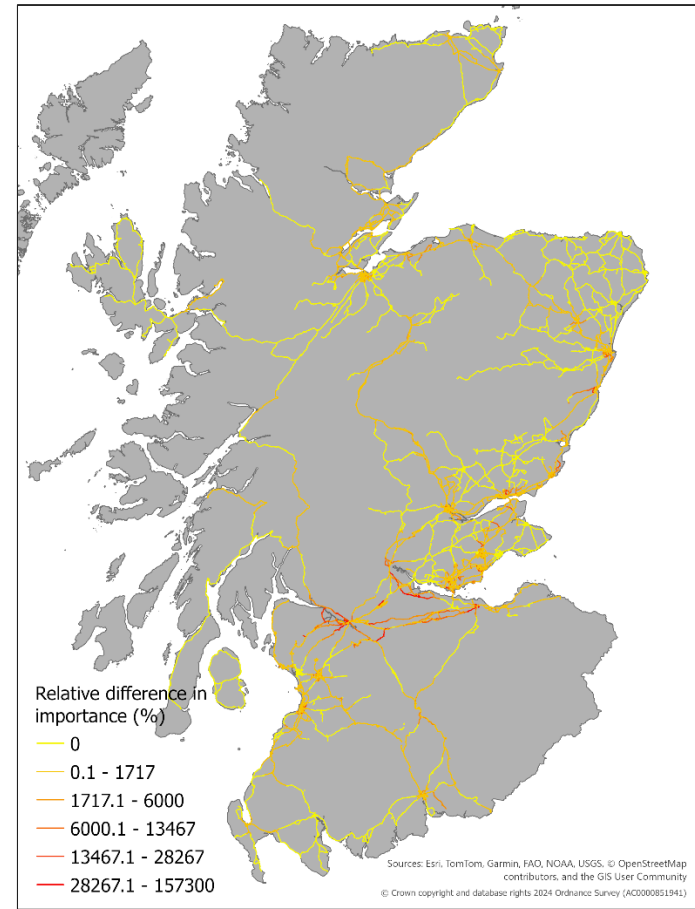
It is observed that for both modes, there are links of low importance which however have very high importance values when considering the neighbouring links of the other mode within their 4km buffer. To ascertain where these links are located, maps were produced showing the geographic distribution of relative differences in importance of links for rail and bus, when considering their geographic interdependencies due to flooding, as shown in Figure 3-6 below.

The results reveal that significant increases in importance of links are observed within and around urban centres of Scotland, such as Glasgow and Edinburgh, for both rail

(Figure 3-6(a)) and bus (Figure 3-6(b)), while low increases are noted for the rest of the country, particularly in North-East Scotland. This could be attributed to the high density of both rail and bus networks, coupled with the high number of trips that operate in these areas. The significant scale of increases in importance for rail and bus links indicate that are traversed by only a few trips of the same mode, while a substantial number of trips of the alternative mode operate within 4 km from those links.



(a) Rail



(b) Bus

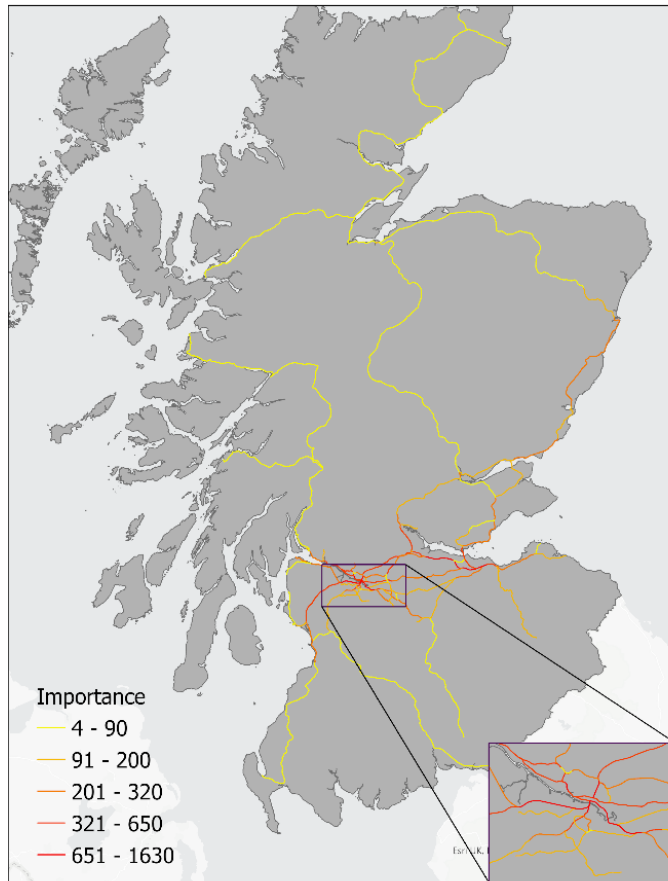
Figure 3-6 Relative increases in importance of (a) rail and (b) bus links as a result of their geographic interdependencies due to rainfall. Note the different classification scales in the two maps. The classification of values was done using the Jenks natural breaks classification method.

To further understand how the geographic distribution of importance values changes for each mode, maps of importance of links and 4km-wide buffers were produced for each mode.

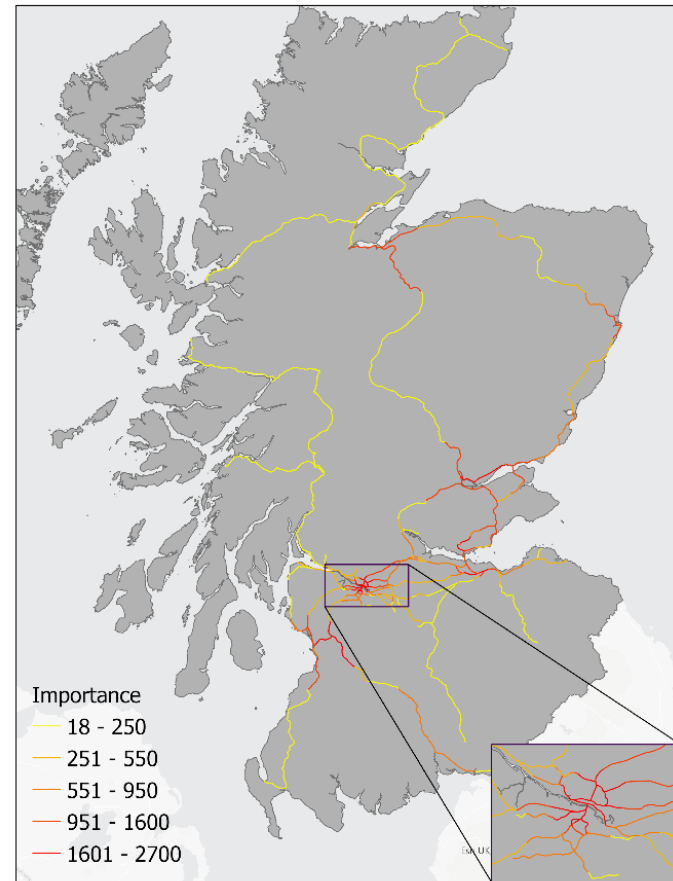
The results of the geographical distribution of importance values for railway are shown in Figure 3-7 below. Note that the importance values were classified using the Jenks natural breaks classification algorithm, because it reveals clusters of values that exist in the data (De Smith *et al.*, 2007). Although the scales of two maps are different and, therefore, direct comparison is not possible, the results can be interpreted qualitatively. In this case, this is sufficient because the focus is on the ranking of links and buffers according to their importance, rather than their absolute values.

In the case of railway links (Figure 3-7(a)), the most important links are clustered in the central part of Scotland (within the inset map), where the two largest and most populated cities of the country are located, and thus generate a significant number of public transport trips. Links of high importance are also observed close to other urban centres, particularly in North-East and South-West Scotland, while rural and remote locations are associated with low importance values. When considering the 4km buffers of the links (Figure 3-7(b)), the results reveal that, while buffers in central Scotland are still characterised of the highest importance, significant increases are also observed in other parts of the country as well, especially in North-East Scotland but also South-West.

It is further apparent that the buffers in North-West and North Scotland, which are in rural and remote areas, remain of low importance. These observations show that important bus links that are traversed by many bus trips on a typical weekday are located in close proximity (less than 4 km) to railway links of high importance, particularly close to large cities and towns of the country. This suggests that if flood events occur within these areas, significant adverse consequences are expected to the public transport network. The lack of increase in importance of railway buffers in rural locations could be attributed to the fact that the bus links within the buffers are of low importance, as shown in Figure 3-8 below.



(a) Rail links

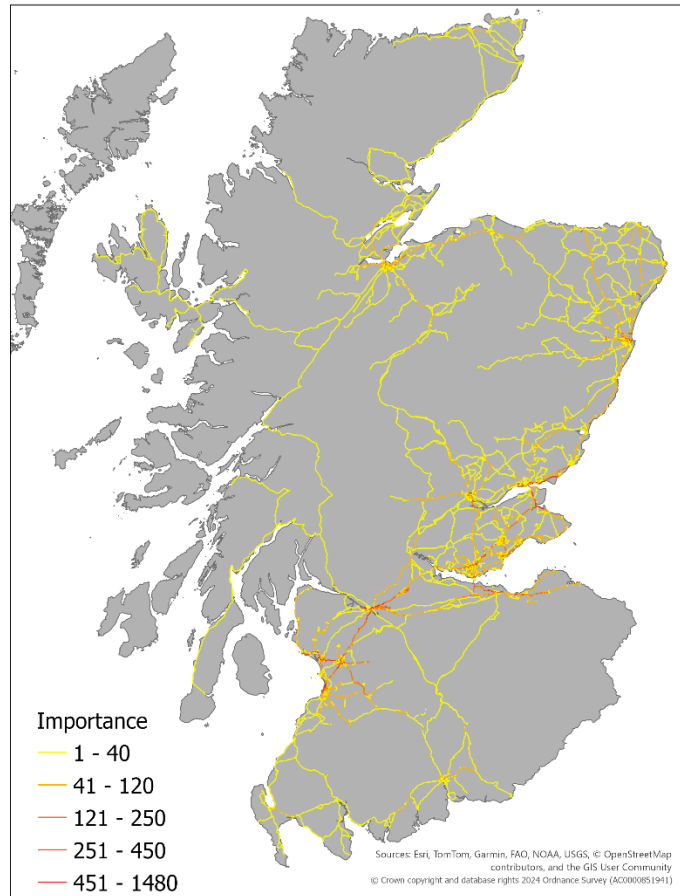


(b) 4km Rail buffers

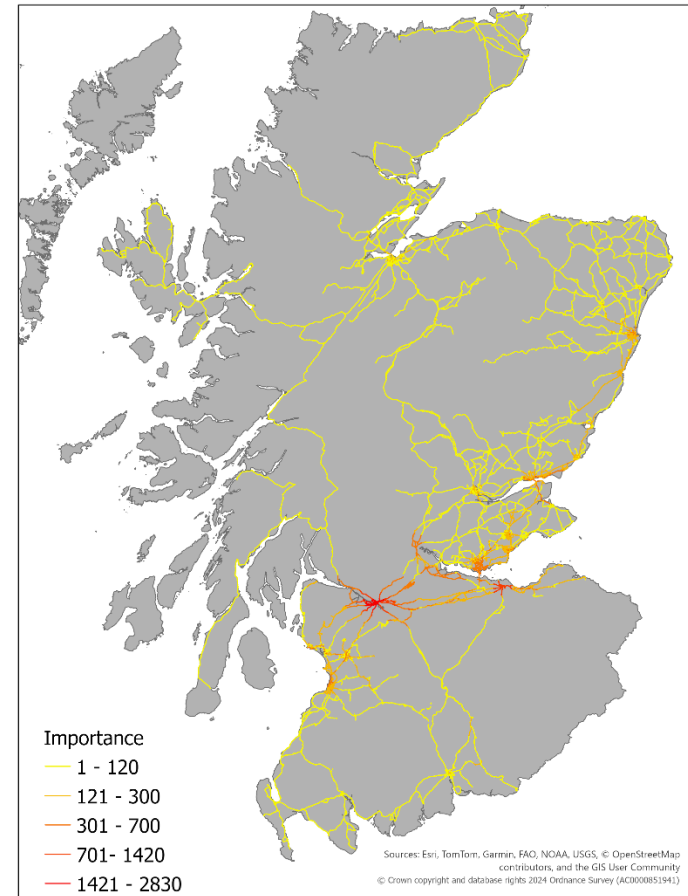
Figure 3-7 Importance of (a) railway links and (b) 4 km railway buffers. Note the different classification scales in the two maps. High values suggest that a significant number of public transport trips traverse the link or buffer. It should be also noted that in the map referring to 4 km buffers of links, the widths of the buffers are not included in order for the results to be clearly shown.

Similarly, Figure 3-8 shows the geographic distribution of importance of links and buffers for the bus network.

The results for the bus links (Figure 3-8(a)) show that most links are characterised of very low importance, meaning that only up to 40 bus trips traverse them on a typical weekday. Unsurprisingly, links of higher importance are observed close to cities and towns of the country, particularly in central, North-East and South-West Scotland; thus, indicating that the geographic distribution of link importance for bus is similar with that of the railway. Regarding the 4 km bus buffers (Figure 3-8(b)), it is observed that the areas in central Scotland are still classified as high importance and that the number of highly important buffers in this area is also increased. This is because railway links of high importance values are located in close proximity (less than 4 km) from these bus links. Furthermore, it is noteworthy that there are bus buffers in smaller towns of the country, specifically in North-West Scotland, of which the importance is higher compared to the corresponding links in Figure 3-8(a), thus indicating that highly important railway links are located within these bus buffers. Again, for the case study, the geographic distribution of bus buffers is very similar to that of rail, with high importance being observed in large urban centres and low importance in rural and remote locations.



(a) Bus links



(b) 4km Bus buffers

Figure 3-8 Importance of (a) bus links and (b) 4 km bus buffers. Note the different classification scales in the two maps. High values suggest that a significant number of public transport trips traverse the link or buffer. It should be also noted that in the map referring to 4 km buffers of links, the widths of the buffers are not included in order for the results to be clearly shown.

3.5.3. Impact of rainfall-related geographic interdependencies on the criticality of public transport links

Whilst the assessment of importance considered the spatial footprint of rainfall events resulting in the concurrent flooding of links, it did not account for the probability of each link experiencing flooding-induced disruptions in the event of heavy rainfall. This limitation can be overcome by computing and assessing the criticality of links and buffers.

Weakness

The average weekly frequency of flooding incidents that occurred on the railway network was equal to 1.76, whilst for bus was 2.18. The Poisson and Negative Binomial distributions were therefore trialled to model the weekly frequency of pluvial flooding for each mode. The distribution fitting process revealed that the Negative Binomial distribution better fitted the frequency values in both cases. This is expected because, as opposed to the Negative Binomial distribution, the Poisson distribution assumes that the mean and variance of the variable of concern are roughly the same, which is not the case for bus ($\mu = 2.17, \sigma^2 = 13.80$) or rail ($\mu = 1.75, \sigma^2 = 18.35$). The parameters of the fitted distributions for rail and bus are provided in Table 3-8 and Table 3-9, respectively.

Table 3-8 Parameters of the fitted Negative Binomial distribution function to the weekly frequency of flooding incidents on the railway network due to rainfall.

	Estimate	Standard error
Size	0.203	0.036
mu	1.766	0.329

Table 3-9 Parameters of the fitted Negative Binomial distribution function to the weekly frequency of flooding incidents on the bus network due to rainfall.

	Estimate	Standard error
Size	0.432	0.0713
mu	2.171	0.288

The selection of this function was concluded based on visual inspection of the fitted functions to the empirical values, as shown in Figure 3-9, and from comparison between goodness-of-fit statistics included in Table 3-10 for rail and Table 3-11 for bus. For both networks, the results reveal that all goodness-of-fit criteria of the Negative Binomial distribution are related to lower values than those of Poisson, as such indicating a higher goodness-of-fit. The high goodness of fit of the former function is further confirmed in Figure 3-9.

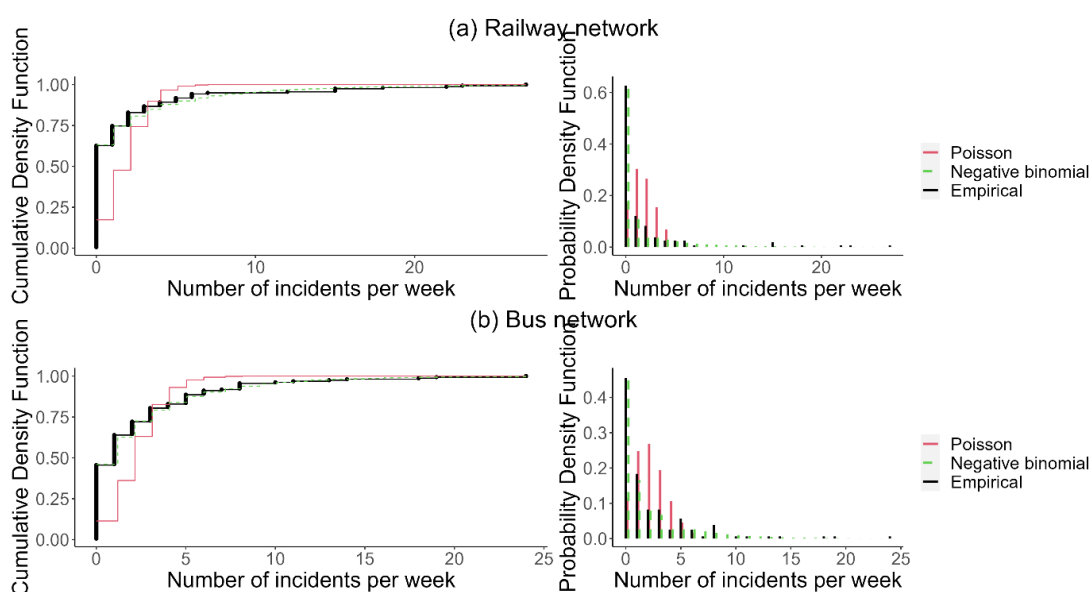


Figure 3-9 Empirical and fitted probability distribution functions for the weekly frequency of flooding incidents on the (a) railway network and (b) bus network.

Table 3-10 Goodness-of-fit criteria for the fitted probability functions to the weekly frequency of flooding incidents on the railway network.

Probability function	Log-likelihood	AIC	BIC
Poisson	-516.695	1035.39	1038.453
Negative binomial	-242.621	489.241	495.366

Table 3-11 Goodness-of-fit criteria for the fitted probability functions to the weekly frequency of flooding incidents on the bus network.

Probability function	Log-likelihood	AIC	BIC
----------------------	----------------	-----	-----

Poisson	-474.571	951.144	954.201
Negative binomial	-299.660	603.319	609.444

Based on the fitted Negative Binomial distributions and using Equation 3-4, the resulting annual frequency of pluvial flooding was computed to be approximately 85 events for railway and 105 events for bus. The expected frequencies of flood events per year were computed for the bus and rail links using Equation 3-5 and the results are included in Table 3-12 and Table 3-13, respectively. Note that these frequencies were not computed for the bus links for which no incident data was available.

Table 3-12 Expected annual number of flood events on bus links due to rainfall.

Expected annual frequency of flood events	Number of bus links	Percentage of bus links
0 < events ≤ 1	57,294	100%
1 < events ≤ 2	0	0%
More than 2 events	0	0%

The results for bus (Table 3-12) reveal that all bus links are expected to experience less than one pluvial flooding incident per year. This is because the expected network-wide frequency of flooding is multiplied by the ratio of each link's length and the total length of all bus links, the latter being significantly higher than the former. Due to the multiplicative form of the equation to estimate the expected frequency of flooding on links from the network-wide frequency (Equation 3-4), no bus links had an expected frequency of zero, which may lead to overestimation of flooding frequency of links in some cases. Comparing these expected frequencies to the observed ones in Table 3-4 shows that a few links experienced more events than expected.

Table 3-13 Expected annual number of pluvial flood events on rail links due to rainfall.

Expected annual frequency of flood events	Number of rail links	Percentage of rail links
0 < events ≤ 1	413	98.57%

1 < events ≤ 2	5	1.19%
More than 2 events	1	0.24%

Similarly for rail, most links were expected to experience less than one flood event per year and only one link was expected to experience more than two events due to rainfall. The comparison of expected frequencies (Table 3-13) with the observed ones in Table 3-5 shows that within the three-year study period, more links experienced at least one flood event per year than expected.

Using Equation 3-5, the weakness of bus and rail links to pluvial flooding was computed and the results are as shown in Table 3-14 below.

Table 3-14 Weakness of bus and rail links to rainfall.

Link weakness	Bus		Rail	
	Number of links	Percentage of links	Number of links	Percentage of links
Below 0	5028	7.99%	278	66.36%
0 to 0.99	57874	91.99%	118	28.16%
1 to 1.99	9	0.01%	15	3.58%
2 to 2.99	2	< 0.01%	5	1.19%
Higher than 3	0	0	3	0.72%

The results of Table 3-14 show that most railway links were associated with negative values of weakness, indicating that most links experienced fewer incidents than expected over the study period. Specifically, only 23 links were identified as weak, which amounts to roughly 5.5% of the total rail links. Furthermore, most bus links had a weakness of approximately zero and only 11 were identified as weak, which corresponds to less than 0.1% of the total links of the bus network. This is because both the average (Table 3-4) and expected (Table 3-12) frequencies of flood events were very close to zero.

Criticality

Spearman's correlation test was performed on the computed criticality values, which measures the strength of relationship between two variables and hypothesizes that no relationship exists between them. The results revealed a statistically significant, moderate association for rail ($\rho = 0.41, p < 0.001$), but very weak for bus ($\rho = 0.07, p < 0.001$). The latter could be attributed to the fact that, when ignoring the geographic interdependencies between bus and rail links, the criticality of bus links is approximately zero due to their weakness being very close to zero. However, when accounting for the railway links located within the 4 km buffers of bus links, the criticality of the buffer of the bus links is significantly higher, due to the criticality of the railway links.

The correlation results are confirmed in Figure 3-10 and further show the absence of strong correlations in both cases, which indicates that even if a link is not critical, in some cases the criticality of the corresponding buffer is markedly higher due to highly critical links located in close proximity.

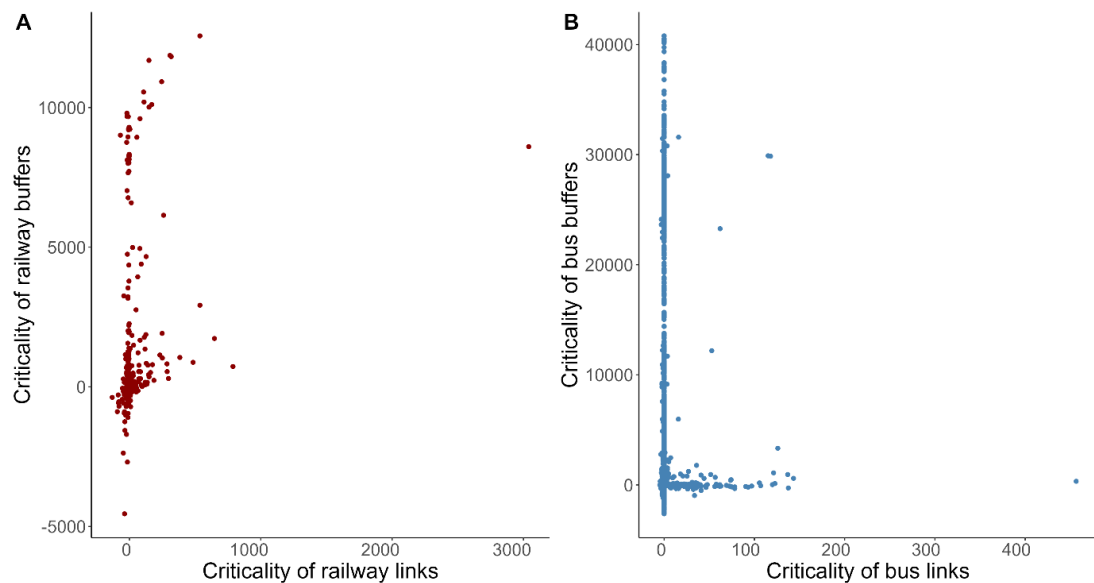
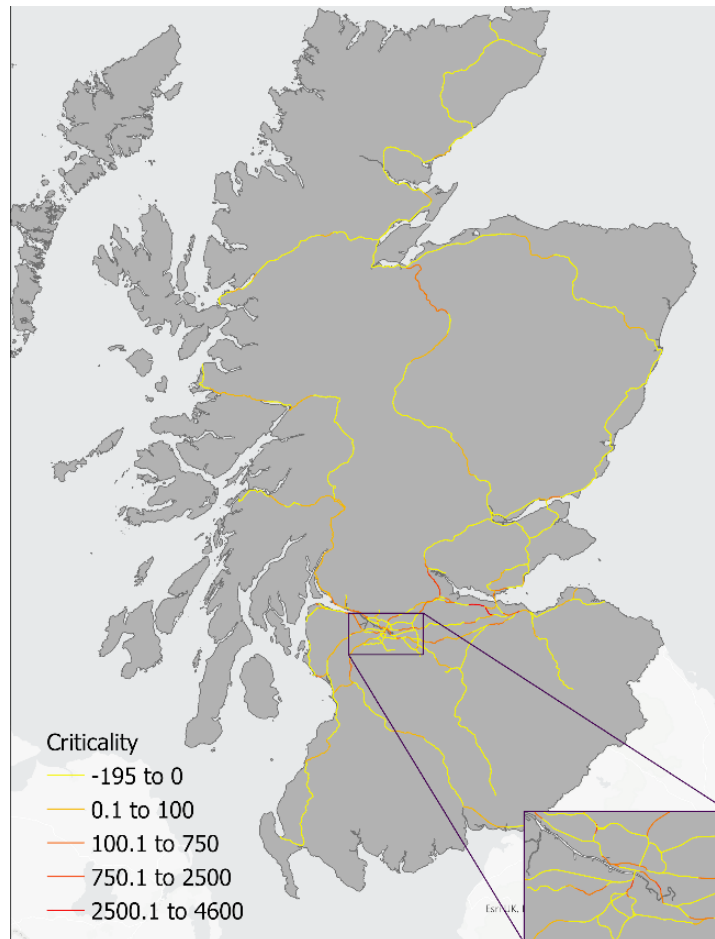


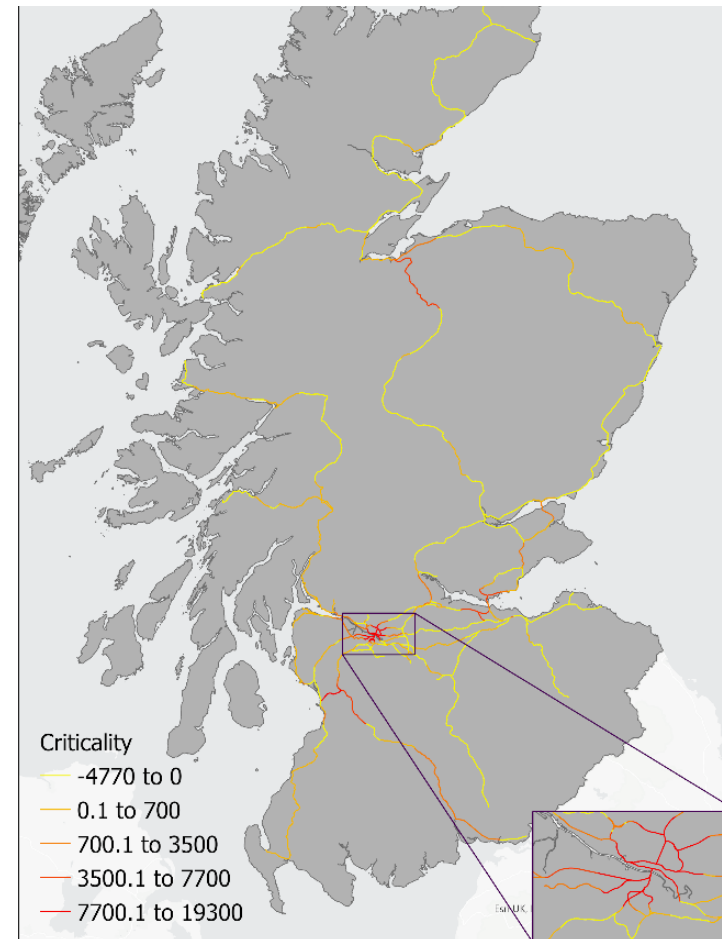
Figure 3-10 Scatterplots of criticality of (A) railway and (B) bus links against the respective values of their corresponding 4 km buffers. Note the difference in the x-axis and y-axis values between plots A and B.

Figure 3-11 shows the geographic distribution of criticality values for the links and buffers of the railway network. As before, the Jenks natural breaks classification of the data was used to reveal groupings inherent to the criticality values of each network.

The results for the railway links (Figure 3-11(a)) reveal that links with the highest criticality are located in central Scotland, particularly on routes connecting Edinburgh and Glasgow. This is because at least three flooding incidents occurred on average per year in this part of the network and this, coupled with the increased importance of these links (Figure 3-7) resulted in significantly high criticality values. The five most critical rail links were identified (Table 3-15) and the results confirm that all are located in these two cities. Links that are relatively critical are observed across the whole of the railway network.



(a) Rail links



(b) 4km Rail buffers

Figure 3-11 Criticality of (a) railway links and (b) 4 km railway buffers. Note the different classification scales in the two maps. High values suggest that a significant number of public transport trips traverse the link or buffer.

Table 3-15 Five most critical rail links

Link Name	Criticality
Winchburgh Junction - Newbridge Junction	4508.55
Linlithgow - Winchburgh Junction	4499.20
Dalmarnock - Bridgeton	2441.34
Edinburgh - Haymarket	1514.97
Glasgow Central - Muirhouse North Junction	1267.07

In the case of railway buffers (Figure 3-11(b)), clusters of buffers of very high criticality values exist in central, North-East and South-West Scotland, where urban centres exist, particularly in Glasgow, Inverness and Ayr. This can be attributed to the fact that these railway buffers include bus links of high importance. However, most buffers are associated with relatively low criticality, particularly in rural areas of the country. Finally, it is worth noting that criticality of several rail buffers located close to bus links for which no incident data were available (e.g., in central and South-East Scotland as shown in Figure 3-12(a)), may be misrepresented.

Table 3-16 Five most critical rail links, when considering their rainfall-related geographic interdependency to bus links.

Link Name	Criticality
Dalmarnock - Bridgeton	19231.36
Glasgow Central - Muirhouse North Junction	15381.26
Glasgow Queen Street - Cowlairs South Junction	13080.45
Charing Cross (Glasgow) - Partick	12692.22
Muirhouse North Junction - Muirhouse West Junction	12628.16

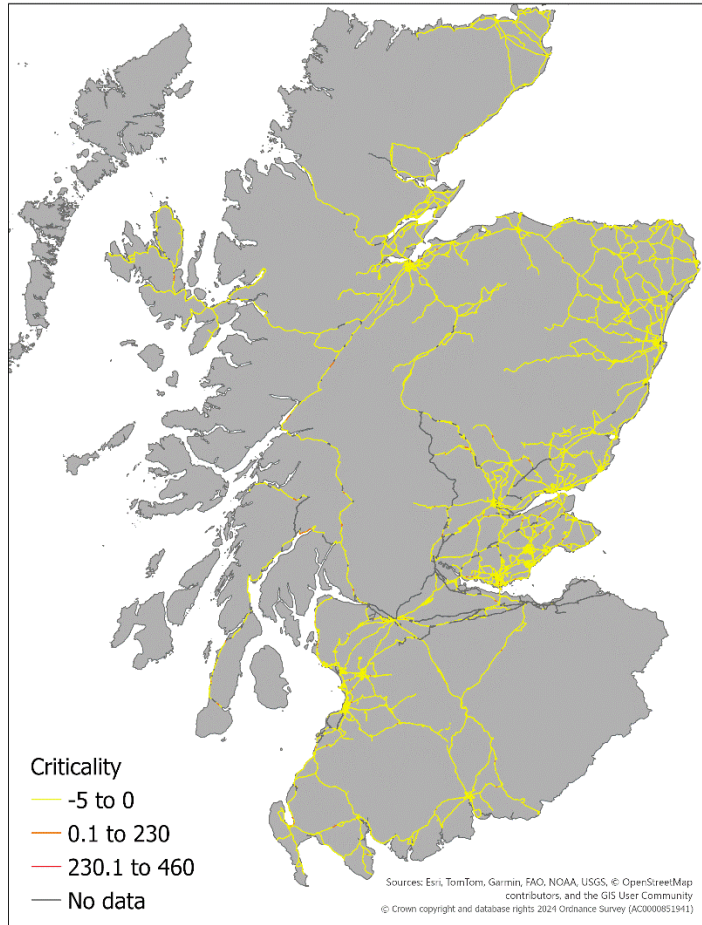
The links, of which the corresponding buffers are related to the five highest criticality values (Table 3-16) were identified and the results show that all buffers are located

in Glasgow. It is further observed that although a few of those buffers are related to the highest criticality links (Table 3-15), exceptions also exist.

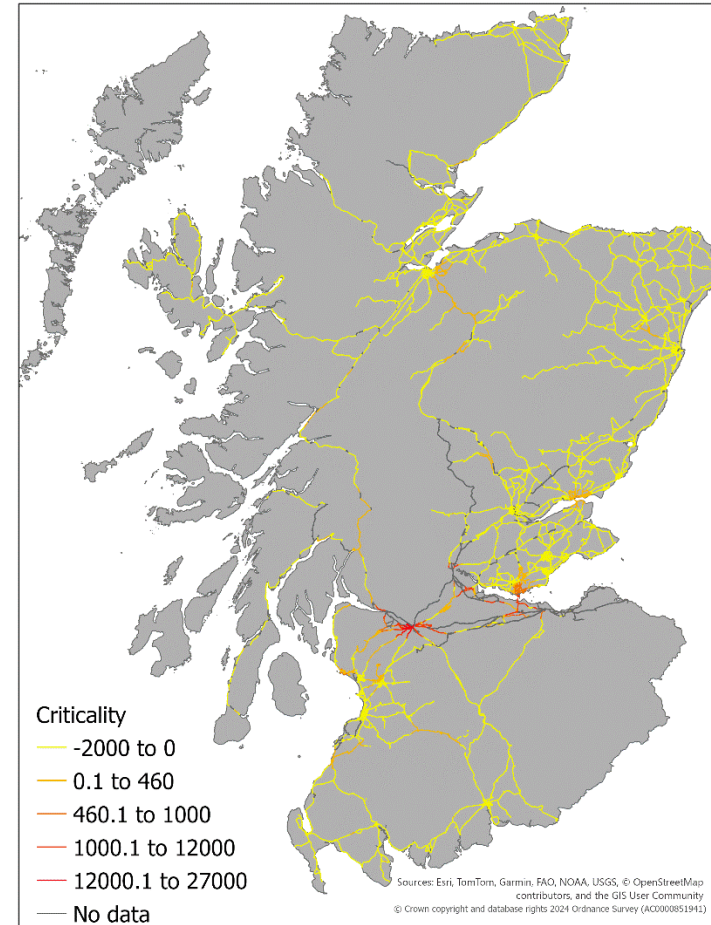
To assess whether differences exist in the criticality of links located in rural areas of the country when considering the geographic interdependency with bus, the five most critical rail links and buffers in rural areas were identified and are included in Table S8 and Table S9 of Appendix B. This was done by intersecting the layer of rail links by the spatial dataset for urban - rural classification of areas in Scotland (Scottish Government, 2020). The results again suggest that the most critical rail links are different from the most critical rail buffers. As such, the ranking of rail links in both urban and rural areas of Scotland is significantly affected when considering the flood-related geographic interdependency between rail and bus.

By comparing the maps of importance and criticality for railway (Figure 3-7 and Figure 3-11, respectively), it is observed that across the network, some buffers are characterised by high values of importance, but rank lower in criticality. This can be attributed to the fact that the railway links and neighbouring bus links experienced no or only a few flooding incidents, which resulted in their weakness and criticality being low.

Figure 3-12 shows the geographic distribution of criticality of the links and 4 km buffers of the bus network.



(a) Bus links



(b) 4km Bus buffers

Figure 3-12 Criticality of (a) bus links and (b) 4 km bus buffers. Note the different classification scales in the two maps. High values suggest that a significant number of public transport trips traverse the link or buffer.

Regarding the bus links (Figure 3-12(a)), unsurprisingly, most of them have very low criticality values because, as previously mentioned, both the historic average and expected flooding frequencies per year were very close to zero and thus their weakness was negligible. Only 262 links were associated with a positive criticality value. The five most critical road links, along with the name of road they are located in, are included in Table 3-17. Contrary to the most critical rail links, these are scattered across Scotland and are not concentrated in any particular location of the country. It is further observed that 4 of these links are part of the local road network and only one is trunk road. This suggests that local roads used by long-distance bus services are more susceptible to flooding-related incidents compared to trunk roads in Scotland.

Table 3-17 Five most critical bus links.

Link ID*	Road name**	Criticality
osgb4000000006892263	A781, Whitesands	456.57
osgb4000000004482004	A92, Tay Bridge Roundabout	143.38
osgb4000000005080393	B7038, Campbell Street	137.61
osgb4000000005074778	B780, South Crescent Road	136.95
osgb4000000005158204	M8	125.96

* Identification code for road links specified in OS MasterMap Highways Network (Ordnance Survey, 2021).

** The name of the road that the link is located. Note that the link may not coincide with the full extent of the road but may be only a part of it.

In the case of bus buffers (Figure 3-12(b)), while again most of the buffers are associated with very low criticality values, two clusters of high values are observed in the central part of the country, and especially within Glasgow. These could be attributed to neighbouring railway links that are highly critical, and thus significantly increase the criticality of these buffers. The results of the five most critical buffers are included in Table 3-18 and confirm this observation. By comparing them with the most critical links (Table 3-17), it is revealed that none of the links of highest criticality

are related to buffers of the highest criticality as well. It is also worth noting that all links are part of the local road network within the city of Glasgow. Although the most critical buffers for both rail and bus are located in the same area, this has different implications for each mode. Specifically, the high density of the road network in Glasgow may provide opportunities for bus services to re-route; however, this is not the case for rail.

Table 3-18 Five most critical bus links, when considering their rainfall-related geographic interdependency to rail links.

Link ID*	Road name	Criticality
osgb5000005130717125	Finnieston Street, Glasgow	26880
osgb5000005230823377	Cathedral Street, Glasgow	25742.40
osgb4000000005391044	Cathedral Street, Glasgow	25742.40
osgb5000005130716787	Govan Road, Glasgow	25068.68
osgb5000005130716793	Golspie Street, Glasgow	25068.68

* Unique identification code for road links as specified in OS MasterMap Highways Network (Ordnance Survey, 2021).

** The name of the road that the link is located. Note that the link may not coincide with the full extent of the road but may be only a part of it.

By comparing the criticality of buffers with their importance for bus, it is apparent that a considerable number of buffers is associated with very high importance but low criticality, particularly in and around cities of the country, which could be attributed to very low values of weakness. Similarly with rail, the five most critical bus links and buffers in rural areas of the country were identified, as shown in Table S10 and Table S11 of Appendix B, respectively. The results revealed that the top 5 critical links are different from the top 5 critical buffers, highlighting that the ranking of bus links in both urban and rural areas of Scotland is substantially different when considering the rainfall-related geographic interdependency with rail.

3.6. Conclusions and Discussion

In this chapter, a method was developed to assess the extent to which discrete transport networks are geographically interdependent as a result of area-wide events and the impact of this interdependency on the importance and criticality of links. The Scottish public transport network consisting of long-distance bus and railway services was used as a case study, and rainfall was selected as the hazard of concern. An empirical probabilistic method was used to determine whether geographic interdependencies exist between the two modes, which were expressed as the potential for links to flood concurrently in the event of heavy rainfall. The proposed criticality measure combines the criticality of public transport link of concern with that of the neighbouring links that are subject to geographic interdependencies.

The results of the application of the method proposed to the case study show that considering the flood-related geographic interdependency did not result in significant differences in the importance of public transport links; however, exceptions to this were identified, as well. On the other hand, in terms of criticality, the results revealed clusters of particularly high values, especially in and around urban centres of the study area, where both the importance of locations and density of networks are high. The ranking of links in terms of criticality was different from that of buffers in both urban and rural areas, indicating that accounting for geographic interdependencies should play an important role in the criticality values.

The findings revealed from the implementation of the method are not confined to the Scottish context but can be generalised to regional or national public transport networks in other geographical areas which are exposed to extreme rainfall events. For instance, in urban areas, where both the density of transport infrastructure networks and the number of public transport services are typically high, the impact of rainfall-related geographic interdependencies on link criticality is more pronounced. This is because urban links are heavily used throughout the day; if these links are more susceptible to rainfall, they become significantly more critical than those in rural areas. Furthermore, the close proximity of links from other transport

networks further increases the criticality of the associated buffers. In contrast, in rural areas, where network density and service frequency are typically low, the criticality of both links and buffers is expected to be low as well. Overall, considering regional variations in both the vulnerability of links to rainfall and network density is likely to result in different criticality rankings of links among public transport networks of similar size.

The novelty of this study lies in the method proposed for the criticality assessment along with the findings derived from its implementation. Various metrics have been proposed to characterise the importance and criticality of transport links using both impact-based (e.g., Jenelius *et al.* 2006; Taylor *et al.* 2006; Rodriguez-Nunez and Garcia-Palomares, 2014) and centrality-based methods (e.g., Lowry, 2014; Cats and Jenelius, 2014; Sarlas *et al.*, 2020). However, these are not appropriate for spatially defined weather events as they consider incidents affecting only one link at a time and do not consider the probability of the disruptive event occurring on the link (i.e., link weakness). Although Cats *et al.* (2016) and Yap and Cats (2021) partially addressed this limitation by estimating the weakness and criticality of links, the disruptions considered were, again, confined to a single link or station. In contrast, the method proposed in this study fills this gap by developing a metric that incorporates both the likelihood of weather events disrupting links and the spatial scale of these events as a proxy for potential concurrent disruptions. Furthermore, this work extends previous studies on the vulnerability assessment of a single transport infrastructure network to area-wide incidents (Jenelius and Mattsson, 2012) and research on the geographic interdependencies between transport networks (Ferrari and Santagata, 2024), by assessing, for the first time, the implications of geographic interdependencies on discrete public transport networks. While this earlier research showed that area-wide events reduce the network redundancy, particularly in densely connected urban areas, this study further demonstrates that, although the ranking of link importance may remain stable for area-wide events, the criticality of links varies markedly when these interdependencies are considered. There are several limitations associated with this

work. Regarding the incident datasets for the railway and bus networks, the original data sources obtained did not provide the exact location of flooding, and this, coupled with the unavailability of incident data for various parts of the bus network, led to high uncertainty associated with the computed empirical probabilities. Ideally, if the coordinates of each incident location were available for the entire rail and bus networks, then the conditional probabilities would be estimated on the basis of buffers around points, thus allowing more accurate characterisation of geographic interdependencies.

Furthermore, the time of day that the incidents occurred was not considered in the estimation of geographic interdependencies, as it was not available for most events. As such, concurrent events were considered as those that occurred on the same day. Likewise, the duration of incidents and their impacts on the infrastructure availability of links (e.g., full or partial closures) were not included in the estimation of weakness, as they were either unavailable or could not be confirmed for most events. Additionally, in the absence of an incident dataset for the entire long-distance bus network, various data were collected and merged from a number of data sources, which, however, did not cover all the bus network. This resulted in some parts of the long-distance bus network being excluded from the assessment of geographic interdependencies or the evaluation of importance and criticality of links. Another limitation associated with the data is the unavailability of information on hazard-specific predictors that would allow the construction of models that predict the frequency of flooding on each link; thus, a semi-descriptive metric of weakness was developed.

A final limitation associated with the available incident data is that because the analysis to estimate geographic interdependencies was not supported by extensive data, the resulting conditional probabilities were very low, and thus a buffer-based approach was adopted to identify links subject to geographic interdependencies. This approach assumes that flooding-related interdependencies are related only to a specific spatial extent and thus links outside this area are ignored. A useful extension to this work could be to directly use the conditional probability of links of the

alternative mode being flooded given the flooding-induced disruption on the link of concern, in conjunction with their importance, to measure criticality when accounting for geographic interdependencies. Moreover, the spatial extent of concurrent flood events is further expected to vary based on the intensity and spatial scale of rainfall events that these are related to. Therefore, the extent of geographic interdependencies could be modelled according to the characteristics of the hazard, consequently resulting in different importance and criticality values of links.

Regarding the measure of importance, a static approach was adopted that does not consider the variability of trips traversing a link over the course of a day. In reality, the adverse impacts of flooding could be expected to be more severe for events occurring at peak times, where the frequency of trips is the highest. Additionally, importance was here perceived in terms of public transport trips, which heavily influenced the ranking of links and buffers; however, other approaches exist that may lead to different conclusions. For example, for rural areas that are serviced by fewer trips, the disruption of links may result in low impacts on the trips of the network but significant consequences in terms of the individuals affected. Exploring how alternative metrics influence these results could complement this work and provide comprehensive conclusions. Finally, the neighbouring links of the same mode were not considered in the importance and criticality of buffers, because this work aimed at analysing the impacts of geographic interdependencies to the ranking of links, rather than comprehensively assess the ranking of areas. A useful extension of this work would therefore be the integration of all links of multiple co-located networks of interest in a single metric.

Despite these limitations, this study offers valuable insights into the vulnerability of public transport networks to extreme weather events and provides a novel framework for identifying areas of public transport networks that require prioritised interventions. Network managers and public transport operators can use readily available information, namely spatial transport network data, public transport timetable and historical records of weather-related disruptions, to estimate the spatial scale of weather events and compute the proposed metrics. By integrating

these datasets and implementing the proposed methods, practitioners can make more targeted and informed decisions on the locations that require prioritisation and develop proactive measures to enhance network resilience.

In this chapter, the second objective of the thesis was addressed by analysing the characteristics of geographic interdependencies between public transport modes for a specific weather-related hazard. Using rainfall as the hazard of concern, the rainfall-related interdependencies between rail and bus were evaluated empirically using historical flood incident records. However, due to the limited availability of data, the geographic interdependencies were captured using a buffer-based approach. In Chapter 4, a model is developed using rainfall data to characterise the geographic interdependencies from a probabilistic standpoint, therefore overcoming the limitation of the “cliff-edge” effect of buffers. The model for geographic interdependencies is subsequently integrated into the model of redundancy proposed in Chapter 2.

4. Assessment of the impact of extreme rainfall on interdependent public transport networks

The empirical assessment presented in Chapter 3 confirmed that geographic interdependencies between discrete public transport networks may occur due to heavy rainfall. However, these were captured using a buffer-based approach and thus did not account for the likelihood of concurrent flood closures of spatially proximate network links due to the same rainfall event. This chapter addresses this by modelling the spatial dependence of rainfall events that can result in the closure of public transport links. This model therefore captures rainfall-related geographic interdependencies in probabilistic terms and is incorporated in the model of redundancy developed in Chapter 2 to assess the impact of concurrent rainfall-induced closures of links on the accessibility of locations. Thus, Chapter 4 addresses the third objective of this thesis, which is to develop a model for the extent of weather-related geographic interdependencies between transport networks and incorporating it to the importance assessment of interdependent public transport modes, for a certain hazard of interest – in this case, rainfall.

4.1. Introduction

Pluvial flooding can damage transportation assets, resulting in disruption to the transport system and substantial economic losses (Jaroszweski *et al.*, 2014). The spatial scale of flood events is closely related to the extent of rainfall (Breugem *et al.*, 2020) and can range from local (Pregolato *et al.*, 2015) to regional (van Ginkel *et al.*, 2021), and, in some cases, international areas (Ulbrich *et al.*, 2003; Fathom Global, 2021). Multimodal transport systems that operate within the spatial footprint of heavy precipitation events may experience disruptions concurrently, thus leaving travellers without options to complete their trips by alternative routes or modes. In the light of climate change, future weather projections indicate increasing trends in both the frequency, severity and, in some cases, spatial extent of rainfall and flooding

in many parts of the world (Seneviratne *et al.*, 2021; Lochbihler *et al.*, 2019; Ghanghas *et al.*, 2023). Hence, the assessment of pluvial flood risk to transport networks has received growing attention in the last few years (Watson and Ahn, 2022). However, research efforts to date have predominantly focused on one transport mode at a time and have overlooked the concurrent impacts of flooding on multiple modes that operate on discrete infrastructure networks. Therefore, the implications of pluvial flood events for the accessibility provided by multimodal public transport networks and, in extreme cases, the loss of connectivity between locations have not been explored.

The potential impacts of weather-related events on transportation networks can be explored through a risk assessment framework. As previously mentioned in Section 1.1, risk is the product of the hazard, exposure and vulnerability of the system of concern. The risk assessment framework encompasses modelling the characteristics of a hazard of a certain return period (e.g., spatial scale, severity, duration) and the exposed system (or systems) of concern, and ultimately estimating the consequences of the event for the functionality of system (Dalziell, 1998). Therefore, the risk assessment framework estimates the *conditional* vulnerability of the transport system given the occurrence of a hazardous event. In contrast, in the general framework of vulnerability assessment, vulnerability of the transport system is assessed through disruption scenarios which are not associated with a certain hazard or likelihood of occurrence.

Despite efforts to assess impacts of pluvial flooding on transportation networks, most works to date have focused on either road or rail individually (Chen *et al.*, 2015; Pyatkova *et al.*, 2019; He *et al.*, 2020; Hong *et al.*, 2015; Pant *et al.*, 2016), thus overlooking the concurrent effect of rainfall on both networks. Therefore, the geographic interdependency between discrete transport infrastructure networks resulting from rainfall has not been adequately explored.

Furthermore, as mentioned in Section 1.1, the pluvial flood maps used for the assessment of rainfall impacts do not provide information on which locations may

experience flooding at the same time, and, as such, do not realistically capture the potential for concurrent impacts on the networks. Thus, although they may be useful to identify particularly susceptible areas that require more detailed assessment, they cannot be used to analyse the geographic interdependencies between discrete modes of the transport system by the occurrence of flood hazard. Although there have been efforts to develop scenarios of concurrent flood events based on these maps (e.g., van Ginkel *et al.*, 2022; Zhu *et al.*, 2022), these are derived from the random sampling of flood locations from the map and, therefore, do not account for the higher likelihood of flooding co-occurrences on spatially proximate locations.

This study aims to assess the impact of extreme rainfall on interdependent public transport modes that operate on discrete infrastructure networks. The assessment explicitly considers the characteristics of rainfall in terms of frequency and intensity and further accounts for the likelihood of flooding affecting two networks concurrently as a result of the same rainfall event. This is achieved by estimating the spatial dependence between historic rainfall-related flood events which have caused the concurrent failure of road and rail links. The model of importance proposed by Taylor *et al.* (2006) is adapted to rank links based on the extent of redundancy loss caused by their failure, as well as to consider the likelihood for geographic interdependencies to occur between discrete public transport networks. The method is applied to the Scottish public transport network consisting of rail and long-distance bus services, where the latter is considered an alternative mode when the former is disrupted due to flooding.

The rest of the chapter is structured as follows. Section 4.2 provides a review of key literature on the risk assessment of transportation networks to flooding. In Section 0, the methods are presented, followed by Section 4.4 which describes the application of methods to the case study network. Section 4.5 includes the results and Section 0 summarises the conclusions of this work.

4.2. Key literature

In light of the climate emergency, assessing the risk of road networks to rainfall-related flooding has received growing attention. Using a flood model, Coles *et al.* (2017) simulated historical pluvial and riverine flood events and estimated their impacts on the accessibility of emergency services to care homes and sheltered accommodations. Pregolato *et al.* (2015) developed a model that represents the impact of water depth on safe speed of road vehicles and subsequently estimated the risk of the urban road network to pluvial flooding based on a flood map and the resulting speed reductions of vehicles. The flood map included events that simultaneously occurred as a result of a statistically possible rainfall event, thus indicating the links of the network that were simultaneously closed. Evans *et al.* (2020) assessed the monetary impacts of flooding due to changes in the traffic flows of two urban road networks, based on synthetic rainfall events that represent current and future climate conditions for the urban areas of concern. The speed of vehicles was adjusted according to the water depth on the road. Pyatkova *et al.* (2019) adopted a dynamic approach where flood and transport models were integrated into a tool to capture the impact of flooding on the road system as the 1-in-100 years' synthetic rainfall event progressed. The impacts estimated included the number of vehicles rerouted, changes in travel distance and time, as well as effects on local air quality due to congestion on roads that remained open.

Van Ginkel *et al.* (2022) assessed the risk of European road networks to concurrent fluvial flood events in terms of number of disrupted routes between regions in each country, number of detours and isolated trips. A large number of flood scenarios were developed by initially randomly sampling a certain number of events from the 100-year flood map of Europe, and then by further sampling flood events in Germany based on a copula-based spatial dependence model for streamflow extremes. The authors interestingly showed that while the randomly sampled flood events disrupted more routes, the spatially correlated floods resulted in a higher number of isolated trips, which was attributed to their more severe impacts on the local scale.

Compared to the road network, less work has been done to assess the risk of public transport networks to flooding. Hong *et al.* (2015) assessed the flood risk of the Chinese railway network by estimating failure probabilities of railway links from past events and by using these to develop disruption scenarios through random sampling to measure adverse impacts in terms of duration of link closures and number of train services affected. Forero-Ortiz *et al.* (2020) assessed the flood risk of the underground metro system in Barcelona in terms of ridership flows by developing pluvial flooding scenarios of certain return periods and using them as input to a hydrodynamic model to estimate the extent and depth of flooding. Then, by overlaying them onto a map showing the number of metro passengers along the network, risk maps were obtained showing the expected impacts.

Similarly, Zhu *et al.* (2022) analysed the risk of the Chinese railway network to riverine flooding in terms of the daily number of train services and passengers affected, as well as travel time increases due to train detours. Flood depth-exceedance probability functions were constructed for each grid cell of the country based on riverine flood maps of various return periods and then multiple national-scale flood scenarios of concurrent flood events were produced through a Monte Carlo sampling process, where depth-exceedance probabilities were randomly assigned to the cells, thus resulting in varying flood depths across the country.

The aforementioned works on public transport networks focus on only one mode, typically railway. The literature on flood risk assessment of multiple transport modes is rare. Indicatively, Hong *et al.* (2019) measured the vulnerability of a multimodal public transport network consisting of bus and subway services to a historical rainstorm event, which however directly affected only the former mode, while the latter remained intact. Ma *et al.* (2019) explored the effects of cascading failures incurred by flooding to the bus and metro networks, by considering the failure probabilities of network elements and the corresponding consequences to passenger volumes. However, only bus services were directly affected, while the metro lines suffered disruptions due to the redistribution of disrupted passenger volumes. He *et al.* (2020) examined the flood risk of the urban multimodal transport network

comprising bus and taxi services and, as such, only modes operating on the road network were considered, whilst railway modes were ignored. It therefore becomes clear that even in cases where multiple modes are assessed, no work to date has considered the concurrent risk of public transport modes that operate on distinct infrastructure networks to flooding; thus, flood-related geographic interdependencies between transportation networks have been overlooked so far.

Because the assessment of geographic interdependencies requires exploring the consequences that arise from concurrent events on multiple infrastructure networks, the most commonly used static approach of flood risk assessment may misrepresent the consequences of pluvial flooding, as it does not account for the temporal progression of extreme rainfall across an area and can be thus only used to estimate the worst potential damages to infrastructure (Pyatkova *et al.*, 2019). With a view to test the vulnerability of transport networks, efforts have been made to develop scenarios of concurrent pluvial and fluvial flood events which typically involve producing multiple simulations through a Monte Carlo process based on static maps (e.g. van Ginkel *et al.*, 2022; Zhu *et al.*, 2022) or require integration of flood and transport models to simulate the progression of consequences as the event propagates across an area (e.g., Pyatkova *et al.*, 2019). However, it is not always possible in practice to employ these approaches, either because of the unavailability of the required modelling tools or due to the limited availability of computational resources that prohibits conducting multiple disruption scenarios.

4.3. Methods

4.3.1. Characteristics of critical rainfall events resulting in the closure of public transport links

To determine the characteristics of rainfall events (e.g., depth, duration) that may cause flooding-induced closure of links on the public transport network, historical disruption records of links due to rainfall and rainfall data were analysed. The former was provided from the incident datasets for bus and rail (Sections 3.4.2 and 3.4.3 respectively), and for the latter, rainfall time series recorded by rain stations were used.

The first step included separating the continuous time series of rainfall of each rain station into statistically independent rainfall events using the minimum inter-event time (MIT), which is the minimum dry period that needs to elapse between two rain events for them to be considered as independent (Joo *et al.*, 2013; Baek *et al.*, 2015; Zeiger and Hubbart, 2021). Events that are temporally separated by a larger time window than the MIT were considered independent, while those separated by a smaller time window than MIT were part of the same event.

Various methods exist for the identification of distinct rainfall events, namely method of autocorrelation, coefficient of variation, average number of rainfall events (Baek *et al.*, 2015; Joo *et al.*, 2013). Here, the method of the coefficient of variation (CVA) was undertaken (Restrepo-Posada and Eagleson, 1982) due to its ease of applicability. This approach assumes that the MIT value for a rain station yields an exponential distribution of the time intervals between rainfall events, which can be thus assumed as Poisson (independent) events. The method involved identifying the dry periods in the rainfall time series of each rain station and progressively testing different MIT values to establish a model between MIT and CVA. The MIT value corresponding to a CVA of one was selected for each rain station. If the computed MIT exceeded 24 hours or the variation coefficient was not close to one, a MIT of 24 hours was applied, assuming that rainfall events separated by at least a day were independent. Once independent rainfall events were established for all rain stations, their total depth, duration, and start and end times were extracted.

To identify those rainfall events that caused closures of public transport links, the rain stations and their respective Thiessen polygons were mapped in GIS, the latter reflecting their area of influence (Brassel and Reif, 1979). Intersection of the polygons with the spatial layers of the public transport network (Figure 3-3) was performed to identify rail and bus links located within each polygon. For each full closure, the corresponding rain station of the closed link was identified, and the rainfall event recorded on the date of closure by that station was derived. In cases where the rainfall event extended beyond the date of closure, only the rainfall depth and duration up to the end of closure date were considered. If a link traversed multiple Thiessen polygons, the average values of rainfall characteristics of the rain stations were derived.

To establish rainfall thresholds for flooding-induced closures of links, the rainfall event-duration method was applied which has been commonly used to identify depth (or intensity) and duration of rainfall events that may result in debris flows, flooding and landslides (e.g., Caracciolo et al., 2017; Zhuang *et al.*, 2015; He *et al.*, 2020; Georganta *et al.*, 2022). For each mode, regression models that best fitted the duration D and depth V of rainfall events previously identified were developed. Rainfall events occurring on a public transport link that are equal to or greater than the modelled characteristics of events have the potential to induce the closure of the link, while for events with a lower intensity than the modelled characteristics, the link is assumed to remain open.

The critical rainfall events obtained through this process are denoted as $E_{cr}(rail) = (V_{cr}^{rail}, D_{cr}^{rail})$ and $E_{cr}(bus) = (V_{cr}^{bus}, D_{cr}^{bus})$ for railway and bus, respectively.

4.3.2. Assessing the geographic interdependencies between public transport modes due to extreme rainfall

To model the geographic interdependencies that may occur between links of two discrete networks co-located within the spatial footprint of extreme rainfall, the

conditional probabilities of links of one mode experiencing a flooding-induced closure due to a rainfall event given the closure of a link of the other mode by the same event were determined. This was achieved by modelling the spatial dependence of critical rainfall events, following the method of conditional probabilities proposed by Ricciardulli and Sardeshmukh (2002) and Israelsson *et al.* (2020). Unlike these works where the critical rainfall conditions were estimated for daily rainfall, the spatial dependence of critical rainfall was estimated here for events of varying durations.

Using the available datasets of rainfall events, a spatial dependence model was developed to establish the conditional probability of a critical rainfall event for mode m_1 occurring given that a critical rainfall event for mode m_2 has been observed at a certain distance, $P(E_{cr}(m_1)|E_{cr}(m_2))$. This was achieved through the following process.

1. Select one rain station of the study area as the origin station, denoted by A , and identify its historical critical rainfall events, $E_A = \{E_{A1}, E_{A2}, E_{A3}, \dots\}$, characterised by start date, rainfall depth and duration.
2. For each event at A , assign 1 to all other rain stations if:
 - i. Their recorded rainfall event starts on the same date as at A ;
 - ii. Their event is critical for mode m_2 , as defined in Section 4.3.1; otherwise, assign zero.
3. Within each equal-width distance bin of A , compute the proportion of stations assigned 1 (observed conditional probabilities).
4. Perform steps 2 and 3 for each critical rainfall event recorded by A , and then repeat for all rain stations.

By plotting the conditional probabilities against the separation distance, d , the spatial dependence patterns between critical rainfall events of modes m_1 and m_2 were derived and modelled using an exponential decay function.

Since the focus is on geographic interdependencies which occur due to the same rainfall event, the spatial scale of a rainfall event d_0 that might result in the

concurrent closure of public transport links was estimated by computing the *decorrelation* distance, which is the separation distance at which the correlation of rainfall values between spatially separate locations falls to $1/e$ (Moron *et al.*, 2007; Ricciardulli and Sardeshmukh, 2002). The standardised conditional probability, Dr , (Equation 4-1) was used as a proxy of statistical dependence. A separation distance at which Dr falls below $1/e$ indicates the statistical independence of rainfall and, therefore, the spatial scale of the rainfall event.

$$Dr = \frac{(P(E_{cr}(m_2)|E_{cr}(m_1)) - P(E_{cr}(m_1)))}{(1 - P(E_{cr}(m_1)))} \approx \exp\left(-\frac{d}{d_0}\right) \quad 4-1$$

Where $P(E_{cr}(m_1))$ is the unconditional probability of the critical rainfall event.

The conditional probability plot $P(E_{cr}(m_2)|E_{cr}(m_1))$ represents the probability of a critical rainfall event of m_2 occurring at a certain distance from one affecting m_1 . Since such events can cause the closure of a public transport link, the model can be used to express the probability of a network link of m_2 closing given the closure of a link of m_1 at a certain distance from it. Therefore, the model serves as a proxy to assess the geographic interdependencies occurring between modes m_1 and m_2 . Estimating the spatial scale of the critical rainfall event that results in geographic interdependencies between modes m_1 and m_2 (Equation 4-1) allows identify links that may be concurrently affected by the same event.

4.3.3. Assessing the impact of extreme rainfall on the redundancy of interdependent public transport networks

Taylor and D'Este (2007) define a network link as important, if “loss (or substantial degradation) of the link significantly diminishes the accessibility of the network”. Based on this concept, Taylor *et al.* (2006) defined the importance of link a as the accessibility loss between O-D pairs resulting from the closure of link, as shown in Equation 4-2.

$$I(a) = \sum_i \sum_j d_{ij} \cdot v_{ij(a)} = \sum_i \sum_j d_{ij} \cdot (acc_{ij(0)} - acc_{ij(a)}) \quad 4-2$$

Where i and j denote origins and destinations of travel, respectively; d_{ij} rerepresents the demand for travel between the O-D pair; $v_{ij(a)}$ represents the consequences for the O-D pair between i and j due to the closure of a ; and $acc_{ij(0)}$ and $acc_{ij(a)}$ are the accessibilities from i to j under normal conditions and when link a has failed, respectively.

Equation 4-2 was adapted to consider the impact of the closure of a given public transport link on accessibility as well as the likelihood of links of an alternative mode concurrently closing due to the same rainfall event.

The consequences of the loss of link a were estimated using the normalised Hansen accessibility index, as shown in Equation 4-3 for origin zone Acc_i .

$$Acc_i = \frac{\sum_j D_j f(c_{ij})}{\sum_j D_j} \quad 4-3$$

Where $f(c_{ij})$ is the cost of travel between i and j and D_j represents the attractiveness of destination zone j , i.e., number of opportunities at j .

Based on Equations 4-2 and 4-3 and taking the destination zones as equally attractive, i.e. $D_j = 1$, the importance of link a can be expressed as shown in Equation 4-4 below.

$$I(a) = \frac{1}{N} \sum_i (Acc_i^{(0)} - Acc_i^{(a)}) = \frac{1}{N} \sum_i \sum_j (acc_{ij}^{(0)} - acc_{ij}^{(a)}) \quad 4-4$$

Where N is the number of destinations, and $acc_{ij}^{(0)}$ and $acc_{ij}^{(a)}$ represent the accessibility between i and j under normal conditions and when link a is closed, respectively.

Let m_1 and m_2 be the preferred and substitute public transport modes and p_{m_1} and p_{m_2} the least-cost routes of m_1 and m_2 respectively, which connect a pair of locations. Under normal conditions, the total accessibility between i and j is provided by both modes m_1 and m_2 as shown in Equation 4-5. This is equivalent to the indicator of redundancy that was proposed in Section 2.3.2.

$$acc_{ij}^{(0)} = acc_{ij}^{m_1} + acc_{ij}^{m_2} = \exp\left(-\frac{C(p_{m_1})}{\beta_{m_1}}\right) + \exp\left(-\frac{C(p_{m_2})}{\beta_{m_2}}\right) \quad 4-5$$

Where $acc_{ij}^{m_1}$ and $acc_{ij}^{m_2}$ is the accessibility for travel from i to j by m_1 and m_2 respectively, $C(p_{m_1})$ and $C(p_{m_2})$ are the times of travel by the least-cost routes of m_1 and m_2 respectively, and β_{m_1} and β_{m_2} represent the maximum cost that travellers are willing to accept between i and j by m_1 and m_2 respectively, which was set to 12 hours for both modes.

When link a of m_1 closes, then all routes that traverse it become unavailable and the accessibility is provided only by the alternative routes, p_{m_2} . Depending on the nature and spatial scale of the hazard, neighbouring links of m_2 may fail as well, leading to the concurrent closure of p_{m_2} . Unlike Chapter 2, where this likelihood was represented by the neighbourhood coefficient (Equation 2-3), here the probability of rainfall-induced geographic interdependencies occurring was considered. Thus, the remaining redundancy is equal to the accessibility offered by p_{m_2} , corrected by its likelihood to close concurrently with p_{m_1} , as shown Equation 4-6.

$$acc_{ij}^{(a)} = (1 - P(p_{m_2}^{flood} | p_{m_1}^{flood})) \cdot acc_{ij}^{m_2} \quad 4-6$$

Where $P(p_{m_2}^{flood} | p_{m_1}^{flood})$ is the probability that p_{m_2} closes due to flooding given the closure of p_{m_1} due to the failure of a .

Aggregating the redundancy losses for all O-D pairs and replacing the accessibilities in Equation 4-4 with those of Equations 4-5 and 4-6, the importance of link a of mode m_1 is then represented by Equation 4-7 below.

$$I(a) = \frac{1}{N} \sum_i \sum_j (acc_{ij}^{m_1} + P(p_{m_2}^{flood} | p_{m_1}^{flood}) \cdot acc_{ij}^{m_2}) \quad 4-7$$

The model of importance was calculated for each link exposed to flooding due to extreme rainfall, for three different scenarios.

Case I: Complete independence of flooding-induced closures (“Best case” scenario)

It is assumed that only one of the locations exposed to rainfall experiences flooding at a time. This corresponds to vulnerability assessments of single-link failures (Taylor *et al.*, 2006; Jenelius *et al.*, 2006; Sohn, 2006). The likelihood of alternative options closing concurrently, and, by extension, the geographic interdependency between m_1 and m_2 is ignored. As such, in the case of closure of link a , $P(p_{m_2}^{flood} | p_{m_1}^{flood})$ is considered as equal to zero and the importance of the link (Equation 4-6) takes its minimum value.

Case II: Complete dependence of flooding-induced closures (“Worst case” scenario)

It is assumed that all locations exposed to rainfall fail concurrently. Because the closure of alternative routes is considered, it can be stated that geographic interdependencies are also considered, but from a “worst case” scenario standpoint.

If there is at least one location of the alternative route exposed to rainfall, its probability of closing concurrently with p_{m_1} is 1 (Equation 4-8); otherwise it is zero. In the former case, the link importance takes its maximum value, while, in the latter case, it takes its minimum value.

$$P(p_{m_2}^{flood} | p_{m_1}^{flood}) = \begin{cases} 1, & \text{if flooding on route } p_{m_2} \text{ exists} \\ 0, & \text{otherwise} \end{cases} \quad 4-8$$

Case III: Spatial dependence of flooding-induced closures

It is assumed that the locations exposed to extreme rainfall may not necessarily close simultaneously and this depends on the separation distance between exposed links. Let A be a location in p_{m_1} which is closed due to flooding caused by a critical rainfall event (Section 4.3.1), and $B = \{B_1, B_2, \dots, B_m\}$ be the set of m locations on p_{m_2} that may concurrently flood. The conditional probability of each location of B closing given the flooding-induced closure at A can be estimated from the spatial dependence model (Section 4.3.2). Since only those locations of B that lie within the spatial extent of the critical rainfall event at A can close simultaneously, the subset of these with a standardised probability of at least $1/e$ (Equation 4-1) are retained. This subset is denoted as $B' = \{B_1, B_2, \dots, B_n\} \subseteq B$, where $n \leq m$.

However, since the Poincaré formula becomes very complex as the number of non-independent B_i events increases, Boole's inequality was employed (Equation 4-9), which can be used to identify the upper bound of the probability of p_{m_2} closing given the closure of p_{m_1} due to the critical rainfall event at A .

$$P(\cup B_i | A) \leq \min \left\{ \sum_{i=1}^n P(B_i | A), 1 \right\} \quad 4-9$$

For the closure of link a , the model of link importance in this case takes a value between those of Case I and Case II.

To assess how the importance of links changes depending on each of the above cases, the model of importance was computed according to Cases I, II and III for each link a of the infrastructure network on which m_1 operates, and for all its locations that are exposed to critical rainfall events. The algorithm that was performed to compute the importance is presented in Appendix C.

For the most important links, the losses in redundancy of origin zones were also computed. For link a , the origin-level losses in accessibility in absolute and relative terms are as shown in Equations 4- and 4-, respectively.

$$\Delta Acc(a)_i^{(ab)} = Acc_i^{(m_1 \leftarrow m_2)(a)} - Acc_i^{(0)} \quad 4-9$$

$$\Delta Acc(a)_i^{(rel)} = (Acc_i^{(m_1 \leftarrow m_2)(a)} - Acc_i^{(0)}) / Acc_i^{(a)} \quad 4-10$$

Where $\Delta Acc(a)_i^{(ab)}$ and $\Delta Acc(a)_i^{(rel)}$ are the absolute and relative losses in accessibility of zone i due to the closure of link a , $Acc_i^{(m_1 \leftarrow m_2)(a)}$ is the origin-level accessibility of i when a is closed, and $Acc_i^{(0)}$ is the accessibility of i under normal conditions. These origin-level accessibility values are obtained by aggregating the accessibility values of location pairs, as shown in Equation 4-3.

4.4. Application of the impact assessment of flooding to the long-distance public transport network in mainland Scotland

The public transport network consisting of long-distance bus and railway services in mainland Scotland as presented in Section 2.4 and the least-cost routes between hexagonal zones were used to illustrate the application of models proposed in Section 0. Considering that rail is significantly less flexible in managing disruptive events due to the limited options of diversions to avoid a closed section, in this study, rail was considered as the primary travel mode, while bus was considered as the alternative.

To identify critical rainfall events (Section 4.3.1), rainfall datasets were obtained from the Scottish Environmental Protection Agency (SEPA), which contain timeseries of rainfall depth recorded at 15-minute intervals for 336 rain stations across Scotland (SEPA, personal communication, May 2020). The datasets acquired, which had previously undergone quality checks by SEPA, span the period between January 2000 and May 2020, with all the time series containing some missing values. Datasets of stations located outside of the mainland Scotland and those containing more than 20% missing values were excluded, resulting in a subset of datasets for 150 stations. These were then aggregated to hourly intervals to reduce their processing time. Figure S5 of Appendix C shows the retained and discarded rain stations. The missing values of the remaining time series were estimated using the Inverse Distance Weighted (IDW) interpolation method as this approach considers the known rainfall depths recorded by neighbouring stations. For each rain station, the independent rainfall events were retrieved as described in Section 4.3.1, which allowed obtaining the total depth, duration as well as start and end dates of events.

The incident datasets containing flooding incidents for rail and bus, as described in Section 3.4, were employed to associate rainfall characteristics to historical closures. Only incidents that resulted in the full closure of links were retained. Then, the characteristics of rainfall events that led to each closure were extracted and, based on these, rainfall thresholds were established for the closure of rail and bus links (Section 4.3.1). Using the constructed rainfall threshold models, the critical rainfall

events recorded by each rain station were identified and their spatial dependence was modelled based on the method presented in Section 4.3.2. Although there are rain stations separated by distances up to 420 km, it was selected to carry out the analysis for distance values up to 300 km to reduce the computational requirements of this task.

The models of importance were applied only to public transport links exposed to pluvial flooding. As such, locations exposed to pluvial flooding were identified by performing a spatial intersection of the rail and bus links with a 1-in-20 years' pluvial flood hazard map for Scotland, which was obtained from Fathom UK (SSBN UK Limited, 2021). To consider links that may fully close, only those bus and rail links submerged by more than 30 cm and 15.5 cm of water were considered, respectively (Pregolato *et al.*, 2015; Pregolato *et al.*, 2020). The spatial layer of floods intersecting these links were used to calculate the proximity between them, as required by the model of redundancy. For further information on the flood map and the processing steps, the reader is referred to Appendix C.

To test the effect of spatial dependence to the importance of rail links, the model of importance proposed in Section 4.3.3 was applied for each link and for the three cases described.

4.5. Results

4.5.1. Characteristics of critical rainfall events causing the closure of public transport links

The MIT value was computed for each rain station using the method described in Section 4.3.1. Figure 4-1 shows the distribution of MIT values for the rain stations of the study area. Based on these estimates, for each rain station, rainfall depths of non-zero value temporally separated by longer periods than the MIT of the station were considered as separate events; otherwise, they were grouped into the same event.

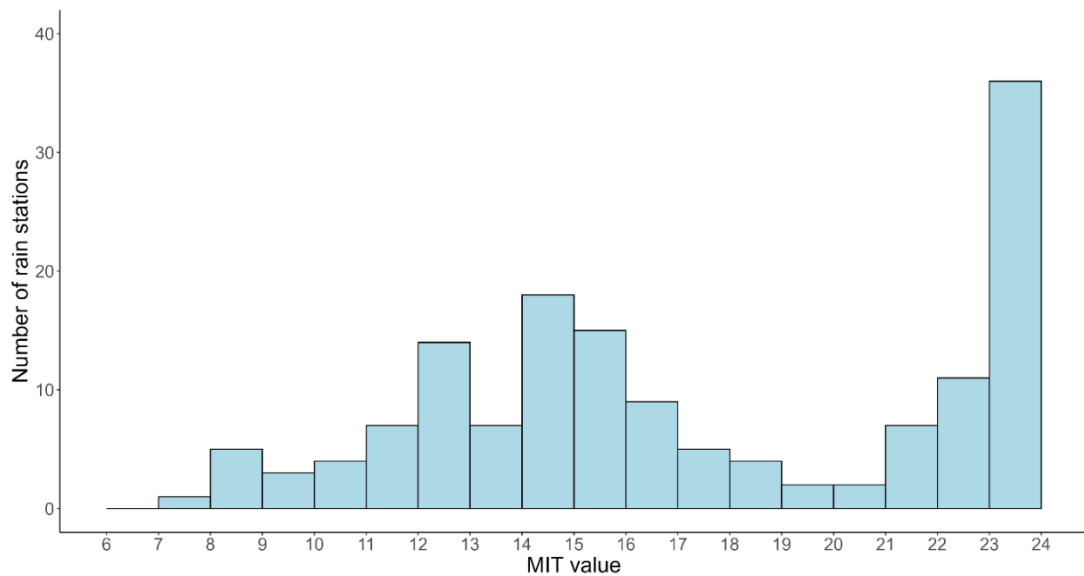


Figure 4-1 Histogram of computed minimum inter-event time (MIT) of rain stations in mainland Scotland.

The results of Figure 4-2 show that the minimum MIT value is 6 hours, while the maximum is 24 hours. The latter corresponds to rain stations for which the coefficient of variation was approximately equal to unity for an MIT value of more than a day. In these cases, the MIT was set to 24 hours on the assumption that non-zero rainfall records separated by a day or more belong to separate rainfall events.

To identify the characteristics of critical rainfall events that led to closures in the public transport network, 62 full closures for rail and 135 closures for bus were extracted from the incident datasets. Based on the estimated rainfall events and the Thiessen polygons of rain stations, the depth and duration of rainfall events that led to closures were identified and regression models were then fitted to them.

As shown in the bagplots (bivariate box plots) of Figure S6 in Appendix C, outliers were observed in the rainfall depth-duration data for both modes and, in this case, linear regression would require their removal. However, these outliers provide valuable information on more extreme rainfall events that disrupted the public transport network. As an alternative, the quantile regression model was fitted to the data of each mode as it allows keeping these outlying observations, while also

resisting their influence. The median line (50% quantile) was selected to establish thresholds for a typical rainfall event that can cause closures. Depending on the scope of analysis, other quantile lines could be used as shown in Figure S7 in Appendix C.

Figure 4-2 shows the data of rainfall characteristics for bus and rail that led to closures between May 2017 and May 2020, along with the fitted median regression lines and fitted model parameters. The results reveal that for both networks, several closures were induced by events of relatively short duration and low depth. Indicatively, for 36 out of 62 closures of rail links were caused by rainfall events that lasted less than 2 days and with corresponding depth of less than 100 mm, while for bus this was the case for 59 incidents out of 135. However, a few exceptions to this also exist, as incidents were observed to be a result of very short rainfall events of less than 4 hours with a corresponding depth between 25 and 30 mm. This was the case for 2 incidents for rail and 1 incident for bus. For 3 bus incidents, no rainfall events were identified on the date that they were reported and were thus excluded from the analysis.

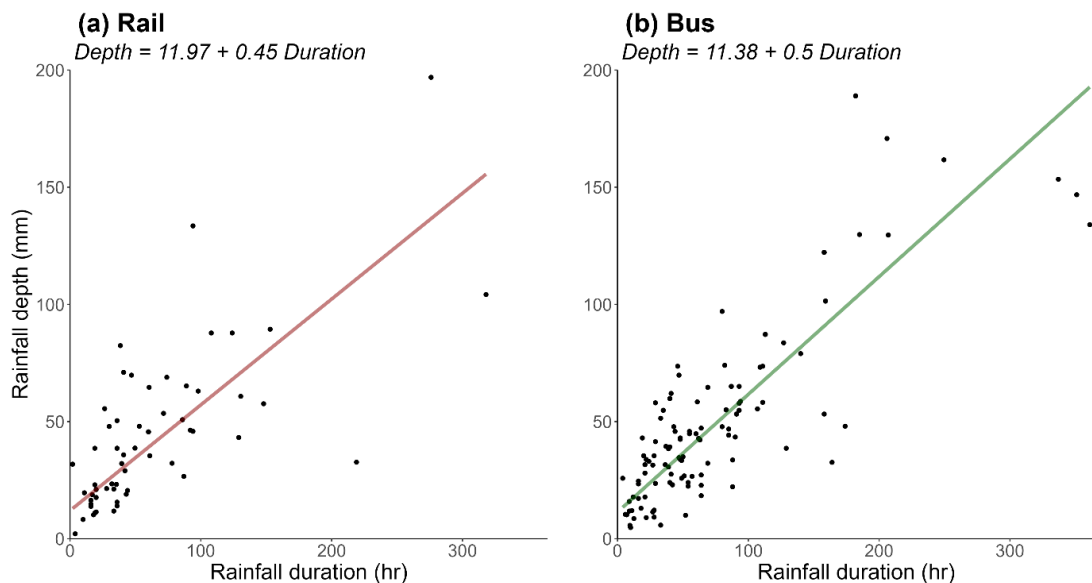


Figure 4-2 Total depth and duration of rainfall events that caused full closure of (a) rail and (b) bus links, along with the fitted median regression lines.

Because it was observed that the median regression lines for railway and bus (Figure 4-3) exhibit very similar intercept and slope values, it was checked whether the difference between them is statistically significant. As such, the dummy variable method was used, where both datasets of rainfall characteristics that caused closures of railway and bus links were joined, and a dummy variable was introduced; in case that the rainfall record came from the rail dataset, the value of the variable was set to 1 and if the record came from the bus dataset, it was set to zero. Fitting a regression line to the merged dataset revealed that the influence of the dummy variable was not statistically significant ($p > 0.05$) and, therefore, the difference between rainfall thresholds for bus and railway was not significant. Thus, a median regression model fitted to the merged dataset was used to establish critical rainfall thresholds for both modes, which is shown in Figure 4-4.

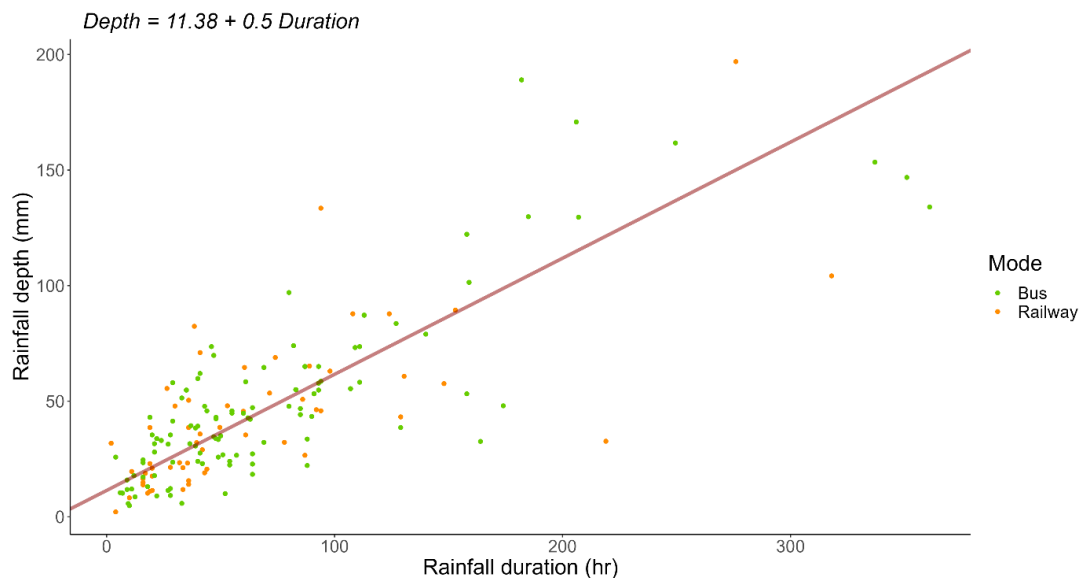


Figure 4-3 Depth and duration of rainfall events that led to full closures of bus and railway links, along with the fitted median regression line.

Table 4-1 shows the parameters of the median regression model. The *pseudo-R²* metric (Koenker and Machado, 1999) was found to be equal to 0.40 which reveals a moderate goodness of fit. Note that this metric refers only to the median regression line and that fitting regression models to other quantiles of the data would result in

different *pseudo-R*² values, as shown in Figure S6 as well as Tables S12 and S13 of Appendix C.

Table 4-1 Fitted parameters of the median regression model that represents the critical rainfall thresholds for rail and bus.

Parameter	Estimated value	Lower bound	Upper bound
Intercept	11.38	6.76	17.19
Duration	0.5	0.38	0.59

Based on the fitted line, critical rainfall events that can induce the closure of a bus or rail link due to flooding are those in which the depth and duration fall on or above the regression line of Figure 4-4. Conversely, rainfall events characterised of lower depth and duration that the critical thresholds fall within the area under the fitted line.

4.5.2. Spatial dependence of critical rainfall events

Based on the characteristics of critical rainfall events for rail and bus and according to the method presented in Section 4.3.1, a model was developed to estimate the probability of co-occurrences of critical rainfall events at spatially separated locations. This model reflects the geographic interdependencies between bus and rail in the event of pluvial flooding, from a probabilistic standpoint.

For each critical rainfall event of each rain station (origin station), the proportion of stations that recorded a critical rainfall event on the same date (target stations) was calculated for each equal-width distance bin from the origin station and an exponential-decay model was fitted to the computed proportions. This process was carried out separately for bins with widths equal to 10 km, 20 km, 40 km, 60 km and 80 km in order to understand how the conditional probabilities may be affected by the size of distance intervals. As shown in Figure S7 of Appendix C, it was observed that the 10 km and 20 km-wide bins lead to significantly higher conditional probabilities compared to the other bins, while for the other bins, the fitted models

appear to be similar. Therefore, the model of the 40 km-wide distance bins was selected.

The box plots for computed proportions of rain stations for each 40 km-wide distance intervals are shown in Figure 4-4.

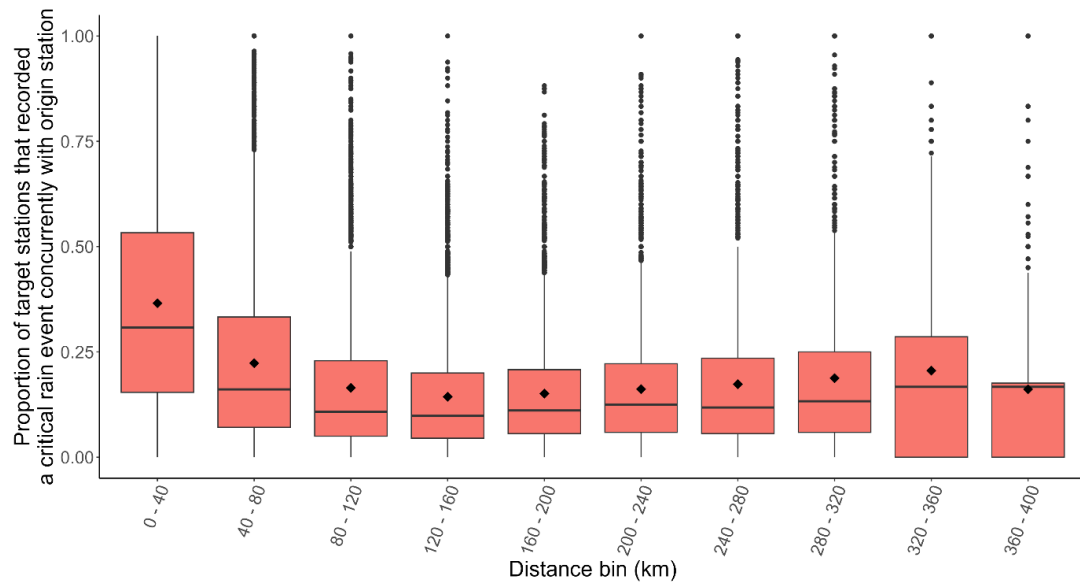


Figure 4-4 Box plots of proportion of rain stations that recorded a critical rainfall event on the same day of occurrence of a critical event at the origin station, along with the mean value of proportions for each distance bin (denoted by diamond symbols).

The results of Figure 4-4 reveal that the mean and median proportions of target stations that recorded a critical rainfall event concurrently with each origin station are higher for proximity values of up to 120 km than those for rain stations located farther from the origin stations. For proximity values higher than 120 km, the mean and median proportions of stations remain roughly the same. This suggests that, as expected, spatially proximate locations are associated with higher likelihood of experiencing critical rainfall events at the same time compared to locations farther apart from each other.

Assuming that the probabilities were observed at the mid-value of each distance bin (e.g., 20 km for the 0 to 40 km bin, 60 km for the 40 km to 80 km bin) and that the conditional probability at zero separation distance is equal to 1 for each event

recorded by the origin station, the exponential regression function was fitted to the values of computed proportions.

Figure 4-5 shows the fitted function and Table 4-2 shows the parameters of the model. The *pseudo-R²* was calculated to be equal to 0.63, revealing a moderate goodness of fit of the model to the data.

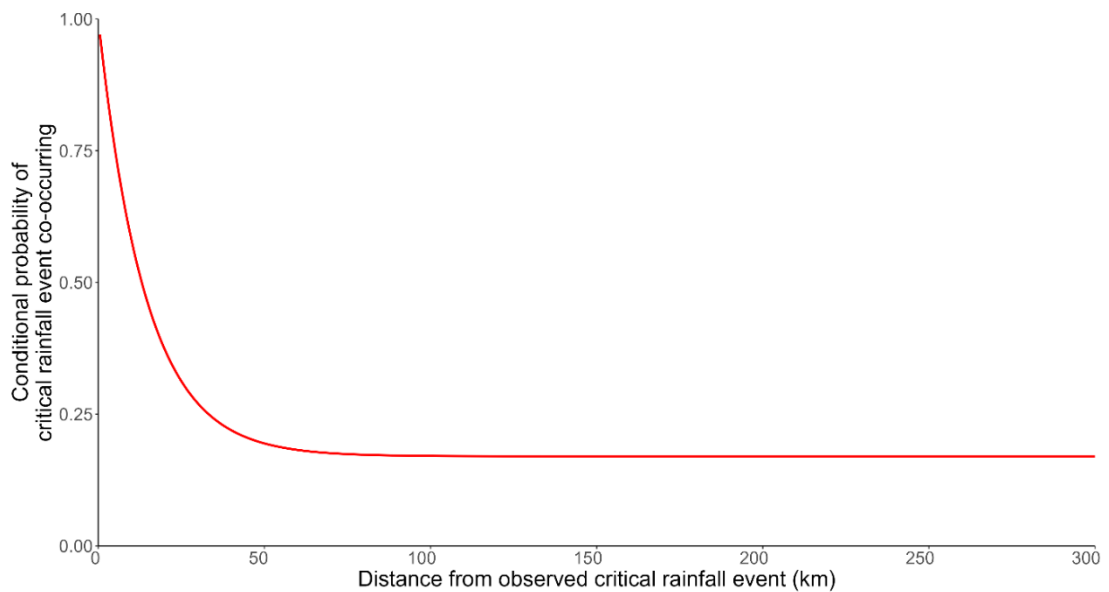


Figure 4-5 Fitted exponential regression model to the estimated conditional probabilities of rainfall.

Table 4-2 Parameters of the fitted exponential decay model to the estimated conditional probabilities of co-occurrences of critical rainfall events.

Model parameter	Estimated value	Standard error	t value	p-value
alpha (α)	0.72	0.002	409.6	< 0.001
beta (β)	-0.04	< 0.001	-170.4	< 0.001
theta (θ)	0.27	< 0.001	371.9	< 0.001

Recalling that the rainfall events that caused the full closure of public transport links were estimated based on the records of their nearest rain station, the spatial

dependence model was used to estimate the likelihood of these events occurring at each link given their occurrence at the corresponding rain stations based on their separation distance. This was done to understand the potential error of the estimated rainfall characteristics that were assumed to occur on the closed public transport links based on the Thiessen polygon method. The results (Figure S9 of Appendix C) show that while, in many cases, the probability of these estimated rainfall depth-duration values being true is more than 75%, there are instances where the probability is as low as 30%.

4.5.3. Impact of pluvial flooding on the redundancy of travel options between locations

The importance was calculated for rail links exposed to critical rainfall events based on the 1-in-20 years' pluvial flood map (Section 4.3.3). Multiple flood locations were observed on some rail links, which resulted in different values of conditional probabilities and importance values for the same link. However, because these differences were small, their average was taken as the importance of the link.

Figure 4-6 shows scatterplots of the importance values of rail links for the spatial dependence of floods (Case III) against the complete independence (Case I) and complete dependence (Case II) of flood events on the bus network.

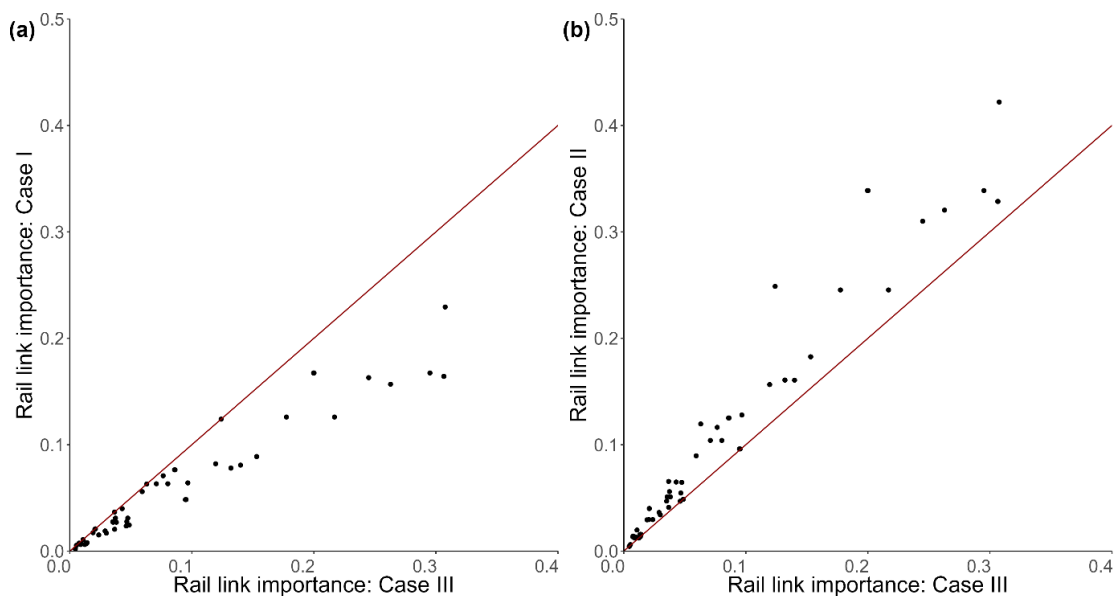


Figure 4-6 Scatterplots of (a) importance of rail links, when considering the spatial dependence of flood events that may occur on the bus network concurrently with those on rail (Case III), against the importance of rail links when assuming that floods on the bus network are independent (Case I), and (b) importance of rail links, when considering the spatial dependence of flood events that may occur on the bus network concurrently with those on rail (Case III), against the importance of rail links when assuming complete dependence of floods on the bus network to them (Case II). In both plots, data points below (above) the 45-degree reference line (in red colour) indicate increase (decrease) in importance of the link compared to Case III, while those falling onto the reference line indicate no change.

Unsurprisingly, the results of Figure 4-6(a) show that when comparing between cases I and III, the importance of all rail links is lower in the former case compared to the latter. This indicates that the losses in redundancy of O-D pairs that traverse each rail link are lower when the geographic interdependency between rail and bus is not considered in the event of rainfall. When comparing the results of case II to case III (Figure 4-6(b)), the importance values of links in the former case are higher than the latter, showing that, as expected, the losses in redundancy of O-D pairs are higher when assuming that all exposed locations of alternative routes are simultaneously inundated, rather than when considering the likelihood of them closing concurrently based on their proximity to each other.

An important observation in both plots of Figure 4-6 is that the importance values of case III against both cases I and II are characterised by a relatively positive linear

relationship, revealing that, in many cases, links related to high importance under case III are also important under the other two cases. As such, the ranking of rail links is expected to be relatively similar regardless of the assumption adopted on the dependence of flood events.

These observations in the ranking of rail links according to their importance in the three cases are further confirmed by the 20 most important links identified in Table 4-3. Specifically, it is observed that for most of the top 10 links with the highest importance when considering the spatial dependence of floods are also within the top 10 links according to the cases of complete independence and complete dependence of floods. However, for links with a corresponding rank that is greater than 10, more differences exist in their ranking between these two assumptions of dependence of floods. This indicates that, despite the similarities mentioned previously, the prioritisation of rail links should be different when considering disruptive events that may directly affect only one link at a time than those that may concurrently affect multiple links in both networks.

Table 4-3 Top 20 rail links identified using the importance measure for Case III, along with their ranking according to their importance under Cases I and II.

Rank	Link Name	Importance	Rank (Case I)	Rank (Case II)
1	Croy - Greenhill Upper Junction	0.3076	1	1
2	Pitlochry - Dunkeld & Birnam	0.3066	5	5
3	Dunkeld & Birnam - Perth	0.3064	6	6
4	Arrochar & Tarbet - Ardlui	0.2951	4	4
5	Ardlui - Crianlarich	0.2628	8	7
6	Greenhill Lower Junction - Carmuir West Junction	0.2449	7	8
7	Balmossie - Broughty Ferry	0.2169	10	11
8	Garelochhead - Arrochar & Tarbet	0.2001	3	3
9	Helensburgh Upper - Garelochhead	0.1997	2	2
10	Arbroath - Carnoustie	0.1775	9	10
11	Crianlarich - Upper Tyndrum	0.1531	12	12
12	Upper Tyndrum - Bridge of Orchy	0.1531	13	13
13	Welsh's Bridge Junction - Carrbridge	0.1399	15	16
14	Bridge of Orchy - Rannoch	0.132	16	14
15	Rannoch - Corrour	0.132	17	15
16	Dalwhinnie - Blair Atholl	0.124	11	9
17	Laurencekirk - Montrose	0.1195	14	17
18	Crianlarich - Tyndrum Lower	0.0967	21	18
19	Dalmally - Loch Awe	0.0953	27	26
20	Tyndrum Lower - Dalmally	0.0947	26	25

To understand the extent to which redundancy losses vary for origin zones, the five most important links identified in Table 4-3 were selected for further assessment. Figure 4-7 shows the absolute and relative losses in redundancy due to the failure of link “Croy - Greenhill Upper Junction” for each case. The classification method of natural breaks (Jenks) was used to classify the redundancy losses as it groups similar values together and accurately identifies trends in the data (Jenks and Caspall, 1971).

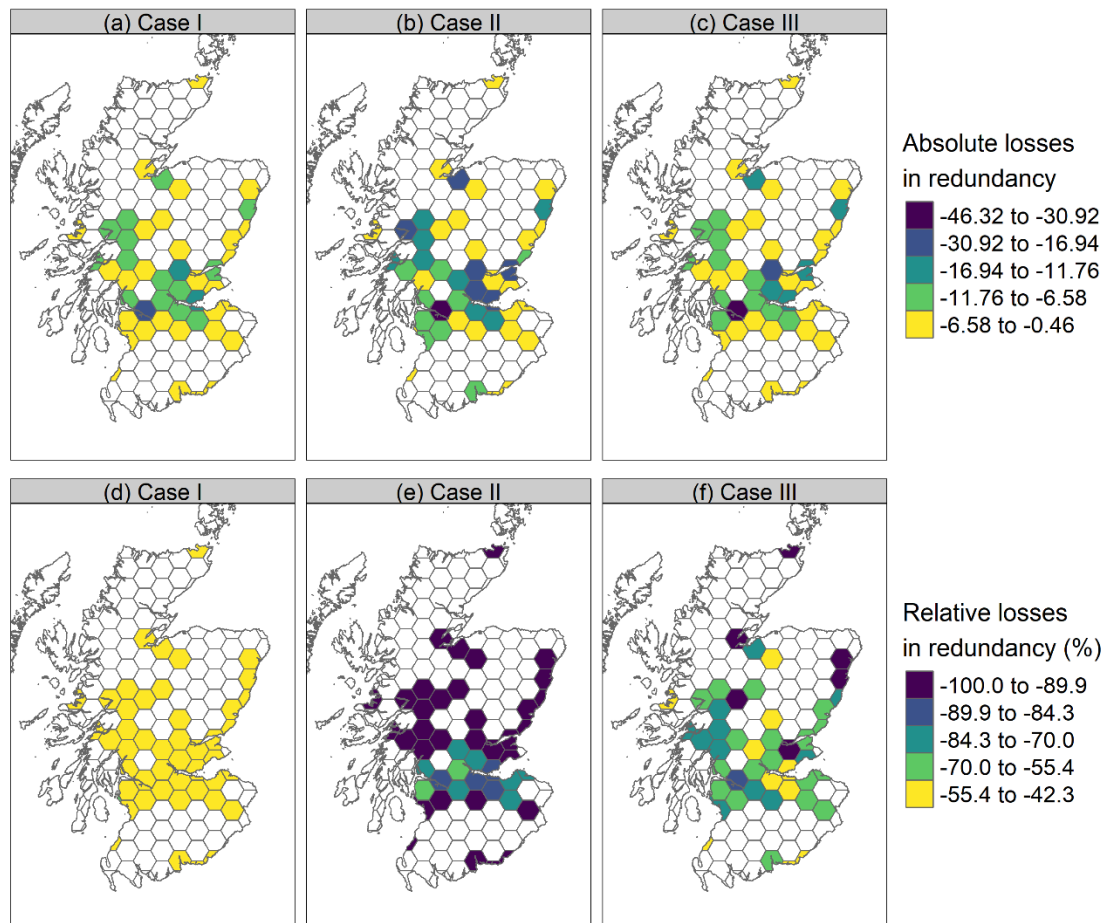


Figure 4-7 Losses in redundancy of origins due to the failure of link spanning from Croy to Greenhill Upper Junction (a) when assuming complete independence of flooding-induced closures on bus routes, in absolute terms (b) when assuming complete dependence of flooding-induced closures, in absolute terms (c) when assuming spatial dependence of flooding-induced closures on bus routes, in absolute terms (d) when assuming complete independence of flooding-induced closures on bus routes, in relative terms (e) when assuming complete dependence of flooding-induced closures on bus routes, in relative terms (f) when assuming spatial dependence of flooding-induced closures on bus routes, in relative terms. Non-shaded zones correspond to origins either not served by both modes or not directly affected by closure of the link.

The results of Figure 4-7 reveal that, in absolute terms, the origin-level losses of case II (Figure 4-7(c)) are much more similar to those of case III (Figure 4-7(b)), than those of case I (Figure 4-7(a)). This can be attributed to the fact that the assumption of case I always assumes that the alternative bus route is available, thus overlooking their likelihood of concurrent closure and consequently resulting in the minimum potential losses of redundancy. On the other hand, cases II and III incorporate this likelihood within the assessment of accessibility losses, which may take the same value when multiple exposed locations to extreme rainfall exist on the alternative route. Generally, in cases II and III, the results show that the absolute losses vary geographically with the highest absolute losses being concentrated in West Scotland, while North-East Scotland is related to the lowest losses.

In relative terms, the maps of Figure 4-7 show that, according to case I (Figure 4-7(d)), all origins are related to the lowest relative losses of accessibility. This shows that if the bus routes stay open, they are an acceptable alternative when the primary rail routes become unavailable. On the other hand, the results according to case II (Figure 4-7(e)) reveal that all origins experience extremely high losses in accessibility, which range between 85% and 100%. Contrary to these two extreme cases, Figure 4-7(f) reveals that there exists variability in the geographic distribution of the changes in accessibility of origins. Specifically, small parts of North and North-East Scotland are characterised by high relative losses which aligns with the results of Figure 4-7(e). This indicates that the alternative routes connecting these zones to the rest of the study area are indeed exposed to extreme rainfall at multiple locations and consequently their probability of closure is unity.

Further, although zones in North-West Scotland are associated with high losses of accessibility under case II (Figure 4-7(e)) they experience lower accessibility losses according to case III (Figure 4-7(f)). This is because the exposed locations on the alternative bus routes originating from these zones are outside of the spatial scale of rainfall event that directly impacted the corresponding primary rail routes, therefore, leading to a zero probability of closure of these bus routes. Finally, for some zones in

the Central Belt, the relative losses in accessibility are slightly lower than those of Figure 4-7(e), indicating that there is a likelihood of the alternative routes experiencing flooding but to a lesser extent than that assumed under case II.

Similarly with above, Figure 4-8 shows the absolute and relative losses in redundancy of origins in the event of closure of the link “Pitlochry - Dunkeld & Birnam” due to pluvial flooding. The observations on the comparison of the results of case III with those case I and case II are equally true for this link as well. This suggests that the geographic distribution of losses in accessibility is more realistic when adopting the assumption of spatial dependence of flooding-induced closures on the alternative routes (Case III), rather than the complete dependence (Case II) or independence (Case I) of them with those on the closed rail route.

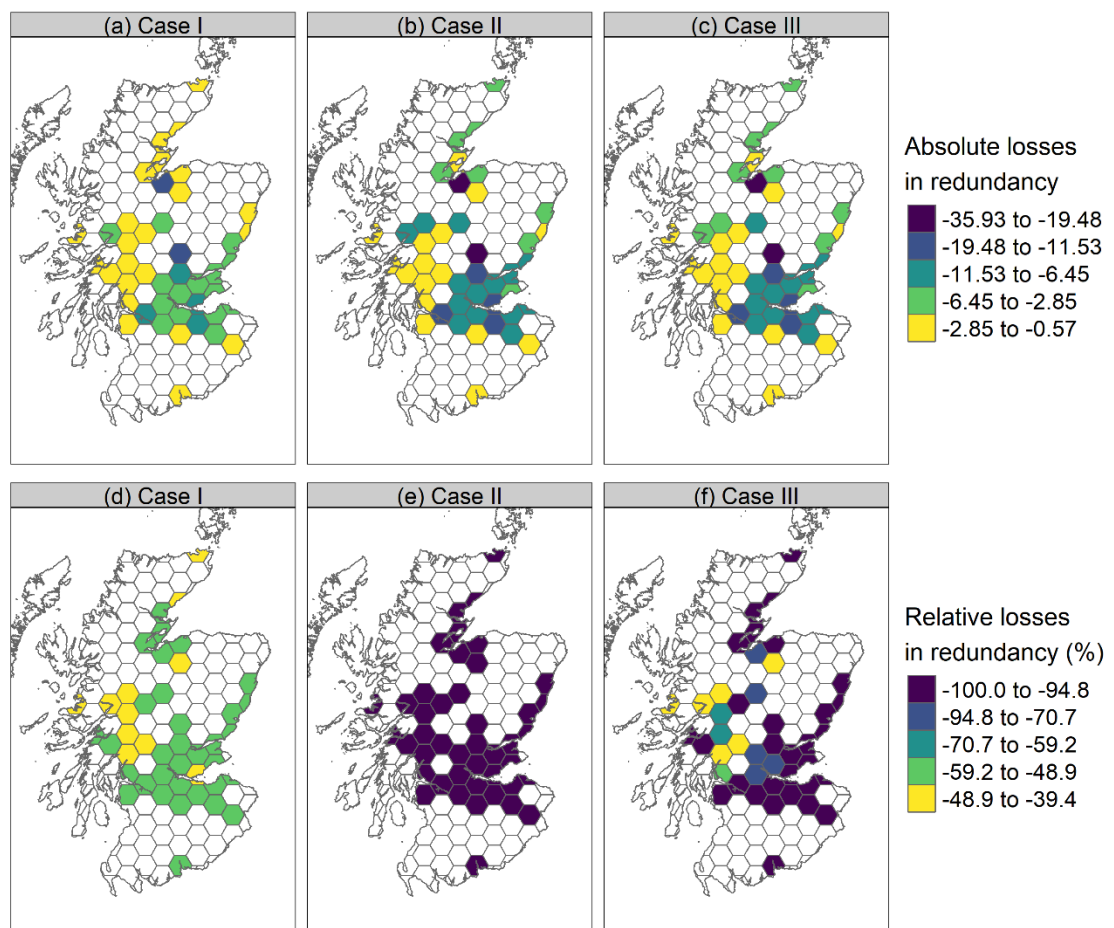


Figure 4-8 Losses in redundancy of origins due to the failure of link spanning from Pitlochry to Dunkeld & Birnam, (a) when assuming complete independence of flooding-induced closures on bus routes, in absolute terms (b) when assuming complete

dependence of flooding-induced closures, in absolute terms (c) when assuming spatial dependence of flooding-induced closures on bus routes, in absolute terms (d) when assuming complete independence of flooding-induced closures on bus routes, in relative terms (e) when assuming complete dependence of flooding-induced closures on bus routes, in relative terms (f) when assuming spatial dependence of flooding-induced closures on bus routes, in relative terms. Non-shaded zones correspond to origins either not served by both modes or not directly affected by closure of the link.

Similar maps were produced for the links “Dunkeld & Birnam - Perth”, “Arrochar & Tarbet - Ardlui” and “Ardlui - Crianlarich” (Figure S10 to Figure S12 of Appendix C), and reveal observations on the comparison of results between the three cases that are very similar to those of Figure 4-7 and Figure 4-8. However, the zones directly impacted by the closure of each link and the geographic distributions of zone-level changes in accessibility significantly depend on which rail link closes, highlighting that the spatial patterns of consequences of rainfall events heavily depend on the location that they occur.

4.6. Conclusions and Discussion

In this study, an approach was proposed to assess the indirect impacts of adverse rainfall events on geographically interdependent public transport networks. The approach extends current impact assessment methods by incorporating the likelihood of flooding closures occurring simultaneously all public transport modes operating in an area due to the same rainfall event and considers the geographic interdependencies between transport networks which carry these modes. This was achieved by estimating the spatial dependence structure of rainfall events that may result in flooding of public transport links using historical data. A new metric of link importance was proposed which considers both the impact of their flooding-induced failure on accessibility, and the probability of concurrent closure of alternative options.

The results of the application of the method to the Scottish public transport network reveal that the ranking of links based on their importance shares some similarities

across the three assumptions on concurrency of flooding-induced closures, although differences were also observed. When ignoring the potential for alternative routes being impacted by pluvial flooding and, by extension, the geographic interdependencies between rail and bus, the ranking of rail links is different than when considering them. This indicates that spatially confined disruptions affecting only one link at a time lead to different prioritisation of links than for flood-related area-covering events. The results also show that the origin-level losses in accessibility are markedly different across the three cases. The “best-case” scenario, which ignores geographic interdependencies, underestimates impacts, with all zones experiencing minimal losses. Conversely, the “worst-case” scenario assumes complete dependence of route closures, leading to widespread high losses. The spatial dependence model offers a more realistic middle ground capturing spatial variability in redundancy losses, which might range from very low to high.

Although the application of the method was undertaken for public transport modes operating on infrastructure networks of a specific geographical area, the conclusions of the results are relevant to other areas that share similarities with the case study. Regional rail and road networks which are located near each other are more susceptible to concurrent disruptions due to rainfall and their alternative routes are more likely to be closed at the same time, therefore leading to higher losses in redundancy. Since the construction of rail and road assets in close proximity is a common practice due to geographical constraints (Thacker *et al.*, 2017), it is expected that the redundancy offered by multiple modes will play a limited role in maintaining connectivity between locations.

A key novel finding of the present study is that scenarios of single-link failures that are commonly used in the vulnerability assessment of geographically interdependent public transport networks (e.g., Cats *et al.*, 2016; Cats and Jenelius, 2014; Taylor *et al.*, 2006) are not appropriate for the assessment of weather-related area-wide events, such as rainfall. Indeed, previous research works have shown that the geographic distribution of impacts of rainfall-related floods on the performance of road and rail networks significantly differ from those arising from spatially confined

events (Hong *et al.*, 2015; van Ginkel *et al.*, 2022). This difference occurs because the redundancy of network, which helps maintain connectivity during single-link failures, is greatly reduced when multiple co-located links fail simultaneously within the event's spatial footprint. To the author's knowledge, no studies have yet assessed the combined effects of rainfall on both road and rail networks. Thus, the rainfall-related geographic interdependency and its implications for the redundancy offered by discrete public transport modes has not been analysed. The novelty of the present study is that it develops a framework that addresses this gap. The application to the case study demonstrates, for the first time, that the contributions of redundancy offered by multiple public transport modes to the connectivity of locations are significantly diminished when rainfall causes multiple flooding-induced closures of links. Furthermore, the novelty of this work is that it shows that common assumptions of ignoring the potential for concurrent link closures during pluvial flood events (e.g., Hong *et al.*, 2019; Ma *et al.*, 2019) leads to markedly different estimates of location losses and link rankings and, therefore, the effect of rainfall on all exposed modes of a study area should be equally considered.

Furthermore, the limited availability of data on historical flooding incidents prevented distinguishing between fluvial and pluvial events or determining return periods of critical rainfall that led to closures. Consequently, only one spatial dependence model was established. In reality, the spatial patterns and dependence structures are expected to vary across events of different frequencies. However, it was not within the scope of this work to develop these more detailed models of rainfall dependencies, but rather to characterise the geographic interdependencies to rainfall-induced flooding as a result of the proximity of transport links and, based on these, identify the most susceptible locations and parts of the networks, which would require more in-depth scrutiny. Future work could focus on integrating spatial dependence and other rainfall characteristics (e.g., seasonality, anisotropy and regional variation) into intensity-duration-frequency curves (e.g., Hefferman and Tawn, 2004; Renard and Lang, 2007; Le *et al.*, 2018) to undertake a comprehensive flood risk analysis for different return periods.

Finally, only one route offered by each mode for travel between locations was considered in the assessment of impacts of extreme rainfall, while multiple routes may exist. Therefore, the method could be extended to consider the k-shortest paths for each mode, and the analysis could be performed using the least-cost routes across the entire set of available options as the preferred choice of travellers, rather than assuming that a specific travel mode is preferred over others.

Despite the abovementioned limitations, the method proposed provides a valuable tool for the assessment of rainfall impacts on transport networks that can be applied to different transport and geographical contexts. From the practitioners' perspective, it is important for network managers to identify those parts of the transport network which if they fail during adverse weather events, including rainfall, would have the most severe consequences on connectivity.

Existing sophisticated methods for the analysis of extreme rainfall on infrastructure systems require the use of flood models which are seldom available to network managers and of which the development requires significant data and computational resources. In contrast, the approach proposed here provides a straightforward method that allows identifying locations subject to concurrent closures and understand the impacts of these simultaneous closures using software tools and data that are readily available to transport practitioners (e.g., spatial data of transport networks and historical closures) or can be easily obtained from other sources (e.g., rainfall data, pluvial flood maps). Furthermore, by accounting for the likelihood of concurrent flooding-induced closures of links, this approach allows practitioners to obtain more realistic estimates of accessibility losses and to better prepare for the potential future indirect costs by taking appropriate engineering measures to adapt susceptible parts of the network to pluvial flooding.

This chapter extended the general and empirical methods for the evaluation of geographic interdependencies presented in Chapters 2 and 3 respectively, by modelling their characteristics of geographic interdependencies in probabilistic terms using records of rainfall timeseries. By incorporating rainfall spatial dependence into the analysis, this study presents a more realistic representation of rainfall impacts on the vulnerability of geographically interdependent public transport networks. The next and final chapter synthesises the key findings of this thesis, discusses broader implications of this research for researchers and practitioners, and outlines future research directions.

5. Discussion

5.1. Completion of the research aim and objectives

The aim of this research was to assess the resilience of public transport modes operating on geographically interdependent transport infrastructure networks to area-wide events, with a particular focus on extreme rainfall. The first study reported in Chapter 2 developed a general framework to characterise the geographic interdependency between two discrete public transport infrastructure networks independent of the nature or intensity of hazardous events. The second study presented in Chapter 3 developed an empirical method to incorporate the characteristics of rainfall-related geographic interdependencies into the assessment of the importance and criticality of public transport links. Finally, Chapter 4 extended this empirical analysis by developing a model of the spatial dependence of flooding-producing rainfall co-occurrences at spatially separate locations, which reflects the likelihood of rainfall-related geographic interdependencies occurring and subsequently incorporating these into the vulnerability assessment. Therefore, as shown in Table 5-1, the research objectives that were previously set out in Table 1-3 were achieved.

Table 5-1 Research objectives achieved in this thesis.

Reference	Research objective	Chapter	Section
OBJ1.1	A review of existing metrics that quantify the redundancy of travel options between locations was carried out.	2	2.2
OBJ2.1	A review of the methods proposed in the literature that quantify the geographic interdependency between infrastructure networks was carried out.	2	2.2
OBJ2.2	A metric was developed that captures the degree of geographic interdependencies between transport infrastructure networks.	2	2.3.2
OBJ3.1	The proposed metric that captures the geographic interdependency was incorporated into selected metrics of redundancy.	2	2.3.2, 2.3.3
OBJ3.2	A general framework was developed to assess the impact of geographic interdependencies between discrete public transport networks on redundancy.	2	2.3
OBJ3.3	Sensitivity analysis on the extent of area-wide events was conducted to assess how the loss of redundancy is affected by the size of footprint of hazardous events.	2	2.5
OBJ4.1	A review of metrics that capture the importance and criticality of transport links was undertaken.	3	3.2

OBJ5.1	Methods that model the likelihood of simultaneous events occurring at spatially distant locations were reviewed, and a method was selected for the purposes of this research.	3	3.3.2
OBJ5.2	The data requirements for the empirical estimation of rainfall-related geographic interdependencies between public transport networks were identified, and datasets were constructed for the purposes of this research.	3	3.4.2, 3.4.3
OBJ6.1	The empirical extent of rainfall-related geographic interdependencies was incorporated into selected metrics of importance and criticality of public transport links.	3	3.3.3, 3.3.4
OBJ6.2	The importance and criticality of public transport links were computed with and without considering the rainfall-related geographic interdependencies, thus allowing to compare the ranking of links for each metric between these two cases.	3	3.5
OBJ7.1	The literature on rainfall-related flood risk assessment of transport networks was reviewed.	4	4.2
OBJ8.1	A method was selected to model the likelihood of concurrent rainfall-induced flood events occurring at spatially proximate locations.	4	4.3.2

OBJ9.1	A framework was proposed for the development of scenarios of concurrent pluvial flood events due to the same rainfall event, which were then incorporated into the vulnerability assessment.	4	4.3.3
OBJ9.2	The losses of redundancy were computed, with and without considering the potential for flooding-producing rainfall co-occurrences in geographically interdependent public transport networks.	4	4.5.3

5.2. Conclusions and Discussion

The methods developed in this thesis were applied to the Scottish public transport network consisting of long-distance bus and rail services. There are several novel findings which were revealed from this research.

In Chapter 2, applying the framework to the case study revealed that losses in network resilience as measured by accessibility indicators are positively correlated to the spatial scale of hazardous events. Specifically, the accessibility losses increase with the scale of area-wide events, suggesting that the contribution of redundancy of travel options to accessibility of locations may be significantly reduced due to the occurrence of these events. As such, ignoring the potential for alternative travel options suffering concurrent disruptions when area-wide events occur, significantly underestimates the true consequences of these events to the accessibility of public transport networks and connectivity of locations. Notably, travel options in close proximity were found to be particularly vulnerable. Furthermore, urban zones experienced higher absolute losses, while rural zones were more vulnerable in relative terms.

Building on this understanding of worst-case accessibility losses, Chapter 3 focused on a specific hazard – in this case, rainfall – by empirically analysing geographic interdependencies using historical disruption records. Importantly, the analysis not only confirmed that geographic interdependencies between rail and bus networks may occur during heavy rainfall events but also informed the selection of an appropriate spatial scale for the assessment of vulnerability of public transport links. Although the ranking of link importance remained relatively unchanged when geographic interdependencies between rail and bus were considered, the criticality of links was significantly affected, particularly in urban centres where clusters of closely spaced links exhibited both high importance and weakness. In practical terms, this means that clusters of spatially proximate rail and bus links, which close frequently due to rainfall and the failure of which will disrupt a significant number of public transport trips, require further scrutiny by infrastructure managers and public transport operators. This is because, in cases of extensive inundation following heavy

rainfall, it is likely that the trips traversing these link clusters will be cancelled simultaneously, thus leaving public transport users with no travel alternative.

Interestingly, the most critical clusters of public transport links identified in Chapter 3 did not overlap the most vulnerable sections of routes shown in Chapter 2. This difference arises from the distinct focuses of each chapter. Chapter 2 assessed geographic interdependencies in terms of accessibility losses, whereas Chapter 3 examined the functionality loss of public transport services. Therefore, these works complement each other and can be used together for a more comprehensive assessment of geographic interdependencies. Furthermore, the empirical findings of Chapter 3 on the geographic interdependencies can inform the buffer-shaped modelling approach used in Chapter 2 for rainfall-specific applications.

Chapter 4 extended the framework of Chapter 2 by incorporating a probabilistic model of rainfall-related geographic interdependencies into the model of redundancy, enabling a more accurate evaluation of concurrent disruptions on the accessibility of locations because of extreme rainfall. The analysis compared the differences in the vulnerability of public transport links and accessibility losses of locations between three separate cases: when ignoring geographic interdependencies (“best case” scenario); when assuming that all exposed links to rainfall will be closed at the same time (“worst case” scenario); and, when assuming that the likelihood of exposed links closing concurrently depends on their separation distance (statistically plausible scenario). Results revealed that, while the overall ranking of rail link importance shared similarities across the scenarios of complete independence, complete dependence, and probabilistic spatial dependence of closures, differences emerged for lower-ranked links, highlighting the need to carefully consider the assumptions adopted on the existence and likelihood of geographic interdependencies. The important links identified in this study are different from the vulnerable route sections of Chapter 2 and critical links of Chapter 3. This can be attributed to the fact that only those links exposed to a rainfall event of a specific frequency were considered, thus targeting the assessment of geographic interdependencies to a subset of the network components as opposed to the two

previous chapters where the links of the entire networks were assessed. Furthermore, in terms of accessibility losses of locations due to the flooding-induced closure of links, the assumption of no interdependency was found to underestimate accessibility losses, whereas adopting the “worst-case” scenario of concurrent closures overestimated them. In contrast, the probabilistic approach produced geographically variable estimates, suggesting it offers a more realistic appraisal of resilience.

Although this findings pertain to the Scotland, they are relevant to areas of similar size and network structure. Specifically, in urban areas, the proximity of transport networks is often constrained by geography. While a significant number of alternative public transport options exist due to high frequency and diversity of services, it is expected that extreme weather-related events have the capacity to concurrently disrupt all these spatially proximate options, thus markedly reducing the available network redundancy and inducing considerable accessibility losses. As such, the worst potential impacts of geographic interdependencies in urban areas will be very high in absolute terms. In contrast, rural areas may have alternative transport options that are more widely spaced, reducing the likelihood of concurrent failures during localised events. However, if large-scale weather events affect these dispersed alternatives simultaneously, redundancy will be significantly reduced, albeit in relative terms.

Findings from the empirical analysis and the impact assessment of rainfall in Chapters 3 and 4 are also relevant to regional and national public transport networks exposed to severe rainfall events, such as those in central Europe and North America. The literature review on the spatial scale of rainfall (Section 1.2.1) highlights that such events can range from localised to regional and even international in extent under both current and future climate conditions. Therefore, considering the extent and likelihood of geographic interdependencies between discrete public transport networks is essential for accurately evaluating the impact of rainfall on transportation systems.

Beyond extreme rainfall, the methods presented in this thesis can be adapted to assess the impact of other weather-related hazards, such as snowfall, hurricanes and windstorms. For example, the framework of Chapter 2 can serve as a preliminary assessment to identify particularly vulnerable sections of routes by selecting an appropriate buffer width for the hazard of concern. The empirical method of Chapter 3 can be applied to characterise the geographic interdependencies that may occur due to the event using historical disruption records for the public transport networks of study. The systematic impact assessment of Chapter 4 can be employed to obtain more accurate estimates of accessibility losses considering both the location and spatial scale of the weather event.

Within the context of vulnerability assessment, previous studies have primarily examined the impacts of isolated link failures on single- or multi-modal networks without considering the spatial correlation of disruptions (e.g., Jenelius et al., 2006; Taylor et al., 2006; Rodriguez-Núñez and García-Palomares, 2014; Cats and Jenelius, 2014). Furthermore, studies to date that have developed general methods for the evaluation of impacts of area-wide events on transport vulnerability, have been limited to individual transport infrastructure networks, namely road or rail (Mattson and Jenelius, 2012; Du et al., 2023; Ouyang et al., 2019). In contrast, this thesis captures the joint exposure of discrete public transport networks to area-wide weather events by integrating resilience indicators with geographic interdependency metrics based on the separation distances of network components. This is achieved through the development of the general framework for the evaluation of geographic interdependencies in Chapter 2 as well as the empirical analysis of their characteristics for a certain hazard in Chapters 3 and 4. To the author's knowledge, no work to date has attempted to analyse historical disruption records for transport networks to characterise the weather-induced geographic interdependency between them and integrate them into the vulnerability assessment to area-wide events.

Using rainfall as the hazard of concern, the research in this work is the first to systematically analyse the consequences of concurrent flood-producing rainfall events on both the functionality of discrete public transport modes and accessibility

of locations. Although extensive research exists on the impacts of pluvial flooding on transportation, most works to date have focused solely on road (e.g., Pregolato et al., 2017; Pyatkova et al., 2019) or rail (e.g., Hong et al., 2015; Forero-Ortiz et al., 2020; Zhu et al., 2022), therefore underestimating the accessibility losses of rainfall across the broader transport system. Even studies that consider multimodal transport networks, ignore the potential for concurrent disruptions across all the modes analysed and, therefore, misrepresent the impacts on the functionality of networks (Hong et al. 2019; Ma et al., 2019; He et al., 2020). In contrast, the research presented in this thesis, takes a thorough approach by first empirically examining geographic interdependencies resulting from historical rainfall events (Chapter 3), confirming that concurrent closures across discrete public transport modes should be incorporated into the impact assessments. This empirical assessment provided the foundation for developing a probabilistic model of interdependencies, which was then used to systematically evaluate the impact of flood-producing rainfall events on interdependent public transport networks (Chapter 4).

5.3. Limitations and recommendations for future research directions

The research presented in this thesis comes with several limitations. Limitations that specifically pertain to each study are reported at the end of Chapters 2, 3 and 4.

Regarding the limitations on methods developed for the purposes of this research, the geographic interdependency between rail and bus was initially defined using a buffer-based approach in the general framework proposed in Chapter 2. This approach assumes that alternative routes lying within the buffer-shaped neighbourhood of the primary routes are concurrently exposed to the same hazardous event, while those parts of the alternative routes lying outside of the buffer are considered to be unaffected. While this approach may be appropriate when exploring the geographic interdependencies for various hazards without necessarily considering their nature, the “cliff edge” effect that results from the delineation of buffers may not provide realistic results when analysing

interdependencies stemming from a given weather-related hazard. Indeed, for flooding, the empirical analysis of concurrent disruptions between rail and bus links (Chapter 3) as well as the spatial dependence structure of rainfall co-occurrences (Chapter 4) revealed that the likelihood of flooding-related geographic interdependencies decays as the separation distance between network components increase.

Therefore, although the general framework of Chapter 2 may provide useful preliminary insights into the susceptibility of geographically interdependent transport networks, efforts should be made to understand how the extent of geographic interdependencies varies with separation distance due to the occurrence of a certain hazard. Similarly, in the empirical analysis of Chapter 3, owing to the limitations of the available data, a buffer-based approach was employed to assess the importance and criticality of public transport links. Although the extent of the buffer-shaped neighbourhood was informed by analysis of the historical datasets of flood events on the two networks considered, the approach did not account for the effect of separation distance between components or the intensity of rainfall to the likelihood of geographic interdependencies occurring. A useful extension of this work would be to incorporate the conditional probability of links being concurrently flooded in the metrics of importance and criticality (e.g. using the spatial dependence model of Chapter 4) based on the separation distance of the links.

In Chapter 4, the limitations of the buffer-shaped neighbourhood were addressed by modelling the conditional probability of critical (flood-producing) rainfall co-occurrences at spatially proximate locations. However, the characteristics of the critical rainfall events were estimated based on the Thiessen polygon method, which assumes that rainfall on a link is the same as that recorded by the nearest rain station, and, as such, this may not provide accurate estimates. By extension, the accuracy of the spatial dependence model used to characterise the geographic interdependencies could be improved by identifying critical rainfall events using radar data or more sophisticated techniques of rainfall interpolation. Additionally, the spatial dependence model for critical rainfall co-occurrences was established

without considering the differences in the spatial dependence structure between intense and milder critical rainfall events or their return periods. It is expected that the spatial extent of rainfall varies according to its frequency and severity and, therefore, a useful extension to this work would be to develop a suite of spatial dependence models that consider the intensity and frequency of critical rainfall events.

Furthermore, in Chapters 2 and 4 only the least-cost rail and bus routes that connect the O-D pairs of concern were considered in the assessment of geographic interdependencies. The methods proposed in these chapters could be extended to incorporate less preferred rail and bus routes for a given OD pair as well as routes offered by other transport modes that may provide feasible alternative options. For the general framework presented in Chapter 2, this would require considering in the neighbourhood coefficient (Section 2.3.2) the extent to which each alternative route lies within the buffers of the already selected options, as shown in Equation S1 of Appendix A. Regarding the flood impact assessment, additional spatial dependence models would need to be established that predict the likelihood of critical rainfall co-occurrences on links of the same infrastructure network (e.g., $P(\text{rail}^{\text{flood}}|\text{rail}^{\text{flood}})$, $P(\text{bus}^{\text{flood}}|\text{bus}^{\text{flood}})$). In a similar vein, the measures of importance and criticality proposed in Chapter 3 could be extended to consider the neighbouring links of the same mode which are located within the buffer of the link of concern. This would provide more comprehensive results on the importance and criticality of buffers.

Moreover, in this research, the assessment of geographic interdependencies was carried out using a static approach, which, for Chapters 2 and 4, involved identifying rail and bus routes that may be concurrently exposed to hazards for a certain time window of a weekday and, for Chapter 3, it involved considering the public transport trips traversing each link on a typical weekday. Repeating these analyses for various time windows would allow identifying the times of day and days of week, where the impact of geographic interdependencies on the resilience of networks is the most significant.

Another limitation in relation to the methods of this research is that the accessibility in Chapters 2 and 4 was estimated on the basis of travel time. However, other components of travel deterrence could be also considered in this work, such as travel distance and economic cost of travel. In addition, the population in the origin zones of travel as well as attractiveness of destinations (e.g., employment, education) could be incorporated into the method to analyse the impact of geographic interdependencies on social components of resilience and the activity system. These additions would provide further insights into the locations most affected by weather-related area-wide events, which require prioritisation for interventions. Regarding Chapter 3, the importance of public transport links was defined on the basis of rail and bus trips that traverse each link. Other metrics could be used to measure the importance, such as the number of shortest paths, number of passengers on the services using the links, or, in a similar direction with Chapter 4, the importance of a link could be defined based on the accessibility loss caused by its failure.

A final limitation on the methods of this work is that the flexibilities and restrictions associated with each public transport mode were not considered in the analysis. For instance, it was not considered whether bus services may divert to avoid the location of the hazardous event or if rail operators could employ replacement bus services to accommodate rail passengers in the event of disruption. As such, this work could be extended to incorporate these characteristics, as well as the ability of travellers to transfer to another mode in order to reach their destination. This would require considering the physical interdependencies between rail and bus in the event of disruptions, e.g. by connecting the bus stops and rail stations that travellers can use to transfer between services using interlinks. An important characteristic that could also be included in the analysis is the capacity of each mode, which could be used to model congestion effects inflicted by the concurrent disruptions on rail and bus. This however would require the use of more sophisticated transport models that realistically capture the travellers' movement and travel behaviour.

Regarding the datasets used for the purposes of this research, there are several limitations associated with them. Specifically, the available GTFS data for bus services

in Scotland, which were used to construct the representation of the long-distance bus network, did not make any distinction between local, regional and long-distance routes. Therefore, with a view to retain only longer-distance services, travel distance was used to exclude routes of local and regional services. However, since no consensus exists on the minimum distance required for routes to be considered as long-distance, an arbitrary distance threshold was selected. Sensitivity analysis would need to be carried out to understand how the results of the analyses vary based on the threshold that defines bus services as long-distance. Furthermore, the selection of bus routes could be further refined by retaining bus services with termini in different localities which exceed a given route distance threshold.

Moreover, several limitations exist in the incident data which were used in Chapters 3 and 4. In the absence of a readily available incident dataset for the entire long-distance bus network, several datasets were obtained and combined. Due to the difficulty in acquiring and fusing these records, only a subset of the long-distance bus network was used, which consisted of services provided by selected coach operating companies. In addition, the incident data did not provide complete coverage even for the selected subset of the long-distance bus network, which increased the uncertainty of results from both the empirical assessment of geographic interdependencies and criticality of public transport links. Another limitation that adversely affected the assessment of geographic interdependencies and criticality of links was that the records provided by the relevant transport authorities did not provide the exact location of flooding for each incident. This resulted in high uncertainty of the estimated level of flooding-related geographic interdependencies between bus and rail as well as the weakness and criticality of links.

Furthermore, since the incident data were available for only a short time period, the conditional probabilities that were used to characterise the flooding-related geographic interdependency between bus and rail links were very low and, therefore, a buffer-based approach was adopted, as previously stated. The availability of records for a longer time period would allow the development of a more robust model of geographic interdependencies which could be incorporated in

the measure of criticality. Although this model was constructed in Chapter 4 using the available rainfall data, the large separation distances between rain stations of the study area did not allow to compute the conditional probabilities of critical rainfall co-occurrences for small distance bins. Thus, the spatial resolution of a model constructed using rainfall data of rain stations would be coarser compared to a similar model developed using incident data between spatially proximate transport links.

The existence of only limited records, coupled with the unavailability of the incident durations, also affected the measure of weakness (and criticality). As such, the measure of weakness was developed to reflect the frequency of flood events on links irrespective of the event duration or severity of flooding impacts on the links (i.e., partial or full closure). In case that long incidents records existed, a metric of weakness could be established for each severity of flooding impact.

A final limitation in relation to the available data is that, in the absence of hazard-specific explanatory variables that could enable the construction of a link-level model of weakness to flooding, only link length was used as an explanatory variable, which is considered as a general property of links, rather than a characteristic which pertains specifically to flooding. To establish hazard-specific link-level models of weakness, further research is needed to identify predictors that affect the frequency of flooding of public transport links, such as average intensity of rainfall on links, topography, surrounding environment etc.

5.4. Contributions of research to theory and practice

This research contributes to the current state of knowledge on the resilience of transport networks to weather-related disruptions in the following ways:

- The development of a general method for the assessment of the impact of geographic interdependencies between transport infrastructure networks on the resilience of discrete public transport modes, from an accessibility perspective. This work provided a robust understanding of the parts of

separate infrastructure networks on which discrete public transport modes operate and which are jointly exposed to spatially defined events stemming from adverse weather conditions. The sensitivity analysis conducted for this work on the impact of the size of area affected on the severity of consequences to the networks allows the implications of the spatial extent of events to the resilience of public transport networks as well as accessibility of areas to be understood.

- The development of an empirical method to characterise the extent of geographic interdependencies between links of discrete public transport networks for a given hazard of concern, which, in this case, was flooding. Incorporating the degree of this interdependency to the criticality assessment enabled the identification of spatially proximate rail and bus links that are both weak (i.e., more frequently closed due to flooding than expected) and important (i.e., used by many public transport trips). The concurrent closure of these links would therefore result in significantly adverse consequences to the functionality of both networks, but also to the potential for public transport users to undertake their trips using either of these modes. The work further demonstrated that the criticality of links is significantly different when accounting for the geographic interdependency between modes than when ignoring it, thereby highlighting that the prioritisation of links to weather-related area-covering events should be different from that for point-based incidents.
- The development of a model that estimates the probability of concurrent rainfall-related flooding incidents occurring based on the degree of spatial proximity between locations. Incorporating this model to the impact assessment of pluvial flooding to discrete public transport modes allows identifying the most important links of a given mode, which have a higher probability of experiencing concurrent closures with nearby links of an alternative mode, as such leading to the most significant losses in

accessibility. Further, the inclusion of geographic interdependencies through this model to the impact assessment provided better estimates of the indirect consequences of flooding to the accessibility of locations.

The work conducted for the purposes of this thesis makes several academic contributions within the context of resilience of public transport networks to weather-related disruptions. Specifically, this research systematically assessed the resilience of public transport modes operating on distinct transport infrastructure networks, while accounting for their likelihood of being concurrently disrupted due to a weather-related area-wide event occurring. The assumption that hydrometeorological events, such as rainfall and flooding, affect only one type of transport infrastructure, while other transport networks remain intact (e.g. Hong *et al.*, 2019; Ma *et al.*, 2019) is not realistic. This is because weather events cover areas, rather than a single spatial point at a time, and, therefore, all infrastructure networks located within their spatial footprint may suffer damage, consequently leading to concurrent disruptions across multiple transport modes. In other words, adverse weather conditions may reveal geographic interdependencies between separate infrastructure networks that are not apparent under normal conditions. While extensive research has been conducted on the implications of geographic interdependencies between other infrastructure networks, very limited work has been done for public transport modes operating on separate transport networks.

Furthermore, in assessing the impacts of weather-related events on the resilience of networks, it cannot be assumed that the redundancy of the transport network helps to maintain the connectivity between locations in the same way as when spatially confined incidents occur. However, research on the losses in redundancy when area-wide events occur is still in its infancy. Therefore, this research work addressed this important gap by analysing the potential losses in redundancy arising from area-covering events, while exploring how impacts in redundancy change based on the size of spatial footprint of events.

Moreover, due to the scarcity of empirical analyses of geographic interdependencies between transport networks to specific weather-related hazards, a part of this research was devoted to empirically assessing the characteristics of flooding-related geographic interdependencies between rail and bus based on historical incident datasets and estimating their impacts on the importance and criticality of public transport links.

A final contribution of this thesis to the current body of research is the construction of a model showing the probability of flooding-related geographic interdependencies occurring at distant locations based on long records of rainfall data and using this model to estimate losses in accessibility as a result of concurrent closures in two discrete public transport networks. Although significant research has been previously carried out to understand the impacts of flooding on the operation of public transport networks, to the author's knowledge, no work has assessed to date the concurrent effects of flooding to the functionality of multiple modes that operate on separate infrastructure networks.

From the practitioners' perspective, current transport policies particularly emphasise the need to transition away from the use of private vehicles and prioritise public transport modes for both short and longer-distance trips. However, in the past decades, public transport networks have been increasingly disrupted to adverse weather, including rainfall-induced flooding, and this vulnerability may deter travellers from using public transport for their trips. This research helps both transport infrastructure owners and public transport operators identify network components, of which the failure has the greatest impact on the performance of networks and connectivity of locations, while also taking into account the potential for the concurrent failure of alternative options. This in turn enables practitioners to identify which sections of their network needs to be prioritised for further assessment and adaptation measures.

Specifically, the general method of impact assessment of geographic interdependencies in Chapter 2 enables practitioners to identify areas where the

potential losses in resilience due to spatially defined events are substantial, thus allowing them to prioritise those areas requiring further scrutiny. Network managers can apply this method using data and tools which are readily available to them. Specifically, they can use spatial data to identify key alternative public transport routes within a region or country, along with the associated travel costs. By delineating buffers around these routes in openly available GIS tools, they can determine which sections of the alternative routes may be exposed to the same area-wide event. The travel costs of the alternative routes can be then adjusted proportionately based on the share of routes that are jointly exposed, allowing for the calculation of redundancy and substitutability indicators for O-D pairs and origin (or destination) zones in the study area. By applying this process with varying buffer widths, the approach can be easily adapted to explore the effects of events at different spatial scales. Therefore, this enables practitioners to identify areas requiring further attention for localised events, as well as those that are only affected by large-scale hazards.

The research conducted in Chapter 3 provides infrastructure managers and public transport operators with an empirical method to identify the areas where susceptible links of separate transport infrastructure networks are co-located. If these links close due to the same weather event, their failure can have severe consequences for the operation of public transport modes that rely on them. To apply this method, timetable data can be used to determine which public transport links carry the highest number of services and are therefore the most important. Historical disruption records can then be analysed to estimate link weakness. When combined with the importance indicator, this allows for the identification of the most critical links within a public transport network. Importantly, these records can also be mapped in GIS and analysed to assess whether links of alternative public transport modes have historically been affected by the same weather-related event, thereby determining the extent of geographic interdependencies between them. By delineating buffers, clusters of links which are highly important and/or critical, can be then identified and prioritised for intervention.

Finally, the work undertaken in Chapter 4 provides transport authorities with a method to identify transport infrastructure links used by alternative public transport modes that are likely to flood simultaneously due to the same rainfall event, consequently leading to high accessibility losses. The method developed is easily applicable using openly available data. Specifically, infrastructure managers can analyse historical disruption records alongside readily available rainfall datasets to estimate the characteristics of rainfall events that have previously caused full link closures. The rainfall datasets can then be used to model the spatial dependence of these rainfall co-occurrences, providing a probabilistic representation of rainfall-related geographic interdependencies between networks. To identify links exposed to the hazard, transport networks can be mapped in GIS and spatially intersected with pluvial flood maps. By considering the closure of these exposed links along with the likelihood of nearby links failing concurrently, redundancy losses can be estimated, allowing for the identification of the most critical links. Accounting for the probability of concurrent closures results in more realistic accessibility loss estimates and enables practitioners to better prepare for the indirect costs associated with rainfall or other weather-related hazards, such as storm surges or heavy snowfall.

6. Conclusions

This thesis presents a novel framework for the assessment of resilience and vulnerability of geographically interdependent public transport networks based on three separate studies.

The first study presents a framework that assesses accessibility losses due to hazards at various spatial scales. Building on this, the second study draws on flood incident data to estimate rainfall-related geographic interdependencies between two discrete public transport networks, which is then used to assess the importance and criticality of links in both networks. The third study captures geographic interdependencies by developing a probabilistic spatial dependence model of flood-producing rainfall events and applies this model to a pluvial flood hazard map in order to estimate the accessibility impacts of heavy rainfall events on public transport networks. The research is applied to the Scottish long-distance bus and rail networks.

Results reveal that losses in accessibility are often substantial even for localised hazards and that these are positively correlated with the spatial scale of event. For rainfall, the empirical analysis confirms the existence of geographic interdependencies between rail and bus and reveals that the criticality of links of both modes is significantly affected when geographic interdependencies due to rainfall are considered. Results of the pluvial flooding impact assessment show that accessibility losses are potentially hi

gher than when geographical interdependencies are ignored. This research provides novel insights into the role of geographic interdependencies to the resilience of public transport networks and enables infrastructure managers to identify locations that require further scrutiny.

Although the findings focus on Scotland's long-distance public transport networks, they are applicable to other regions and countries exposed to heavy rainfall.

References

- Adjetey-Bahun, K., Birregah, B., Châtelet, E., & Planchet, J. L. (2016). A model to quantify the resilience of mass railway transportation systems. *Reliability Engineering & System Safety*, 153, 1-14.
- Agarwal, J. (2015). Improving resilience through vulnerability assessment and management. *Civil Engineering and Environmental Systems*, 32(1-2), 5-17.
- Anas, A (1983) 'Discrete choice theory, information theory, and the multinomial logit and gravity models', *Transportation Research B*, vol. 17, pp. 13-23.
- Aparicio, J. T., Arsenio, E., & Henriques, R. (2022). Assessing robustness in multimodal transportation systems: a case study in Lisbon. *European transport research review*, 14(1), 28.
- Association of Train Operating Companies (2020). ATOC GTFS [Data set]. <https://transitfeeds.com/p/association-of-train-operating-companies/284>. Accessed 21/09/2020.
- Aultman-Hall, L. (2018). Incorporating long-distance travel into transportation planning in the United States.
- Baek, S. S., Choi, D. H., Jung, J. W., Lee, H. J., Lee, H., Yoon, K. S., & Cho, K. H. (2015). Optimizing low impact development (LID) for stormwater runoff treatment in urban area, Korea: Experimental and modeling approach. *Water research*, 86, 122-131.
- Ben-Akiva, M. E. and Lerman, S. R. (1985). Discrete Choice Analysis: Theory and Application to Travel Demand, *MIT Press, Cambridge, Ma*.
- Berche, B., Von Ferber, C., Holovatch, T., & Holovatch, Y. (2009). Resilience of public transport networks against attacks. *The European Physical Journal B*, 71, 125-137.
- Berche, B., FERBER, C. V., Holovatch, T., & Holovatch, Y. (2012). Transportation network stability: a case study of city transit. *Advances in Complex Systems*, 15(supp01), 1250063.
- Berdica, K. (2002). An introduction to road vulnerability: what has been done, is done and should be done. *Transport policy*, 9(2), 117-127.
- Betts, R.A. and Brown, K. (2021) Introduction. In: *The Third UK Climate Change Risk Assessment Technical Report* [Betts, R.A., Haward, A.B. and Pearson, K.V.(eds.)]. Prepared for the Climate Change Committee, London
- Bevacqua, E., Shepherd, T. G., Watson, P. A., Sparrow, S., Wallom, D., & Mitchell, D. (2021). Larger spatial footprint of wintertime total precipitation extremes in a warmer climate. *Geophysical Research Letters*, 48(8), e2020GL091990.

- Birch, C. P., Oom, S. P., & Beecham, J. A. (2007). Rectangular and hexagonal grids used for observation, experiment and simulation in ecology. *Ecological modelling*, 206(3-4), 347-359.
- Bondemark, A., Kopsch, F., & Johansson, E. (2021). Accessibility and uncertainty. *Journal of Transport and Land Use*, 14(1), 463-477.
- Bowyer, P., Hänsel, S., Smalley, E., Velegrakis, A., Dagan, M., & Wyrowski, L. (2020). Climate Change Impacts and Adaptation for Transport Networks and Nodes (No. ECE/TRANS/283).
- Brassel, K. E., & Reif, D. (1979). A procedure to generate Thiessen polygons. *Geographical analysis*, 11(3), 289-303.
- Breugem, A. J., Wesseling, J. G., Oostindie, K., & Ritsema, C. J. (2020). Meteorological aspects of heavy precipitation in relation to floods—an overview. *Earth-Science Reviews*, 204, 103171.
- Bruneau, M., Chang, S. E., Eguchi, R. T., Lee, G. C., O'Rourke, T. D., Reinhorn, A. M., ... & Von Winterfeldt, D. (2003). A framework to quantitatively assess and enhance the seismic resilience of communities. *Earthquake spectra*, 19(4), 733-752.
- Brunner, M. I., Gilleland, E., Wood, A., Swain, D. L., & Clark, M. (2020). Spatial dependence of floods shaped by spatiotemporal variations in meteorological and land-surface processes. *Geophysical Research Letters*, 47(13), e2020GL088000.
- Cao, N., & Cao, H. (2020). Exploring the robustness of urban bus network: a case from Southern China. *Chinese Journal of Physics*, 65, 389-397.
- Caracciolo, D., Arnone, E., Conti, F. L., & Noto, L. V. (2017). Exploiting historical rainfall and landslide data in a spatial database for the derivation of critical rainfall thresholds. *Environmental Earth Sciences*, 76, 1-16.
- Cats, O., and Jenelius, E. (2014). Dynamic vulnerability analysis of public transport networks: mitigation effects of real-time information. *Networks and Spatial Economics*, 14(3), 435-463.
- Cats, O. and Jenelius, E. (2015) 'Planning for the unexpected: The value of reserve capacity for public transport network robustness', *Transportation Research Part A: Policy and Practice*. Elsevier Ltd, 81, pp. 47–61. doi: 10.1016/j.tra.2015.02.013.
- Chan, H. Y., Xu, Y., Chen, A., & Zhou, J. (2023). Choice and equity: A critical analysis of multi-modal public transport services. *Transport Policy*, 140, 114-127.
- Chang, W., Stein, M. L., Wang, J., Kotamarthi, V. R., & Moyer, E. J. (2016). Changes in spatiotemporal precipitation patterns in changing climate conditions. *Journal of Climate*, 29(23), 8355-8376.

Chatzigeorgiadis, M., Dogani, I., Doganis, T. (2023, October 11). Thessaly flood (Storm Daniel): A multi-temporal analysis of the flood impact using Sentinel-1 and Sentinel-2 images. <https://storymaps.arcgis.com/stories/e7dca3fe3d114860872f3108587c23db>

Chen, X. Z., Lu, Q. C., Peng, Z. R., & Ash, J. E. (2015). Analysis of transportation network vulnerability under flooding disasters. *Transportation research record*, 2532(1), 37-44.

Coles, D., Yu, D., Wilby, R. L., Green, D., & Herring, Z. (2017). Beyond 'flood hotspots': Modelling emergency service accessibility during flooding in York, UK. *Journal of hydrology*, 546, 419-436.

Crucitti, P., Latora, V., & Porta, S. (2006). Centrality measures in spatial networks of urban streets. *Physical Review E—Statistical, Nonlinear, and Soft Matter Physics*, 73(3), 036125.

D'Este, G. A., & Taylor, M. A. (2003). Network vulnerability: an approach to reliability analysis at the level of national strategic transport networks. In *The network reliability of transport (Vol. 1, pp. 23-44)*. Emerald Group Publishing Limited.

Dalziell, E. (1998) 'Risk assessment methods in road network evaluation: a study of the impact of natural hazards on the Desert Road, New Zealand'. Available at: <http://ir.canterbury.ac.nz/handle/10092/5633>.

Dalziell, E., & Nicholson, A. (2001). Risk and impact of natural hazards on a road network. *Journal of transportation engineering*, 127(2), 159-166.

De Smith, M. J., Goodchild, M. F., & Longley, P. (2007). *Geospatial analysis: a comprehensive guide to principles, techniques and software tools*. Troubador publishing ltd.

Dong, S., Wang, H., Mostafizi, A., & Song, X. (2020). A network-of-networks percolation analysis of cascading failures in spatially co-located road-sewer infrastructure networks. *Physica A: Statistical Mechanics and its Applications*, 538, 122971.

Du, C., Ouyang, M., Zhang, H., Wang, B., & Wang, N. (2023). Resilience patterns of urban road networks under the worst-case localized disruptions. *Risk analysis*.

Dudenhoeffer, D. D., Permann, M. R., & Manic, M. (2006, December). CIMS: A framework for infrastructure interdependency modeling and analysis. In *Proceedings of the 2006 winter simulation conference* (pp. 478-485). IEEE.

Evans, B., Chen, A. S., Djordjević, S., Webber, J., Gómez, A. G., & Stevens, J. (2020). Investigating the effects of pluvial flooding and climate change on traffic flows in Barcelona and Bristol. *Sustainability*, 12(6), 2330.

- Fang, C., Dong, P., Fang, Y. P., & Zio, E. (2020). Vulnerability analysis of critical infrastructure under disruptions: An application to China Railway High-speed. *Proceedings of the Institution of Mechanical Engineers, Part O: Journal of Risk and Reliability*, 234(2), 235-245.
- Fang, C., Chu, Y., Fu, H., & Fang, Y. (2022). On the resilience assessment of complementary transportation networks under natural hazards. *Transportation research part D: transport and environment*, 109, 103331.
- Fathom Global (2021). Flood Emergency Report Germany 2021. https://www.fathom.global/wp-content/uploads/2021/12/Flood-Emergency-Report-Germany-2021-1_compressed.pdf
- Ferrari, C., & Santagata, M. (2023). Vulnerability and robustness of interdependent transport networks in north-western Italy. *European Transport Research Review*, 15(1), 6.
- Forero-Ortiz, E., Martínez-Gomariz, E., Cañas Porcuna, M., Locatelli, L., & Russo, B. (2020). Flood risk assessment in an underground railway system under the impact of climate change—A case study of the Barcelona metro. *Sustainability*, 12(13), 5291.
- Forbes H., Ball K., McLay F. (2015). Natural Flood Management Handbook. *Scottish Environment Protection Agency*. <https://www.sepa.org.uk/media/163560/sepa-natural-flood-management-handbook1.pdf>
- Frappier, A., Morency, C., & Trépanier, M. (2018). Measuring the quality and diversity of transit alternatives. *Transport Policy*, 61, 51-59.
- Freeman, L. C., Borgatti, S. P., & White, D. R. (1991). Centrality in valued graphs: A measure of betweenness based on network flow. *Social networks*, 13(2), 141-154.
- Galiano, E. F. (1982). Pattern detection in plant populations through the analysis of plant-to-all-plants distances. *Vegetatio*, 49(1), 39-43.
- Georganta, C., Feloni, E., Nastos, P., & Baltas, E. (2022). Critical Rainfall Thresholds as a Tool for Urban Flood Identification in Attica Region, Greece. *Atmosphere*, 13(5), 698.
- Geurs, K. T., & Van Wee, B. (2004). Accessibility evaluation of land-use and transport strategies: review and research directions. *Journal of Transport geography*, 12(2), 127-140.
- Ghanghas, A., Sharma, A., Dey, S., & Merwade, V. (2023). How is spatial homogeneity in precipitation extremes changing globally?. *Geophysical Research Letters*, 50(16), e2023GL103233.

- Guinard, K., Mailhot, A., & Caya, D. (2015). Projected changes in characteristics of precipitation spatial structures over North America. *International Journal of Climatology*, 35(4), 596-612.
- Gvoždíková, B., Müller, M., & Kašpar, M. (2019). Spatial patterns and time distribution of central European extreme precipitation events between 1961 and 2013. *International Journal of Climatology*, 39(7), 3282-3297.
- Hackl, J., Lam, J. C., Heitzler, M., Adey, B. T., & Hurni, L. (2018). Estimating network related risks: A methodology and an application in the transport sector. *Natural Hazards and Earth System Sciences*, 18(8), 2273-2293.
- Han, C., & Liu, L. (2009, September). Topological vulnerability of subway networks in China. In *2009 International Conference on Management and Service Science* (pp. 1-4). IEEE.
- Hansen, W. G. (1959). Accessibility and residential growth (Doctoral dissertation, Massachusetts Institute of Technology).
- He, Y., Thies, S., Avner, P., & Rentschler, J. (2020). The Impact of Flooding on Urban Transit and Accessibility.
- Heffernan, J. E., & Tawn, J. A. (2004). A conditional approach for multivariate extreme values (with discussion). *Journal of the Royal Statistical Society Series B: Statistical Methodology*, 66(3), 497-546.
- Hong, L. *et al.* (2015) 'Vulnerability assessment and mitigation for the Chinese railway system under floods', *Reliability Engineering and System Safety*. Elsevier, 137, pp. 58–68. doi: 10.1016/j.ress.2014.12.013.
- Hong, L., Yan, Y., Ouyang, M., Tian, H., & He, X. (2017). Vulnerability effects of passengers' intermodal transfer distance preference and subway expansion on complementary urban public transportation systems. *Reliability Engineering & System Safety*, 158, 58-72.
- Hong, L., Zhong, X., Ouyang, M., Tian, H., & He, X. (2019). Vulnerability analysis of public transit systems from the perspective of urban residential communities. *Reliability Engineering & System Safety*, 189, 143-156.
- Hughes, J. F., Wild, A. J., & Muzyk, C. (2020). *Developing a method for quantifying transport interdependencies* (No. 671). Waka Kotahi= NZ Transport Agency.
- Huizinga, J., De Moel, H., & Szewczyk, W. (2017). *Global flood depth-damage functions: Methodology and the database with guidelines* (No. JRC105688). Joint Research Centre (Seville site).

Hunt, J. C. R. (2005). Inland and coastal flooding: developments in prediction and prevention. *Philosophical Transactions of the Royal Society A: Mathematical, Physical and Engineering Sciences*, 363(1831), 1475-1491.

IPCC, 2022: Summary for Policymakers [H.-O. Pörtner, D.C. Roberts, E.S. Poloczanska, K. Mintenbeck, M. Tignor, A. Alegría, M. Craig, S. Langsdorf, S. Löschke, V. Möller, A. Okem (eds.)]. In: *Climate Change 2022: Impacts, Adaptation and Vulnerability*. Contribution of Working Group II to the Sixth Assessment Report of the Intergovernmental Panel on Climate Change [H.-O. Pörtner, D.C. Roberts, M. Tignor, E.S. Poloczanska, K. Mintenbeck, A. Alegría, M. Craig, S. Langsdorf, S. Löschke, V. Möller, A. Okem, B. Rama (eds.)]. Cambridge University Press, Cambridge, UK and New York, NY, USA, pp. 3–33, doi:10.1017/9781009325844.001.

Islam, T., & Moselhi, O. (2012). Modeling geospatial interdependence for integrated municipal infrastructure. *Journal of Infrastructure Systems*, 18(2), 68-74.

Israelsson, J., Black, E., Neves, C., Torgbor, F. F., Greatrex, H., Tanu, M., & Lamptey, P. N. L. (2020). The spatial correlation structure of rainfall at the local scale over southern Ghana. *Journal of Hydrology: Regional Studies*, 31, 100720.

Jaroszweski, D., Hooper, E., & Chapman, L. (2014). The impact of climate change on urban transport resilience in a changing world. *Progress in Physical Geography*, 38(4), 448-463.

Jenelius, E., Petersen, T., & Mattsson, L. G. (2006). Importance and exposure in road network vulnerability analysis. *Transportation Research Part A: Policy and Practice*, 40(7), 537-560.

Jenelius, E. and Mattsson, L. G. (2012) 'Road network vulnerability analysis of area-covering disruptions: A grid-based approach with case study', *Transportation Research Part A: Policy and Practice*. Elsevier Ltd, 46(5), pp. 746–760. doi: 10.1016/j.tra.2012.02.003. Jenelius, E., & Mattsson, L. G. (2020). Resilience of transport systems. *Encyclopedia of Transportation*.

Jenelius, E., & Mattsson, L. G. (2020). Resilience of transport systems. *Encyclopedia of Transportation*.

Jenks, G. F., & Caspall, F. C. (1971). Error on choroplethic maps: definition, measurement, reduction. *Annals of the Association of American Geographers*, 61(2), 217-244.

Jing, W., Xu, X., & Pu, Y. (2019). Route redundancy-based network topology measure of metro networks. *Journal of Advanced Transportation*, 2019.

Johansson, J. and Hassel, H. (2010) 'An approach for modelling interdependent infrastructures in the context of vulnerability analysis', *Reliability Engineering and*

- System Safety*. Elsevier, 95(12), pp. 1335–1344. doi: 10.1016/j.res.2010.06.010.
- Joo, J., Lee, J., Kim, J. H., Jun, H., & Jo, D. (2013). Inter-event time definition setting procedure for urban drainage systems. *Water*, 6(1), 45-58.
- Kays, H. I., Sadri, A. M., Muraleetharan, K. M., Harvey, P. S., & Miller, G. A. (2023). Exploring the Interdependencies Between Transportation and Stormwater Networks: The Case of Norman, Oklahoma. *Transportation Research Record*, 2678(5), pp.491-513.
- Klau, G. W., & Weiskircher, R. (2005). Robustness and resilience. In *Network Analysis: Methodological Foundations* (pp. 417-437). Berlin, Heidelberg: Springer Berlin Heidelberg.
- Koenker, R., & Machado, J. A. (1999). Goodness of fit and related inference processes for quantile regression. *Journal of the american statistical association*, 1296-1310.
- Koks, E. E., Rozenberg, J., Zorn, C., Tariverdi, M., Vousdoukas, M., Fraser, S. A., & Hallegatte, S. (2019). A global multi-hazard risk analysis of road and railway infrastructure assets. *Nature communications*, 10(1), 2677.
- Koks, E., Van Ginkel, K., Van Marle, M., & Lemnitzer, A. (2021). Brief communication: Critical infrastructure impacts of the 2021 mid-July western European flood event. *Natural Hazards and Earth System Sciences Discussions*, 2021, 1-11.
- Laporte, G., Marin, A., Mesa, J. A., & Perea, F. (2011). Designing robust rapid transit networks with alternative routes. *Journal of advanced transportation*, 45(1), 54-65.
- Latora, V., & Marchiori, M. (2001). Efficient behavior of small-world networks. *Physical review letters*, 87(19), 198701.
- Le, P. D., Leonard, M., & Westra, S. (2018). Modeling spatial dependence of rainfall extremes across multiple durations. *Water Resources Research*, 54(3), 2233-2248.
- Lee, H., Calvin, K., Dasgupta, D., Krinner, G., Mukherji, A., Thorne, P., ... & Zommers, Z. (2023). Climate change 2023: synthesis report. *Contribution of working groups I, II and III to the sixth assessment report of the intergovernmental panel on climate change*. The Australian National University.
- Lengfeld, K., Winterrath, T., Junghänel, T., & Becker, A. (2019). Characteristic spatial extent of rain events in Germany from a radar-based precipitation climatology. In *Rainfall Monitoring, Modelling and Forecasting in Urban Environment. UrbanRain18: 11th International Workshop on Precipitation in Urban Areas. Conference Proceedings* (pp. 61-66). ETH Zurich, Institute of Environmental Engineering.
- Li, T., Rong, L. and Yan, K. (2019) 'Vulnerability analysis and critical area identification

of public transport system : A case of high-speed rail and air transport coupling system in China', *Transportation Research Part A*. Elsevier, 127(June), pp. 55–70. doi: 10.1016/j.tra.2019.07.008.

Li, J. Y., Teng, J., & Wang, H. (2024). Measuring route diversity in spatial and spatial-temporal public transport networks. *Transport Policy*, 146, 42-58.

Liao, F. and van Wee, B. (2017) 'Accessibility measures for robustness of the transport system', *Transportation*. Springer US, 44(5), pp. 1213–1233. doi: 10.1007/s11116-016-9701-y.

Liu, K., Wang, M., Cao, Y., Zhu, W., Wu, J., & Yan, X. (2018). A comprehensive risk analysis of transportation networks affected by rainfall-induced multihazards. *Risk analysis*, 38(8), 1618-1633.

Lochbihler, K., Lenderink, G., & Siebesma, A. P. (2017). The spatial extent of rainfall events and its relation to precipitation scaling. *Geophysical Research Letters*, 44(16), 8629-8636.

Lochbihler, K., Lenderink, G., & Siebesma, A. P. (2019). Response of extreme precipitating cell structures to atmospheric warming. *Journal of Geophysical Research: Atmospheres*, 124(13), 6904-6918.

Lowry, M. (2014). Spatial interpolation of traffic counts based on origin–destination centrality. *Journal of Transport Geography*, 36, 98-105.

Lyu, H. M., Sun, W. J., Shen, S. L., & Arulrajah, A. (2018). Flood risk assessment in metro systems of mega-cities using a GIS-based modeling approach. *Science of the Total Environment*, 626, 1012-1025.

Mamun, S. A., Lownes, N. E., Osleeb, J. P., & Bertolaccini, K. (2013). A method to define public transit opportunity space. *Journal of Transport Geography*, 28, 144-154.

Ma, F., Liu, F., Yuen, K. F., Lai, P., Sun, Q., & Li, X. (2019). Cascading failures and vulnerability evolution in bus–metro complex bilayer networks under rainstorm weather conditions. *International Journal of Environmental Research and Public Health*, 16(3), 329.

Matte, D., Christensen, J. H., & Ozturk, T. (2022). Spatial extent of precipitation events: when big is getting bigger. *Climate Dynamics*, 58(5), 1861-1875.

Mattsson, L. G. and Jenelius, E. (2015) 'Vulnerability and resilience of transport systems - A discussion of recent research', *Transportation Research Part A: Policy and Practice*, 81, pp. 16–34. doi: 10.1016/j.tra.2015.06.002.

McCull, L., Palin, E. J., Thornton, H. E., Sexton, D. M., Betts, R., & Mylne, K. (2012).

Assessing the potential impact of climate change on the UK's electricity network. *Climatic change*, 115, 821-835.

Met Office (2023). Storm Babet, 18 to 21 October 2023. https://www.metoffice.gov.uk/binaries/content/assets/metofficegovuk/pdf/weather/learn-about/uk-past-events/interesting/2023/2023_08_storm_babet.pdf

Mishra, A., Mukherjee, S., Merz, B., Singh, V. P., Wright, D. B., Villarini, G., ... & Stedinger, J. R. (2022). An overview of flood concepts, challenges, and future directions. *Journal of hydrologic engineering*, 27(6), 03122001.

Moron, V., Robertson, A. W., Ward, M. N., & Camberlin, P. (2007). Spatial coherence of tropical rainfall at the regional scale. *Journal of Climate*, 20(21), 5244-5263.

National Infrastructure Commission. (2020). Anticipate, react, recover. Resilient infrastructure systems. National Infrastructure Commission.

Network Rail (2017) 'Delivering a better railway for a better Britain Route Specifications 2017 Scotland'. Available at: <https://www.networkrail.co.uk/wp-content/uploads/2017/04/Route-Specification-Scotland-2017.pdf>.

Network Rail (2020) 'Scotland's Railway Weather Resilience and Climate Change Adaptation Plan' – Version 1 – September 2020. Available at: <https://www.networkrail.co.uk/wp-content/uploads/2020/10/Scotlands-Railway-WRCCA-Plan-2020-CP6.pdf>

Niemeier, D. A. (1997). Accessibility: an evaluation using consumer welfare. *Transportation*, 24, 377-396.

OpenStreetMap (2022). Scotland-latest.osm.pbf [Data set]. <https://download.geofabrik.de/>. Geofabrik GmbH. Accessed 22/06/2022.

OpenTripPlanner (2022) (version 2.1.0) [Computer software] <https://repo1.maven.org/maven2/org/opentripplanner/otp/2.1.0/>. Accessed 22/06/2022.

Ordnance Survey (GB) (2021) *OS MasterMap Highways Network* [GML3 geospatial data], Scale 1:2500, Tiles: GB, Updated: 1 March 2021, Ordnance Survey (GB), Using: EDINA Digimap Ordnance Survey Service, <<https://digimap.edina.ac.uk>>, Downloaded: 2021-06-18 18:34:18.522

Outwater, M., Bradley, M., Ferdous, N., Trevino, S., & Lin, H. (2015). Foundational Knowledge to Support a Long-Distance Passenger Travel Demand Modeling Framework: Implementation Report.

Ouyang, M. (2014). Review on modeling and simulation of interdependent critical infrastructure systems. *Reliability engineering & System safety*, 121, 43-60.

- Ouyang, M., Pan, Z., Hong, L., & He, Y. (2015). Vulnerability analysis of complementary transportation systems with applications to railway and airline systems in China. *Reliability Engineering & System Safety*, 142, 248-257.
- Ouyang, M., Tian, H., Wang, Z., Hong, L., & Mao, Z. (2019). Critical infrastructure vulnerability to spatially localized failures with applications to Chinese railway system. *Risk Analysis*, 39(1), 180-194.
- Palko, K., & Lemmen, D. S. (2017). Climate risks and adaptation practices for the Canadian transportation sector 2016.
- Pant, R., Hall, J. W., & Blainey, S. P. (2016). Vulnerability assessment framework for interdependent critical infrastructures: case-study for Great Britain's rail network. *European Journal of Transportation and Infrastructure Research*, 16(1), 174-194.
- Patterson, S. A. and Apostolakis, G. E. Ā. (2007) 'Identification of critical locations across multiple infrastructures for terrorist actions', 92, pp. 1183–1203. doi: 10.1016/j.res.2006.08.004.
- Pebesma, E. J. (2018). Simple features for R: standardized support for spatial vector data. *R J.*, 10(1), 439.
- Peruccacci, S., Brunetti, M. T., Luciani, S., Vennari, C., & Guzzetti, F. (2012). Lithological and seasonal control on rainfall thresholds for the possible initiation of landslides in central Italy. *Geomorphology*, 139, 79-90.
- Pitt, S. M. (2007). The Pitt review: learning lessons from the 2007 floods. *Cabinet Office*.
- Pregolato, M., Ford, A. and Dawson, R. (2015) 'Analysis of the risk of Transport infrastructure disruption from extreme rainfall', *12th International Conference on Applications of Statistics and Probability in Civil Engineering, ICASP 2015*, (July).
- Pregolato, M., Jaroszewski, D., Ford, A., & Dawson, R. J. (2020). Climate extremes and their implications for impact modeling in transport. In *Climate Extremes and Their Implications for Impact and Risk Assessment* (pp. 195-216). *Elsevier*.
- Pyatkova, K., Chen, A. S., Butler, D., Vojinović, Z., & Djordjević, S. (2019). Assessing the knock-on effects of flooding on road transportation. *Journal of environmental management*, 244, 48-60.
- Rebally, A., Valeo, C., He, J., & Saidi, S. (2021). Flood impact assessments on transportation networks: a review of methods and associated temporal and spatial scales. *Frontiers in Sustainable Cities*, 3, 732181.

- Renard, B., & Lang, M. (2007). Use of a Gaussian copula for multivariate extreme value analysis: Some case studies in hydrology. *Advances in Water Resources*, 30(4), 897-912.
- Restrepo-Posada, Pedro J., and Peter S. Eagleson. "Identification of independent rainstorms." *Journal of Hydrology* 55, no. 1-4 (1982): 303-319.
- Ricciardulli, L., & Sardeshmukh, P. D. (2002). Local time-and space scales of organized tropical deep convection. *Journal of climate*, 15(19), 2775-2790.
- Rinaldi, S. M., Peerenboom, J. P. and Kelly, T. K. (2001) 'Identifying, understanding, and analyzing critical infrastructure interdependencies', *IEEE Control Systems Magazine*. IEEE, 21(6), pp. 11–25. doi: 10.1109/37.969131.
- Rodríguez-Núñez, E., & García-Palomares, J. C. (2014). Measuring the vulnerability of public transport networks. *Journal of transport geography*, 35, 50-63.
- Rogelis, M. C. (2015). Flood risk in road networks.
- Rosenzweig, B. R., McPhillips, L., Chang, H., Cheng, C., Welty, C., Matsler, M., ... & Davidson, C. I. (2018). Pluvial flood risk and opportunities for resilience. *Wiley Interdisciplinary Reviews: Water*, 5(6), e1302.
- Saito, H., Nakayama, D., & Matsuyama, H. (2010). Relationship between the initiation of a shallow landslide and rainfall intensity—duration thresholds in Japan. *Geomorphology*, 118(1-2), 167-175.
- Sarlas, G., Páez, A., & Axhausen, K. W. (2020). Betweenness-accessibility: Estimating impacts of accessibility on networks. *Journal of Transport Geography*, 84, 102680.
- Schintler, L. A., Kulkarni, R., Gorman, S., & Stough, R. (2007). Using raster-based GIS and graph theory to analyze complex networks. *Networks and Spatial Economics*, 7(4), 301-313.
- Scottish Government (2020). Urban Rural Classification - Scotland [Geospatial data]. Retrieved from <https://spatialdata.gov.scot/geonetwork/srv/api/records/564db46c-3153-423c-ac84-90d41ec2652c>
- Scottish Government. (2023). Localities, Scotland [Data set]. National Records of Scotland. <https://www.data.gov.uk/dataset/1a9d2abf-9050-42ac-b508-02cf2f4532b2/localities-scotland>
- Seneviratne, S. I., Zhang, X., Adnan, M., Badi, W., Dereczynski, C., Di Luca, A., ... & Zhou, B. (2021). Weather and climate extreme events in a changing climate (Chapter 11).

- Shelat, S., & Cats, O. (2017, June). Measuring spill-over effects of disruptions in public transport networks. In *2017 5th IEEE international conference on models and technologies for intelligent transportation systems (MT-ITS)* (pp. 756-761). IEEE.
- Slingo, J. (2021) Latest scientific evidence for observed and projected climate change. In: The third UK Climate Change Risk Assessment Technical Report [Betts, R.A., Haward, A.B. and Pearson, K.V. (eds.)] Prepared for the Climate Change Committee, London
- Sohn, J. (2006). Evaluating the significance of highway network links under the flood damage: An accessibility approach. *Transportation research part A: policy and practice*, 40(6), 491-506.
- Steen, B., Chowdhury, R., Fletcher, A., & Standing-Tattersall, C. (2022). Climate Change Adaptation and Transport Infrastructure.
- Taylor, M. A., & D'Este, G. M. (2007). Transport network vulnerability: a method for diagnosis of critical locations in transport infrastructure systems. In *Critical infrastructure: Reliability and vulnerability* (pp. 9-30). Berlin, Heidelberg: Springer Berlin Heidelberg.
- Taylor, M. A., Sekhar, S. V., & D'Este, G. M. (2006). Application of accessibility based methods for vulnerability analysis of strategic road networks. *Networks and Spatial Economics*, 6(3), 267-291.
- Taylor, M. A. (2017). Accessibility Methods. In *Vulnerability Analysis for Transportation Networks*. Elsevier.
- Tennekes, M., Nowosad, J., Gombin, J., Jeworutz, S., Russell, K., Zijdeman, R., Clouse, J., Lovelace, R., & Muenchow, J. (2021). Tmap: Thematic Maps. <https://cran.r-project.org/web/packages/tmap/index.html>
- Thacker, S., Barr, S., Pant, R., Hall, J. W., & Alderson, D. (2017). Geographic hotspots of critical national infrastructure. *Risk Analysis*, 37(12), 2490-2505.
- Touma, D., Michalak, A. M., Swain, D. L., & Diffenbaugh, N. S. (2018). Characterizing the spatial scales of extreme daily precipitation in the United States. *Journal of Climate*, 31(19), 8023-8037.
- Traveline (2019). GB Bus services [Data set]. <https://transitfeeds.com/p/traveline/1033>. Accessed 21/09/2020.
- Ulbrich, U., Brücher, T., Fink, A. H., Leckebusch, G. C., Krüger, A., & Pinto, J. G. (2003). The central European floods of August 2002: Part 1-Rainfall periods and flood development. *Weather*, 58(10), 371-377.

- van de Velde, D. (2013). Long-distance coach services in Europe. In *Regulating transport in Europe* (pp. 115-139). Edward Elgar Publishing.
- Van Ginkel, K. C., Dottori, F., Alfieri, L., Feyen, L., & Koks, E. E. (2021). Flood risk assessment of the European road network. *Natural Hazards and Earth System Sciences*, 21(3), 1011-1027.
- Van Ginkel, K. C., Koks, E. E., de Groen, F., Nguyen, V. D., & Alfieri, L. (2022). Will river floods 'tip' European road networks? A robustness assessment. *Transportation Research Part D: Transport and Environment*, 108, 103332.
- Vanneuville, W., De Maeyer, P., Maeghe, K., & Mostaert, F. (2003). Model the effects of a flood in the Dender catchment based on a risk methodology. *Bulletin of the Society of Cartography*, 37(2), 59-64.
- Wang, X., Koç, Y., Derrible, S., Ahmad, N., & Kooij, R. E. (2015). Quantifying the robustness of metro networks. In *INSTR 2015-6th International Symposium on Transportation Network Reliability*, August 2-3, Nara, Japan. Kyoto University-Japan Society of Transportation Engineering.
- Wang, N., Wu, M., & Yuen, K. F. (2023). A novel method to assess urban multimodal transportation system resilience considering passenger demand and infrastructure supply. *Reliability Engineering & System Safety*, 238, 109478.
- Wasko, C., Sharma, A., & Westra, S. (2016). Reduced spatial extent of extreme storms at higher temperatures. *Geophysical Research Letters*, 43(8), 4026-4032.
- Watson, G., & Ahn, J. E. (2022). A systematic review: to increase transportation infrastructure resilience to flooding events. *Applied Sciences*, 12(23), 12331.
- Wee, B. Van, Cranenburgh, S. Van and Maat, K. (2019) 'Substitutability as a spatial concept to evaluate travel alternatives', *Journal of Transport Geography*. Elsevier, 79(January), p. 102469. doi: 10.1016/j.jtrangeo.2019.102469.
- Westra, S., Fowler, H. J., Evans, J. P., Alexander, L. V., Berg, P., Johnson, F., ... & Roberts, N. (2014). Future changes to the intensity and frequency of short-duration extreme rainfall. *Reviews of Geophysics*, 52(3), 522-555.
- White, P., Pelling, M., Sen, K., Seddon, D., Russell, S., & Few, R. (2005). Disaster risk reduction: a development concern. *London: DfID*.
- Wickham, H., Averick, M., Bryan, J., Chang, W., McGowan, L. D. A., François, R., ... & Yutani, H. (2019). Welcome to the Tidyverse. *Journal of open source software*, 4(43), 1686.

- Wickham, H. (2011). ggplot2. *Wiley interdisciplinary reviews: computational statistics*, 3(2), 180-185.
- Xi, Y., Miller, E. J., & Saxe, S. (2018). Exploring the impact of different cut-off times on isochrone measurements of accessibility. *Transportation Research Record*, 2672(49), 113-124.
- Xu, X., Chen, A., Jansuwan, S., Yang, C., & Ryu, S. (2018). Transportation network redundancy: Complementary measures and computational methods. *Transportation Research Part B: Methodological*, 114, 68-85.
- Xu, X., Huang, A., Shalaby, A., Feng, Q., Chen, M., & Qi, G. (2024). Exploring cascading failure processes of interdependent multi-modal public transit networks. *Physica A: Statistical Mechanics and its Applications*, 638, 129576.
- Yang, X., Chen, A., Ning, B., & Tang, T. (2016). Measuring route diversity for urban rail transit networks: A case study of the Beijing metro network. *IEEE Transactions on Intelligent Transportation Systems*, 18(2), 259-268.
- Yap, M. D., van Oort, N., van Nes, R., & van Arem, B. (2018). Identification and quantification of link vulnerability in multi-level public transport networks: a passenger perspective. *Transportation*, 45(4), 1161-1180.
- Yap, M., & Cats, O. (2021). Predicting disruptions and their passenger delay impacts for public transport stops. *Transportation*, 48, 1703-1731.
- Young, M. (2020). otplr: an R wrapper for the OpenTripPlanner REST API.
- Zeiger, S. J., & Hubbart, J. A. (2021). Measuring and modeling event-based environmental flows: An assessment of HEC-RAS 2D rain-on-grid simulations. *Journal of Environmental Management*, 285, 112125.
- Zhang, H., Ouyang, M., Sun, W., & Hong, L. (2023). An approach for accessibility assessment and vulnerability analysis of national multimodal transport systems. *Risk analysis*, 43(11), 2312-2329.
- Zhu, W., Liu, K., Wang, M., Ward, P. J., & Koks, E. E. (2022). System vulnerability to flood events and risk assessment of railway systems based on national and river basin scales in China. *Natural Hazards and Earth System Sciences*, 22(5), 1519-1540.
- Zhuang, J., Cui, P., Wang, G., Chen, X., Iqbal, J., & Guo, X. (2015). Rainfall thresholds for the occurrence of debris flows in the Jiangjia Gully, Yunnan Province, China. *Engineering Geology*, 195, 335-346.
- Zimmerman, R. (2004, October). Decision-making and the vulnerability of interdependent critical infrastructure. *In 2004 IEEE International Conference on*

Systems, Man and Cybernetics (IEEE Cat. No. 04CH37583) (Vol. 5, pp. 4059-4063).
IEEE.

Zorn, C., Pant, R., Thacker, S., & Shamseldin, A. Y. (2020). Evaluating the magnitude and spatial extent of disruptions across interdependent national infrastructure networks. *ASCE-ASME Journal of Risk and Uncertainty in Engineering Systems, Part B: Mechanical Engineering*, 6(2), 020904.

Appendices

Appendix A: Supplementary Material for Chapter 2

Table S1 Results of post-hoc comparisons of redundancy values for rail and bus routes using Dunn's test with Bonferroni correction to p-values.

Comparison groups	Railway		Bus	
	Z	Mean redundancy losses due to geographic interdependencies (%) **	Z	Mean redundancy losses due to geographic interdependencies (%) **
proximity ignored and 0.10km-wide buffer	-4.79***	-4.03	-4.87***	-3.89
proximity ignored and 0.25km-wide buffer	-10.13***	-8	-10.08***	-7.57
proximity ignored and 0.50km-wide buffer	-15.52***	-12	-15.12***	-11.23
proximity ignored and 0.75km-wide buffer	-19.63***	-14.95	-18.88***	-13.86
proximity ignored and 1km-wide buffer	-22.84***	-17.17	-21.77***	-15.82
proximity ignored and 1.25 km-wide buffer	-25.56***	-19.05	-24.18***	-17.46
proximity ignored and 1.50km-wide buffer	-27.73***	-20.55	-26.16***	-18.82
proximity ignored and 1.75km-wide buffer	-29.26***	-21.62	-27.64***	-19.85

proximity ignored and 2km-wide buffer	-30.68***	-22.6	-28.99***	-20.8
proximity ignored and 4km-wide buffer	-39.57***	-28.91	-37.86***	-27.2
proximity ignored and 6km-wide buffer	-45.19***	-32.93	-43.15***	-31.14
proximity ignored and 8km-wide buffer	-48.76***	-35.57	-46.75***	-33.95
proximity ignored and 10km-wide buffer	-52***	-38	-49.91***	-36.49

** Mean relative losses in redundancy of travel between OD pairs when comparing the redundancy where proximity between routes is ignored with the redundancy when buffer zones are applied around the primary routes.

*** adjusted p-value < .05

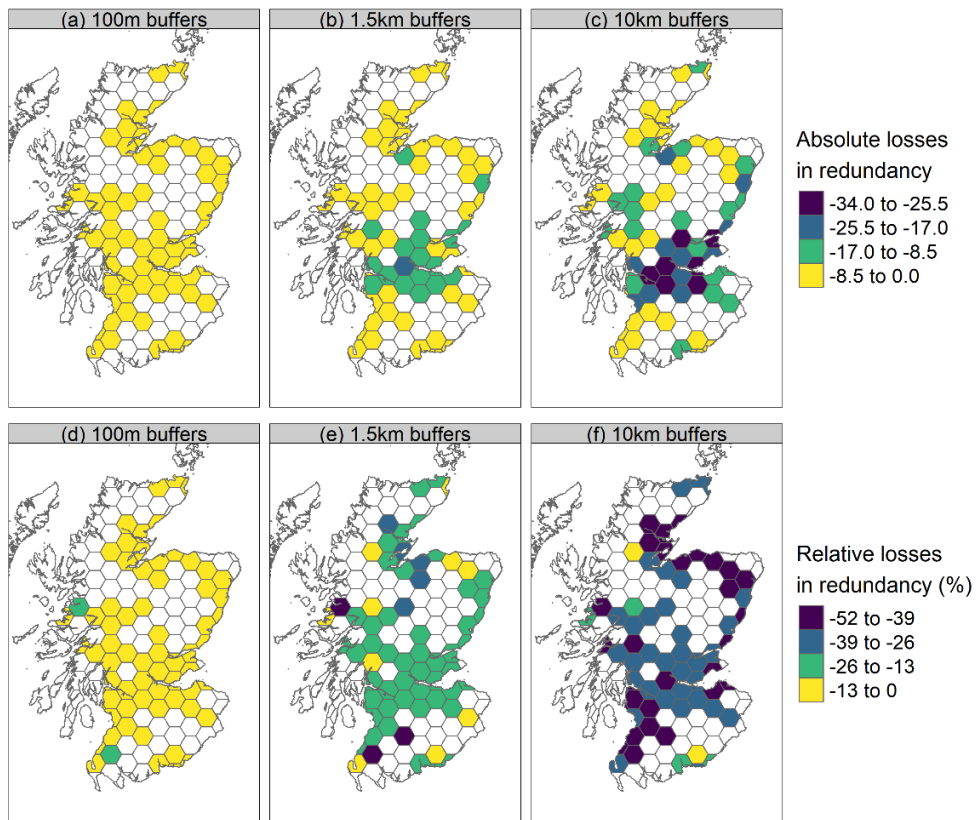


Figure S1 Losses in redundancy for origins (a) in absolute terms due to hazards of 100m footprint (b) in absolute terms due to hazards of 1.5km footprint (c) in absolute terms due to hazards of 10km footprint (d) in relative terms due to hazards of 100m footprint (e) in relative terms due to hazards of 1.5km footprint, and (f) in relative terms due to hazards of 10km footprint, when bus is the primary travel mode and rail is alternative. Non-shaded zones are those origins not served by both modes. Zones in lighter colours are less susceptible to losses due to geographic interdependencies.

Table S2 Results of post-hoc comparisons of normalised substitutability values for rail and bus routes using Dunn’s test with Bonferroni correction to p-values.

Comparison groups	Railway		Bus	
	Z	Mean substitutability losses due to geographic interdependencies (%) **	Z	Mean substitutability losses due to geographic interdependencies (%) **
proximity ignored and 0.10km-wide buffer	-10.06***	-4.79	10.96***	- 4.54
proximity ignored and 0.25km-wide buffer	-17.97***	-9.48	19.25***	- 8.83
proximity ignored and 0.50km-wide buffer	-24.94***	-14.14	26.28***	- 13.10
proximity ignored and 0.75km-wide buffer	-29.78***	-17.62	31.05***	- 16.23
proximity ignored and 1km-wide buffer	-33.21***	-20.39	34.35***	-18.64
proximity ignored and 1.25 km-wide buffer	-36.05***	-22.82	37.04***	-20.66
proximity ignored and 1.50km-wide buffer	-38.33***	-24.89	39.23***	-22.41
proximity ignored and 1.75km-wide buffer	-39.88***	-26.25	40.84***	-23.78
proximity ignored and 2km-wide buffer	-41.28***	-27.54	42.28***	-25.00

proximity ignored and 4km-wide buffer	-49.83***	-38.20	-	50.87***	-34.89
proximity ignored and 6km-wide buffer	-54.98***	-45.01	-	55.76***	-41.23
proximity ignored and 8km-wide buffer	-58.43***	-50.80	-	59.08***	-46.24
proximity ignored and 10km-wide buffer	-61.48***	-55.98	-	62.04***	-51.98

** Mean relative losses in normalised substitutability of travel between OD pairs when comparing the normalised substitutability where proximity between routes is ignored with normalised substitutability when buffer zones are applied around the primary routes.

*** adjusted p-value < .05

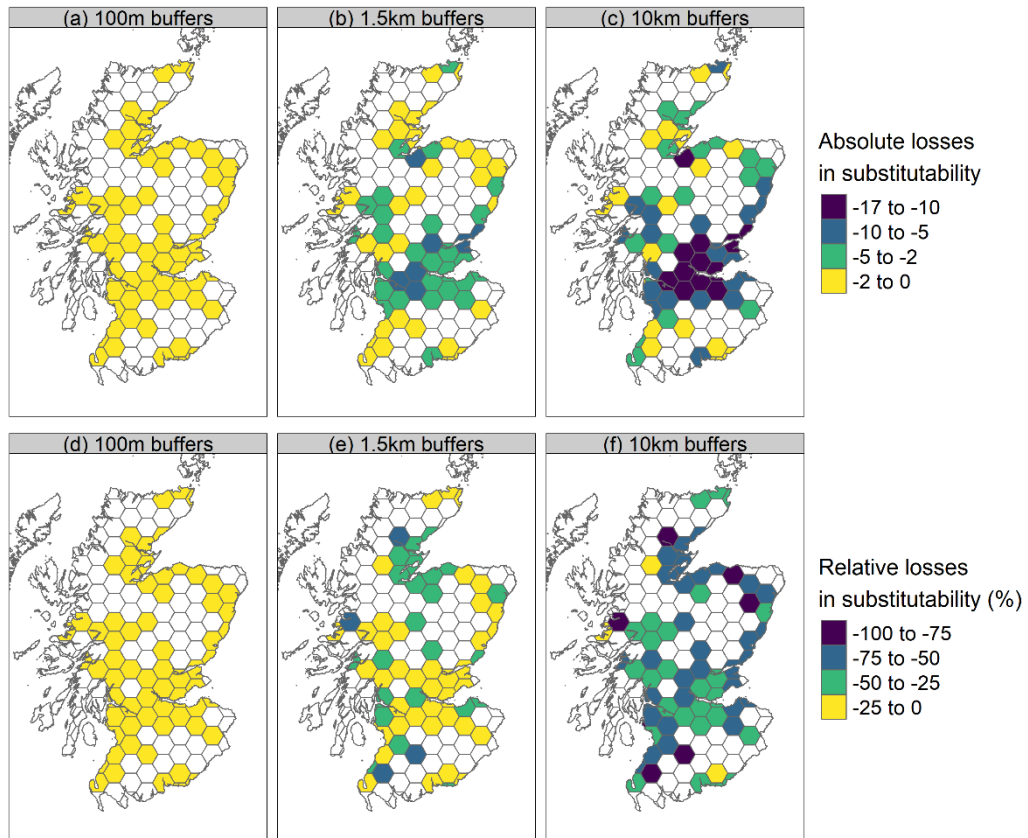


Figure S2 Losses in normalised substitutability for origins (a) in absolute terms due to hazards of 100 m footprint (b) in absolute terms due to hazards of 1.5 km footprint (c) in absolute terms due to hazards of 10 km footprint (d) in relative terms due to hazards of 100m footprint (e) in relative terms due to hazards of 1.5 km footprint, and (f) in relative terms due to hazards of 10 km footprint, when bus is the primary travel mode and rail is substitute. Non-shaded zones are those origins not served by both modes. Zones in lighter colours are less susceptible to losses due to geographic interdependencies.

Equation S1 below shows the proposed general model of redundancy that accounts for the number of opportunities at the destination, along with the feasible routes offered by all available modes for travel between the O-D pair.

$$acc_{OD}^{m_1 \leftarrow M} = D \left(\exp \left(- \frac{C(p_{m_1}^*)}{\beta_{m_1}} \right) + \sum_{n=1}^k \exp \left(- \frac{C(p_m^{(n)})}{\beta_m} \right) \left[1 - \max \{ R_C(p_m^{(n)}, p_l), \forall n < l \} \right] \right) \quad S1$$

Where D represents the number of opportunities at the destination, $M = \{m_1, m_2, m_3, \dots\}$ is the set of travel modes which include alternative routes that may substitute the preferred one, $p_{m_1}^*$ is the preferred route of primary mode m_1 , k is the number of feasible paths between OD (apart from $p_{m_1}^*$).

The first term of the right-hand side of Equation S1 represents the preferred choice of m_1 for travel between OD . The second term includes the contributions to redundancy offered by the shortest paths of each mode included in the set M that may substitute the preferred option $p_{m_1}^*$, while also considering the risk of them being concurrently disrupted due to their proximity to already selected routes. This is achieved by introducing the term “ $\max \{ R_C(p_m^{(n)}, p_l), \forall n < l \}$ ” in Equation S1, which represents the maximum proximity between any additional alternative route of M and the ones that are already selected.

Table S3 Information on flooding incidents on trunk roads included in the IRIS dataset.

	Variable	Description
Location of incident	Road Name	The name of the trunk road that the flood incident occurred, e.g. A78.
	Section Code	The ID of the section of the trunk road where the incident occurred, e.g., 14010/05. Trunk roads are divided into several sections; hence, this variable provides more specific information on the exact location of flooding, compared to “Road Name”.
Time progression of incident	Start Time	The start date of the incident. Note that the time of incident occurrence is not provided.
	Incident End Date	The date that the incident ended. Note that time of day is not provided.
	Duration of incident	The duration of incident, e.g., 2 days 3 hours 45 mins.
Details of event	Description	These variables provide further information about each incident in free-text format. For example, for some incidents the location is provided in alternative terms (e.g., M8 – Junction 14/15 W/B). It was observed that for some incidents the cause of flooding was provided, allowing events that did not occur due to extreme
	Comments	

		weather, such as flooding from burst water mains, to be excluded. Additionally, for other events, no flooding was found, and these incidents were excluded as well.
Hazard impact	Road condition	<p>Indicates the condition of the location of incident. It takes the following values:</p> <ul style="list-style-type: none"> · Dry · Wet of Damp · Flood over 3cm deep · Frost or ice · Snow · Other · Unknown
	Disruption caused	<p>Denotes whether the flood event caused disruption on the trunk road section. It takes the following values:</p> <ul style="list-style-type: none"> · TRUE · FALSE
	Disruption type	<p>Indicates the impact of the hazard on the road and is a proxy of type of road closure. Values:</p> <ul style="list-style-type: none"> · 1 – Full Road closure (Both directions of dual) · 2 – Carriageway closed · 3 – Lane or lanes closed · 4 – Reduced Lane width · 5 – Other · Unknown

The types of impacts included in the IRIS dataset were re-classified as shown in Table S4 below. Specifically, for incidents where the road experienced full road closure and carriageway closure, the impact was reclassified to full capacity reduction, whilst when only certain lane(s) were closed or experienced reduced width, the impact was reclassified to partial capacity reduction. For the events that the type of impact was originally reported as unknown, the variable of road conditions was employed to determine whether the event caused road closures, or speed restrictions.

Table S4 Types of impacts in the IRIS dataset and reclassified impacts for the bus incident dataset.

Type of impact and road conditions (where applicable) in IRIS dataset	Re-classified and/or assumed type of impact for the bus dataset
Disruption type: Full road closure (both ways of dual)	Full capacity reduction
Disruption type: Carriageway closed	
Disruption type: Reduced lane width	Partial capacity reduction
Disruption type: Lane or lanes closed	
Disruption type: Unknown, and Road conditions: Flood over 3cm deep	
Disruption type: Unknown, and Road conditions: Wet or damp	Partial capacity reduction
Disruption type: Other, and Road conditions: Wet or damp	
Disruption type: Unknown, and Road conditions: Snow	Unknown
Disruption type: Unknown, and Road conditions: Frost or ice	
Disruption type: Unknown, and Road conditions: Other	

Disruption type: Unknown, and

Road conditions: Unknown

Table S5 below shows how each incident was mapped based on the type of location reported to be flooded. The flood events were selected to be mapped onto the road infrastructure layer that contains the road links used by the long-distance services, rather than the layer of GTFS segments. This is because the GTFS segments span between bus stops that are consecutively serviced by bus trips, and since some express trips may skip intermediate stops along a route, segments may overlap with one another. The identification of road links where each incident occurred was implemented in a semi-automatic way. Based on the information provided, the reported location of flooding was either a road segment stretching between two junctions or bus stops, a locality/village that could not be serviced due to flooding, or a specific spatial point, such as a bridge.

Table S5 Types of flooding locations reported by Stagecoach and local authorities, and corresponding process undertaken to map them in GIS.

Type of location	Example	Process for mapping location	Data used
Road stretch between two junctions	A823 Queensferry Road northbound between Laburnum Road & Carnegie Avenue	<ul style="list-style-type: none">The relevant junctions were identified in the road nodes layer.Route analysis was performed in ArcGIS between the selected points using the road network dataset of Ordnance Survey (Ordnance Survey, 2021).	Vector point layer of road junctions in OS Mastermap – Highways – Roads layer (Ordnance Survey, 2021). Road network dataset

				2021) to identify the flooded road links.	(Ordnance Survey, 2021).
Road stretch between two localities/villages	B9027 between Cuminestown and New Byth			<ul style="list-style-type: none"> The first junctions on the boundaries of the localities/villages were selected. In some cases, it was not clear which junctions should be chosen, and their selection was arbitrary. Route analysis was performed in ArcGIS between the selected points to identify the flooded road links. 	Vector point layer of road junctions in OS Mastermap – Highways – Roads layer (Ordnance Survey, 2021). Road network dataset (Ordnance Survey, 2021).
Road stretch without any start and end points specified	Station Road, Elgin			<ul style="list-style-type: none"> The junctions corresponding to the start and end nodes of the road were selected. The subsequent process was similar as in the previous cases. 	Vector point layer of road junctions in OS Mastermap – Highways – Roads layer (Ordnance Survey, 2021). Road network dataset (Ordnance Survey, 2021).
Specific point along a road	A709 at Shillahill Bridge			The point was identified by overlaying the bus	–

			<ul style="list-style-type: none"> spatial layer over the OpenStreetMap basemap in GIS, and it was manually mapped. The mapped point was intersected with the road network layer to identify the flooded road links.
One or more bus stops that cannot be serviced	Harbour and Ravenscraig flats stops		<ul style="list-style-type: none"> The relevant bus stops were selected from the layer of GTFS bus stops. Intersection were performed with the road layer to identify the flooded road links.
Locality that cannot be serviced	Dundonald		<ul style="list-style-type: none"> Intersection was performed between the layer containing the boundaries of locality and the road network layer to identify the flooded road links.

Table S6 Information on flooding-induced incidents included in the incident dataset obtained from Network Rail.

Variable	Description
Incident start date & time	The date and time of day that the incident occurred.
Incident end date & time	The date and time of day that the incident ended.
Incident description	Brief description of the incident. This largely varies between the records, for example it can contain in some cases further information on the location of the event in abbreviated terms, whether the line where the incident occurred closed or was subject to speed restrictions, or it simply confirms that flooding was the cause of disruption.
Incident section name	The location of the flooding-induced incident. The section name in the dataset could either be a railway station, or a railway segment between two (not necessarily consecutive) stations.
Reason code	<p>According to the FOI response received, this variable takes the following values:</p> <ul style="list-style-type: none"> · X2: This code refers to events resulting from severe flooding beyond that which could be mitigated on Network Rail infrastructure and is used for incidents that are related to specific severe weather criteria that Network Rail uses. · JK: This code refers to flooding-induced incidents that occurred not due to exceptional weather and typically correspond to events that are associated with failure in the infrastructure maintenance.

Table S7 Types of locations of flooding incidents reported on the railway network and corresponding process undertaken to map them in GIS.

Type of location	Example	Process for mapping location	Data used
Railway station	Shotts railway station	<ul style="list-style-type: none"> The infrastructure links having the station as their start or end node were identified. The links were then intersected with the layer of the GTFS links to obtain the affected links of the GTFS network representation. 	<ul style="list-style-type: none"> Infrastructure links layer GTFS links layer
Railway segment between two stations	Section between Aviemore and Inverness	<ul style="list-style-type: none"> The relevant railway stations were identified and selected as origin and destination. Routing was performed between the selected points. The resulting railway segment was intersected with the GTFS links layer. 	<ul style="list-style-type: none"> Infrastructure links layer GTFS links layer

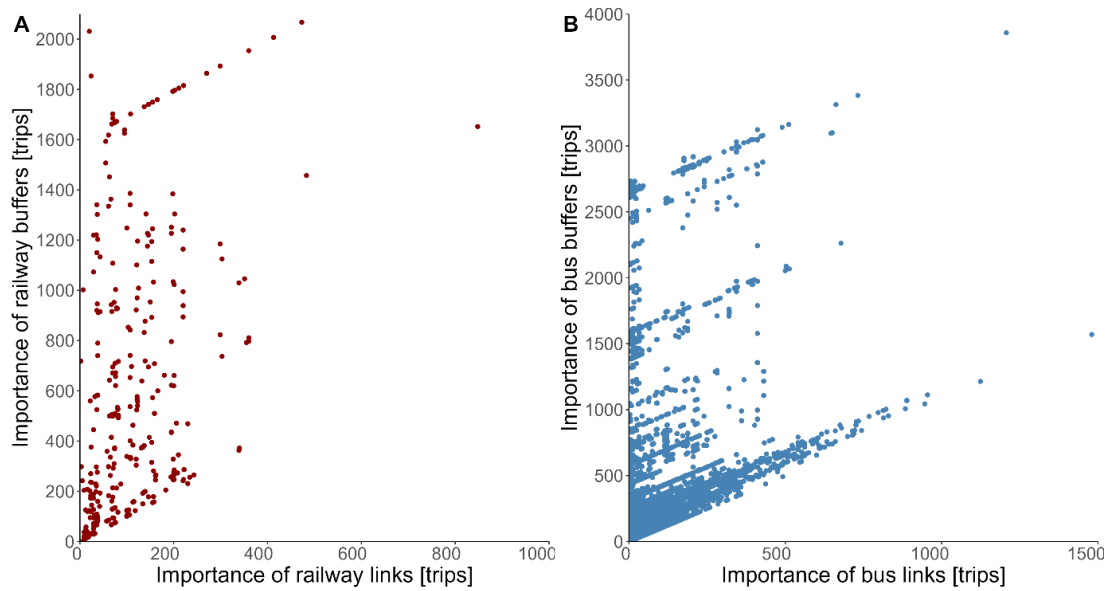


Figure S3 Scatterplots of trip-based importance of (A) railway and (B) bus links against the respective values of their corresponding 4km buffers. Note the difference in the x-axis and y-axis values between plots A and B.

Table S8 Most critical rail links in rural areas.

Link Name	Criticality
Winchburgh Junction - Newbridge Junction	4508.55
Linlithgow - Winchburgh Junction	4499.20
Stirling - Larbert	1036.95
Cardross - Craigendoran	592.91
Greenhill Lower Junction - Carmuir's West Junction	502.48

Table S9 Most critical rail buffers in rural areas.

Link Name	Criticality
Sighthill East Junction - Robroyston	9656.32
Barassie - Kilmarnock	8573.18
Kilmarnock - Auchinleck	13080.45
Kilmaurs - Kilmarnock	12692.22
Winchburgh Junction - Newbridge Junction	6701.76

Table S10 Most critical bus links in rural areas.

Link ID*	Road name**	Criticality
osgb4000000004482004	A92, Tay Bridge Roundabout	143.38
osgb4000000006279318	A955	122.76
osgb4000000005368529	A71	106.92
osgb4000000006373730	A90, Queensferry Road	105.60
osgb4000000005104093	B7073, Main Road	93.06

* Unique identification code for road links as specified in OS MasterMap Highways Network (Ordnance Survey, 2021)

** The name of the road that the link is located. Note that the link may not coincide with the full extent of the road but may be only a part of it.

Table S11 Most critical bus buffers in rural areas.

Link ID*	Road name**	Criticality
osgb4000000006241096	M9	6499.50
osgb4000000006241095	M9	6499.50
osgb4000000006242179	A904, Builyeon Road	6385.50
osgb4000000005165320	B765, Gartloch Road	5413.84
osgb4000000005165291	A80, Cumbernauld Road	5305.28

* Unique identification code for road links as specified in OS MasterMap Highways Network (Ordnance Survey, 2021)

** The name of the road that the link is located. Note that the link may not coincide with the full extent of the road but may be only a part of it.

Poincare formula

The Poincare formula which can be used to estimate the probability of at least one event B_i given the occurrence of the event at A is given in the Equation S2 below.

$$\begin{aligned}
 P(\cup B_i | A) &= \\
 &= \sum_{i=1}^n P(B_i | A) - \sum_{i < j} P(B_i | A, B_j | A) + \dots + (-1)^{n-1} \cdot P(B_1 | A, B_2 | A, \dots, B_n | A)
 \end{aligned}
 \tag{S2}$$

Where $P(B_i | A)$ is the conditional probability of B_i occurring, $P(B_i | A, B_j | A)$ is the joint probability of B_i and B_j occurring simultaneously given the event at A , $P(B_1 | A, B_2 | A, \dots, B_n | A)$ is the joint probability of all n events of set B occurring given the event at A .

Figure S4 illustrates an example of a flooding-induced closure at A observed on a part of p_{m_1} and three floods that may result in the concurrent closure of p_{m_2} .

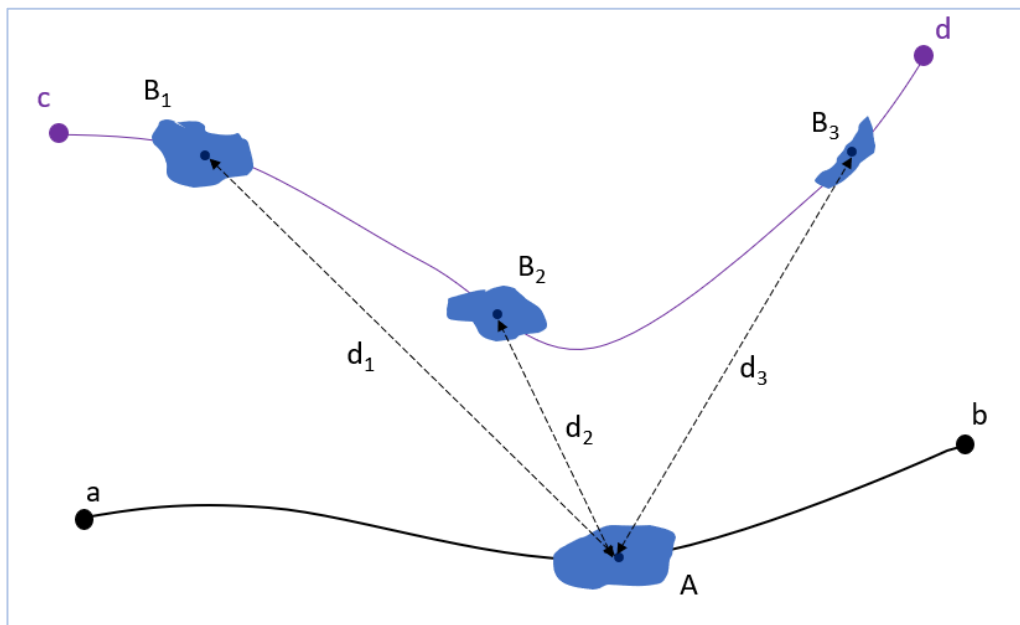


Figure S4 Example of a flood A on a part of the primary route of m_1 and three floods $\{B_1, B_2, B_3\}$ that may occur on a part of the alternative route of m_2 , along with their respective distances from A , i.e. $\{d_1, d_2, d_3\}$.

Computation of importance according to the three assumptions on geographic interdependencies

The algorithm for the computation of link importance according to each of the three assumptions on geographic interdependency is as follows. For simplicity, the value in the right-hand side of Equation 4-9 is hereafter denoted as $P(p_{m_2}^{flood} | p_{m_1}^{flood})_{upper}$.

1. Select link a , on which at least one flood event may occur according to the flood map. Select a flood location A_j of set A on the link and consider it as an observed flood event. Identify the routes of m_1 that traverse link a and thus are directly affected by A_j and the corresponding O-D pairs.
2. Calculate the importance of link, $I(a)$ (Equation 4-5), according to **Case I**.
3. Identify whether the alternative routes for the impacted O-D pairs are exposed to flooding (i.e., at least one flood hazard location intersects them) and calculate the importance of link, according to **Case II**.
4. For the set of flood locations $B = \{B_1, B_2, \dots, B_n\}$ on the alternative routes, compute the Euclidean distances between the observed event, A_j , and each flood location of set B , along with the corresponding conditional probability of each event of B occurring given the occurrence of A_j . This results in a set of conditional probabilities denoted by $P = \{P(B_1|A_j), P(B_2|A_j), \dots, P(B_n|A_j)\}$.
5. Compute the standardised conditional probabilities of events of B (Equation 4-1), where $P(E_{cr}) = 1/RP$, and retain only the flood events B_i that are statistically dependent on the occurrence of A_j , i.e. $Dr \geq 1/e$. This results in the subset of floods $B' \subseteq B$.
6. For each OD pair directly affected by A_j , calculate the overall probability $P(p_{m_2}^{flood} | p_{m_1}^{flood})_{upper}$ (Equation 4-9) based on the conditional probabilities of events of B' occurring and, by extension, compute the importance of link $I(a)$ according to **Case III**.
7. Repeat steps 4 to 6 for each event of set A .
8. Repeat steps 1 to 7 for each link of m_1 .

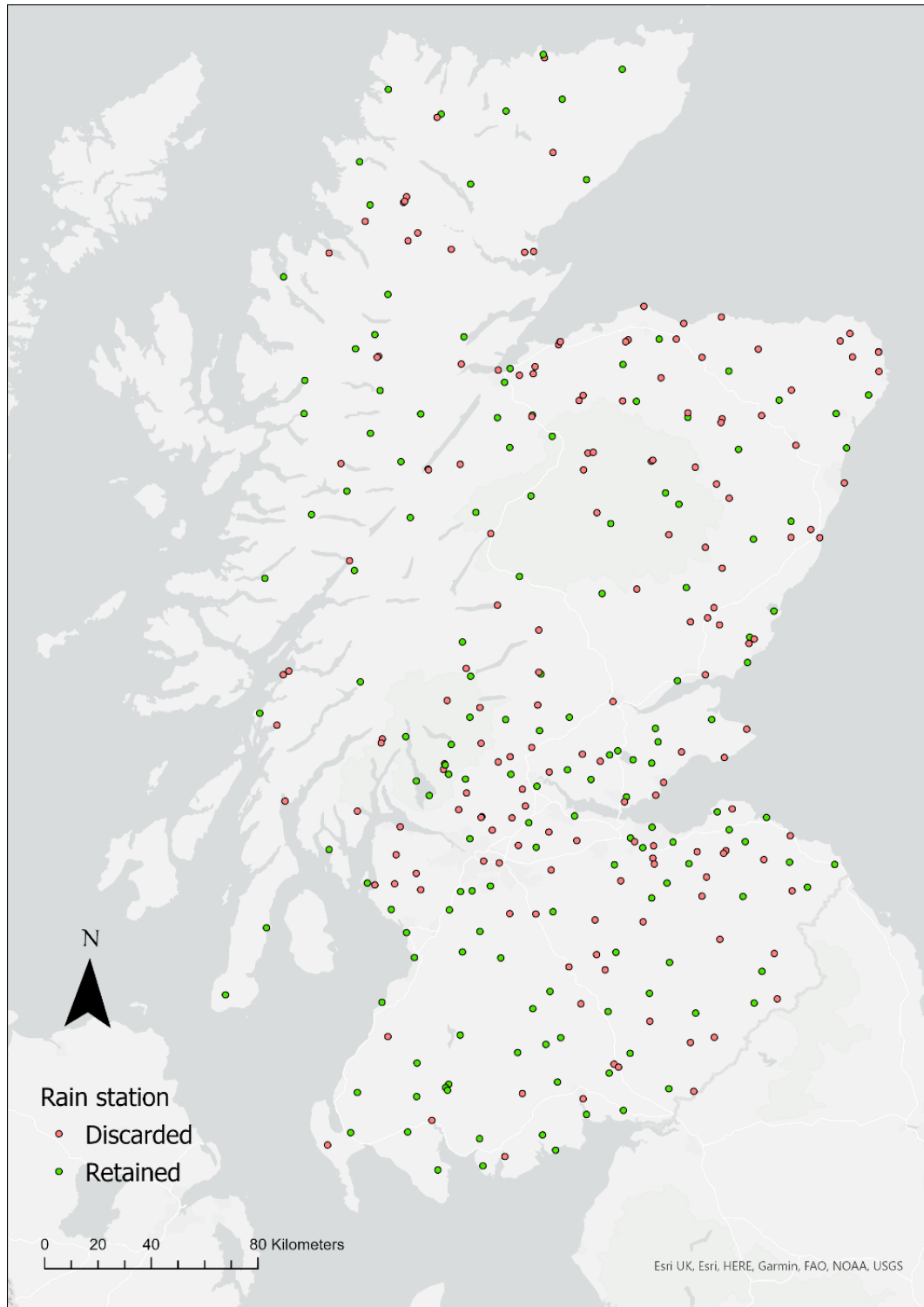


Figure S5 Rainfall stations in mainland Scotland.

Locations exposed to the pluvial flood, for which the conditional probabilities of route closures were estimated, were retrieved from a pluvial flood hazard map for Scotland which was obtained from Fathom (SSBN UK Limited, 2021). Based on CEH GEAR1h, which is a 1-km hourly gridded rainfall dataset for UK, maps were produced by constructing Intensity-Duration-Frequency curves that show 1-hour, 6-hour and 12-hour gridded rainfall intensities for certain return periods, and by subsequently using them as input onto the 2D base LISFLOOD-DP model, coupled with a 1D model solver for small channels to obtain surface water flows (Ponti *et al.*, 2022). The LISFLOOD-DP numerical scheme is a hydraulic modelling framework that provides a simplification of shallow water equations (Bates *et al.*, 2010).

The pluvial flood maps derived from this process were provided in GeoTIFF raster format at 10 m spatial resolution. Each raster cell contains the floodwater depth measured in centimetres, and its values range from zero to 9999, the latter indicating permanent water. Although maps of various return periods were available, for the purposes of this work, it was selected to use only the map of the 20-year return period, as the incident datasets, from which critical rainfall events were extracted, as well as the rainfall time series, for which the spatial dependence model was established, span for short time periods (namely from 2017 to 2020, and from 2000 to 2020, respectively). The cells of the map containing permanent water were removed to avoid considering links traversing water bodies (e.g., bridges) as flooded.

In many cases, floods on a route were adjacent or in very close proximity to each other and accounting for each of these as a separate event would inflate the upper bound of conditional probability (Equation 4-9). Thus, it was selected to group floods spanning up to 50 m from each other into a single event and calculate the conditional probability for the cluster of floods occurring concurrently with the observed event, rather than the conditional probability for each of these floods separately.

Further information on characteristics of critical rainfall events and spatial dependence model

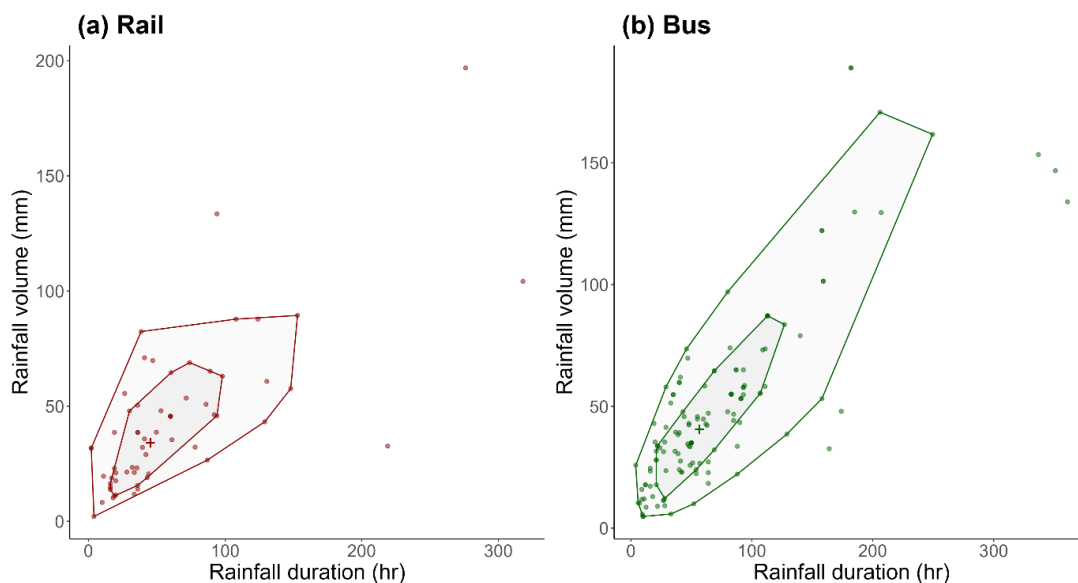


Figure S6 Bagplots of volume and duration of rainfall events that led to full closure of (a) rail and (b) bus links between May 2017 and May 2020.

The bagplots shown in Figure S6 for (a) rail and (b) bus are an extension to the commonly used box plots and show distributions of values for bivariate data (Rousseeuw *et al.*, 1999). For each bagplot, the median rainfall event is represented by the cross at the center of the plot. The inner polygon is the bag, which corresponds to the box of the univariate box plot and the outer polygon is the fence, which corresponds to the whiskers of the univariate box plot. Data points that fall outside of the fence are considered as outliers.

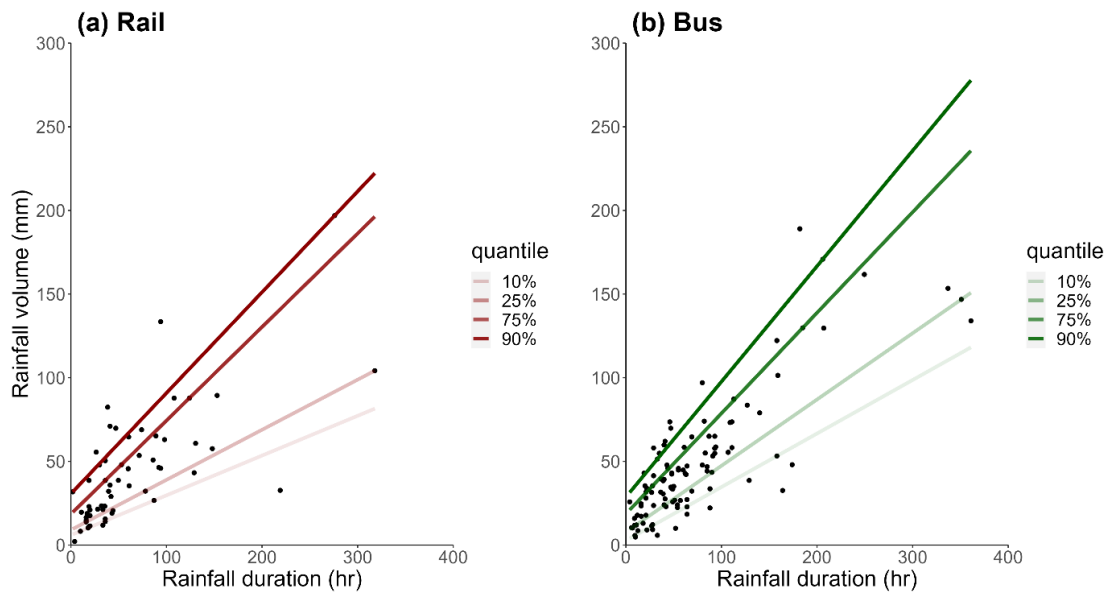


Figure S7 Fitted regression lines for various quantiles to the rainfall event characteristics that led to closures of (a) railway links and (b) bus links.

Table S12 Model parameters and goodness-of-fit values of fitted regression lines to various quantiles of rainfall depth-duration data that led to the closures of railway links.

Model	Intercept	Slope	Pseudo R ²
10%	5.92	0.24	0.18
25%	9.01	0.3	0.25
75%	18.47	0.56	0.32
90%	30.59	0.6	0.41

Table S13 Model parameters and goodness-of-fit values of fitted regression lines to various quantiles of rainfall depth-duration data that led to the closures of bus links.

Model	Intercept	Slope	Pseudo R ²
10%	2.66	0.32	0.28
25%	7.74	0.4	0.34
75%	18.57	0.6	0.5
90%	28.62	0.69	0.58

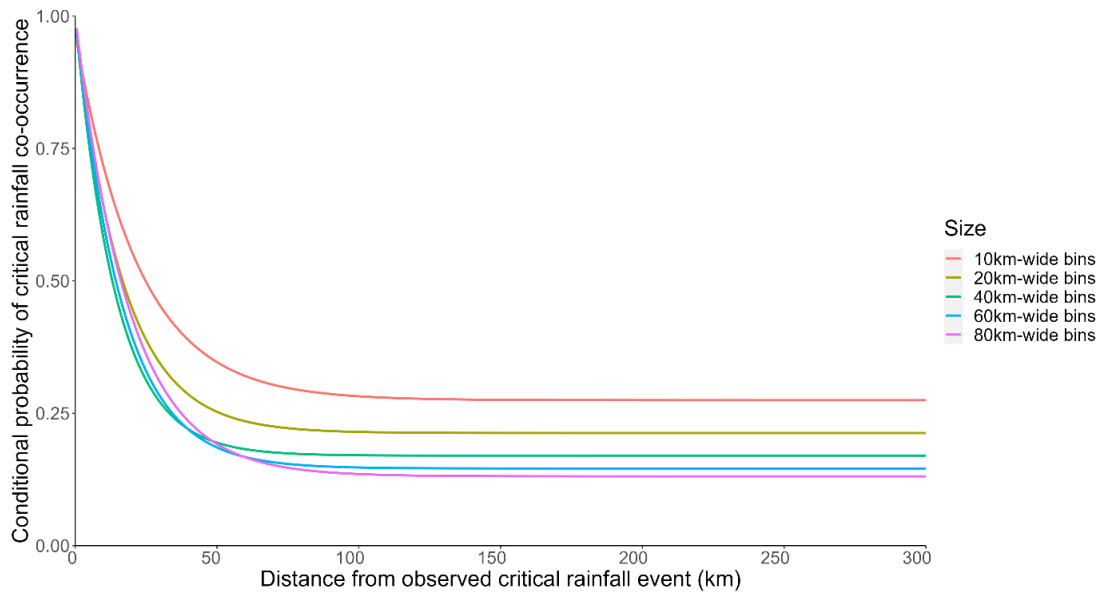


Figure S8 Fitted exponential-decay models to the computed observed conditional probabilities of critical rainfall co-occurrences when measuring proportions of target stations in 10 km, 20 km, 40 km, 60 km and 80 km-wide distance bins from the origin station.

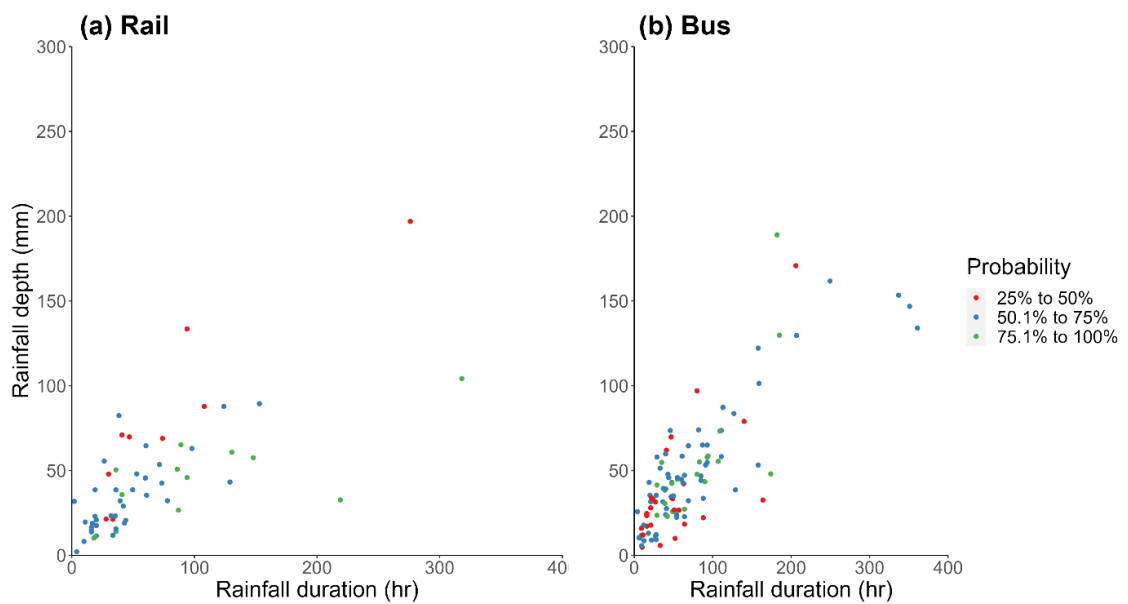


Figure S9 Characteristics of critical rainfall events that led to closures of (a) railway links and (b) bus links, weighted by their conditional probability of occurrence at the flooded locations given their occurrence at the rain station corresponding to the closed links.

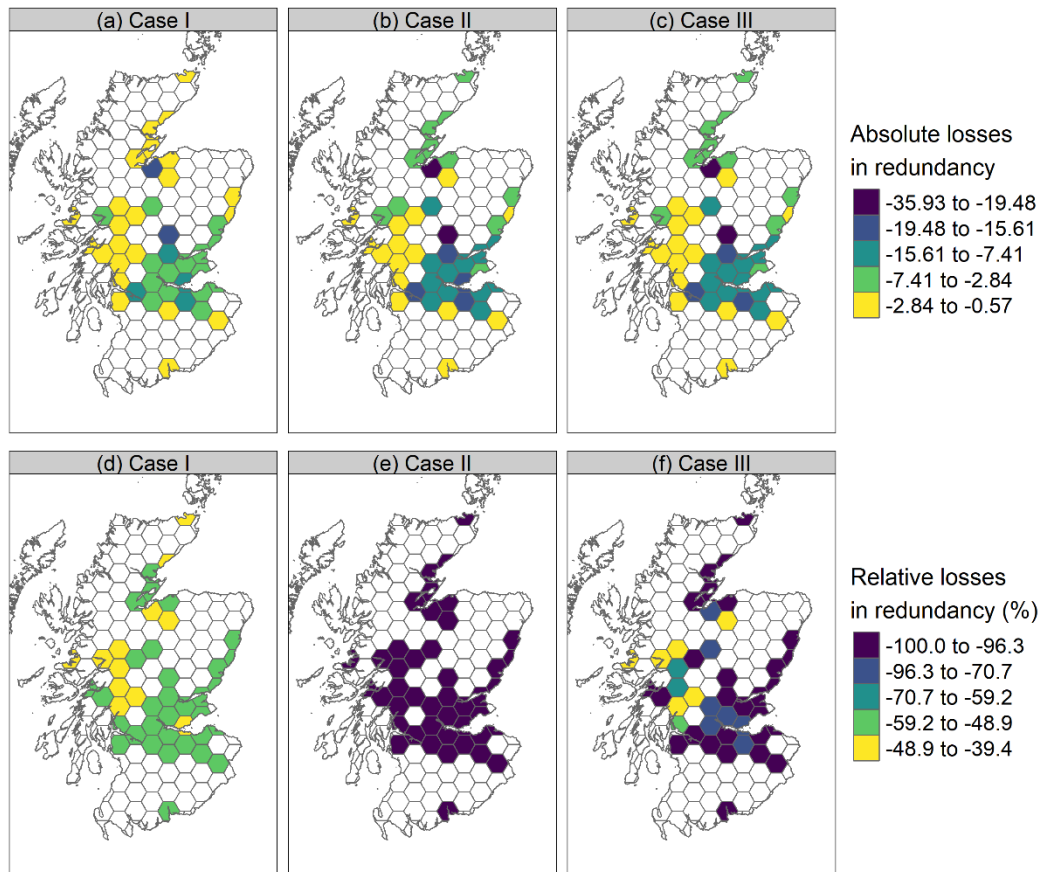


Figure S10 Losses in redundancy of origins due to the failure of link spanning from Dunkeld & Birnam to Perth, (a) when assuming complete independence of floods on bus routes, in absolute terms (b) when assuming complete dependence of floods, in absolute terms (c) when assuming spatial dependence of floods on bus routes, in absolute terms (d) when assuming complete independence of floods on bus routes, in relative terms (e) when assuming complete dependence of floods on bus routes, in relative terms (f) when assuming spatial dependence of floods on bus routes, in relative terms. Non-shaded zones correspond to origins either not served by both modes or not directly affected by closure of the link.

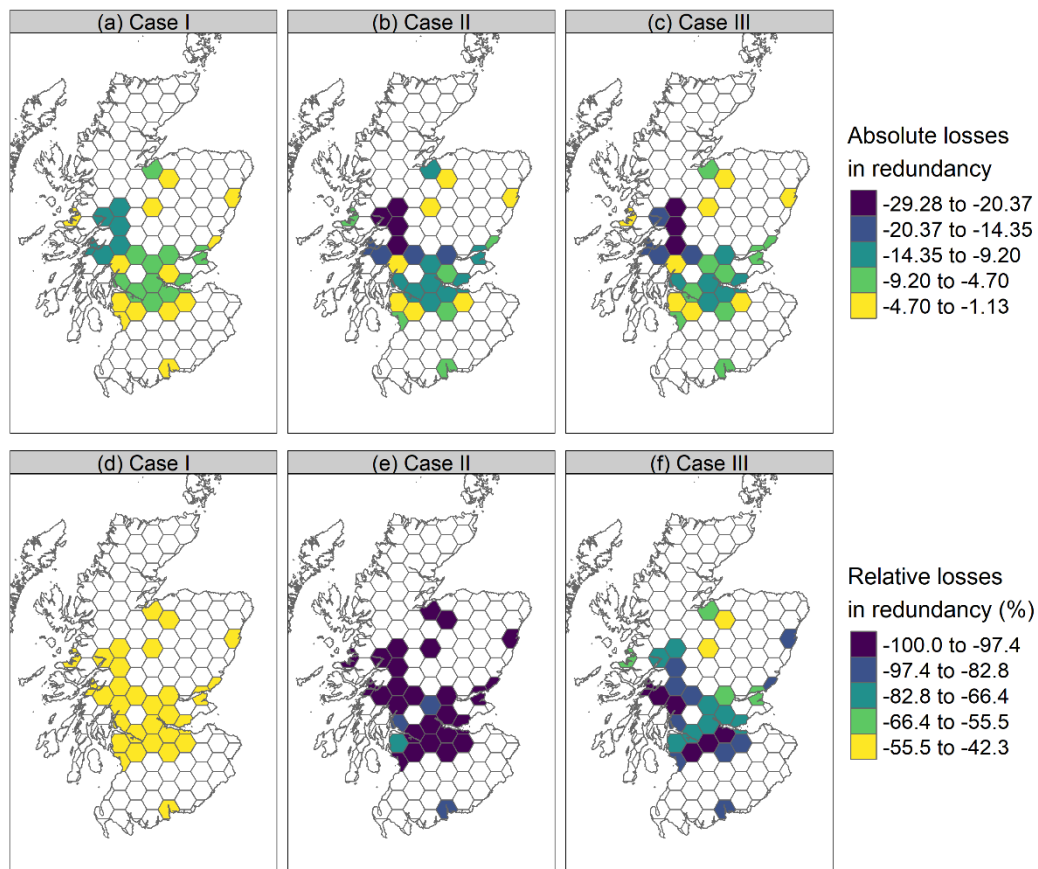


Figure S11 Losses in redundancy of origins due to the failure of link spanning from Arrochar & Tarbet to Ardlui, (a) when assuming complete independence of floods on bus routes, in absolute terms (b) when assuming complete dependence of floods, in absolute terms (c) when assuming spatial dependence of floods on bus routes, in absolute terms (d) when assuming complete independence of floods on bus routes, in relative terms (e) when assuming complete dependence of floods on bus routes, in relative terms (f) when assuming spatial dependence of floods on bus routes, in relative terms. Non-shaded zones correspond to origins either not served by both modes or not directly affected by closure of the link.

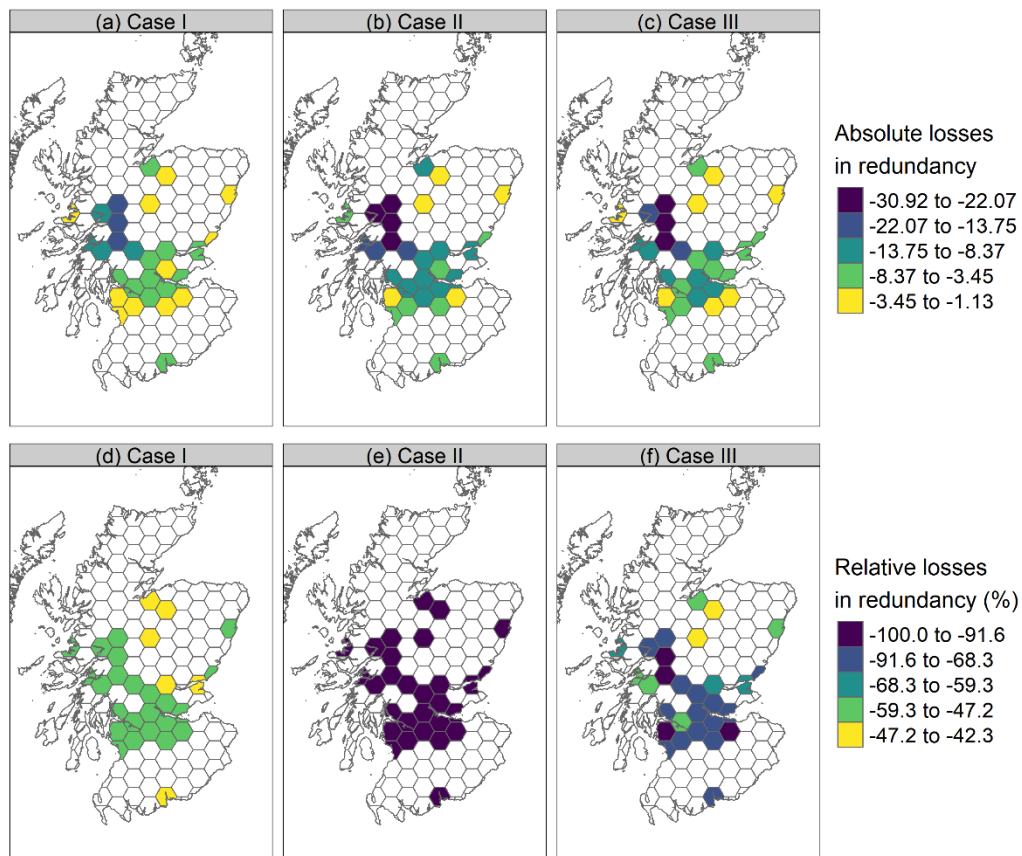


Figure S12 Losses in redundancy of origins due to the failure of link spanning from Ardlui to Crianlarich, (a) when assuming complete independence of floods on bus routes, in absolute terms (b) when assuming complete dependence of floods, in absolute terms (c) when assuming spatial dependence of floods on bus routes, in absolute terms (d) when assuming complete independence of floods on bus routes, in relative terms (e) when assuming complete dependence of floods on bus routes, in relative terms (f) when assuming spatial dependence of floods on bus routes, in relative terms. Non-shaded zones correspond to origins either not served by both modes or not directly affected by closure of the link.

References:

Bates, P. D., Horritt, M. S., & Fewtrell, T. J. (2010). A simple inertial formulation of the shallow water equations for efficient two-dimensional flood inundation modelling. *Journal of hydrology*, 387(1-2), 33-45.

Ponti, M. G., Allen, D., White, C. J., Bertram, D., & Switzer, C. (2022). A framework to assess the impact of flooding on the release of microplastics from waste management facilities. *Journal of Hazardous Materials Advances*, 7, 100105.

Rousseeuw, P. J., Ruts, I., & Tukey, J. W. (1999). The bagplot: a bivariate boxplot. *The American Statistician*, 53(4), 382-387.